UNIVERSIDAD AUTONOMA DE MADRID

DEPARTAMENTO BIOQUIMICA

SPLICING ALTERNATIVO EN *SERPING1*:

Expresión del ARNm total y de dos variantes alternativas del mensajero del gen del inhibidor de C1 en pacientes con angioedema hereditario

MARÍA DEL ROCÍO MENA DE LA CRUZ

Madrid, 2016

Departamento de Bioquímica
FACULTAD DE MEDICINA
UNIVERSIDAD AUTÓNOMA DE MADRID

SPLICING ALTERNATIVO EN *SERPING1*:

Expresión del ARNm total y de dos variantes alternativas del mensajero del gen del inhibidor de C1 en pacientes con angioedema hereditario

Memoria para optar al grado de Doctora:
María del Rocío Mena de la Cruz
Licenciada en Bioquímica

Directora: Dra. Margarita López-Trascasa
Jefa de Sección de la Unidad de Inmunología
del Hospital Universitario La Paz

AGRADECIMIENTOS

Este trabajo no habría sido posible sin el apoyo de la Dra. López-Trascasa y su gran laboratorio formado, entre otros, por Mª Ángeles y Sofía, quienes confiaron en mí desde el primer momento y me hicieron participe del proyecto que empezaba a emerger. Sin Gracia, quien siempre ha tenido esa frase de amiga que te levanta el ánimo. Sin Alberto con quien he compartido tardes de PCRs hasta las mil, y a cada uno de los residentes con los que he compartido poyata.

Aunque este trabajo es fruto de la colaboración con el grupo de Inmunoquímica del hospital, en realidad lleva una montaña de granos de arena aportados por todos y cada uno de los que formaron parte de la Unidad de Investigación del Hospital Universitario La Paz. Con ellos fui y sigo siendo una aprendiz en Biología Molecular. Con ellos me he sentido parte de una gran familia con la que viví momentos duros, pero también enormes alegrías. De allí me llevo a mis "Cukis", grandes investigadoras con las que he compartido y seguiré compartiendo la energía de seguir en la investigación y una enorme amistad, por muchos kilómetros que nos separen. Son muchos los entrañables momentos vividos tanto con ellas como con un grupo más extenso de alocados acompañantes de innumerables aventuras. Ahora muchos de esos acompañantes forman parte de mis chicos INGEMM. Del primero al último, gracias por soportarme todo este tiempo.

Este trabajo no podría haber sido posible, sobre todo, sin mis chicas SEC con las que he crecido profesional y personalmente. Ellas, sin dudarlo un minuto, han dedicado parte de su tiempo para que este trabajo pudiera salir adelante. A ellas debo darle las gracias por haberme aportado la visión práctica de las cosas.

Como salida de la caverna de Platón, deslumbrada por la luz y la realidad, llegué a esta ciudad de la mano de mi hermana pequeña, Carmen. Parecía que este reto iba a ser cosa de unos días o un mes y, quién me lo iba a decir, ya llevamos unos años por aquí. Un reto al que se nos unió la hermana mediana (Clara,) y toda una familia madrileña. Son tantas las experiencias vividas con vosotras cuatro que podría escribir un libro de dos mil páginas. Mil páginas serían de psicología y otras mil de terapia aventurera.

Consecuencia de esa terapia aventurera es Juanjo, a quien tengo que agradecer que camine junto a mí, sea cual sea el camino que se nos presente, pero siempre con

ilusión y esperanza. Él ha conseguido darme la racionalidad a velocidad crucero junto con grandes momentos de locura, una entrañable familia madrileña adoptiva y un grupo de personas que me han hecho ver la amistad desde otro punto de vista. Sin él no hubiera conseguido sacar energía para afrontar esta última etapa.

Como digo líneas arriba, mucha gente ha puesto granitos de arena para que este trabajo haya llegado hasta aquí, pero nada de esto habría sido posible sin la familia que me vio nacer: MI FAMILIA. Mi hermano, con quien comparto cada una de mis aventuras y desventuras tanto en ciencia como en otros ámbitos de mi vida, ahora y siempre. Mi madre, que tiene ese don de sacarme la garra de dentro para afrontar cosas inimaginables por mí misma. Debe ser eso del "don de madre".

Mi PADRE. Si hay una estrella que me guía día a día, esa tiene que ser él. Si he llegado hasta aquí es gracias a que fue capaz de poner la parte racional por delante de la emocional y me aconsejó volar del nido para desarrollarme como persona, aún con gran dolor de su corazón. Ojalá estuviera hoy aquí y pudiera ver que el polluelo que en su día voló de su nido está creciendo mientras intenta poner en práctica todas y cada una de sus enseñanzas. Va por ti.

Resumen

El angioedema hereditario por deficiencia del inhibidor del C1 (AEH-C1INH) se caracteriza por recurrentes edemas localizados en tejidos subcutáneos.

Es una enfermedad genética con herencia autosómica dominante debido a mutaciones en el gen *SERPING1* que limitan la producción del inhibidor de C1(C1INH) impidiendo la regulación de las cascadas enzimáticas sobre las que actúa. En el 85% de los pacientes se debe a una deficiencia cuantitativa de la proteína (AEH-C1INH tipo I), con síntesis de proteína disminuida por debajo del 50% esperado. En el 15% restante (AEH-C1INH tipo II), la deficiencia es cualitativa. En este último grupo, la mutación está localizada en los aminoácidos que conforman el centro reactivo o sus inmediaciones y, aunque los niveles del C1INH están normales o elevados, la proteína no es funcional.

Este trabajo ha profundizado en la expresión del mensajero del inhibidor de C1 en 30 pacientes con AEH-C1INH. El estudio detectó que la producción de mensajero en los pacientes tipo I está disminuida por debajo del 50%, hecho que cabría esperar por el aporte del alelo sano. En cambio, los pacientes tipo II mostraron una síntesis del ARN mensajero cercana al 72% respecto a los valores normales.

En 2006, Duponchel *et al.* publicaron un estudio mostrando una variante alternativa de *splicing* del gen del inhibidor de C1 (*SERPING1*) con ausencia de exón 3 que se expresaba en monocitos de sangre periférica, pero no en hígado. En nuestro trabajo se ha analizado la expresión de ambas variantes, variante completa (todos los exones) y variante sin exón 3, en 32 pacientes. Dos tercios de los pacientes portaban mutaciones tipo I y un tercio mutaciones tipo II. En el primer grupo (tipo I), la producción de la variante completa era mayor que la alternativa cuando las mutaciones estaban localizadas dentro del dominio serpina, pero el patrón de expresión se invertía cuando estas se localizaban en el dominio no serpina, o en los extremos del dominio serpina. Estos datos parecen indicar que el patrón es independiente del tipo de mutación. En los pacientes tipo II, los niveles de expresión para ambas variantes fue más uniforme siendo la variante corta la más expresada en todos los individuos.

Para profundizar en las posibles funciones de la variante corta en monocitos, realizamos estudios de expresión de variantes en poblaciones celulares aisladas a partir de células mononucleadas de sangre periférica (PBMCs) de donantes sanos con y sin estimulación por IFN-γ a 24 y 48 horas. Este estudio ha mostrado que las células NK expresan Inhibidor del C1en un entorno inflamatorio.

Summary

Hereditary angioedema due to C1 inhibitor deficiency (HAE-C1INH) is a rare disease that causes recurrent localized oedemas in subcutaneous tissues.

It is a genetic disease with dominant autosomal inheritance caused by mutations in the gene *SERPING1*, reducing either the synthesis or the function of C1 inhibitor and leading to uncontrolled activation of serum enzymatic over which it operates.

In about 85% of patients, the disease is caused by quantitative protein deficiency where protein synthesis decrease below the expected 50% (HAE-C1INH type I). In the remaining 15% of patients, it is due to a qualitative deficiency because a mutation is located in the reactive centre loop or its surroundings. In the latter type, C1 inhibitor levels can be either normal or above normal. In either case, such production is non-functional.

This work contains a thorough study of C1 inhibitor expression in 30 patients suffering from HAE-C1INH. The study has found that messenger production in type I patients is also below 50% as could be expected from the single normal allele. On the other hand, patients with type II showed messenger synthesis around 72% of normal levels.

In 2006, Duponchel *et al.* published a study showing that an alternative *SERPING1* transcript lacking exon 3 is expressed by peripheral blood monocytes but not liver. We analysed the expression of both transcripts, the complete transcript (all exons) and the one without exon 3, in peripheral blood monocytes of 32 HAE patients. Two thirds of the patients carried type I mutations, and one third carried type II mutations. In the first group, the production of the complete transcript was observed to be higher than that of the alternative transcript when mutations were located in the serpin domain. However, mutations in non-serpin domain, and those in marginal regions of the serpin domain were observed to have an inverted expression pattern. Such behaviour did not depend on the mutation type. As for patients with type II mutations, the transcript with highest levels was the one without exon 3, the expression pattern being more uniform in all cases.

In order to deepen our understanding of the expression pattern of the short transcript in monocytes, we studied the expression of both complete and short transcripts in isolated peripheral blood cells (PBMCs) of healthy individuals with and without IFN-γ stimulation during 24 and 48 hours. The results showed that NK cells also express C1 inhibitor in inflammatory environment.

Índice

INTRODUCCIÓN.

1. EL ANGIOEDEMA HEREDITARIO 1

1.1. Introducción general 1

1.2. Manifestaciones clínicas en AEH por deficiencia del inhibidor de C1 2

1.3. Diagnóstico 3

- Diagnóstico de laboratorio 3
- Diagnóstico diferencial con otros tipos de angioedemas 3

1.4. Profilaxis y tratamiento 5

- Profilaxis a largo plazo 5
- Profilaxis a corto plazo 6
- Tratamiento de los ataques agudos 6

1.5. Fisiopatología del angioedema hereditario por deficiencia del inhibidor de C1 7

1.6. Base molecular del AEH 8

2. INHIBIDOR DE C1 10

2.1. Introducción y estructura de la proteína 10

2.2. Biosíntesis del inhibidor de C1 11

2.3. Serpinas, la familia del inhibidor de C1 11

- Estructura de las serpinas, conformación y mecanismo inhibitorio 11

2.4. Función del inhibidor de C1 14

- Regulación del sistema del complemento 14
- Regulación del sistema de la coagulación 15
- Regulación del sistema de la fibrinólisis 15
- Regulación del sistema de cininas 15

3. GEN DE *C1INH/ SERPING1* 15

3.1. Estructura y localización del gen 15

3.2. Regulación transcripcional de *SERPING1* dependiente de tejido 18

OBJETIVOS 23

MATERIALES Y MÉTODOS

4. ANÁLISIS DE LA EXPRESIÓN DE *SERPING1* EN PBMCs DE PACIENTES AEH-C1INH 27

4.1. Criterios de inclusión y exclusión 27

4.1.1. Población estudiada 27

- Análisis de expresión del ARN mensajero de *SERPING1* **27**
- Análisis de expresión del *splicing* alternativo del exón 3 de *SERPING1* **28**

4.2. Extracción de ADN y ARN **28**

4.3. PCR cuantitativa para la detección del ARNm de *SERPING1* **29**

4.3.1. Trascripción inversa (RT) **29**

4.3.2. PCR a tiempo real **29**

4.3.3. Cebadores utilizados para técnicas de PCR a tiempo real **31**

- Análisis de expresión de *SERPING1* **31**
- Análisis de expresión del *splicing* alternativo del exón 3 **32**

4.3.4. Desarrollo de la PCR cuantitativa **33**

- Análisis de la expresión de *SERPING1* **33**
- Análisis de expresión del splicing alternativo del exón 3 **33**

5. ANÁLISIS ESTADISTICO **34**

6. AISLAMIENTO DE POBLACIONES CELULARES EN CONTROLES **34**

6.1. Población estudiada **34**

6.2. Extracción de muestras y obtención de suspensión leucocitaria **35**

6.3. Selección poblacional **35**

- Selección inmunomagnética **35**
- Aislamiento por citometría de flujo **38**

6.4. Estimulación de células con IFN-γ **40**

6.5. Extracción de ARN **40**

RESULTADOS

7. ESTUDIO DE LA EXPRESIÓN DE *SERPING1* EN SANGRE PERIFÉRICA **45**

7.1. Población estudiada **45**

7.2. Análisis de la expresión de *SERPING1* en pacientes con AEH **46**

7.3. Análisis de expresión por tipo de mutación **48**

8. ESTUDIO DE LA EXPRESIÓN DE VARIANTES DE *SPLICING* DE *SERPING1* EN SANGRE PERIFÉRICA **49**

8.1. Análisis semicuantitativo de la expresión de *SERPING1* por PCR con transcriptasa reversa **50**

8.2.Población estudiada **51**

8.3. Análisis de expresión de las variantes de *splicing* que afectan al exón 3 **52**

9. ESTUDIO DE LA EXPRESIÓN DE *SERPING1* DEPENDIENTE DE TIPO CELULAR. 56

- Separación inmunomagnética. **56**
- Separación por citometría de flujo. **60**

10. DISCUSIÓN. 67

10.1. Expresión total de *SERPING1* en pacientes con AEH-C1INH 67

10.2. Expresión de variantes de *splicing* de *SERPING1* en pacientes con AEH-C1INH 70

10.3. Efecto del tratamiento en la expresión de *SERPING1* en pacientes con AEH-C1INH 73

10.4. Expresión de *SERPING1* dependiente de tipo celular 74

CONCLUSIONES 79

BIBLIOGRAFÍA 81

ANEXOS 93

ABREVIATURAS

ADN: Ácido desoxirribonucleico.

ADNc: ADN de cadena sencilla.

ADN-H: Estructura de ADN de hélice triple.

AEA-C1INH: Angioedema adquirido con deficiencia del inhibidor de C1.

AEA-IECA: Angioedema adquirido mediado por inhibidores de la enzima convertidora de angiotensina.

AEH: Angioedema hereditario.

AEH-C1INH: Angioedema Hereditario por deficiencia del inhibidor de C1.

AEH-FXII: Angioedema hereditario por mutación en FXII.

APC: Aloficocianina.

ARN: Ácido ribonucleico.

ARNm: Ácido ribonucleico mensajero.

B1R: Receptores endoteliales de bradicinina tipo 1.

B2R: Receptores endoteliales de bradicinina tipo 2.

C1INH: Inhibidor de la esterasa C1.

C1INH-C1r-C1s-C1INH: Complejo covalente C1INH y subcomponentes de C1.

C1r: Subcomponente r de C1.

C1s: Subcomponente s de C1.

C2: Segundo componente del sistema del complemento.

C3: Tercer componente del sistema del complemento.

C4: Cuarto componente del sistema del complemento.

CD14: Receptor de lipopolisacáridos de monocitos (*cluster of differentiation 14*).

CD16: Receptor de la fracción Fc de la IgG (*cluster of differentiation 16*).

CD19: Marcador clínico linfocitos B (*cluster of differentiation 19*).

CD3: Complejo con el receptor de célula T (TCR) (*cluster of differentiation 3*).

CD41: Glicoproteína IIb/IIIa (*cluster of differentiation 41*).

CD45: Antígeno común leucocítico (*cluster of differentiation 45*).

CD56 : Molécula de adhesión de la célula neuronal (*Cluster of differentiation 56*).

CH50: Actividad hemolítica 50.

CpG: Citosina y guanina enlazados por fosfatos.

Ct: Ciclo umbral (*Cycle threshold*).

DEPC: Dietil pirocarbonato.

EDTA: Ácido etilendiaminotetraácetico.

FITC: Isotiocianato de fluoresceína.

FXI: Factor XI de la coagulación.

FXIa: Factor XI de la coagulación activado.

FXII: Factor XII de la coagulación.

FXIIa: Factor XII de la coagulación activado.

GAPDH: Gliceraldehido-3-fosfato deshidrogenasa.

GAS: Secuencia activada por INF-γ.

HAWK: *Hereditary Angioedema International Working Group*

HGMD: Base de datos de mutaciones en genes humanos (*Human Gene Mutation Database*)

HMWK: Cininógeno de elevado peso molecular.

IECA: Inhibidores de la enzima convertidora de angiotensina.

IFN-γ: Interferón gamma.

IL-6: Interleuquina 6.

ISREs: Elementos de secuencias de nucleótidos con respuesta a estimulo con IFN-γ .

MASP-1: Serín proteasa 1 asociada a la lectina de unión a manosa.

MASP-2: Serín proteasa 2 asociada a la lectina de unión a manosa.

MBL: Lectina de unión a manosa (*Mannose Binding Lectin).*

$MgCl_2$: Cloruro de magnesio.

NK: Células *Natural Killer*.

NMD: Degradación del ARN mensajero mediada por mutaciones de codón de parada (*Nonsense mediated decay).*

PAI1: Inhibidor del activador del plasminógeno-1

PBMCs: Células mononucleadas de sangre periférica (*Peripheral Blood Mononuclear cells*).

PBS: Solución salina amortiguada por fosfatos (***P****hosphate* ***B****uffered* ***S****aline*).

PCR: Reacción en cadena de la polimerasa.

PE: Ficoeritrina.

PerCP: Proteína peridinina-clorofila.

PMPs: Micropartículas plaquetarias.

RCL: Bucle del centro reactivo.

RefSeq: Secuencia de referencia nucleotídica.

RNasas : Ribonucleasas.

RPMI: Medio de cultivo empleado en células humanas (***R****oswell* ***P****ark* ***M****emorial* ***I****nstitute medium*)

RT: Retrotranscripción inversa.

RT-PCR: Reacción en cadena de la polimerasa con transcriptasa inversa.

qPCR: Reacción en cadena de la polimerasa cuantitativa**.**

Serpina: Inhibidor de serín proteasa.

***SERPING1*:** Gen que codifica el inhibidor de C1.

STF: Suero de ternera fetal.

UTR: Región no traducida de un gen.

Introducción

1. EL ANGIOEDEMA HEREDITARIO

1.1. Introducción general

El angioedema hereditario (AEH) por deficiencia del inhibidor de C1 [MIM#106100] (en adelante AEH-C1INH) es una enfermedad con patrón de herencia autosómica dominante y penetrancia incompleta.

En 1882, Quincke fue el primer autor que consideró el angioedema como una entidad clínica al documentar varios casos de angioedema en distintas generaciones de una misma familia. En 1888, Osler describió el carácter hereditario de la enfermedad y la definió como "edema angioneurótico".

La asociación entre la deficiencia genética del inhibidor del C1 y el angioedema fue propuesta por primera vez en 1963 por Donaldson y Evans. Nueve años más tarde, Cadwell y colaboradores relacionaron la deficiencia de C1INH adquirida, no hereditaria, con un linfosarcoma concomitante (Caldwell et al., 1972).

La última forma de angioedema hereditario fue descrita en 2000. Esta se presenta con niveles antigénicos y funcionales de C1INH normales, y se debe a mutaciones en el gen *F12* que codifica el Factor XII del sistema de la coagulación (FXII). Este factor es dependiente de estrógenos, ya que se desencadena en las fases hiper-estrogénicas afectando, predominantemente, al sexo femenino (Bork et al., 2000). La dependencia de estrógenos ha supuesto que sea denominado AEH dependiente de estrógeno (Binkley and Davis, 2000) o AEH asociado a estrógenos (Agostoni et al., 2004).

El angioedema puede producirse también sin déficit de C1INH, o de mutación en el gen *F12*. Ante estas situaciones se propuso el término AEH sin déficit de C1INH de causa desconocida (Bork et al., 2009).

Roche y colaboradores estimaron la prevalencia mínima del AEH-C1INH en España en 1,09 individuos por cada 100.000 habitantes (Roche et al., 2005a). El mismo estudio realizado en población noruega estableció una prevalencia de la enfermedad de 1,51 por cada 100.000 habitantes (Stray-Pedersen et al., 2000). Esta baja prevalencia le hace ser considerada como enfermedad rara según la definición de la Unión Europea, que define como "enfermedad rara" aquella que presenta una prevalencia no mayor de 5 cada 10.000 ciudadanos.

En el caso del AEH sin déficit de C1INH no se conoce la prevalencia debido a la ausencia de estudios epidemiológicos.

1.2. Manifestaciones clínicas en AEH por deficiencia del inhibidor de C1.

El AEH-C1INH se manifiesta con episodios recurrentes de edemas localizados en el tejido subcutáneo y/o submucoso. Estos se desencadenan por la liberación de vasodilatadores como la bradicinina que aumentan de forma transitoria la permeabilidad vascular dando lugar a una tumefacción en la zona afectada.

Los edemas cutáneos suelen aparecer principalmente en cara (labios, párpados), extremidades, o genitales. Pero son los edemas en vías respiratorias superiores (laringe, nariz o boca) los de mayor riesgo para los pacientes, ya que pueden resultar letales al provocar la muerte por asfixia (Moore et al., 1988).

El 75% de los pacientes desarrollan los primeros síntomas de la enfermedad durante la primera o segunda década de vida. Pero es en la juventud del afectado donde los episodios se producen con mayor frecuencia (Agostoni and Cicardi, 1992). Aproximadamente uno de cada tres pacientes de AEH padece en el transcurso de su vida por lo menos un episodio en las vías respiratorias superiores y, en uno de cada cuatro pacientes, los edemas se producen predominantemente en la región intestinal, manifestándose en forma de náuseas, vómitos y espasmos gástricos. Las manifestaciones intestinales pueden retrasar el correcto tratamiento y seguimiento durante años debido a un diagnóstico erróneo.

La aparición de los episodios no tiene una clara relación causal. Por esto no se puede predecir en qué lugar del cuerpo se producirá el siguiente episodio. Además, la frecuencia de aparición, duración e intensidad del edema varían de un episodio a otro y entre individuos. Por lo general, los episodios se desarrollan durante las primeras 12 a 36 horas y permanecen de 2 a 5 días, tiempo desde el que desaparecen gradualmente (Gompels et al., 2005, Moore et al., 1988).

La expresión clínica de la enfermedad es muy variable de un paciente a otro, ya que algunos pueden permanecer asintomáticos durante toda la vida (Agostoni and Cicardi, 1992), mientras que otros sufren ataques incapacitantes recurrentes y potencialmente mortales, afectando su calidad de vida (Gower et al., 2011).

1.3. Diagnóstico

- Diagnóstico de laboratorio**.**

El diagnóstico clínico de AEH-C1INH siempre requiere de su confirmación en el laboratorio que se realiza mediante la medición de los niveles de C4 y C1INH séricos, así como la funcionalidad de C1INH.

Cuando un paciente presenta manifestaciones clínicas, el primer parámetro que puede hacer pensar en esta deficiencia son los niveles de C4 disminuidos (Tarzi et al., 2007, Donaldson and Rosen, 1964). Posteriormente, la medición los niveles y funcionalidad de C1INH confirman la sospecha de angioedema por deficiencia de C1INH.

En el 85% de los casos, se observa una disminución cuantitativa de C1INH por debajo del 30% respecto a los valores de referencia (AEH-C1INH tipo I). En el 15% restante de los casos (AEH-C1INH tipo II), los niveles de la proteína en suero son normales o aumentados, pero la funcionalidad de C1INH en plasma se encuentra disminuida por debajo del 50% de los valores de referencia (Wagenaar-Bos et al., 2008).

- Diagnóstico diferencial con otros tipos de angioedemas**.**

Los episodios de AEH se desarrollan por edemas localizados que tienen lugar sin prurito, una de las características diferenciales con la urticaria.

Diferentes grupos de trabajo dirigieron su investigación a la comprensión de la fisiopatología de angioedema por deficiencia del inhibidor del C1 que llevaron a conocer que el daño es mediado por la bradicinina, un nonapetido con función vasodilatadora que se libera durante el proceso de inflamación y favorece la extravasación de fluidos al medio (Cicardi et al., 2014, Agostoni et al., 2004, Cichon et al., 2006).

Se conoce una forma de angioedema adquirido por deficiencia de C1INH (AEA-C1INH) que, a diferencia de la forma heredada, aparece a edades más tardías, entre la quinta y sexta década de la vida, y que se clasifica en dos tipos. En el AEA-C1INH tipo I el aumento del consumo de C1INH está asociado a síndromes linfoproliferativos y enfermedades autoinmunes. En este tipo se ha observado que los episodios de angioedema preceden a los síndromes linfoproliferativos.

En el tipo II (AEA-C1INH), los niveles de proteína son normales o ligeramente elevados pero la presencia de autoanticuerpos frente al C1INH interfieren en la funcionalidad de la proteína.

Otra forma de angioedema es la mediada por inhibidores de la enzima convertidora de angiotensina (AEA-IECA). En este caso, la inhibición de la enzima convertidora de angiotensina disminuye la degradación de la bradicinina aumentando los niveles de bradicinina en el medio que favorece la vasodilatación y desencadena el episodio de angioedema. En la actualidad, el uso de IECA en el tratamiento de la hipertensión arterial, insuficiencia cardiaca y la enfermedad renal crónica supone un aumento de la incidencia de angioedema mediada por estos inhibidores convirtiéndole en la segunda causa más frecuente de hospitalización por enfermedades alérgicas después del asma (Lin et al., 2005).

Ante el amplio espectro de tipos de angioedema se ha hecho necesario generar un algoritmo de diagnóstico que permita proporcionar un tratamiento adecuado a los pacientes. En 2012, el grupo de expertos HAWK (***H****ereditary* ***A****ngioedema International* ***W****or****k****ing Group*) proporcionó recomendaciones para el diagnóstico y, por tanto, el tratamiento de los diferentes tipos de angioedema (Caballero et al., 2012, Cicardi et al., 2012). En la Tabla 1 se recogen los criterios diagnósticos basados en los datos de laboratorio para discriminar adecuadamente una sospecha de angioedema hereditario o adquirido, así, como sus subtipos.

El trabajo que aquí se presenta se centrará en el estudio de los dos tipos de angioedema hereditario por deficiencia del inhibidor de la esterasa C1.

Tabla 1: Perfil de Complemento en los diferentes tipos de angioedemas

Presentación clínica			Niveles C4	Niveles C1INH	CH50 C1INH	Niveles C1q	Gen *F12*
HEREDITARIO	AEH-C1INH	TIPO I	⇓	⇓	⇓	Normal	Normal
		TIPO II	⇓	Normal / ⇑	⇓	Normal	Normal
	AEH-FXII		Normal	Normal	Normal	Normal	Mutación
ADQUIRIDO	AEA-C1INH	TIPO I	⇓	⇓	⇓	⇓	Normal
		TIPO II	⇓	Normal / ⇑	⇓	⇓	Normal
OTROS	AEA-IECA		Normal	Normal	Normal	Normal	Normal

1.4. Profilaxis y tratamiento

El tratamiento en los pacientes con angioedema por deficiencia en C1INH tiene varios objetivos: (1) la prevención a largo plazo de los ataques agudos en aquellos individuos donde la recurrencia es alta, (2) la prevención a corto plazo cuando el paciente tenga que someterse a procedimientos que puedan desencadenar ataques y (3) tratamiento de los ataques agudos.

La función de los diferentes tratamientos es evitar la mortalidad y aliviar o prevenir los síntomas debidos a la progresión del edema de laringe, y reducir la morbilidad, donde ésta es dependiente de la recurrencia y severidad de los ataques.

- Profilaxis a largo plazo

El tratamiento profiláctico se debe establecer en los pacientes con una calidad de vida reducida por presentar episodios muy recurrentes y/o que ponen en peligro la vida del paciente al presentarse edemas en laringe. Así, está indicado este tipo de tratamiento cuando el paciente presente más de un ataque al mes o si se superan los 24 días al año con angioedema (Navarro Ruiz, 2013).

Ante estos supuestos, el tratamiento, fundamentalmente preventivo, consiste en la administración de andrógenos atenuados, como son el Danazol o el Stanazolol. Ambos son derivados sintéticos de la 17α-etiniltestosterona. Aunque no se conoce el mecanismo de acción, se ha observado que reducen el número de ataques (Agostoni et al., 1980b, Fabiani et al., 1990), y aumentan la expresión del ARNm y la síntesis del inhibidor del C1 (Agostoni et al., 1980b, Egidio Fabiani et al., 1987, Fabiani et al., 1989, Fabiani et al., 1990, Gelfand et al., 1976, Pappalardo et al., 2003, Tappeiner et al., 1979, Agostoni and Cicardi, 1992, Sheffer et al., 1987). Existe cierta controversia en su uso como profilaxis a largo plazo debido a los efectos secundarios asociados, pero la alternativa con antifibrinolíticos parece tener menos eficacia. Así, los andrógenos atenuados han sido el tratamiento elegido durante años para la mayoría de los pacientes en edad adulta.

Los antifibrinolíticos (ácido tranexámico o ácido ε-aminocaproico) son la profilaxis elegida principalmente en niños por ser el sector de la población con mayor riesgo a los efectos secundarios de los andrógenos atenuados. Se cree que su beneficio se debe a la actividad antiplasmina Esta actividad ejerce un efecto neutralizador del sistema de la fibrinólisis bloqueando la actividad proteolítica de los activadores del plasminógeno, el cual participa en la disolución de coágulos sanguíneos. El aumento del

riesgo de trombosis en la administración de antifibrinolíticos implica la suspensión del tratamiento antes de intervenciones quirúrgicas en estos pacientes.

- Profilaxis a corto plazo

Está indicado cuando el paciente deba someterse a cualquier procedimiento traumático, incluidos los procedimientos odontológicos. Se suelen utilizar principalmente andrógenos atenuados (Farkas et al., 1999) y, en algunos casos, se administra un concentrado de inhibidor del C1 (Langton et al., 1994) o antifibrinolíticos (Sheffer et al., 1977). Además, para evitar el traumatismo, consecuencia de la intubación orofaríngea, se recomienda el uso de anestesias locales (Wall et al., 1989).

- Tratamiento de los ataques agudos

El tratamiento de elección en las crisis agudas es la administración de un concentrado de C1INH obtenido de plasma humano. Con este concentrado los episodios disminuyen entre 30 y 60 minutos después de la infusión intravenosa, alcanzando niveles máximos de C1INH a los 15 minutos y de C4 a las 12 horas (Agostoni et al., 1980a, Bork and Barnstedt, 2001). La dosis recomendada oscila entre 1000 y 2000 U intravenosas y su acción puede durar 4-5 días.

En España se dispone de Berinert® (Behring, Marburg, Alemania), inhibidor del C1 derivado de plasma humano y que, por tanto, suministra el inhibidor de la esterasa.

Sólo en lugares donde no se dispone del derivado de plasma se recurre a la perfusión de plasma fresco, aunque su uso supone un aporte de C2 y C4 que pueden generar un agravamiento del episodio, además de ser fuente de posibles infecciones virales.

En 2008, la Agencia Europea de Medicamentos aprobó la administración de Icatibant, antagonista de los receptores de la bradicinina de tipo 2 (B2R) para el tratamiento sintomático de los ataques agudos de angioedema (Caballero et al., 2012). Los estudios presentados por Mauer en 2013 indican que la administración temprana de Icatibant en episodios de angioedema pueden reducir significativamente la duración y el tiempo de estos (Caballero et al., 2012, Maurer et al., 2013).

El mayor riesgo de los pacientes de AEH-C1INH son los episodios agudos en las vías respiratorias superiores, ya que suponen una amenaza a la vida por el riesgo de asfixia. Episodios en otras localizaciones como los edemas agudos abdominales llevan al paciente a una situación incapacitante. Ante estos supuestos la administración de un tratamiento de choque debe ser inmediata.

1.5. Fisiopatología del angioedema hereditario por deficiencia del inhibidor de C1.

En los pacientes de AEH-C1INH los episodios de angioedema se desencadenan al no poder regular la activación de cascadas enzimáticas como el sistema del complemento, contacto (cininas), coagulación y fibrinolisis. La activación de estos sistemas desencadena, en último término, la liberación de péptidos vasodilatadores como la bradicinina.

A nivel del sistema de coagulación el C1INH regula la activación del factor XI (FXI) y el factor XII (FXII). Cuando el C1INH no puede ejercer su función, el FXII activado (FXIIa) induce la activación de calicreína desde precalicreína que se encuentra mayoritariamente unida a cininógenos de alto peso molecular (HMWK) en la superficie endotelial. La calicreína está activada es capaz de escindir el HMWK. Esta escisión da lugar a la liberación de bradicinina, un nanopéptido que actúa como potente vasodilatador con propiedades permeabilizantes en los vasos sanguíneos (Colman, 1999, Colman et al., 1999, Bhoola et al., 1992).

En humanos se conocen dos tipos de receptores endoteliales para bradicinina. Los receptores B1 (B1R) reconocen predominantemente el producto de degradación parcial des-Arg^{9}-bradicinina. Su expresión es inducible por daño tisular y presentan niveles máximos de expresión en endotelio 6 horas después del estímulo y permanece elevada durante 2 días. Por su parte, los receptores de bradicinina tipo 2 (B2R) se expresan de forma constitutiva a bajos niveles en la mayoría de células y tejidos y son estos los activados por bradicinina intacta (Trabold et al., 2010).

Así, la activación de los receptores B2R como consecuencia de la unión de bradicinina, aumenta la permeabilidad vascular y favorece la liberación de óxido nítrico y prostaglandina E que aumentan la vasodilatación (Han et al., 2002, Schmaier, 2008, Zhao et al., 2001).

Por otro lado, la activación de la calicreína por el sistema de contacto tiene diversos efectos sobre otros sistemas proteolíticos. La calicreína media la degradación de plasminógeno a plasmina, iniciando de este modo la cascada de la fibrinólisis. La actividad proteolítica de la plasmina, que es igualmente regulada por C1INH, puede activar recíprocamente a la calicreína, así como a los componentes C1 y C3 de la vía clásica del complemento, iniciando complejos bucles de retroalimentación entre las diferentes cascadas de proteasas del suero.

Cuando los niveles de C1INH están disminuidos, el aumento de la plasmina actúa como retroalimentación positiva de la síntesis de calicreína (Bergamaschini et al., 1999, Egidio Fabiani et al., 1987, Cugno et al., 1996, Davis, 2005). A nivel del sistema del complemento, la insuficiente síntesis de C1INH funcional supone un aumento del catabolismo de C2 y C4.

Las cascadas enzimáticas sobre la que actúa el C1INH se activan ante cualquier situación traumática, estrés, u otras enfermedades, pero también pueden activarse sin factores desencadenantes (Donaldson and Rosen, 1964, Donaldson and Rosen, 1966). Ante la ausencia de una regulación adecuada por parte de C1INH, la liberación de bradicinina desencadenará un episodio de angioedema. La Figura 1 muestra un esquema de los puntos de control del inhibidor del C1 en cada una de las casadas.

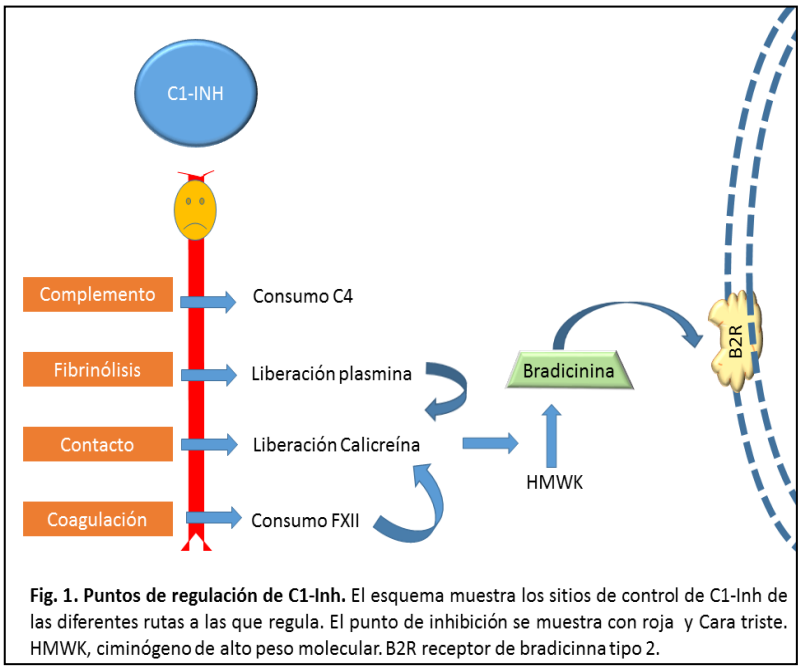

Fig. 1. Puntos de regulación de C1-Inh. El esquema muestra los sitios de control de C1-Inh de las diferentes rutas a las que regula. El punto de inhibición se muestra con roja y Cara triste. HMWK, ciminógeno de alto peso molecular. B2R receptor de bradicinna tipo 2.

1.6. Base molecular del AEH

En los pacientes con angioedema hereditario, la presencia de una mutación en uno de los alelos del gen *SERPING1* es suficiente para que se produzca la desregulación de la homeostasis vascular y de todos los sistemas sobre los que actúa el C1INH.

En el AEH-C1INH tipo I, el 85% de los casos, la presencia de una mutación en uno de los alelos supone una deficiencia cuantitativa C1INH. Esta mutación puede encontrarse a lo largo de todo el gen. Se han descrito tanto puntuales como grandes deleciones y duplicaciones. La consecuencia final es la disminución de la síntesis de proteína.

En el 15% restante de casos (AEH-C1INH tipo II) aunque presentan niveles de proteína normales o elevados, su deficiencia se debe a la no funcionalidad de la proteína (Agostoni et al., 2004). En este grupo, la mutación se localiza en los nucleótidos que codifican los aminoácidos localizados en el centro activo (Arg444 y Thr445), o bien aminoácidos en las proximidades del mismo.

Una mutación en heterocigosis con un modelo de herencia dominante produce un 50% de la proteína nativa. Se considera dominancia negativa cuando el alelo mutado interfiere en la producción del alelo normal de manera que no se alcance el 50% de proteína nativa. Los pacientes con AEH presentan entre un 5% y un 30% de C1INH funcional. Cuando Kramer analizó en un paciente con angioedema hereditario por deficiencia de C1INH el efecto que causaba una mutación que producía un mensajero de *SERPING1* que no incluía exón 7 observó que la tasa de síntesis apenas alcanzaba un 30% (Kramer et al., 1993). Él utilizó el término transinhibición para catalogar el efecto de la dominancia negativa del alelo mutado sobre el alelo sano en AEH-C1INH.

Aunque se han descrito más de 200 mutaciones en *SERPING1* asociadas a angioedema hereditario por deficiencia del inhibidor de C1, hasta el momento sólo se han descrito cinco familias con individuos que portaban la misma mutación en ambos alelos. Tres con mutación en la región codificante del gen de *SERPING1* (Bafunno et al., 2013, Blanch et al., 2006, López-Lera et al., 2010), y dos familias con cambios en homocigosis en la región promotora (-103C>T y -101A>G) (Verpy et al., 1996, Büyüköztürk et al., 2009).

En nuestro laboratorio se han descrito los tres primeros casos de individuos con mutaciones en homocigosis en la región codificante. Dos individuos de una misma familia presentaban la mutación p.Ile440Ser (Blanch et al., 2006), y cuatro años más tarde, en otra familia, un individuo presentaba el cambio p.Arg378Cys (López-Lera et al., 2010). En 2013, Bafunno y colaboradores describieron un individuo con perfil de complemento acorde a un AEH-C1INH tipo I que portaba la mutación p.Lys216Serfs*4 en homocigosis.

En las cinco familias descritas, los individuos homocigotos mostraron un perfil de complemento acorde a AEH-C1INH tipo I. En el caso de los familiares heterocigotos, estos cursaron un perfil de complemento tipo II (Blanch et al., 2006, López-Lera et al., 2010) y sin clínica. La baja incidencia de homocigotos en la enfermedad parecía sugerir un efecto letal en estado embrionario en la mayoría de los

eventos, y sólo podrían ser viable las mutaciones en homocigosis asociadas a fenotipos leves (Blanch et al., 2006).

No se conoce el mecanismo por el que la presencia de un alelo mutado suponga niveles inferiores al 50%. Nuestro grupo ha estudiado la implicación de la isla CpG presente en el promotor (5.740 pares de bases del exón 1) y la isla CpG de 345 pares de bases localizadas en el exón 2 como posible efecto epigenético en el gen *SERPING1*, pero no se han obtenido resultados vinculantes con la dominancia negativa (López-Lera et al., 2014).

2. INHIBIDOR DE C1

2.1. Introducción y estructura de la proteína

C1INH es una proteína sérica de cadena polipeptídica única altamente glicosilada. La proteína inmadura presenta un péptido señal (22 aminoácidos) que marcará su transporte a membrana que debe ser eliminado para la liberación de la proteína al medio y para su activación (Gaboriaud et al., 2004, Sim and Tsiftsoglou, 2004). La proteína madura contiene 478 aminoácidos que se pueden dividir en dos dominios (Carter et al., 1991):

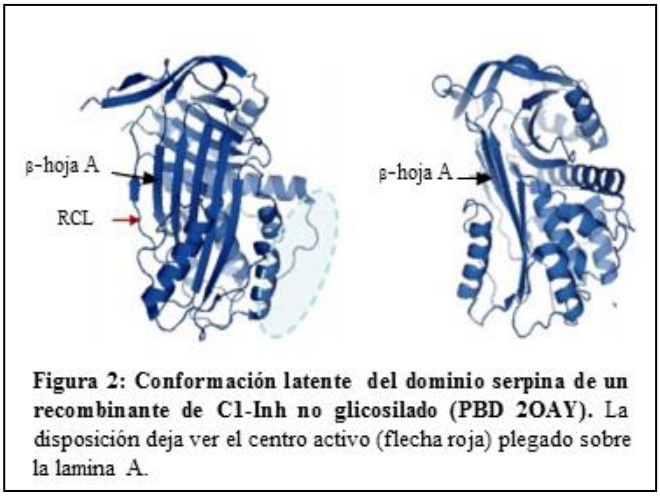

Figura 2: Conformación latente del dominio serpina de un recombinante de C1-Inh no glicosilado (PBD 2OAY). La disposición deja ver el centro activo (flecha roja) plegado sobre la lamina A.

- *Dominio NO Serpina*. Localizado en la región N-terminal. Formado por 100 aminoácidos, contiene la mayoría de N- y O-glicosilaciones. Esta región no presenta homología con otras proteínas de la familia.
- *Domino Serpina*. Localizado en la región C-terminal. Contiene 378 aminoácidos y presenta homología con otras serpinas (**Ser**ina **p**roteasas **in**hibidoras) como α1-antitripsina y antitrombina III. Ver Figura 2

Ambos dominios se encuentran estabilizados por dos enlaces disulfuro entre ambos dominios (Simonovic and Patston, 2000). El centro reactivo se encuentra en el dominio Serpina, al igual que el resto de la familia a la que pertenece. En el caso de C1INH el centro reactivo se localiza en el enlace peptídico entre el residuo 444Arg (P1) y el 445Thr (P1´) localizados en el exón 8 del gen.

2.2. Biosíntesis del inhibidor de C1.

Estudios de inmunofluorescencia indican que los hepatocitos del parénquima son el mayor productor de C1INH *in vivo* (Johnson et al., 1971). Otros tipos celulares como monocitos de sangre periférica (Randazzo et al., 1985), células de la microglía (Walker et al., 1995), fibroblastos (Katz and Strunk, 1989), células endoteliales (Lappin et al., 1992, Schmaier et al., 1989) y plaquetas también son capaces de sintetizar y secretar C1INH tanto *in vivo* como *in vitro* (Prada et al., 1998, Heda et al., 1990, Schmaier et al., 1993).

En 1987, Lotz observó un aumento de la producción de C1INH cuando estimulaba monocitos en cultivo con IFN-γ (Lotz and Zuraw, 1987). Diferentes estudios *in vitro* han observado un aumento de la expresión del ARN mensajero de *SERPING1* bajo un estimulo con interferón gamma en monocitos cultivados varios días (Heda et al., 1990, Lappin et al., 1992, Lotz and Zuraw, 1987, Prada et al., 1998, Zahedi et al., 1994). Esto es debido a que el promotor de la serpina presenta elementos de respuesta a la citoquina entre los que se incluyen los de respuesta a estímulo por interferón gamma (ISREs) y secuencias de unión a factores de transcripción dependiente de interferón gamma (GAS, Interferon-**G**amma **A**ctivateed **S**equence). Estos elementos regulan la producción basal de *SERPING1* y la respuesta en fase aguda de inflamación.

El promotor contiene un potencial elemento de respuesta a andrógenos y parece mediar en la síntesis del inhibidor de la esterasa de C1 en distintos tipos celulares como monocitos y hepatocitos (Falus et al., 1990a, Falus et al., 1990b, Falus, 1990, Pappalardo et al., 2003, Tappeiner et al., 1979).

2.3. Serpinas, la familia del inhibidor de C1

- Estructura de las serpinas, conformación y mecanismo inhibitorio

Las serpinas (inhibidores de serín proteasas) son la superfamilia más amplia de inhibidores de proteasas (Irving et al., 2000). En todos los grupos de organismos (virus, arqueas, bacterias y eucariotas) se han localizado genes de esta familia (Silverman et al., 2001). Pese a la diversidad de procesos en los que se encuentran implicadas, mantienen una estructura terciaria muy conservada, aunque puedan sufrir modificaciones post-traduccionales como la glicosilación.

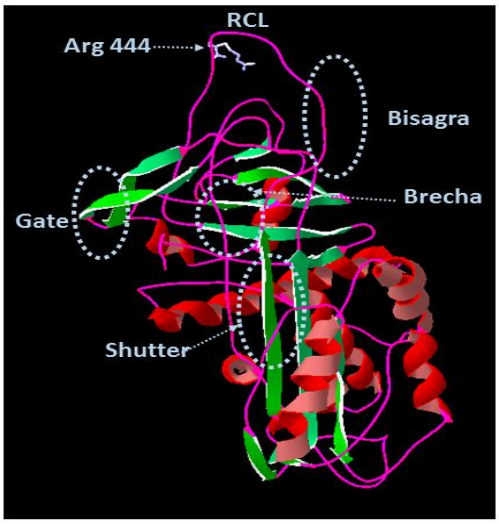

Figura 3. Estructura nativa de C1-Inh. En la conformación nativa de C1-Inh (pdb1m6q, Protein Data Bank (PBD)) se observan las regiones móviles del domino serpina (marcadas en azul) y el centro activo (RCL). Se ha indicado en azul el residuo P1 (Arg 444).

A nivel estructural, tal y como se muestra en la Figura 3, todas presentan tres láminas β (nombradas de la A a la C) y, entre siete y nueve hélices-α, siendo nueve el número predominante (nombradas de la A a la I). Además, presentan un lazo móvil formado por una región expuesta y flexible en forma de bucle constituido por aproximadamente veinte aminoácidos desde el aminoácido P17 en dirección N-terminal y hasta el P3´ del extremo C-terminal (según nomenclatura de Schechter and Berger) (Abramowitz et al., 1967).

El bucle (RCL, *Reactive Centre Loop*) se localiza entre las láminas A y C y contiene el centro reactivo en los residuos P1 (Arg444) y P1´ (Thr445) que actúan como pseudosubstrato de la proteasa diana, ver Figura 3.

Adyacente al RCL se localiza la región denominada *bisagra* (residuos P15-P9) que permite el desplazamiento del centro activo hacia la lámina A tras la escisión del enlace peptídico P1-P1´ que une los aminoácidos del centro activo. En la lámina A se localizan las regiones *shutter* y *brecha*, que sufren un desplazamiento para permitir la inserción del RCL en la lámina A. La región *gate* está localizada entre las hojas 3C y 4C. Estas dos láminas sufren un giro β para conectar las láminas C y A (Stein and Carrell, 1995) (Fig.3). Para que el RCL pueda ser determinante de la especificidad y forma de interacción con la proteína diana debe estar expuesto tal y como se muestra en la Figura 3. Esta conformación nativa es conocida como metaestable y es la requerida para su actividad inhibitoria (Stein and Carrell, 1995) (Fig.4 A).

Las serpinas pueden sufrir cambios estructurales transitorios que conllevan el movimiento del bucle del centro activo hacia la lamina A y formen una hoja antiparalela. Estos cambios estructurales se producen sin escisión del centro activo, por tanto, son reversibles. Así, la serpina tendrá conformación latente (Fig. 4B). En esta conformación, la serpina no tiene función inhibitoria. Estas dos conformaciones son alternantes en las serpinas y el paso de una a otra puede darse por reestructuración o por desnaturalización. Se ha descrito que la temperatura necesaria para que PAI1 cambie de

la forma latente a la forma nativa y, por tanto inhibitoria, son 17 ºC (Silverman et al., 2001).

La forma más estable de las serpinas inhibitorias es la forma escindida donde el centro activo escindido y el RCL se insertan en la lámina A sin necesidad de extraer la hoja 1C (Fig. 4C). Se estima que la temperatura necesaria para deshacer esta conformación es >120 ºC (Kaslik et al., 1997). Así, el mecanismo de acción de las serpinas está basado en las tres conformaciones. Cuando la serpina inhibitoria se encuentra en conformación nativa, el centro activo puede unir a la proteasa diana formando un complejo Michaelis (Fig. 4D) (Ye et al., 2001). Si este no se revierte, la serpina sufre un cambio conformacional hacia la forma latente donde, seguidamente, se produce la acción inhibitoria al escindirse el bucle que contiene centro activo. Ahora la serpina presenta conformación escindida y se convierte en la verdadera trampa para la proteasa diana al ser esta unión irreversible (Fig. 4E). Esta característica les lleva a ser considerados inhibidores suicidas porque cada proteína inhibidora sólo puede ejercer su función una vez sobre sus proteasas dianas quedando en estado latente y, por tanto, inactivo una vez producida la interacción.

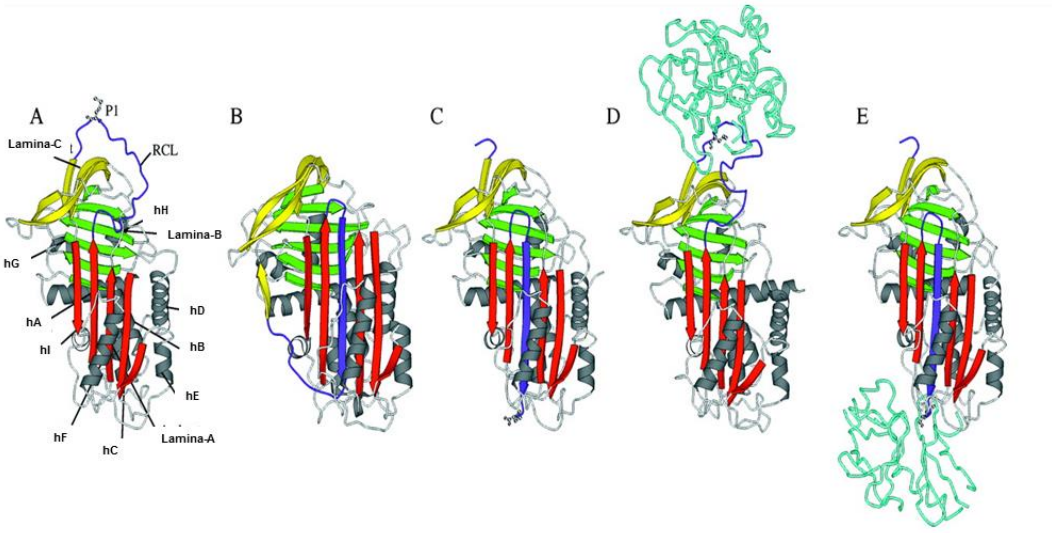

Figura 4: Conformaciones de las serpinas. A) conformación nativa de α1AT donde se observa el centro activo expuesto, B) conformación latente de ATIII. C) α1AT en conformación escindida en el centro activo; D) Formación del complejo Michaelis entre Serpin 1 y tripsina. E) Complejo covalente entre la α1-AT y la tripsina con la tripsina distorsionada en el polo opuesto de la serpina. Lamina A se muestra en rojo, la lamina B en verde y la lamina C en amarillo. La hélices se marcan en gris. El bucle que contiene el centro activo se representa en morado. En cian se muestra la molécula de tripsina.

2.4. Función del inhibidor de C1.

El C1INH está implicado en la regulación de la activación del sistema del complemento, de la coagulación, de la fibrinólisis y de síntesis de las cininas. En la Figura 5 se muestra la interacción entre las cascadas y los puntos de actuación del C1INH.

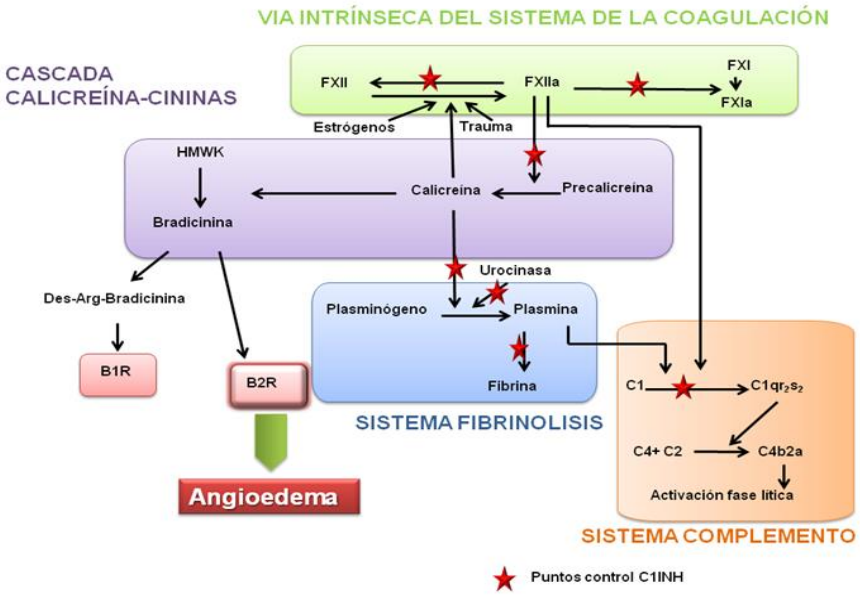

Fig 5: Fisiopatología del angioedema y puntos de control del C1INH. HMWK: cininógeno de elevado peso molecular; B1R: receptor B1 de bradicinina; B2R: receptor B2 de bradicinina; C1: componente 1q del complemento; C1qrs: componente 1 del complemento activo; C1INH: inhibidor de la esterasa C1; C2: componente 2 del complemento; C4: componente 4 del complemento; C4b2a: convertasa C3; FXI: factor XI de la coagulación; FXIa: factor XI de la coagulación activado; FXII: factor XII de la coagulación; FXIIa: factor XI de la coagulación activado.

- Regulación del sistema del complemento

El C1INH está considerado uno de los principales reguladores del sistema del complemento. A nivel de la vía clásica, es el único punto de control de la activación del primer componente (C1) por medio de una unión covalente con C1s y C1r (C1INH-C1r-C1s-C1INH) (Laurell et al., 1990). En la vía de las lectinas, inactiva a las serín proteasas asociadas a MBL (MASP1 y MASP 2) (Gaboriaud et al., 2004, Sim and Tsiftsoglou, 2004). Tanto el complejo C1 como MASP2 escinden C2 y C4 dando lugar a la convertasa C3. A nivel de la vía alternativa, C1INH, se une a C3b impidiendo la unión del factor B (Sim and Tsiftsoglou, 2004).

- Regulación del sistema de la coagulación

La activación del Factor XI (FXI) por el Factor XII (FXII) a través de la vía intrínseca se ve reforzada por la acción de la trombina. Está ultima es liberada por el factor tisular de las células subendoteliales (vía extrínseca) y así se desencadena la fase de amplificación y posteriormente la de propagación, donde la liberación de fibrina estabilizará la formación del coágulo. En condiciones normales, C1INH es el único regulador de la vía intrínseca impidiendo la activación tanto de FXI como de FXII , mientras que por vía extrínseca existen otros inhibidores (Caliezi et al., 2000, Ziccardi, 1981).

- Regulación del sistema de la fibrinólisis

En la región de daño tisular, la plasmina es la encargada de la degradación de las redes de fibrina y, por tanto, de la desestabilización del coágulo. La formación de plasmina se produce a partir del plasminógeno (por la vía intrínseca). Esta activación es potenciada por la presencia de FXIIa y la activación de la calicreína. C1INH actúa inhibiendo la formación del plasminógeno acomplejándose con la calicreína libre.

- Regulación del sistema de cininas

La activación de los factores de coagulación FXI y FXII se produce *in vivo* ante un traumatismo. *In vitro,* suele asociarse a la presencia de superficies con carga negativa. Al final de la cascada, la fibrina será la encargada de dar forma a los coágulos blandos. El FXIIa es capaz de inducir la activación calicreína a partir de precalicreína. C1INH mantiene los niveles tisulares de FXIa y FXIIa, a la vez que regula la activación de calicreína por FXIIa (Davis, 2005). La calicreína es una proteasa que libera bradicinina a partir de cininógeno de alto peso molecular. La bradicinina es un potente vasodilatador dependiente del endotelio, que causa la contracción del músculo liso no vascular y aumenta la permeabilidad vascular permitiendo la extravasación de líquidos al intersticio por la unión de la bradicinina a los receptores tipo 2.

3. GEN DE *C1INH/SERPING1*

3.1. Estructura y localización del gen

El gen *SERPING1* (MIM*606860; GenBank NG_009625.1; ID 710) con localización cromosómica 11q12.1, está constituido por 17,3 Kb y codifica el inhibidor del primer componente del complemento C1 (C1INH). La transcripción de *SERPING1*

genera dos variantes de ARN mensajero: la más larga de 1.966 pb (NM_000062.2) con 8 exones y 7 intrones, y otra más corta de 1.814 pb (NM_001032295.1), a la que le falta el exón 1 y utiliza un sitio alternativo de *splicing* (procesamiento) en la región 5´UTR comparada con la primera variante. En adelante las posiciones de los elementos que contiene el gen se refieren al ATG de inicio en la secuencia de referencia NM_000062.2.

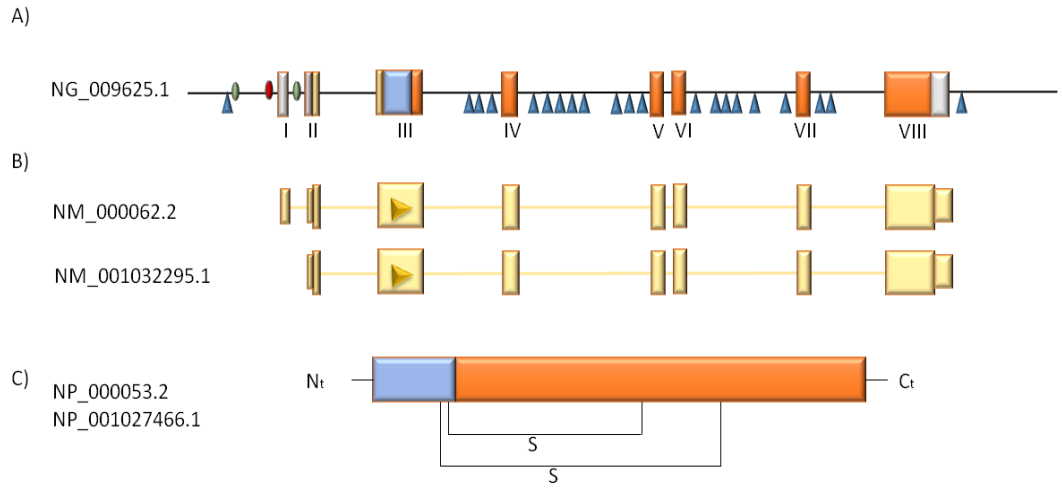

Figura 6: Representación del gen de *SERPING1*. A) Distribución de los exones a lo largo de la secuencia. Las secuencias *Alu* se representan con triángulos azules. Los círculos verdes indican regiones reguladora dependientes de IFN-γ. Los elementos *Cajas CAAT* se indican con un círculo rojo. Las cajas grises indican las regiones 5´y 3´ no codificantes. Las cajas amarillas indican la localización del péptido señal. Las cajas de color azul indican el dominio no-Serpina y el color naranja indica el dominio Serpina. **B)** Variantes de ARN mensajero que codifican proteína. **C)** Representación de los puentes disulfuro entre los dos dominios de la proteína. Nt y Ct corresponden a los extremos NH_2 y COOH de la proteína, respectivamente.

El gen presenta alta densidad de *clusters* de secuencias *Alu* en diferentes orientaciones. Carter, en 1991, describió hasta 19 *clusters* donde diecisiete están distribuidos a lo largo de cuatro intrones y dos en las regiones 5´UTR y 3´UTR del gen. Mediante la aplicación web RepeatMasker (Tempel, 2012) se han rastreado las secuencias *Alu* en la variante de mensajero más larga (NM_000062.2) y 1.120 nucleótidos de las regiones intragénicas adyacentes al gen. El análisis indica la presencia de dos secuencias *Alu* no descritas por Carter. La primera se localiza en el intrón cuatro, y la segunda en el intrón siete (Figura 6A). Las secuencias *Alu* ,elementos móviles, son las secuencias cortas y repetitivas más frecuentes en el genoma humano (Jelinek and Schmid, 1982, Stoppa-Lyonnet et al., 1990). Forman parte del genoma no codificante, por lo que es factible encontrarlo en intrones, tal y como sucede en el gen

del C1INH. Estas estructuras de trasposones confieren al gen elevada frecuencia de reordenamientos (Ariga et al., 1990, Carter et al., 1991, Stoppa-Lyonnet et al., 1990), de ahí que el 12% de las alteraciones moleculares del gen sean grandes deleciones o inserciones (dato extraído de la base de datos de mutaciones HGMD *Public*) (Stenson et al., 2003).

El promotor del gen del inhibidor de C1 no presenta elemento regulador caja TATA. Los genes sin este elemento regulador presentan una serie de elementos iniciadores (Weis and Reinberg, 1992). Este tipo de genes comparten dos características, por un lado, prácticamente se consideran genes constitutivos, y, por otro, la mayor parte poseen un único sitio de inicio de la transcripción. En *SERPING1* el elemento iniciador (CTCAGTCT) se localiza entre las posiciones -3 y +5 respecto al codón de inicio.

La región dónde se esperaría que estuviera localizado el elemento regulador TATA (posición -48 al -17) presenta una región rica en pirimidinas que da lugar a una estructura ADN-H (-48 del -3) (Carter et al., 1991, Zahedi et al., 1994). Esta estructura de triple hélice es similar a la encontrada en el gen *c-myc* y tiene capacidad de unión con ribonucleótidos y factores de transcripción que podrían actuar como reguladores de la transcripción (Davis et al., 1989). Otros elementos reguladores corriente arriba del inicio de la transcripción del gen de C1INH son dos caja CAAT en posición -103 al -100 y -61 al 58. Círculo rojo en Figura 6A.

Desde la posición -83 a la posición -77 se encuentra la secuencia CTGGGCA que es similar a un elemento de respuesta a IL-6, una citoquina con múltiples funciones biológicas, incluida la inducción de respuesta en fase aguda (Hattori et al., 1990) donde el inhibidor de C1 juega un papel importante (Morgan and Gasque, 1997).

La expresión de *SERPING1*, *in vitro*, es fuertemente inducida por INF-γ (Hamilton et al., 1987, Heda et al., 1990, Lotz and Zuraw, 1987, Prada et al., 1998, Zahedi et al., 1994). Esta potente inducción se debe a que el gen presenta dos regiones intensificadoras de la transcripción dependientes de proteínas de unión a ADN inducibles por interferón gamma (Zahedi et al., 1994). La primera se localiza entre las posiciones -582 y -252, mientras que la segunda está en el primer intrón (+373, +410). Círculos verdes en la Figura 6A.

De los ocho exones, no todos son codificantes. En la variante de mensajero más larga (NM_000062.2) el primer exón contiene el codón de iniciación para la transcripción de eucariotas (Bucher and Trifonov, 1986). El segundo exón contiene el

codón de inicio de la traducción (ATG), a partir del cual se traducen los primeros 17 aminoácidos del péptido señal (22 aminoácidos). El péptido señal se extiende hasta el exón 3 a partir del cual se codifica para la proteína. La Figura 6A ilustra la disposición de los elementos reguladores y las secuencias *Alu*. En la Figura 6B se indica las regiones de las dos variantes ARN mensajero recogidas en GenBank con los extremos UTR representados con recuadros más estrechos.

La base de datos Human Gene Mutation Database en su versión pública (HGMD Public, http://www.hgmd.cf.ac.uk/ac/index.php)(Stenson et al., 2003) ha recogido, hasta el momento 389 alteraciones en el gen *SERPING1* (NM_000062.2) (dato obtenido en Junio de 2016). *SERPING1* presenta una elevada tasa de mutaciones *de novo,* en torno al 20%, y se distribuyen a lo largo de todo el gen.

3.2. Regulación transcripcional de *SERPING1* dependiente de tejido.

Las células hepáticas son las mayores productoras de C1INH circulante, aunque otros tipos celulares, como plaquetas, fibroblastos, etc. también poseen la capacidad de secretar C1INH (Lappin et al., 1992, Schmaier et al., 1989, Schmaier et al., 1993, Zahedi et al., 1994).

Entre los tipos celulares de menor aporte se encuentran los monocitos (Lappin et al., 1992, Hamilton et al., 1987, Randazzo et al., 1985). Mucho se ha descrito del papel del C1INH en la regulación de la homeostasis celular y que los niveles de C1INH a nivel localizado son debidos a la secreción del mismo por macrófagos. Pero para que se produzca la activación de monocitos a macrófagos es necesario un entorno inflamatorio. Los estudios publicados se centran en la expresión de *SERPING1* y la producción de proteína en macrófagos. No se han realizado estudios de expresión de *SERPING1* en población monocítica antes de su diferenciación a macrófagos en entorno inflamatorio.

Duponchel, en 2006, realizó un estudio semicuantitativo de la expresión del ARNm de *SERPING1* en monocitos de un paciente que portaba la mutación c.51+3A>G. El cambio detectado en el paciente se localizaba en el segundo intrón del gen, en la secuencia de reconocimiento del sitio 5´del proceso de corte y empalme de intrones (en adelante *splicing).* Los estudios funcionales con RT-PCR en monocitos del paciente revelaron una forma alternativa de mensajero con ausencia de exón 2 y exón 3. Además, en monocitos de controles sanos, el mismo análisis mostró una variante alternativa con ausencia de exón 3. Al no detectar esta variante alternativa en líneas

celulares de hepatomas, Duponchel concluye que su expresión debe ser dependiente de tejido.

La base de datos *NCBI* sólo recoge dos variantes de *splicing* del gen *SERPING1* indicadas en el apartado 3.1. Sin embargo, en el navegador genómico de *Ensembl* (*http://www.ensembl.org*) se mencionan hasta 12 variantes, de las cuales sólo 7 producirían proteína. De ellas, el navegador contempla una posible variante alternativa sin exón 3 (*ENST00000531133*). Según esta aplicación, la variante sin exón 3 presenta un truncamiento del péptido señal dejando sólo 17 aminoácidos de los 22 existentes en la variante con los ocho exones (variante completa).

Por otro lado, la eliminación del exón 3 produce un cambio de la pauta de lectura durante la traducción que da lugar a una proteína truncada con sólo 43 aminoácidos, siempre que esta variante presentase el inicio de traducción en el mismo ATG que en la variante más larga.

Tanto Duponchel, como la aplicación en línea *Ensembl* proponen la acción del mecanismo de NMD (***N****onsense* ***m****ediated* ***d****ecay*) sobre esta variante para evitar que la proteína truncada sea expresada. Estas sospechas deberían demostrarse mediante western blot con anticuerpos contra la parte COOH final de C1INH.

Siguiendo la línea del hallazgo de Duponchel, en el presente trabajo se realizó un estudio de la expresión de la variante con exón 3 (variante completa) y la variante sin exón 3 (variante corta) en PBMCs (*Peripheral Blood Mononuclear Cells*) de distintos pacientes con angioedema hereditario. Conocer el patrón de expresión de la variante corta en pacientes de angioedema hereditario podría explicar su implicación a nivel local.

Los estudios de inducción de la expresión del ARN mensajero de *SERPING1* en monocitos publicados (Prada et al., 1998) no contemplan la existencia de esta variante alternativa sin exón 3, por lo que se asumieron los niveles de expresión obtenidos, tanto a nivel basal, como bajo estímulo, como procedentes de una sola forma de mensajero, la completa. Es posible que la expresión de esta serpina esté regulada por el ambiente y que otros tipos celulares cobren protagonismo en la regulación de la homeostasis vascular a nivel localizado sin restar importancia al aporte de las células hepáticas sobre los niveles del C1INH circulante.

En este trabajo, se pretendía investigar el patrón de expresión de dos variantes de *splicing* en población monocítica de individuos sanos en presencia o ausencia de estimulación con IFN-γ.

Objetivos

Objetivo I:

Estudio de la repercusión de mutaciones puntuales en la expresión del ARN mensajero del inhibidor de C1 en pacientes con angioedema hereditario.

Objetivo II:

Análisis de la expresión de dos variantes de ARN mensajero (completa y con ausencia de exón 3), producto del *splicing* alternativo en *SERPING1,* en células mononucleadas de sangre periférica de pacientes con angioedema hereditario.

Objetivo III:

Estudio de los niveles de expresión de las variantes de ARN mensajero del inhibidor de C1 en población monocítica de individuos sanos en respuesta a inflamación (respuesta a interferón-γ).

Materiales y Métodos

4. ANÁLISIS DE LA EXPRESIÓN DE *SERPING1* EN PBMCs DE PACIENTES AEH-C1INH

4.1. Criterios de inclusión y exclusión

En el estudio de la expresión del ARN mensajero de *SERPING1* se incluyeron pacientes diagnosticados previamente de angioedema hereditario tipo I y tipo II debido a mutaciones puntuales en heterocigosis. Los pacientes incluidos podían estar en tratamiento profiláctico con andrógenos atenuados en el momento de la extracción de la muestra.

Se recogieron muestras de 24 individuos sanos que también fueron caracterizados bioquímica y molecularmente para descartar angioedema hereditario por deficiencia de C1INH. Estos individuos constituyeron el grupo control.

4.1.1. Población estudiada

- Análisis de expresión del ARN mensajero de *SERPING1*

El grupo de pacientes seleccionados para cuantificar niveles de expresión de C1INH total estaba constituido por 30 individuos. 22 pacientes estaban diagnosticados de AEH-C1INH tipo I (9 de ellos se encontraban bajo profilaxis a largo plazo con andrógenos atenuados en el momento de la inclusión en el estudio (ver Tabla 2). De los 8 pacientes con AEH-C1INH tipo II, 3 estaban siendo tratados con andrógenos atenuados y/o antifibrinolíticos como profilaxis a largo plazo (ver Tabla 2). Estas cuantificaciones fueron comparadas con los niveles de expresión del grupo control.

Tabla 2: Distribución de pacientes con AEH-C1INH incluidos en la cohorte del estudio de la expresión del ARN mensajero de *SERPING1*

Pacientes	TIPO AEH	TTO	CAMBIO	Nº (tto./no tto.)	controles
30	Tipo I 22	9 tto / 13 no tto	Parada prematura	4 (2/2)	**24**
			Cambio de aminoácido	8 (3/5)	
			Splicing	8 (3/5)	
			Cambio de pauta lectura	2 (1/1)	
	Tipo II 8	3 tto / 5 no tto	Cambio de aminoácido	8 (3/5)	

Tto: tratamiento. En la columna *Nº (tto/no tto)* se indica el número total de pacientes por cada tipo de mutación y, entre paréntesis se indican los pacientes con tratamiento (tto), seguido de los pacientes sin tratamiento (no tto)

- Análisis de expresión del *splicing* alternativo del exón 3 de *SERPING1*

El análisis de la expresión de la variante sin exón 3 (en adelante variante corta) y la variante con exón 3 (en adelante, variante completa) del gen *SERPING1* se realizó en 32 pacientes con AEH-C1INH.

Aproximadamente, un tercio eran pacientes que presentaban AEH-C1INH tipo II. De ellos, 3 estaban en tratamiento en el momento de la extracción de la muestra (ver Tabla 3).

De los 22 pacientes incluidos en la cohorte con AEH-C1INH tipo I, la mitad se encontraban en profilaxis a largo plazo con andrógenos atenuados en el momento de la extracción de la muestra (Tabla 3). Como grupo control se seleccionaron 25 donantes sanos.

Tabla 3: Distribución de pacientes con AEH incluidos en la cohorte del estudio de la expresión de variantes de *SERPING1*.

Pacientes	TIPO AEH	TTO	CAMBIO	Nº CASOS (tto/ no tto)	Controles
32	Tipo I	11 tto / 11 no tto	Parada prematura	4 (2/2)	**25**
			Cambio de aminoácido	7 (3/4)	
			Splicing	6 (4/2)	
			Cambio de pauta lectura	5 (2/3)	
	tipo II	4 tto / 6 no tto	Cambio de aminoácido	10 (4/6)	

Tto: tratamiento. En la columna *Nº (tto/no tto)* se indica el número total de pacientes por cada tipo de mutación y, entre paréntesis se indican los pacientes con tratamiento (tto), seguido de los pacientes sin tratamiento (no tto)

4.2. Extracción de ADN y ARN

Tanto el ADN como el ARN fueron extraídos a partir de 10 ml de sangre periférica obtenidos por punción venosa en tubo con el anticoagulante EDTA.

En el caso de la extracción de ADN se siguieron las instrucciones del fabricante del kit de Puregene (Gentra systems, Minneapolis, MN). Las muestras de ADN fueron almacenadas a -20 ºC hasta su uso.

El ARN total procedente de células mononucleares de sangre periférica (PBMCs) fue extraído por medio del kit QIAamp RNA Blood Midi Kit (Qiagen, Hilden, Germany), siguiendo las indicaciones del fabricante. Para determinar la

concentración y pureza del ARN se utilizó el cociente entre la medida de la densidad óptica (D.O.) a 260 y a 280 nm. Posteriormente, cargando 1 µgr. de ARN en un gel de agarosa 1% y DEPC al 0.01%, se comprobó la integridad de los ARN extraídos. El material utilizado para la formación del gel y la cubeta fueron lavados previamente con agua con DEPC al 0,01%, enjuagados con agua oxigenada al 3% y dejado secar al aire tras un último lavado con etanol al 70 %. Las muestras se almacenaron a -80 ºC hasta su utilización.

4.3. PCR cuantitativa para la detección del ARNm de *SERPING1*

4.3.1. Trascripción inversa (RT)

El ADN complementario (ADNc) fue generado a partir de 1 µg de ARN total de sangre periférica utilizando el enzima SuperScript II RT (50 unidades/µl) y cebadores aleatorios incluidos en el kit SuperScriptII First-Strand Synthesis System for RT-PCR (Invitrogen, Carlsbad, California) siguiendo las indicaciones del fabricante.

4.3.2. PCR a tiempo real

A diferencia de la PCR convencional, en la que se analizan los productos finales de reacción, la técnica de PCR en tiempo real (o cuantitativa) está fundamentada en el análisis de la cinética de reacción y en la detección de moléculas de ADN presentes en cada ciclo de amplificación y durante la fase exponencial de la reacción.

La determinación de las moléculas de ADN se basa en la correlación entre la cantidad de producto de la PCR en cada ciclo y la señal de intensidad de fluorescencia emitida por marcadores fluorescentes del ADN incluidos en la mezcla de reacción.

Entre los marcadores fluorescentes del mercado se eligió SYBR Green I. Esta molécula tiene afinidad por el ADN y se intercala en la doble cadena emitiendo fluorescencia creciente en cada ciclo de PCR. El ciclo en el cual la intensidad de emisión del fluocromo aumenta diez veces respecto al ruido de fondo se conoce como ciclo umbral (Ct, *Cycle threshold*). El valor de Ct es inversamente proporcional al número de copias de la región diana a amplificar presentes al inicio de la reacción, por lo tanto, a mayor número de copias de mensajero (variante) en el comienzo de la reacción menor será el valor de Ct obtenido.

Para la cuantificación de los niveles de expresión de C1INH se recurrió a un método relativo. Este permite estimar la cantidad de ADNc de partida en una muestra

problema interpolando los valores de Ct obtenidos en una curva patrón generada a partir de diluciones seriadas de una muestra de concentración arbitraria. Para minimizar las variaciones de la técnica, la cuantificación de la expresión del gen de interés se normaliza en relación a los valores obtenidos tras la cuantificación, en la misma muestra, de un gen de referencia con expresión constante (constitutivo). El gen de referencia elegido para normalizar la expresión del gen de interés fue la gliceraldehido-3-fosfato deshidrogenasa (*GAPDH*). Este gen se expresa en todas las células de sangre periférica lo que permitiría normalizar sobre la población total de células mononucleadas de sangre periférica. Además, en los análisis iniciales no se observaron variaciones en las mediciones de *GAPDH.*

Todas las cuantificaciones fueron realizadas a partir de una curva patrón de diluciones seriadas de una muestra de donante sano a la que se le asignó un valor arbitrario (1µg de ADNc total).

Para establecer la variabilidad inter-ensayo, todas las muestras fueron cuantificadas por triplicado: se llevaron a cabo dos mediciones en un primer ensayo y una tercera medición en un ensayo independiente.

Idealmente, durante la fase exponencial, cada ciclo de amplificación de PCR duplica la muestra de partida, lo que significa que el rendimiento, o eficiencia, es de 2. La eficiencia puede ser calculada a partir de la pendiente de una curva patrón aplicando la siguiente fórmula:

$$E=10^{(-1/\text{pendiente})}$$

La eficiencia puede verse influida por diversos factores, como el diseño de los cebadores o el tamaño del amplificado. Este aspecto supuso que las cuantificaciones realizadas fueron incluidas en el estudio solo cuando la eficiencia de la curva patrón estuviese comprendida en el rango 1.8 - 2.2, tanto en el caso de C1INH (*SERPING1*) como en el de *GAPDH.* Al obtener la misma eficiencia en ambas amplificaciones, podríamos aplicar la ecuación:

$$[\text{Concentración gen diana}]=\frac{Ct_{diana}}{Ct_{\ referencia}}$$

Por otro lado, cuando en una PCR a tiempo real se recurre a un fluorocromo con afinidad por doble cadena de ADN, se pueden utilizar las curvas de disociación o desnaturalización para conocer la pureza del amplificado. Así, siempre que el

amplificado de la reacción sea único, se observará una temperatura en la cual la fluorescencia detectada será mínima.

De esta forma, la técnica de PCR a tiempo real nos permite conocer tanto la concentración de partida como la pureza de la amplificación en un único proceso.

4.3.3. Cebadores utilizados para técnicas de PCR a tiempo real

- Análisis de expresión de *SERPING1*

Para la detección de la expresión de C1INH se recurrió a los cebadores diseñados por Pappalardo y colaboradores (Pappalardo et al., 2004) (ver Tabla 4) donde el cebador en sentido directo se localizaba en mitad del exón 6, mirentras que el cebador en sentido reverso se localizaba *a caballo* entre el final del exón 6 y princpio del exón 7 del gen *SERPING1* [MIN*606860]. El tamaño del intrón 6 (5.169 pb) permitió amplificar sólo ARN y evitar el efecto de la contaminación con ADN genómico (Bustin et al., 2009). Además, la mayoría de los pacientes incluidos en el estudio no presentaban mutaciones en esta región, de manera que la fluorescencia detectada se debió sólo a los niveles del ARN mensajero de *SERPING1* presente en las células de sangre periférica de los individuos estudiados. El factor último que influyó en el diseño de los cebadores fue la ausencia, en la bibliografía y las bases de datos consultadas, de ninguna variante alternativa específica de tejido con ausencia de estos exones, de manera que esta región cumplía con la finalidad de cuantificar todo el ARN mensajero de C1INH.

Mediante el programa en línea *Primer3Plus* www.bioinformatics.nl/cgi-bin/primer3plus/primer3plus.cgi/ se diseñaron los cebadores para el gen normalizador siguiendo el mismo criterio que en el gen *SERPING1*. La Tabla 4 muestra los cebadores utilizados indicando la posición en la secuencia diana utilizada.

Tabla 4: Cebadores utilizados en el análisis de la expresión del ARN mensajero de *SERPING1* y *GAPDH*.

Región diana	Cebador	Secuencia cebadores (tamaño)	POSICION	Sec. referencia (Núm acceso)
SERPING1	SERPING1-6-directo	5´-CCCATGATGAATAGCAAGAAGTACC-3´ (25 ntos)	1158-1182	NM_000062.2
	SERPING1-6,7-reverso	5´-*GCTGCAGCTGCCCCAC*CTTGGCTT-3´ (24 ntos)	1213-1236	
GAPDH	GAPDH-directo	5´- TCCTGCACCACCAACTGCTTA-3' (21 ntos)	639-659	NM_002046.5
	GAPDH-reverso	5´-ACCACCCTGTTGCTGTAGCC-3' (20 ntos)	1143-1162	

En la secuencia del cebador en sentido reverso de *SERPING1* se han diferenciado la región de cada exón utilizando el estilo cursiva en la secuencia de hibridación con el exón 7

- Análisis de expresión del *splicing* alternativo del exón 3

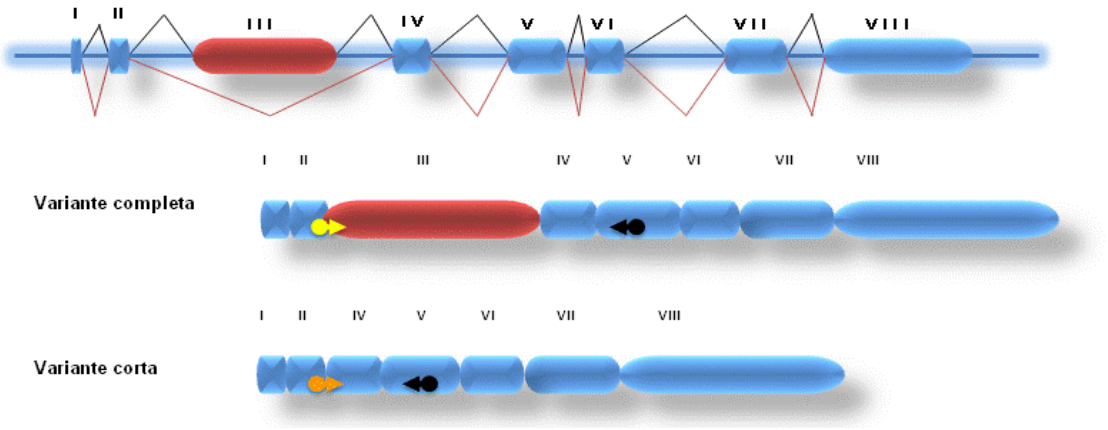

Figura 7: Disposición de los cebadores específicos de las variantes en el ARN mensajero NM_000062.2. En el diseño del ensayo, el cebador reverso hibrida en la misma región del exón 5 para ambas variantes (punta de flecha negra). La detección específica de cada variante se debe a la región de hibridación de los cebadores directos: final del exon 2 y comienzo del exón 3 para la variante completa (flecha amarilla), final del exon 2 y comienzo del exón 4 para la detección de la variante sin exon 3 (flecha naranja en variante corta). El exón 3 es el que diferencia una variante de la otra, por eso se ha representado en otro color (rojo).

Con la finalidad de cuantificar la expresión de dos variantes producidas durante la maduración del ARN mensajero (variante completa/ variante sin exón 3) de forma independiente, se diseñaron cebadores específicos de secuencia para cada variante con el programa en línea *Primer3Plus*. Para la detección específica de la variante completa, el cebador en sentido directo hibridaría en la conexión de los exones 2 y 3, mientras que el cebador en sentido directo para la variante corta requirió una hibridación en la conexión entre los exones 2 y 4 (Figura 7).

Como en el análisis de los niveles de expresión del mensajero total en PBMCs, el gen de referencia elegido fue *GAPDH*. La Tabla 5 muestra la secuencia de cebadores y la posición de los mismos en la secuencia diana.

Tabla 5: Lista de cebadores utilizados en el análisis de expresión de las variantes de *splicing*.

Región diana	Cebador	Secuencia cebador	POSICION	Secuencia de referencia (Núm de acceso)
Variante completa	SERPING1-2,3-directo	5´-*GCTGGG*GATAGAGCCTCCT-3´ (19 ntos)	237-255	NM_000062.2
	SERPING1-5-reverso	5´-GGGGCTGCTGCTGTACAGGG-3´ (20 ntos)	916-935	
Variante corta	SERPING1-2,4-directo	5´-*TGGCTGGG*GGGCTGGGGAGAA-3´ (21 ntos)	235-242/ 742-754	NM_000062.2
	SERPING1-5-reverso	5´-GGGGCTGCTGCTGTACAGGG-3´ (20 ntos)	916-935	
GAPDH	GAPDH-directo	5´- TCCTGCACCACCAACTGCTTA-3´ (21 ntos)	639-659	NM_002046.5
	GAPDH-reverso	5´-ACCACCCTGTTGCTGTAGCC-3´(20 tos)	1143-1162	

En la secuencia de nucleótidos del cebador que se une en sentido directo en cada variante se ha identificado la secuencia de hibridación con el final del exón 2 utilizando el estilo cursiva. Para el cebador en sentido directo diseñado para la variante corta se ha indicado en la columna de localización en la secuencia de referencia las posiciones de hibridación en el exón 2 y del exón 4 separadas por una barra inclinada

4.3.4. Desarrollo de la PCR cuantitativa

Para el desarrollo de estos análisis, se adaptó el protocolo de PCR en tiempo real a la química del intercalador SYBR Green I y el termociclador Light Cycler 1.5 (Roche Applied Science).

- Análisis de la expresión de *SERPING1*

La mezcla de la reacción contenía 3,125 mM de $MgCl_2$, 0.5 pmol/µl de cebadores, 1X Light Cycler FastStart DNA Master SYBR Green I (Roche Applied Science) y 1 µg de ADNc. En la Tabla 6 se muestran las condiciones de PCR para las amplificaciones.

Tabla 6: Condiciones de PCR a tiempo real utilizadas en la cuantificación de la expresión de C1 inhibidor

Gen	Activación	Desnat.	Hibridación	Extensión	Adquisición	Curva disociación
SERPING1		----------40 ciclos----------				
	95 ºC, 10 min.	95 ºC, 10 sec	63 ºC, 10sec	72 ºC, 10sec	72 ºC 10 sec	65 ºC-95 ºC
GAPDH		----------40 ciclos----------				
	95 ºC, 10 min.	95 ºC, 10sec	63 ºC, 10sec	72 ºC, 10sec	79 ºC, 10 sec	65 ºC-95 ºC

- Análisis de expresión del *splicing* alternativo del exón 3

La mezcla de reacción contenía 3,75 mM de $MgCl_2$, 0,5 pmol/µl de cebadores, 1X Light Cycler FastStart DNA Master SYBR Green I (Roche Applied Science) y 1 µg de ADNc. En la Tabla 7 se muestran las condiciones de PCR para las amplificaciones.

Tabla7: Condiciones de PCR a tiempo real utilizadas en la cuantificación de la expresión de las variantes de *SERPING1* y *GAPDH.*

Gen	Activación	Desnat.	Hibridación	Extensión	Adquisición	Curva disociación
Variante corta		----------40 ciclos----------				
	95 ºC, 10 min.	95 ºC, 10sec	69 ºC, 10sec	72 ºC, 10sec	72 ºC 10 sec	65ºC-95 ºC
Variante completa		----------40 ciclos----------				
	95 ºC, 10 min.	95 ºC, 10sec	63 ºC, 10sec	72 ºC, 10sec	72 ºC 10 sec	65ºC-95 ºC
GAPDH		----------40 ciclos----------				
	95 ºC, 10 min.	95ºC, 10sec	63 ºC, 10sec	72 ºC, 10sec	79 ºC, 10 sec	65ºC-95 ºC

5. ANALISIS ESTADISTICO

Mediante el Coeficiente de Correlación Intra-clase (ICC) se valoró la variabilidad de las tres mediciones en la misma muestra y mismo gen. Dicho coeficiente nos permitiría valorar la reproducibilidad inter-ensayo teniendo en cuenta que las dos primeras mediciones en cada paciente fueron realizadas en un primer experimento y la tercera medición se realizó en un segundo ensayo independiente.

Para analizar la inferencia de los datos agrupados por la variable "tener mutación" o "no presentarla" se aplicó el test Shapiro-Wilk. Debido a que los datos no presentaban una distribución normal o de homogeneidad de varianzas se aplicaron test no-paramétricos. Así, para las comparaciones entre dos grupos se aplicó el test de U Mann-Whitney. En las comparaciones múltiples, se aplicó el test estadístico de Kruskal-Wallis. De este modo, se podría conocer la existencia de diferencias entre las medianas de los niveles de expresión de los tres grupos. Como método *Post hoc* se aplicó el test de Dunn para las comparaciones dos a dos entre los tres grupos.

Los diferentes test estadísticos se llevaron a cabo utilizando la aplicación GraphPad Prism versión 5.00 para Windows, (GraphPad Software, San Diego California USA, www.graphpad.com).

6. AISLAMIENTO DE POBLACIONES CELULARES EN CONTROLES

Diferentes autores indican que la capacidad de los monocitos de secretar C1INH podría tener importancia a nivel localizado (Vinci et al., 2002, Duponchel et al., 2006). Por eso, nos propusimos conocer la expresión de C1INH total y de ambas variantes en respuesta a estímulo con INF-γ en la población monocítica de individuos sanos.

6.1. Población estudiada

Se aislaron las poblaciones monomorfonucleadas de sangre periférica de cuatro donantes sanos de la población española mediante separación inmunomagnética.

Los resultados obtenidos inicialmente mediante la separación inmunomagnética requirieron de la obtención de elevadas purezas. Esta condición disminuía el rendimiento de células en cada población haciendo difícil el desarrollo de los estudios moleculares posteriores.

La separación celular por citometría de flujo (sorting) es una metodología que permite obtener altos niveles de pureza a la vez que la obtención de un número

adecuado de células de las poblaciones celulares específicas y de baja presencia en sangre periférica. Se solicitó, entonces, la participación en el estudio a dos de los cuatro donantes sanos que habían sido estudiados por separación inmunomagnética y poder validar los datos con la separación por citometría de flujo.

6.2. Extracción de muestras y obtención de suspensión leucocitaria

La formación de gradiente de densidad con ficoll es una técnica ampliamente utilizada para la obtención de las poblaciones leucocitarias monomorfonucleares de sangre periférica. Se debe a que aprovecha las diferencias de densidad entre cada tipo celular permitiendo obtenerlas de forma rápida.

Se extrajeron 50 ml de sangre periférica en heparina de litio por punción venosa a los donantes sanos. La sangre extraída se diluyó ½ en una solución tampón fosfato salina (NaCl 137mM, KCl 2.7mM $NaHPO_4$ 10mM, KH_2PO_4 1.8mM y pH 7.2) (en adelante PBS) y se centrifugó durante 30 minutos a 400x g a temperatura ambiente en un gradiente en Ficoll-Histopaque (Ficoll-paque, GE Healthcare Bio-Sciences AB, Suecia) sin acelaracion, ni freno. Bajo este procedimiento se recogieron las células de la serie blanca monomorfonucleadas del sedimento localizado sobre la fase de ficoll, y se lavaron dos veces con solución salina (PBS).

Para calcular la viabilidad celular se siguió el método de tinción con azul tripán (colorante de exclusión) en una cámara hemocitométrica de Neubahuer. El cálculo de la viabilidad permitió conocer el rendimiento del enriquecimiento de leucocitos que oscilaba entre 50 millones y 80 millones de células totales.

Posteriormente, se obtuvo la formula leucocitaria de cada muestra mediante el uso de un contador celular basado en técnica de impedancia (Beckman Coulter), que nos permitiría estimar el rendimiento teórico del aislamiento celular.

6.3. Selección poblacional

- Selección inmunomagnética

La separación inmunomagnética es una técnica de aislamiento celular que utiliza microesferas magnéticas de 50 µm revestidas de anticuerpos monoclonales dirigidos contra antígenos celulares. Con un sistema configurado con un imán y columna magnética se aplica el campo magnético sobre la columna. Se hace pasar a través de la columna la suspensión de células marcadas con microesfereas y las no marcadas. Con el

campo magnético se retienen en la columna las poblaciones de interés unidas a las microesferas magnéticas mediante el marcaje con los anticuerpos monoclonales. Las poblaciones no marcadas y, por tanto, no unidas a las microesferas eluirán. La posterior retirada del campo magnético de las columnas permitirá eluir las poblaciones celulares deseadas. De esta forma obtendremos las poblaciones de interés mediante selección positiva (Ver Figura 8).

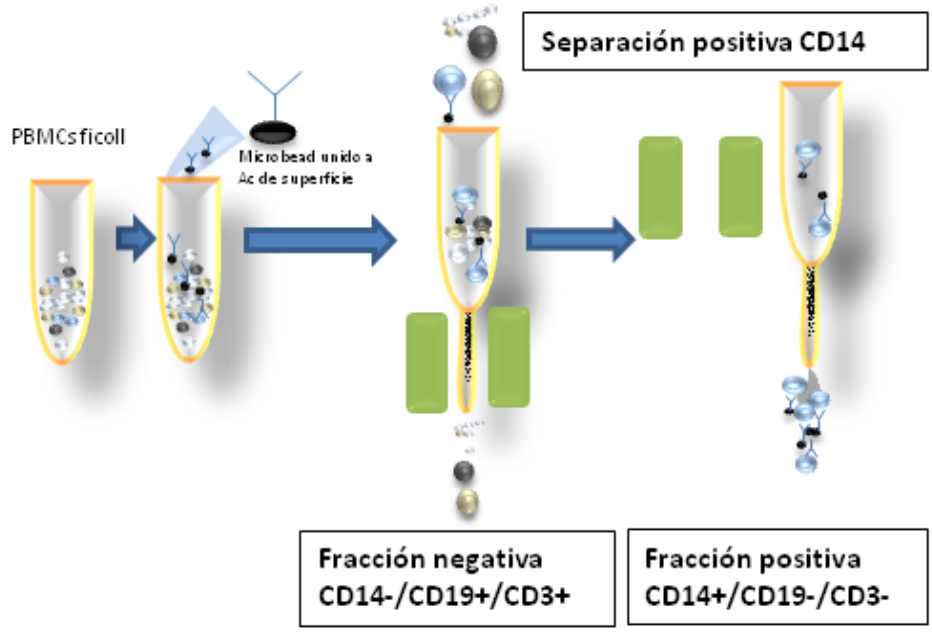

Figura 8: Fundamento de la separación inmunomagnética por selección positiva. Mediante un imán obtenemos la población de interés, previamente marcada con anticuerpos unidos a microbolas magnéticas. La población deseada permanece en la columna mientras esté unida al imán. El resto de células son eluidas.

Determinado el número de células obtenidas por centrifugación en gradiente, se sedimentaron las células a 300x g durante 10 minutos y el sedimento se resuspendió en el tampón de elución (PBS+STF 0.5%) a razón de 80 µl por cada 10^7 células. Se aplicó una suspensión de microesferas magnéticas (Miltenyi Biotec) unidas a marcadores de superficie (ver Tabla 8) a razón de 20 µl por 10^7 células totales. Se incubó la mezcla durante 15 minutos a 4 ºC. Las células marcadas resuspendidas en el tampón de elución (500 µl de tampón) se incluyeron en una columna LS unida a un imán de elevada fuerza magnética (MidiMACS™ Separator, Miltenyi Biotec) que permitió una selección positiva de las poblaciones celulares marcadas por retención en la columna por la fuerza

magnética del imán frente al resto de poblaciones eluídas de la columna. La separación de la columna del imán permitió eluir la población retenida en la columna.

Para el aislamiento de la población monocítica se recurrió al kit de microesferas marcadas con los anticuerpos para los receptores de superficie CD14 (CD14 MicroBeads, human, BD Biosciences, San José, CA). La fracción de células eluídas de la columna fue incubada con el kit que presentaba anticuerpos para el clúster de diferenciación CD19 (CD19 MicroBeads, human, BD Biosciences, San José, CA) que nos permitió obtener la población de linfocitos B. Ahora, la fracción no retenida en la columna fue incubada con el kit que contenía las microesferas unidas a anti-CD56/16 (CD16/CD56 MicroBeads, human, BD Biosciences, San José, CA) recogiendo en este paso la población de células *Natural Killer* (en adelante NK). La última población eluída en la columna contenía la población de linfocitos T.

La Tabla 8 muestra la caracterización fenotípica de las poblaciones obtenidas mediante la separación inmunomagnética.

Tabla·8: Fenotipo de poblaciones a estudiar

Marcaje / Población	**CD14**	**CD16/56**	**CD3**	**CD41**	**CD19**	**CD45**
MØ	+	-	-	-	-	+
MØ-plaquetas	+	-	-	+	-	+
Linf. T	-	-	+	-	-	+
Natural Killer	-	+	-	-	-	+

MØ: población monocítica

Con las subpoblaciones así preparadas, se recogieron dos alícuotas con 300.000 células por población separada que se incubaron durante 15 minutos en oscuridad con los anticuerpos monoclonales. La primera alícuota se marcó con el siguiente panel de anticuerpos marcados con distintos fluorocromos: anti-CD14-PercP, anti-CD19-APC, anti-CD3-FITC y anti-CD16/56-PE (BD Biosciences, San José, CA). La segunda alícuota se marcó con anti-CD45-APC (BD Biosciences, San José, CA). El análisis de la pureza en las poblaciones celulares aisladas se realizó con un citómetro de flujo BD FACSCalibur™ (BD Biosciences, San José, CA) y configuración óptica de cuatro colores. Sólo poblaciones con pureza superior al 90% fueron aceptadas.

El análisis de los datos se realizó mediante una estrategia de análisis jerárquico con el software CellQuestPro 3.7® (BD Biosciences, San José, CA) para Macintosh®.

- Aislamiento por citometría de flujo

Las plaquetas y micropartículas de plaquetas (PMPs) participan en la regulación de la activación de la vía clásica del sistema del complemento liberando C1INH a través de gránulos α (Blair and Flaumenhaft, 2009, Coppola et al., 2002, Harrison and Cramer, 1993, Yin et al., 2008). Esta población, cuando es activada, tiende a formar agregados con leucocitos (Cerletti et al., 2012, Hamad et al., 2012). Por esta razón, la presencia residual de población plaquetaria o gránulos α debía ser tenida en cuenta en el momento de la separación por citometría de flujo y no se tuvo en cuenta en las selecciones positivas realizadas mediante separación inmunomagnética. En cambio, en la separación de poblaciones celulares por citometría de flujo se realizaron estudios previos con diferentes abordajes de aislamiento celular para la obtención de células monomorfonucleadas libres de la fracción megacariocítica.

El abordaje técnico establecido partía de 40 ml de sangre periférica en el anticoagulante heparina de litio por punción venosa que se centrifugó a bajas revoluciones (152x g) durante 10 minutos a temperatura ambiente, sin freno ni acelerador. Tras este tiempo se obtuvieron tres fracciones:

- Plasma rico en plaquetas (parte superior del tubo).
- Leucocitos con plaquetas (anillo intermedio del tubo).
- Eritrocitos y reticulocitos (parte inferior del tubo).

La fracción que contenía la serie blanca (anillo intermedio) se recogió en un nuevo tubo y se le adicionó PBS hasta obtener un volumen igual al extraído (40 ml). Una vez eliminada la mayor parte de la población plaquetaria, se siguió el protocolo de separación de PBMCs con Ficoll-Histopaque.

La viabilidad celular se valoró mediante citometría de flujo incorporando a la muestra el colorante vital yoduro de propidio. Este estudio se realizó también en los ensayos de puesta a punto de la separación por citometría realizados para testar la técnica y comprobar que durante la fase de separación celular (*sorting*) no se producía apoptosis celular.

Conocida la fórmula leucocitaria, las células se concentraron por centrifugación. Se descartó el sobrenadante y se prepararon para la separación por citometría de flujo.

Se utilizó un separador celular digital de alta velocidad FACSARIA II configurados con dos láseres (azul de 488 nm y rojo de 633 nm) y configuración óptica de 7 detectores ópticos, que permiten la cuantificación de la expresión de hasta 9 parámetros de emisión de fluorescencia a la vez, además de los parámetros de tamaño y complejidad celular. En la Figura 9 se ilustra el fundamento de la separación por citometría de flujo.

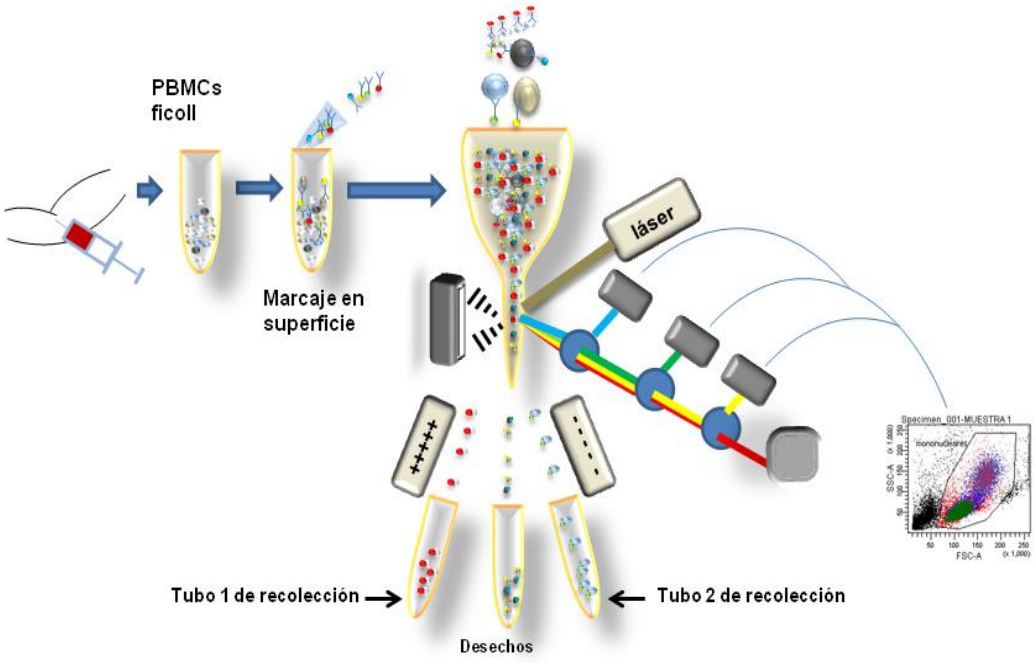

Figura 9: Fundamento de la separación por citometría de flujo. La dispersión de la luz de cada célula determina el tamaño y complejidad (FSC-A, SSC-A). El marcaje en superficie permite discriminar entre tipos celulares de tamaño y complejidad similares.

Para este proceso, el sedimento de células se resuspendió en tampón de citometría de flujo (PBS con EDTA 3 mM y suplementado con suero de ternera fetal (STF) al 3%) a razón de 10^6 células/300 µl en tubos estériles. Las células resuspendidas se marcaron con anticuerpos monoclonales validados por titulación en concentración y fluorescencia para citometría. El panel utilizado fue: antiCD14 FITC, anti-CD16/56 PE, anti-CD19 PercP Cy5.5, anti-CD41 APC y anti-CD3 APC-C750. Estos marcadores de superficie nos permitieron conocer el porcentaje de expresión de cada linaje celular y estimar el rendimiento de la separación. En la Tabla 9 se indican los marcadores de superficie diana para cada población de interés.

Tabla·9: Fenotipo de poblaciones a estudiar

Marcaje / Población	CD14 FITC	CD16/56 PE,	CD3 APC-C750	CD41 APC	CD19 PercP Cy5.5
MØ	+	-	-	-	-
MØ-plaquetas	+	-	-	+	-
Linf. T	-	-	+	-	-
Natural Killer	-	+	-	-	-

MØ: población monocítica. Linf.: linfocitos

Las poblaciones positivas fueron recogidas en medio RPMI-1640 (Sigma Chemical Co., St. Louis, MO, USA), que es un medio de cultivo con alto contenido en fosfatos, al que se le suplementó con suero de ternera fetal al 3% en tubos estériles para citometría, y se sembraron a razón de 10^6 células/ml en medio RPMI 1640 al 10% de STF y se les sometió a un tiempo de descanso (*resting*) de 16 horas de duración. Transcurrido ese tiempo de procedió a la estimulación con citoquinas.

6. 4 Estimulación de células con IFN-γ

IFN-γ es una citoquina proinflamatoria potente y ampliamente estudiada su implicación en la activación del sistema del complemento *in vitro* (Falus et al., 1990a, Heda et al., 1990, Katz and Strunk, 1989, Lappin et al., 1992, Lotz and Zuraw, 1987).

Tanto en la separación inmunomagnética como por citometría de flujo se recurrió a la estimulación con IFN-γ para el estudio de respuesta inflamatoria.

Se estimularon cada una de las poblaciones aisladas por ambas técnicas de separación con 10 ng/ml de IFN-γ durante 24 horas a razón de 10^6 células/ml de RPMI-1640 y un 10% de suero de ternera fetal (STF). La misma densidad de células se mantuvo sin la citoquina durante las 24 horas de estímulo.

Como en la separación por citometría de flujo se obtuvieron rendimientos mayores, se pudo incluir un punto de recogida muestra con y sin IFN-γ a 48 horas.

6. 5 Extracción de ARN

Transcurrido el tiempo de estimulación, se aislaron las células por centrifugación para la obtención de ARN para el estudio de la expresión de *SERPING1*, y el sobrenadante se almacenó para posteriores estudios funcionales.

Para la extracción de ARN se utilizó el método de tiocianato de guanidinio-fenol-cloroformo con el reactivo TRIzol (InvitrogenTM, Life Techonologies, Carlsbad, CA) de Chomczynsky (Chomczynski and Sacchi, 1987, Chomczynski, 1993,

Chomczynski and Sacchi, 2006, Hummon et al., 2007). Este método basado en una solución monofásica de fenol y tiocianato de guanidino permite el lisado de las células protegiendo al ARN de la acción de la RNasas liberadas durante la lisis celular.

La adición y homogenización de Trizol (750 µl/10^6 células) al sedimento de células libres de sobrenadante permitió la liberación de ARN al medio. Posteriormente se adicionó cloroformo (1/2 volumen de Trizol) al homogenizado. Tras la homogenización de ambos reactivos y posterior centrifugación (10.000 rpm durante 15 minutos a 4º C) se obtuvo la separación de la muestra en dos fases:

- Fase acuosa superior: Contiene el ARN.
- Fase orgánica inferior: Contiene el ADN y las proteínas desnaturalizadas.

Se transfirió la fase acuosa a un tubo de 1.5 ml y se adicionaron 350 µl de isopropanol para la precipitación de ARN por centrifugación a 10000 rpm durante 10 minutos a 4 ºC. El precipitado se lavó con etanol al 75 % (750µl) y se centrifugó a 10.000 rpm durante 10 minutos a 4 ºC (2 veces). Posteriormente, el precipitado se secó durante 10 minutos y por último se resuspendió en 30 µl de agua estéril con DEPC al 0,1%

Este método robusto permite obtener el máximo rendimiento de ácido ribonucleico, además de obtener material genómico y material proteico de origen intracelular necesario para estudios funcionales posteriores.

Para testar la integridad, pureza y concentración (ng/µl) del ARN extraído se recurrió a la medida de la densidad óptica (OD) a 260 nm y 280 nm medidos en un espectrofotómetro NanoDrop® D-1000 (NanoDrop Technologies, Wilmington, Estados Unidos).

Con las muestras de ARN recogidas de cada población obtenida mediante separación inmunomagnética, o separación por citometría de flujo, se analizaron los niveles de mensajero total de C1INH en las poblaciones celulares bajo estímulo con IFN-γ siguiendo el protocolo establecido para PBMCs de pacientes de angioedema hereditario por deficiencia de C1INH

Resultados

7. ESTUDIO DE EXPRESION DE *SERPING1* EN SANGRE PERIFERICA

7.1. Población estudiada

Para el análisis de la expresión del mensajero de *SERPING1* se recogió muestra de 30 individuos con AEH causado por mutaciones puntuales. En el proceso de caracterización molecular de los individuos se diagnosticaron tres familias con cambios no descritos hasta el momento que han sido recogidos en dos publicaciones (de la Cruz et al., 2012, López-Lera et al., 2011). En la Tabla 10 se muestran las mutaciones de los individuos incluidos en la serie de pacientes.

Tabla 10: Pacientes estudiados en el análisis de expresión total de *SERPING1*.

Pac.	Ex.	Cambio ADNc *HGVS*	Cambio proteína *Tradicional*	Predicción efecto	Tipo AEH	Tratamiento
DA	2	c.51+3A>G		Splicing	I	SI
BN	3	c.270delC	Thr69fsX57	C. pauta lectura	I	NO
AG	3	c.512C>T	Pro149leu	Cambio aa	I	SI
D	3	c.550+2T>C		Splicing	I	NO
M	3	c.550+5G>C	-	Splicing	I	SI
AZ	3	c.550G>A	Gy162Arg	Splicing	I	NO
BI	3	c.550G>A	Gy162Arg	Splicing	I	SI
FN	3	c.550G>A	Gly162Arg	Splicing	I	NO
BM	4	c.578T>C	Leu171Pro	Cambio aa	I	NO
FF	4	c.614G>A	Cys183Ser	Cambio aa	I	SI
DY	5	c.686-3C>G	-	Splicing	I	NO
AI	6	c.990C>G	Tyr308Stop	Stop prematuro	I	NO
GM	7	c.1033 G>A	Gly323Arg	Cambio aa	I	NO
GO	7	c.1048T>C	Ser328Pro	Cambio aa	I	NO
O	7	c.1226T>C	Met387Thr	Cambio aa	I	NO
B	7	c.1249+2delT	-	Splicing	I	NO
BW	8	c.1328 A>G	His421Arg	Cambio de aa	I	NO
GI4	8	c.1331T>C	Leu425Pro	Cambio aa	I/II	SI
Y	8	c.1350dupA	Glu429ArgfsX22	C. pauta lectura	I	NO
I	8	c.1367C>A	Ala434Gln	Cambio aa	II	SI
ED	8	c.1396C>A	Arg444His	Cambio aa	II	NO
FT	8	c.1396C>G	Arg444Gly	Cambio aa	II	SI
EH	8	c.1396C>G	Arg444Gly	Cambio aa	II	NO
GY	8	c.1396C>G	Arg444Gly	Cambio aa	II	NO
DT	8	c.1396C>T	Arg444Cys	Cambio aa	II	SI

Tabla 10 continuación

DT5	8	c.1396C>T	Arg444Cys	Cambio aa	II	NO
BL3	8	c.1399A>C	Thr445Pro	Cambio aa	II	NO
AP	8	c.1480C>T	Arg472Stop	Stop prematuro	I	NO
DR	8	c.1480C>T	Arg472Stop	Stop prematuro	I	SI
Q	8	c.1480C>T	Arg472Stop	Stop prematuro	I	SI

Pac: paciente estudiado. Ex: exón. HGVS: Human genome variation society ADNc: ADN codificante.

7.2. Análisis de la expresión de *SERPING1* en pacientes con AEH

Para cada individuo se realizaron tres mediciones, tanto de la expresión del mensajero de *SERPING1*, como del gen constitutivo *GAPDH* (gliceraldehido-3-fosotato deshidrogenasa). Mediante una curva patrón con cinco diluciones seriadas de un donante sano, se calculó el número de copias relativas del gen de interés y del gen constitutivo para cada individuo. El valor de expresión de *SERPING1* fue normalizado por la cuantificación relativa de la expresión del gen constitutivo para minimizar las variaciones debidas a la técnica. Posteriormente, la normalización sufrió una transformación tal y como se indica en la siguiente ecuación:

$$\frac{\text{número copias SERPING1}}{\text{número copias GAPDH}} \times 1.000.000 = \text{expresión SERPING1}$$

Los datos se agruparon en dos poblaciones (controles y pacientes) que presentaron una gran dispersión alejándose en ambas de la distribución normal (p-valor< 0,0001 para controles, y p-valor=0,0017 en pacientes; test Shapiro-Wilk).

El primer nivel de comparación mostró una disminución estadísticamente significativa del ARN mensajero de *SERPING1* en el grupo de pacientes (144,7 [7,846-624,7]) respecto a controles (377,8 [35,02-5484]) (p-valor=0,0006, test Mann-Whitney), (ver Figura 10a). Este perfil de ARN mensajero disminuido en pacientes respecto a donantes sanos ha sido observado también en otros trabajos (Donaldson and Evans, 1963, Pappalardo et al., 2000, Pappalardo et al., 2003, Pappalardo et al., 2004, Cicardi et al., 2014).

Un análisis más detallado evidenció diferencias estadísticamente significativas en la producción del inhibidor de C1 según el tipo de AEH (*p-valor*=0,0003). El análisis *post hoc* mediante el test de *Dunn* matizó las diferencias estadísticamente significativas entre los pacientes tipo I (99,49 [7,846-551,3]) y el grupo control (*p-valor*<0,001). (Figura 10b y Tabla 11).

Tabla 11: Expresión de *SERPING1* en controles y tipos de AEH.

Grupo	Número copias *(Mediana [máx.-min.])*	Kruskall-Wallis
Controles	377,8 [35,02-5484]¥	0,0003
AEH I	99,49 [7,846-551,3] ¥	
AEH II	272,9 [104,1-624,7]	

En la tabla se indica el valor de la mediana [mínimo-máximo] en cada grupo. ¥ indica diferencias estadísticamente significativas entre ambos por el test de Dunn (p<0,05).

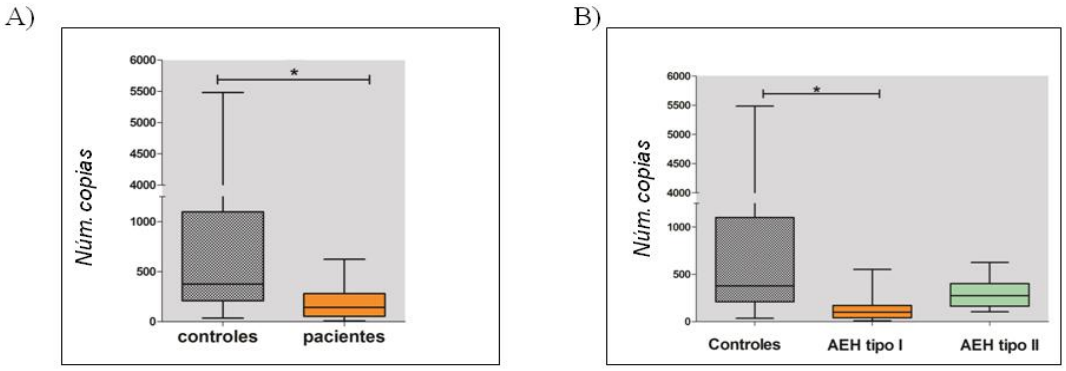

Figura 10. **Niveles de expresión de mensajero de *SERPING1* en pacientes con AEH**. Los gráficos representan el número de copias en medianas [máximo–mínimo] en cada categoría. A) Niveles de expresión en pacientes frente controles. B) Niveles de expresión según el tipo de angioedema.* indica los grupos con p-valor <0.05 para los test estadísticos aplicados.

En nuestra serie de pacientes estaban incluidos tanto pacientes tratados a largo plazo como pacientes sin tratamiento. Desde finales del siglo pasado se observó que la administración de andrógenos atenuados y/o antifibrinolíticos induce la producción del C1INH y disminuye la frecuencia y severidad de los episodios de angioedema (Pappalardo et al., 2003, Agostoni et al., 1980b, Sheffer et al., 1987, Agostoni and Cicardi, 1992, Agostoni et al., 1980a). Al analizar el efecto del tratamiento, se observó que los pacientes tratados presentaban mayor expresión de mensajero total de *SERPING1* que aquellos que no tenían profilaxis (ver Figura 11 y Tabla 12). Esta diferencia fue más marcada en el grupo de pacientes tipo I.

Tabla 12: Expresión en controles y tipos de AEH en tratamiento o sin tratamiento

Grupo	Tratamiento *Número copias Mediana [máx.-min.]*	Sin tratamiento *Número copia Mediana [máx.-mín.]*	Kruskall-Wallis
Controles		377,8 [35,02-5484]¥	0,0003
AEH I	222,1 [19,16-551,3]	66.89[7,846-184,5] ¥	
AEH II	403,4[179,1.4-624,7]	257.1[104,1-400,8]	

Los valores son expresados en mediana [mínimo-máximo] ¥ indica diferencias estadísticamente significativas entre ambos por el test de Dunn (p<0,05).

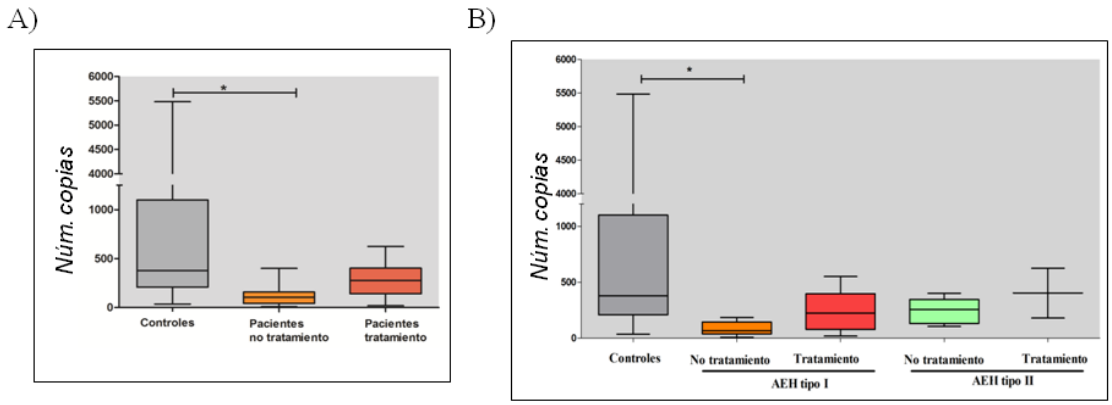

Figura 11. **Efecto del tratamiento sobre la expresión de *SERPING1* en pacientes con AEH**. Los gráficos representan el número de copias en medianas [máximo –mínimo] en cada categoría. **A)** Niveles de expresión pacientes en tratamiento y sin tratamiento. **B)** Niveles de expresión según tratamiento en cada tipo de angioedema. * indica los grupos con p-valor <0.05 para los test estadísticos aplicados.

7.3. Análisis de expresión por tipo de mutación

Nuestra cohorte estaba formada mayoritariamente por pacientes tipo I, dos tercios del total, pero sólo las mutaciones de *splicing* (108,9 [7,8-403,4]) y las alteraciones que producen un cambio de aminoácido (127,5 [19,16-277,8]) mostraron diferencias estadísticamente significativas respecto al grupo control según el test *post hoc* de *Dunn*. Los pacientes con cambio de la pauta de lectura, con los niveles más bajos de expresión de *SERPING1*, no cumplieron los criterios necesarios para aplicar los métodos estadísticos por el tamaño muestral (n=2) de este grupo. En la Figura 12 se muestra el porcentaje de expresión de los grupos respecto al grupo control.

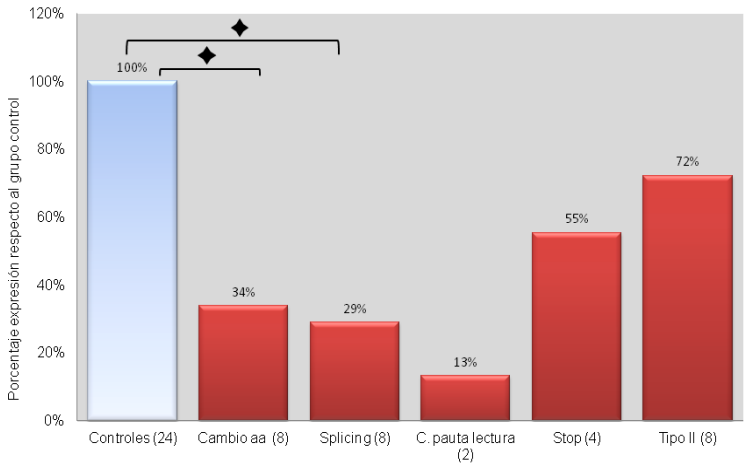

Figura 12. Análisis de expresión de *SERPING1* por tipo de mutación. El gráfico de histogramas indica la expresión obtenida en cada grupo de mutaciones respecto a la expresión del grupo control.
◆ indica las comparaciones con *p-valor* <0,05 para el test estadístico de Dunn.

Por su parte, el grupo con alteración de codón de parada prematura formado por cuatro pacientes (DR, Q, AP y AI), presentó una expresión superior al 50% respecto al grupo control. Este comportamiento no parecía concordar con la dominancia negativa de la enfermedad descrita por Kramer (Kramer et al., 1993) y otros grupos.

En los pacientes DR, Q y AP estaba presente el mismo cambio c.1480C>T, localizado en el exón 8, pero los niveles de expresión fueron marcadamente menores (10%) en el paciente AP. Estos datos eran similares al paciente AI con alteración de parada prematura en el exón 6.

Por su parte, los pacientes DR y Q, con tratamiento a largo plazo, presentaron un número de copias (379 copias y 551 copias, respectivamente) muy similares al grupo control. Así, la diferencia de expresión dependiente de profilaxis podría explicar los valores de la mediana obtenidos para este grupo.

8. ESTUDIO DE EXPRESION DE VARIANTES DE *SPLICING* DE *SERPING1* EN SANGRE PERIFERICA

En la base de datos *Ensembl* se han recogido doce formas de mensajero producto de diferentes patrones de maduración del mensajero de *SERPING1*. De todos ellos, sólo el transcrito ENST00000278407 (NM_000062.2) que codifica para la proteína de 500 aminoácidos y que contiene el péptido señal completo, por lo que puede ser secretada.

En 2006, Duponchel describió una variante alternativa de ARN mensajero del gen *SERPING1* que no contenía el exón 3. Sus datos indicaron que su expresión es constitutiva de monocitos de sangre periférica, mientras que en líneas celulares de hepatomas esta variante no se detectaba (Duponchel et al., 2006). Dicha variante alternativa sin exón 3 no está recogida en ninguna base de datos de transcritos consultada (*NCBI, UCSC Genome Broswser).*

La ausencia del exón 3, en el caso de que utilizase el mismo codón de inicio que la secuencia de referencia NM_000062.2, supone la pérdida de 499 nucleótidos respecto de la variante completa y altera la pauta de lectura produciendo una proteína truncada de 43 aminoácidos (p.Asp18Gly fs*26).

Basándonos en los estudios publicados en 2006, nos propusimos conocer la expresión de esta variante específica de células blancas en pacientes con AEH causada por cambios puntuales y en donantes sanos.

8.1. Análisis semicuantitativo de la expresión de *SERPING1* por PCR con transcriptasa reversa.

Se realizó un análisis preliminar a partir de 1 µg de ARN de PBMCs mediante transcripción reversa y posterior PCR de los exones 1 al 5 de *SERPING1*. La secuencia de cebadores en la reacción de PCR en sentido directo hibridaba en los ultimos 10 nucleótidos del exón 1 y lo primeros 11 nucleótidos del exón 2 (5´ GAAGTTTGGAGTCCGCTGACG 3´) y el cebador en sentido reverso hibridaba en el interior del exón 5 (5´ GGGGCTGCTGCTGTACAGGG 3´).

El estudio por PCR a tiempo final se realizó en tres pacientes estudiados en el apartado 7 (Tabla 10) (GO, Q, y DT5), el paciente AK con mutación de *splicing* en el exón 3, y el paciente G con mutación de cambio de la pauta de lectura (estos dos pacientes no estaban incluidos en la serie anterior), además de un donante sano (C65). Tras la migración en un gel de agarosa al 2%, se observó que las mutaciones asociadas a AEH-tipo I no presentaban un patrón de expresión homogéneo para ambas variantes. Los datos del patrón de expresión de las variantes se muestran en la Figura 13.

Para llevar a cabo un análisis más detallado se realizaron estudios de cuantificación de las variantes en una serie de pacientes más amplia.

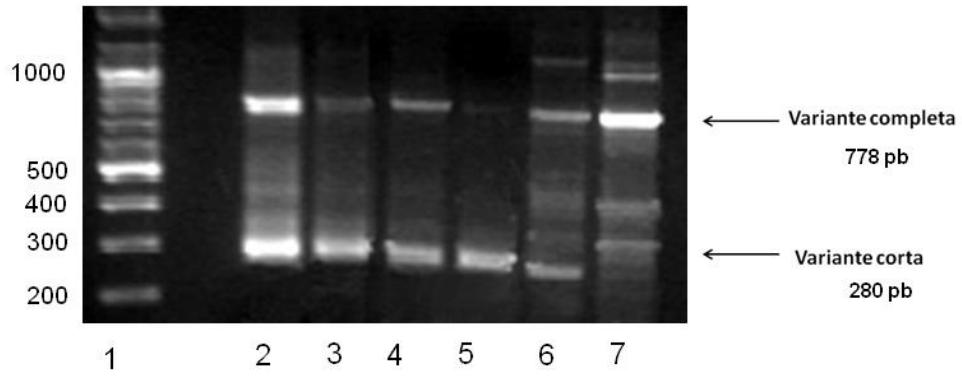

Figura 13. Análisis del patrón de expresión de las variantes en diferentes tipos de alteraciones mediante PCR por transcripción reversa. El ADNc se obtuvo a partir de 1µgr de ARNm total con cebadores aleatorios. Posterior amplificación con cebadores específicos exones 1 al 5. Migración en Agarosa 2%. **1:** Marcador de ADN de 100 pb de tamaño **2:** Control sano (C65); **3:** AK con mutación de *splicing* (c.550G>C, exón 7); **4:** GO mutación cambio de aminoácido (c.1048T>C, exón 8); **5:** DT5, mutación en centro activo (c.1396T>C, exón 8); **6:** G, mutación de cambio pauta de lectura (c.291_295del, exón 3); **7:** Q mutación de parada prematura (c.1480C>T, exón 8).

8.2. Población estudiada.

En la serie de pacientes se incluyeron 32 individuos con mutaciones puntuales distribuidas a lo largo del gen que han sido recogidas en la Tabla 13.

Tabla 13: Pacientes estudiados en el análisis de expresión de variantes de *splicing* de *SERPING1*

Pac.	Ex.	Cambio ADNc HGVS	Cambio proteína Tradicional	Predicción efecto	Tipo AEH	Tratamiento
FP	2	c.51+3A>G		Splicing	I	NO
FU	3	c.267delA	GLn63fs59	C. pauta lectura	I	No idea
BN	3	c.270delC	Thr69fsX57	C. pauta lectura	I	NO
G	3	c.291_95del	Gln75fsx34	C. pauta lectura	I	NO
FJ	3	c.473C>G	Arg136Stop	Stop prematuro	I	SI
AG	3	c.512C>T	Pro149Leu	Cambio aa	I	SI
J	3	c.550+5G>C		Splicing	I	SI
M	3	c.550+5G>C		Splicing	I	SI
AK	3	c.550G>C	Gly162Arg	Splicing	I	SI
AZ	3	c.550G>C	Gly162Arg	Splicing	I	NO
BI	3	c.550G>C	Gly162Arg	Splicing	I	SI
FF	4	c.614G>A	Cys183Ser	Cambio aa	I	SI
GE	4	c.669_670del	Gln201Hisfs*33	C. pauta lectura	I	SI
K	5	c.795G>A	Trp243Stop	Stop prematuro	I	No idea
K3	5	c.795G>A	Trp243Stop	Stop prematuro	I	No idea
GM	7	c.1033 G>A	Gly323Arg	Cambio aa	I	NO
GO	7	c.1048T>C	Ser328Pro	Cambio aa	I	NO
O	7	c.1226T>C	Met387Thr	Cambio aa	I	NO
GI4	8	c.1331T>C	Leu425Pro	Cambio aa	II/I	SI
Y	8	c.1350_1351insA	Glu429fs*22	C. pauta lectura	I	NO
I	8	c.1367C>A	Ala434Gln	Cambio aa	II	SI
AA	8	c.1396C>T	Arg444Cys	Cambio aa	II	NO
DT	8	c.1396C>T	Arg444Cys	Cambio aa	II	SI
DT5	8	c.1396C>T	Arg444Cys	Cambio aa	II	NO
ED	8	c.1396C>T	Arg444Cys	Cambio aa	II	NO
EH	8	c.1396C>T	Arg444Cys	Cambio aa	II	NO
EH3	8	c.1396C>T	Arg444Cys	Cambio aa	II	NO
FT	8	c.1396C>T	Arg444Cys	Cambio aa	II	SI
FK	8	c.1397G>A	Arg444His	Cambio aa	II	NO
BL3	8	c.1399A>C	Thr445Pro	Cambio aa	II	SI
Q	8	c.1480C>T	Arg472Stop	Stop prematuro	I	SI
FQ	8	c.1493C>T	Pro476Thr	Cambio aa	I	NO

Pac: paciente estudiado. Ex: exón. HGVS: Human genome variation society. ADNc: ADN codificante

8.3. Análisis de expresión de las variantes de *splicing* que afectan al exón 3

Como se puede observar en la Tabla 14, el patrón de expresión de las variantes en el grupo control y el grupo de pacientes fue igual. En ambos grupos se observó una tendencia hacia una mayor expresión de la variante corta respecto a la completa, sin diferencias estadísticamente significativas entre las agrupaciones (p-valor=0.3643, test de Kruskal-Wallis). A pesar de los valores obtenidos en el apartado 7.2, los niveles de expresión de las dos variantes en pacientes y en controles fueron similares.

Tabla 14: Valores de expresión en controles y pacientes.

Grupo	Casos	Núm. copias Variante completa	Núm. copias Variante corta	*Kruskal-Wallis*
Controles	25	172.2[14.10-2664]	210.8[11.37-7078]	0.3643
Pacientes	32	186.5[7.9-618.6]	207.8[8.2-2046]	

Los valores son expresados en mediana [mínimo-máximo].

Con los resultados obtenidos en la expresión del ARN mensajero total de *SERPING1* teniendo en cuenta las dos formas de AEH, y por los datos obtenidos en los estudios preliminares (apartado 8.1), sospechamos que los valores obtenidos en la Tabla 14 podrían enmascarar patrones de expresión diferentes según el tipo de AEH. Por eso, analizamos los datos según el tipo de angioedema. Con este análisis, las mutaciones tipo II mostraban mayor expresión que el resto de grupos para ambas variantes. Por su parte, tal y como sospechábamos en base a los resultados obtenidos en el primer objetivo, los pacientes tipo I fueron el grupo con menor expresión de ambas variantes, mostrando diferencias estadísticamente significativas respecto al grupo de pacientes tipo II (Tabla 15).

Tabla 15: Expresión de las variantes según el tipo de AEH

Grupo	Casos	Núm. copias Variante completa	Núm. copias Variante corta	*Kruskal-Wallis*
Controles	25	172.2[14.10-2664]	210.8[11.37-7078]	0.0103
AEH tipo I	22	131.4 [7.9-618.6] ¥	192.2[8.2-1034] ¢	
AEH tipo II	10	238.7[56.8-571.5]	686[108.7-2046] ¢¥	

Valores de expresión en controles y pacientes expresados en mediana [mínimo-máximo] ¥ indica diferencias estadísticamente significativas entre ambos por el test de Dunn (p<0.05). ¢ indica diferencia estadísticamente significativa entre ambos grupos por el test de Dunn (p<0.05).

Basándonos en los estudios con PCR con transcriptasa reversa realizados en los cuatro pacientes con AEH-tipo I donde se observó un patrón de expresión de ambas variantes dependiente del tipo de mutación (Figura 13) reagrupamos la cohorte de pacientes tipo I según la mutación que portaban. La proporción de ambas variantes fue

similar en pacientes de cambio de aminoácido (ratio 1:1; completa: corta). Por su parte, el grupo de pacientes con mutaciones que producen un codón de parada prematura mostró un ratio 2:1 (completa: corta). En cambio, el resto de mutaciones (*splicing*, cambio de la pauta de lectura, pacientes tipo II) presentaron un patrón de expresión como el del grupo control, aproximadamente doble expresión de la variante corta que la completa (1:2). Los datos de este análisis se recogen en la Tabla 16.

Tabla 16: Análisis de la expresión en controles y por tipo mutación.

Grupo	Casos	Núm. copias Variante completa	Núm. copias Variante corta	U Mann-Whitney	Kruskal-Wallis
Controles	25	172.2[14.10-2664]	210.8[11.37-7078]	P=0.1116	0.0099
Cambio de aa	7	280.0[48.05-618.6] **¢£**	218.9[83.49-1034]	P=0.4531	
Stop	4	184.9[128.0-403.8] **¢£**	43.31[8.2-164.3]**¥**	**P=0.0462**	
C. pauta lectura	5	59.36[28.25-256.7] **£**	197.65[31.5-322.2]	P=0.3125	
Splicing	6	63.91[7.9-174.6]**¢**	94.65[39.83-801.8]	P=0.0625	
AEH tipo II	10	238.7[56.8-571.5]	686[108.7-2046] **¥**	**P=0.0078**	
Kruskal-Wallis		***P=0.043***	***P=0.0062***		

Valores expresados en mediana [mínimo-máximo] ¥ indica diferencias estadísticamente significativas entre ambos por el test de Dunn ($p<0.05$). ¢ indica diferencia estadísticamente significativa entre ambos grupos por el test de Dunn ($p<0.05$). £ indica diferencia estadísticamente significativa entre estos grupos según el test de Dunn ($p<0.05$).

Según la base de datos *HGMD* (***H**uman **G**enome **M**utation **D**atabase*) (Stenson et al., 2003), el 43% de las mutaciones asociadas a angioedema hereditario se deben al cambio de un aminoácido. El grupo de pacientes con este tipo de mutación de nuestra serie mostró valores de mediana similares para ambas variantes (ratio 1:1, completa: corta), aunque la dispersión de los valores obtenidos para la variante corta esra mayor que en el resto de los grupos. Este dato en el tipo de mutación más común en la patología nos hizo plantearnos un análisis individualizado en los pacientes con cambio de aminoácido teniendo en cuenta la localización de la mutación a lo largo del gen.

Cuando se estudió el patrón de expresión en función de la localización del cambio pudimos observar que las mutaciones en la región interna del dominio serpina invertían el patrón de expresión de las variantes, favoreciendo la producción de la variante completa en detrimento de la variante corta. Por contra, las mutaciones localizadas en los extremos del dominio serpina, y a lo largo del dominio no serpina, mostraron un patrón de expresión de variantes como el grupo control (variante completa menor que variante corta). Sólo en el paciente GI4 (con el cambio c.1331T>C) rompía la uniformidad del criterio de un patrón de expresión dependiente de la localización del

cambio. Este paciente presentaba un fenotipo de tipo intermedio con niveles de C1INH ligeramente disminuidos (11,6mg/dl), pero funcionalidad muy reducida.

Los datos obtenidos en el grupo de pacientes mayoritario motivaron un replanteamiento del análisis y se estudiaron el resto de los cambios que daban un fenotipo de AEH tipo I según su localización .Tal y como se muestra en la Figura 14, se observó que el patrón de expresión de las mutaciones parecía ser dependiente de la localización de la mutación de la misma forma que lo habíamos observado en las mutaciones de cambio de aminoácido. Con independencia de las consecuencias en la transcripción, las mutaciones en el interior del dominio serpina presentaron ratios de expresión de las variantes invertidos respecto del grupo control (2:1; completa: corta). El patrón de expresión de aquellas mutaciones que se localizaban tanto en los extremos del dominio serpina como a lo largo de todo el extremo no serpina era similar al patrón de expresión de los controles (1:2; completa: corta).

Las mutaciones de cambio de la pauta de lectura recogidas en nuestra serie de pacientes se localizaban en ambos dominios de la proteína. Las dos familias (FU y BN) con alteraciones en el dominio no serpina mantenían el mismo patrón de expresión que el grupo control. Por su parte, los pacientes con este tipo de alteraciones en el dominio serpina (G, GE, Y) presentaron un patrón de expresión de las variantes invertido respecto a controles (2:1).

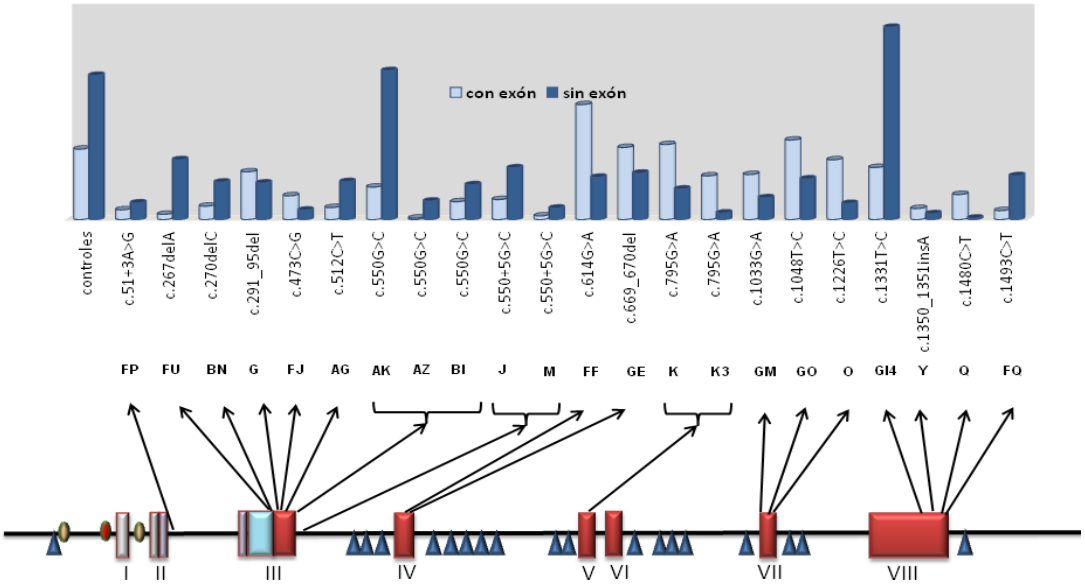

Figura 14. Expresión de las variantes en los pacientes con mutaciones tipo I incluidos en la cohorte. El gráfico de histogramas indica la expresión obtenida en cada paciente. Las flechas indican la localización de la mutación en el ADNc de *SERPING1* (NM_000062.2) para cada paciente.

El paciente FP con mutación de *splicing* e incluido sólo en el estudio del patrón de expresión de las variantes (Tabla 13), portaba la mutación c.51+3A>G localizado a 3 nucleótidos del comienzo del intrón 2. En este paciente la producción obtenida fue de un 10% en el caso de la variante completa y un 14% en el de la variante corta. Este cambio en el inicio del intrón 2 impide que el segundo exón del gen sea incluido en el mensajero maduro (Duponchel et al., 2006). En nuestro estudio sólo detectábamos la producción del alelo salvaje. Esto se debía a que el diseño de la PCR a tiempo real estaba dirigido a la detección de la variante con el exón 3 (completa) y la variante sin exón 3 (corta), los cebadores se diseñaron sobre el exón 2 (Figura 7).

El resto de mutaciones que afectan al *splicing* incluidas en la serie estaban localizaban en el extremo 3´del exón 3 de *SERPING1* (c.550G>C y c.550+5G>C). Estos cambios promueven la no inclusión del exón 3 en el mensajero maduro. Y ese efecto se observó en estos pacientes (AK, AZ, BI, J y M) donde fue mayor la expresión de la variante corta que la variante completa. Se observó una inversión del patrón de expresión de las variantes desde el sitio donador de *splicing* en el intrón 3 que se mantuvo hasta la posición 1480 en el ADNc que se localizaba próximo al extremo carboxilo terminal del dominio serpina. Esta inversión del patrón de expresión no dependía del tipo de mutación. En nuestra serie de pacientes no había ningún caso con mutación de *splicing* entre los exones 4 al 8 que nos permitiese comparar los patrones de expresión de las variantes con los observados en las posiciones c.550 y c.550+5G>C. Sería interesante realizar el mismo análisis en pacientes con mutaciones de *splicing* en exones posteriores para comparar ambos patrones de expresión de variantes.

En el caso de los pacientes tipo II, el análisis individualizado mostró un patrón de expresión igual en todos los casos, con mayor expresión de la variante corta que de la completa. (Figura 15)

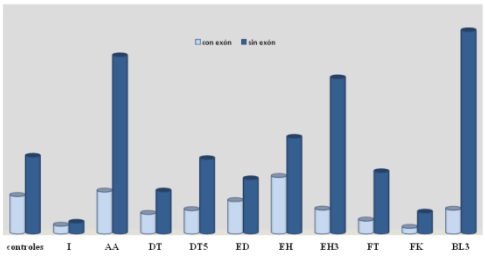

Figura 15. Patrón de expresión de las dos variantes estudiadas en los pacientes con mutaciones tipo II incluidos en la cohorte. El gráfico de histogramas indica la expresión obtenida en cada paciente para la variante completa (relleno azul claro) y para la variante corta (relleno azul oscuro).

9. ESTUDIO DE LA EXPRESION DE *SERPING1* DEPENDIENTE DE TIPO CELULAR.

Estudios de inducción de expresión del gen *SERPING1* en diferentes tipos celulares han mostrado que células hepáticas y monocíticas incrementan la tasa de transcripción de *SERPING1* bajo estímulo con IFN-γ (Lappin et al., 1992, Falus, 1990, Lappin et al., 1990b, Lappin et al., 1990a, Heda et al., 1990, Schmaier et al., 1989). De estas dos poblaciones, las células hepáticas son las mayores productoras del C1-Inh circulante (Zuraw and Lotz, 1990). Es probable que la capacidad de secreción del inhibidor de la esterasa C1 por la población monocítica en sangre periférica pueda tener un papel importante en la regulación de la respuesta inflamatoria a nivel local (Duponchel et al., 2006). Se ha observado que monocitos humanos en cultivo estimulados con dosis entre 0,1 y 100 ng/ml de IFN-γ aumentaban la síntesis de ARN mensajero total de *SERPING1* de forma dependiente de la dosis de IFN-γ (Waddell et al., 2010, Heda et al., 1990, Lappin et al., 1990b, Lappin et al., 1990a). Para conocer cómo la citoquina influye en el patrón de expresión de las variantes previamente analizadas (completa y sin exon 3), se realizó una estimulación con una dosis de 10 ng/ml de IFN-γ en este tipo celular aislado de sangre periférica de donantes sanos.

- Separación inmunomagnética.

Se aislaron por separado las tres poblaciones de interés (monocitos, linfocitos B y linfocitos T) mediante separación positiva con *microbeads* conjugados con anticuerpos específicos de cada población celular. El rendimiento de la separación permitió obtener 10^6 células en la población minoritaria (monocitos y linfocitos B) y $20x10^6$ células en la población mayoritaria (linfocitos T). En el caso de las poblaciones minoritarias con alta pureza (monocitos y linfocitos B) se requirieron varios pases por la columna. En la Figura 16 se muestra un ejemplo de los rendimientos de purificación obtenidos en las poblaciones de interés.

Los estudios se realizaron en 250.000 células de cada población en 250 µl de medio RPMI-1640 y se estimularon con 10 ng/ml de IFN-γ. Se establecieron cuatro puntos de recogida (0, 0.5, 5 y 24 horas). Sólo en el punto de recogida de 24 horas se detectó expresión de ARN mensajero de *SERPING1*.

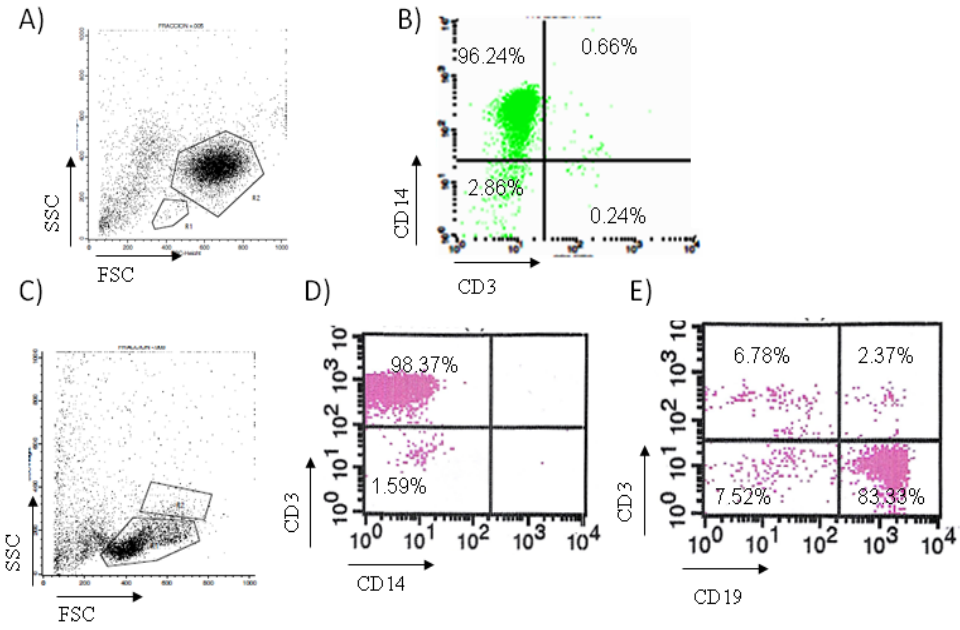

Figura 16. Pureza de la fracción post-enriquecimiento celular. En los *dot plot* se muestran la purezas obtenidas en tras la primera separación inmunomagnética para obtener la población de interés. **A)** *Dot plot* SSC-FSC (morfología-tamaño) de la población monocítica post-separación. **B)** *Dot plot* PE-CD14 frente FITC-CD3 de la población monocítica. **C)** *Dot plot* SSC-FSC de la población PBLs post-separación PercP-CD14 frente FITC-CD3 **D)**, *Dot plot* post-separación de PBLs PercP-CD14 frente FITC-CD3, **E)** *Dot plot* post-separación de PBLs FITC-CD3 frente APC-CD19.

En la población monocítica se obtuvo un incremento de la expresion del ARN mensajero para *SERPING1* en más de tres ordenes de magnitud (1485 copias) respecto al momento de comienzo de estímulo (t=0) (ver Figura 17A). Con la misma concetración de IFN-γ que la adicionada a los monocitos, la población de linfocitos T respondió al estímulo inflamatorio activando la expresión de inhibidor hasta alcanzar 461 copias. Este fue un resultado no esperado, cuando se incluyeron las poblaciones de linfocitos T y B como controles negativos; pues hasta el actual estudio no se conocía que la población de linfocitos T mostrase respuesta a IFN-γ expresando *SERPING1*.

En el análisis de expresión de las variantes (completa y corta), ambas poblaciones (monocitos y linfocitos T) aumentaron la producción de la variante completa a las 24 horas de estímulo con la citoquina proinflamatoria (Figura 17B). En monocitos, se detectaron 920 copias de la variante completa, mientras que la variante corta mostró un ligero aumento de expresión que apenas alcanzó un orden de magnitud (9 copias) respecto a la ausencia del estímulo (ver Figura 17B y Figura 17C). La población de linfocitos T presentó, también, mayores niveles de expresión de la variante completa (76 copias) que de la variante corta con apenas 4 copias (Figura 17B).

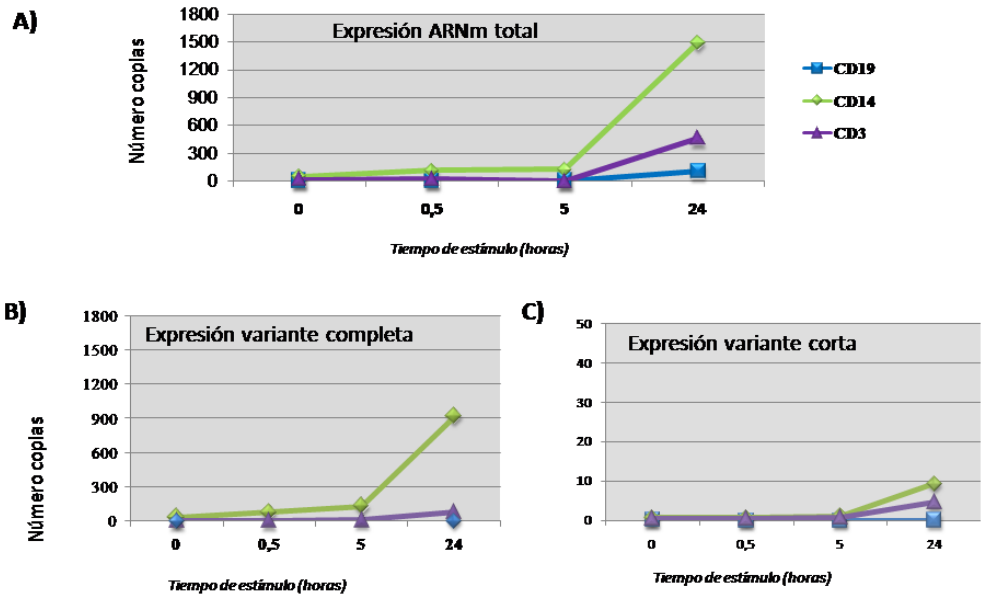

Figura 17. Niveles de expresión del ARNm total de *SERPING1* y sus variantes en las diferentes poblaciones celulares estudiadas. Las graficas muestran diferentes tiempos (t=0, t=30 minutos, t=5 horas y t= 24 horas) de recogida de ARNm en las poblaciones celulares estudiadas **A)** Cuantificación de *SERPING1* total. **B)** Cuantificación de variante completa. **C)** Cuantificación variante corta.

Los resultados obtenidos en la población de linfocitos T para la detección de ARN mensajero de *SERPING1* podrían deberse a la presencia de población monocítica residual en el procedimiento de aislado celular por tanto, estuviéramos observando su respuesta a estímulo con IFN-γ. Para comprobar esa hipótesis, se realizaron dos nuevos ensayos de estimulación en donantes sanos obteniendo purezas del 98%. Los resultados de estimulación, de nuevo, mostraron que la población de linfocitos T respondía al estímulo con la citoquina produciendo ARN de *SERPING1*. Quizás una proporción de linfocitos T podrían presentar inducción de la transcripción de *SERPING1* en respuesta a la citoquina proinflamatoria.

Por otro lado, desde hace unos años se conoce que, compartiendo marcaje en superficie con los linfocitos T de sangre periférica (CD3+), se encuentra una subpoblación de células *Natural Killer* (en adelante NK) conocida como células NKT (con marcaje en superficie CD16+/CD56+/CD3+) (Berzins et al., 2004, Montalvillo et al., 2014). Esta población, al igual que las células NK propiamente dichas, presenta dos perfiles subpoblacionales: Th1 (productor de IFN-γ) y Th2 (productor de IL-4 e IL-13, y con disminución de la producción de IFN-γ) (Geffner and Fainboim, 2008, Montalvillo et al., 2014). En estudios mediante microarrays de expresión en células aisladas de sangre periferica detectaron que células NK estimuladas con 100 U de IFN-γ eran capaces de aumentar la expresión de *SERPING1* (Waddell et al., 2010). Con los datos

obtenidos, nos planteamos la posibilidad de que las células NK tengan capacidad de inducir expresión de *SERPING1* en un entorno inflamatorio.

Se realizó un análisis semicuantitativo de expresión de ARN mensajero de *SERPING1* por PCR de transcripción reversa a partir de 1 µg de ARN de las poblaciones que podrían expresarlo (NK y linfocitos T), así como en líneas celulares de población NK (NKL y NK92, cedidas por el grupo 44 de IdiPAZ, Madrid). Además, se incluyó en el estudio ARN de PBMCs y de la línea HuH-7 (línea celular hepática con expresión de *SERPING1*) que nos servirían como control positivo. Tal y como se muestra en la Figura 18, las mayores producciones de ARN mensajero de *SERPING1* se obtuvieron en población monocítica, en la línea celular de hepatocitos y PBMCs. Por su parte, en linfocitos T se detectó una ligera producción de ARN mensajero de *SERPING1* y en las líneas celulares de NK no se detectó síntesis de mensajero de *SERPING1*. Por este motivo se planteó obtener una fracción extra para separar la población celular NK mediante *microbeads* conjugados con CD56 y estimularla durante 24 horas con 10 ng/ml de IFN-γ, de la misma forma que al resto de las poblaciones.

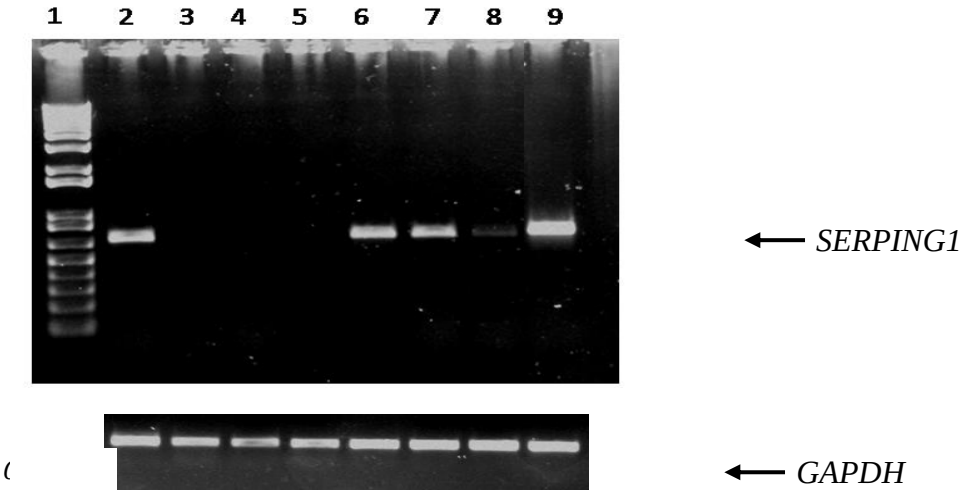

Figura 18: Análisis semicuantitivo de la expresión de *SERPING1* en células de sangre periférica y líneas celulares. Resultado de la RT-PCR a tiempo final de los exones 2 al 5 de C1INH para la detección de la variante completa en diferentes tipos celulares obtenidos por separación inmunomagnetica del donante C62 y de líneas celulares, todos sin estimulación con γ-IFN. ***Carril 1***: marcador 1kb invitrogen; C***arril 2:*** PBMCs; ***Carril 3***: línea celular NKL; ***Carril 4***: línea celular NK92; ***Carril 5*****:** control negativo de PCR; ***Carril 6*****:** Monocitos; ***Carril 7*****:** Natural Killer (NK); C***arril 8***: Linfocitos T; ***Carril 9:*** Línea celular hepática *HuH-7*. En el gel de agarosa inferior se muestra la migración de detección de la expresión de *GAPDH* por RT-PCR de los ochos casos arriba mostrados.

Tras el estímulo durante 24 horas con IFN-γ se recogió el ARN y se cuantificó la expresión de *SERPING1* en las cuatro poblaciones detectándose expresión de *SERPING1* en población monocítica, células NK, linfocitos T. La Figura 19 muestra los niveles de expresión obtenidos para las cuatro poblaciones.

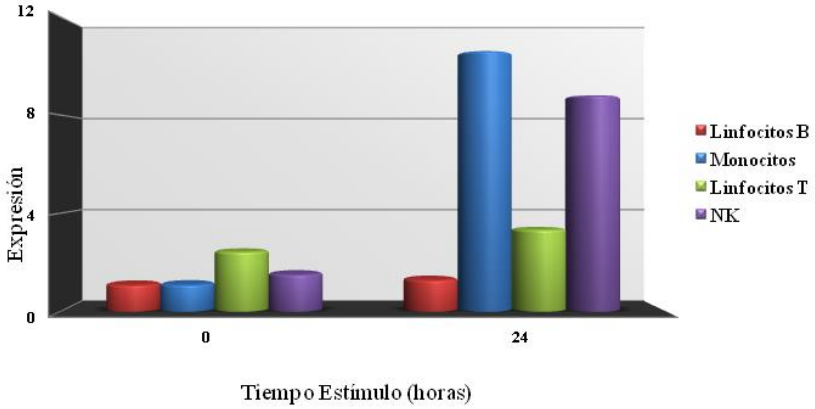

Figura 19. Niveles de expresión del ARNm total de *SERPING1*. La grafica muestra la media de los niveles de expresión de *SERPING1* de los dos pacientes estudiados para las diferentes poblaciones celulares obtenidas en la separación inmunomagnética y estimuladas con 0,01ng/µl de IFN-γ a dos tiempos de recogida de ARNm (t=0 y t= 24 horas).

- Separación por citometría de flujo

Las purezas de la separación inmunomagnética (Figura 16) se habían obtenido tras varios pases a través de la columna y este proceso suponía un rendimiento bajo que obligaba a partir de un mayor volumen de muestra. Además, el tiempo de obtención de las poblaciones resultaba prolongado, pudiendo alterar los resultados por una activación dependiente de estrés. Por tanto, se hacía necesaria una técnica más robusta que nos permitiese obtener mayor rendimiento en la recogida de poblaciones con purezas elevadas, además de que permitiese validar, o no, los datos obtenidos por *microbeads.* La técnica de elección fue la separación por citometría de flujo (*sorting*), por ser una técnica de aislamiento de poblaciones ampliamente utilizada. Esta técnica permitió caracterizar fenotípicamente la muestra a separar y, a su vez, conocer el rendimiento teórico de la separación.

El proceso de separación por citometría de flujo se realizó en dos donantes sanos que participaron en los ensayos realizados con aislamiento celular por *microbeads.* De esta forma se minimizaba la variación interindividual para comparar la expresión de *SERPING1* por ambos abordajes en las poblaciones aisladas.

Para evitar posibles expresiones inespecíficas, durante el desarrollo técnico se debía eliminar todo posible artefacto y/o interferencias como la población plaquetaria o los derivados de la misma, cuya producción de *SERPING1* se conoce desde 1993 (Schmaier et al., 1993, Yin et al., 2008). Con esta finalidad se incluyó un paso de centrifugación previa al gradiente con Ficoll. De esta forma, podríamos obtener la fracción de células mononucleares libre de la fase de plasma rico en plaquetas.

Tabla 17: Panel de marcadores de superficie para la selección celular por enriquecimiento celular.

	CD14-FITC	CD3-PE-Cy7	CD16/56-PE	CD41-APC
Monocitos	+	-	-	-
Linfocitos T	-	+	-	-
NK	-	-	+	-
Monocitos/ plaquetas	+	-	-	+

Se diseñó un panel con marcadores de superficie celular (Tabla 17) que permitía seleccionar la población de monocitos, linfocitos T y NK en tubos de recogida diferentes. También se incluyó un cuarto tubo de recogida donde se seleccionaron aquellos eventos con marcaje tanto para población monocítica (CD14), como para población plaquetaria (CD41) y se denominó co-cultivo monocitos/ plaquetas.

El rendimiento de la técnica ($2x10^6$ células de las poblaciones minoritarias) permitió sembrar 250.000 células/pocillo para cada punto de recogida tras estímulo con IFN-γ (24 y 48 horas). La Figura 20 muestra los resultados de purezas obtenidos en las poblaciones tras la separación por citometría de flujo en el segundo donante sano (C80).

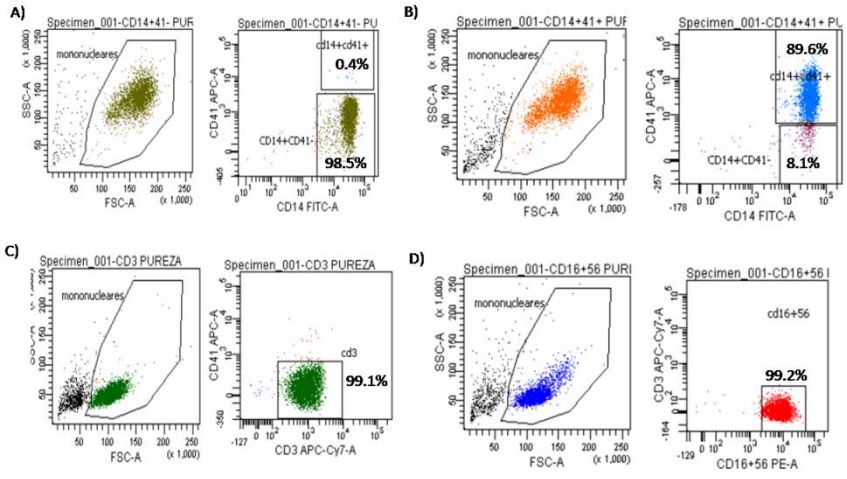

Figura20. Pureza de las fracciones post-enriquecimiento celular por *sorting*. En los *dot plots* se muestra el rendimiento teórico de la separación y las purezas obtenidas reales post-separación. **A)** *Dot plot*s pureza de la población monocítica post-separación. **B)** *Dot plot*s pureza de la población monocítica y plaquetaria post-separación. **C)** *Dot plot*s pureza de la población Linfocitos T post-separación. **D)** *Dot plot*s pureza de la población NK post-separación.

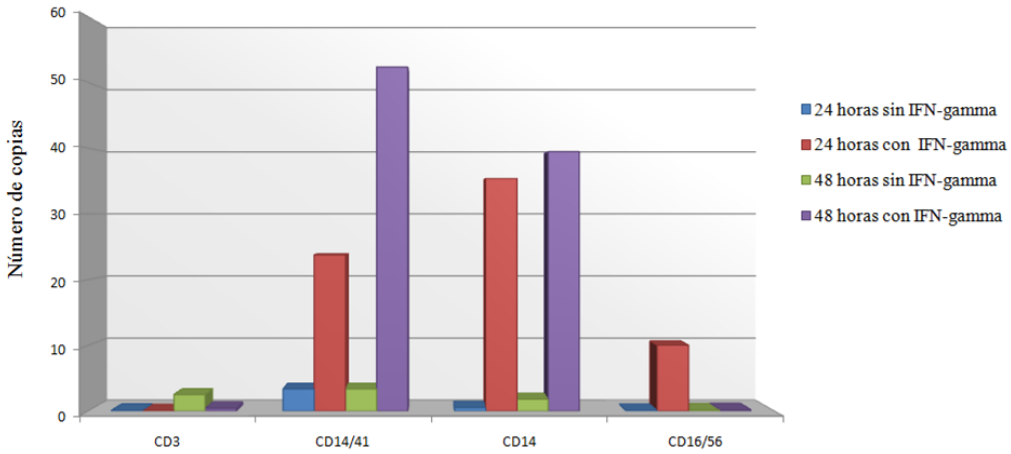

Figura 21: **Niveles expresión de *SERPING1* en diferentes poblaciones celulares separadas por citometría de flujo en dos controles sanos**. La figura indica la media de los niveles de expresión de *SERPING1* en diferentes poblaciones para los dos individuos analizados. La población de monocitos y el co-cultivo de plaquetas-monocitos muestran inducción de la expresión de *SERPING1* bajo estímulo con IFN-γ a 24 y 48 horas. En NK sólo se detecta expresión a 24 horas.

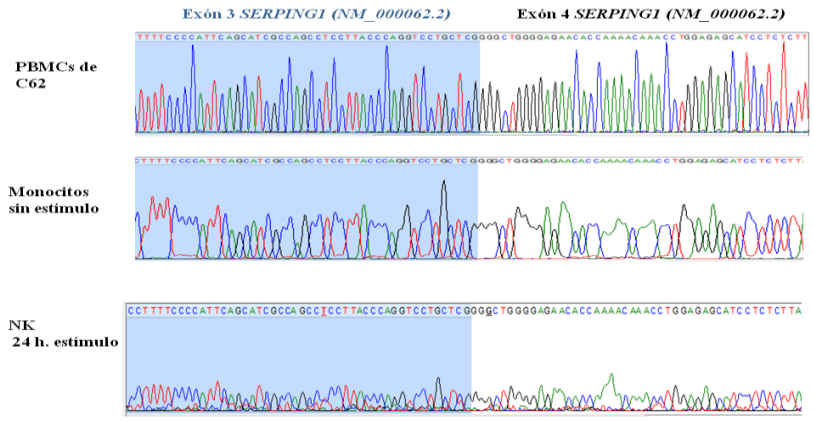

Figura 22: Secuenciación Sanger de los productos purificados obtenidos en qPCR de la variante completa. Los productos purificados de qPCR del fragmento conteniendo los exones 2 al 5 (variante completa) de la población monocítica y NK, ambas separadas por citometría de flujo, se secuenciaron por Sanger. El electroferograma superior procede de la secuenciación del producto de qPCR del ADNc de PBMCs del control C62, muestra con la que se han realizado todas las curvas patrón de los amplificados. Los electroferogramas intermedio e inferior son el resultado de la secuenciación de la población monocítica y de *Natural Killer* , respectivamente. En sombreado azul se indica la secuencia que corresponde al exón 3., seguida dela secuencia del exón 4 (sin sombreado).

Tanto la población de monocitos, como el co-cultivo de monocitos-plaquetas mostraron respuesta al estímulo a las 24 y 48 horas. Además, la respuesta correlacionaba con el tiempo de exposición a la citoquina. A mayor tiempo de exposición, mayor nivel de expresión para la población (ver Figura 21).

La síntesis de mensajero detectada en población monocítica (CD14) estimulada con IFN-γ mostró niveles de expresión similares en los dos puntos de recogida (24 y 48 horas). En cambio, en el co-cultivo de monocitos y plaquetas en el

punto de recogida de 48 horas se detectó el doble número de copias que el mismo cultivo sometido a la citoquina durante 24 horas (ver Figura 21).

La población NK presentó respuesta a estímulo a 24 horas de estimulación con 10 ng/ml de INF-γ (Figura 21), por lo que se repetían los resultados observados en el enriquecimiento inmunomagnético. En el punto de recogida de 48 horas la población de células NK no mostraron respuesta al estímulo.

Para descartar falsos positivos, en todos los casos donde obtuvimos amplificado se secuenciaron los fragmentos obtenidos y el resultado se alineó con el programa Sequencher 4.8 y la base de datos *UCSC Genome Browser* con identidad completa con el gen del inhibidor de C1(*SERPING1*) tal y como muestra la Figura 22 para la variante completa. Nuestros resultados muestran que la población de NK presente en sangre periférica es capaz de inducir la transcripción de *SERPING1* bajo estímulo de IFN-γ durante 24 horas.

Discusión

10. DISCUSION.

10.1. Expresión total de *SERPING1* en pacientes con AEH-C1INH.

AEH-C1INH es una enfermedad con herencia autosómica dominante causada por alteraciones en el gen del inhibidor de C1 (*SERPING1*). Hasta el momento se han asociado con AEH-C1INH más de 230 cambios puntuales a lo largo de *SERPING1*. El 85% de las mutaciones puntuales dan lugar a un fenotipo tipo I, donde la producción de proteína está disminuida por debajo del 50% (Kramer et al., 1993, Prada et al., 1998, Donaldson and Evans, 1963, Donaldson and Rosen, 1964, Johnson et al., 1971, Frank et al., 1976). El restante 15% de los pacientes se incluyen en el tipo II de AEH-C1INH y muestran niveles normales o elevados de C1INH en suero, pero este no es funcional.

En el AEH-C1INH tipo I, la causa radica en mutaciones que pueden estar localizadas a lo largo de todo el gen, menos en la región del centro activo de la proteína (Arg444, Thr445), que es donde se localizan las mutaciones asociadas al AEH-C1INH tipo II.

Diferentes estudios de expresión en pacientes AEH-C1INH tipo I describen que el ARN mensajero está disminuido en los individuos con este fenotipo (Pappalardo et al., 2004, Zahedi et al., 1994, Cumming et al., 2003, Colobran et al., 2014). En nuestra serie, la mayoría de los pacientes tipo I presentó una disminución del 70% en los niveles de expresión respecto al grupo control (Tabla 11). Sólo el grupo de pacientes con codón de parada prematura formado por cuatro individuos presentó una disminución del 45%. El estudio individualizado mostró que la diferencia respecto al resto de los pacientes tipo I podría deberse al efecto del tratamiento. Del grupo de pacientes con codón de parada prematura, los dos individuos sin tratamiento (AI y AP) apenas alcanzaban el 15% de expresión de ARN mensajero total de *SERPING1*, mientras que los pacientes con tratamiento (DR y Q) presentaron niveles similares al grupo control (apartado 7.3). Así, el aumento de la expresión observado en los pacientes con parada prematura se debía a que los dos pacientes con tratamiento presentaron niveles superiores al 50% respecto al grupo control. Nuestros datos muestran, una vez más, el efecto inductor del tratamiento con andrógenos atenuados en la transcripción de *SERPING1* (ver Figura 11).

Estudios previos en nuestro laboratorio analizaron, mediante RT-PCR, la presencia de ambos alelos en el mensajero a partir de ARN de pacientes con diferentes mutaciones que dan fenotipo AEH-C1INH tipo I. Se observó que ambos alelos son

expresados en situación basal en células de sangre periférica de los individuos afectados (Roche et al., 2005b).

Mediante la utilización de la técnica de PCR a tiempo real hemos podido determinar de forma más precisa que la producción de ARN mensajero total de *SERPING1* en estos pacientes en situación basal se encuentra disminuida entre el 90% y el 70% respecto al grupo control.

La observación de coexistencia de dos formas de mensajero (salvaje y mutado), junto con la baja capacidad de producción de mensajero total a nivel basal en los pacientes tipo I podrían suponer una limitación de la capacidad de regular la autoactivación en las cascadas enzimáticas sobre las que actúa el C1INH.

Nuestros datos son una evidencia más de la dominancia negativa del alelo mutado que fue descrita por Kramer como transinhibición del alelo mutado sobre el alelo sano (Kramer et al., 1993). La observación resultó del estudio de la expresión del mensajero de *SERPING1* en un paciente con AEH-C1INH con una deleción del exón 7. En este individuo sólo se producía un 30% del mensajero de *SERPING1* siendo esta producción la suma de ambos alelos, mutado y salvaje. La transinhibición en la expresión del gen podría estar determinada por diferentes mecanismos de regulación transcripcional. Los datos obtenidos en el presente trabajo parecen indicar que los mecanismos celulares que regulan la transcripción podrían estar limitando la producción de mensajero en *SERPING1* en aquellos casos en los que el cambio puntual altera la estructura, o genera una proteína truncada. Este dato fue también observado en la serie analizada por Pappalardo et al. en 2004.

Los pacientes de AEH-C1INH tipo II tienen capacidad de producir niveles normales de proteína o incluso superiores que los controles, pero esta proteína no es funcional. Como consecuencia, el C1INH producido no es capaz de regular la autoactivación de las cascadas enzimáticas sobre las que actúa. En la serie de pacientes incluidos en el actual trabajo se estudió una representación de pacientes clasificados como AEH-C1INH tipo II. El mensajero en estos pacientes no mostró la misma regulación negativa ejercida por el alelo mutado observada en los pacientes tipo I ya que se alcanzaron niveles superiores al 50%.

Debido a que el diseño experimental utilizado se centró en la cuantificación de fragmentos de ARNm de la conexión entre el exón 6 y 7 (ver apartado 4.3.3), en este trabajo no pudimos cuantificar la expresión específica de cada alelo (salvaje y mutado). Pero trabajos anteriores (Pappalardo et al., 2004) han confirmado la expresión de ambos

alelos en los mensajeros de células de sangre periférica de pacientes de AEH-C1INH tipo II. Estos datos sugieren que los niveles de ARN mensajero total obtenidos en los pacientes tipo II estudiados en nuestro laboratorio correspondían a la suma de ambos alelos (salvaje y mutado).

Por otro lado, nuestro grupo de pacientes con AEH-C1INH tipo II presentó niveles de expresión superiores (72% respecto a controles) que el observado en la serie de Pappalardo en 2004 (46% respecto al grupo control). En el grupo de Pappalardo, intentaron minimizar los errores de la técnica mediante dos consideraciones. Por un lado, se recogió el mismo número de PBMCs por individuo. Por otro, se empleó la normalizaron con el antígeno de superficie CD64 (específico de monocitos). Así, se asumió que el mensajero de *SERPING1* detectado procedía únicamente de la población de monocitos (población minoritaria en PBMCs). Aún con estas premisas, ambos grupos hemos observado gran variación interindividual en la cuantificación del mensajero de *SERPING1* en PBMCs, tanto en pacientes como en el grupo control. Esta dispersión de los datos en ambos grupos podría ser la causa de la diferencia de expresión obtenidas en las dos series de pacientes.

Las alteraciones de *SERPING1* que reducen la síntesis de proteína han sido estudiadas previamente (Colobran et al., 2014, Kramer et al., 1993, Roche et al., 2005b, López-Lera et al., 2011). Estos trabajos han propuesto diferentes mecanismos de regulación de la expresión del mensajero (NMD, NSD, NGD, NAC…). La finalidad de todos estos mecanismos celulares es evitar la presencia de un complejo ribosómico problemático en la célula que debe ser resuelto por niveles: (1) un ARNm sin función celular debe ser eliminado. (2) A nivel de traducción, el coste energético que supone a la célula perder ribosomas es demasiado elevado como para no recuperar las subunidades estancadas para las siguientes rondas de traducción y, generada la secuencia polipeptídica, estos mecanismos deben proteger a la célula de la producción de proteína incompleta, o mal plegada, que podría favorecer el aumento de la toxicidad celular por depósitos intracelulares (Shoemaker and Green, 2012).

En los pacientes tipo II, los mecanismos celulares de control de la transcripción no parecen actuar limitando la producción del mensajero producido por el alelo mutado. La evasión a los mecanismos regulatorios de la transcripción por el alelo mutado permite, así, que ambos mensajeros (salvaje y mutado) produzcan C1INH y que este sea secretado.

10.2. Expresión de variantes de *splicing* de *SERPING1*en pacientes con AEH-C1INH.

Partiendo de los hallazgos realizados en 2006 por Duponchel y colaboradores donde describen la existencia de una variante corta de ARNm en la que el exón 3 está ausente, se diseñó una estrategia para la cuantificación de las variantes completa y sin exón 3. Esta última variante corta da lugar a una proteína truncada de 43 aminoácidos, frente a los 500 aminoácidos de la salvaje, y con la secuencia del péptido señal alterada.

Los mensajeros que contienen codones de parada prematuros son reconocidos y degradados por la maquinaria celular a través de un mecanismo conocido como *Nonsense-mediated decay* (NMD). En ciertos casos, el NMD está acoplado al *splicing* como un mecanismo de regulación postranscripcional según el cual, la expresión de proteína de un determinado gen puede bloquearse al inducir en sus mensajeros un patrón de *splicing* improductivo que introduce un codón de parada prematuro e induce secundariamente su degradación (RUST, de *Regulated Unproductive Splicing and Translation*).

Este parece ser el caso de la expresión de *SERPING1* en monocitos humanos. En experimentos con PBMCs humanos de individuos control, la cuantificación de ambas isoformas de ARNm mostró mayor expresión de la variante corta en condiciones basales (ratio 1:2, completa: corta). El proceso de *splicing* está dirigido durante la maduración de mensajeros por la unión de determinadas proteínas de unión al ARN (RBP, de *RNA-Binding Proteins*) a secuencias específicas del pre-ARNm para el control de la producción de formas alternativas que dan lugar al enriquecimiento del transcriptoma (Keren et al., 2010). No todas las células expresan las mismas RBPs debido que están condicionadas por señales de transducción dependiente de entorno interno y externo. De esta forma, cada variante alternativa de un determinado ARNm es producto de la unión del conjunto de RBPs que cada tipo celular expresa (Fu and Ares, 2014). El patrón de RBPs que expresan las células hepáticas podría no ser igual al de PBMCs al encontrarse en entornos diferentes. Unido al diferente patrón celular de las proteínas RBPs es posible que exista un mecanismo dependiente de señales de transducción que module el proceso de maduración de mensajero de *SERPING1* dependiente del entorno. De este modo, los niveles de la proteína funcional podrían regularse a través del *splicing* alternativo observado que produciría una proteína truncada y limitaría la secreción y funcionalidad de C1INH a nivel local.

La ausencia de la variante corta en líneas hepáticas y su presencia en PBMCs debe ser atribuida al ambiente, t8al y como sucede con la expresión de fibronectina, ya que el gen *FN1* (MIM*135600, NG_012196.1, ID: 2335) genera formas de ARN mensajero con diferente número de exones en hepatocitos y fibroblastos. El splicing de fibronectina en fibroblastos da lugar a un mensajero que contiene los exones EIIIA y EIIIB que codifican dominios que interactúan con los receptores de superficie celular de multitud de tipos celulares. En cambio, estos exones no son incluidos en el ARN mensajero de fibronectina de hepatocitos. De ahí, que la fibronectina secretada por hepatocitos no se adhiera a la superficies celulares (Lodish et al., 2000)

En el paciente FP (c.51+3 A>G), el diseño de la detección las dos variantes de ARNm de *SERPING1* (corta y completa) mediante qPCR nos permitió conocer los niveles de expresión aportados por el alelo sano, ya que la localización de los cebadores en la unión de los exones 2 y 3 (detección variante completa), y conexión exones 2 y 4 (detección de variante corta) impedía la cuantificación de todas las formas de ARN mensajero que no portasen el exón 2. De esta forma, la variante con ausencia de los exones 2 y 3 descrita en un paciente por Duponchel como consecuencia de la mutación no pudo ser detectada. En nuestro paciente, la producción del alelo sano no fue superior al 20% respecto al grupo control en ninguna de las dos variantes (apartado 8.3, Figura 14). Estos niveles de expresión del alelo sano muestran, una vez más, una regulación negativa del alelo mutado sobre el salvaje en aquellas mutaciones que afectan a la estructura de la proteína.

Cambios en la secuencia de nucleótidos del mensajero pueden tener un impacto significativo en el balance de expresión de las diferentes isoformas del mensajero de un gen. Este hecho se ha observado en la demencia y Parkinsonismo asociado al cromosoma 17 (FDTP-17) causado por una mutación en *MAPT*, gen que codifica tau. Esta proteína está involucrada en el ensamblaje y estabilidad del microtúbulo y presenta dos variantes que difieren entre ellas en la inclusión o no del exón 10. Mutaciones en el gen pueden alterar el procesado del exón 10 y alterar la relación de las dos variantes de tau (Ward and Cooper, 2010).

En nuestra serie de pacientes con AEH-C1INH tipo I además de observar una expresión de ambas variantes (completa y corta) inferior a lo observado en el grupo control, se observaron dos patrones de expresión diferentes para las dos variantes. En el caso de las mutaciones localizadas en posiciones que afectan al dominio no serpina y a los extremos del domino serpina, el patrón de expresión de las variantes observado fue

el mismo que en el grupo control (ratio 1:2, completa:corta). En cambio, las mutaciones localizadas dentro del dominio serpina mostraron un ratio invertido (2:1; completa: corta). Por su parte, el ratio entre variantes en los pacientes tipo II fue en todos los casos como en el grupo control (ratio 1:2, completa: corta). Ver Tabla 16.

En la conformación nativa de C1INH, ambos dominios están estabilizados tridimensionalmente por dos puentes disulfuro uniendo la cisteína 101 a la cisteína 406, y la cisteína 108 a la cisteína 183. Mientras que las dos primeras se localizan en el dominio no serpina, único de la serpina C1INH, Cys183 y Cys406 forman parte del dominio serpina, homólogo al resto de la familia serpina. Estudios publicados por Bos y colaboradores, en 2003, muestran cómo mutaciones en las cisteínas 101 y 108, o en aminoácidos próximos, desestabilizan el dominio serpina permitiendo que la lámina-β central quede al descubierto. De esta forma, el bucle del centro reactivo escindido puede desplazarse sobre la lámina-β acompañado del cambio conformación hacia la forma latente, con capacidad de formar polímeros. Lo mismo se ha observado en otras serpinas como la antitrombina (ATIII) (Bos et al., 2003, Huntington, 2011). En el caso de ATIII, la heparina se une a las cisteínas implicadas en los puentes disulfuro del dominio no serpina de ATIII e impide la formación de agregados producidos por la unión de las formas latentes. En ausencia de heparina, ATIII es menos estable que C1INH. Bos propone que en el caso de C1INH debe haber un mecanismo de modulación constitutivo y diferente al observado en otras serpinas.

El diferente patrón de expresión de ambas variantes del ARN mensajero de *SERPING1* observado en nuestra serie de pacientes tipo I podría estar mostrando un mecanismo post- transcripcional que module la maduración del mensajero hacia formas aberrantes que sean degradas. Para comprobar esta hipótesis serían necesarios estudios *in vitro* bajo entorno inflamatorio con células de pacientes portadores de mutaciones.

En los pacientes tipo II, ambas variantes mostraron niveles de expresión mayores que en los del tipo I y del grupo control. Este dato parece discrepar con lo obtenido en el estudio de la cuantificación del ARN total de *SERPING1*, pero las base de datos *Ensembl* y *AceView* (NCBI), basándose en secuencias de *Homo sapiens* recogidas en *GenBank, dbEST, Trace* y *SRA*, apoyan que el proceso de *splicing* en *SERPING1* da lugar, al menos, a 16 variantes alternativas. Una de estas variantes (*ENST00000528996*) contiene sólo los exones del 5 al 8. Esta variante, así como otras similares que puedan existir, también habría sido cuantificada cuando se estudió el ARNm total pero no en el análisis de variantes. Estudios futuros del transcriptoma

podrían incrementar el número de variantes de *SERPING1*. En nuestro trabajo aportamos una aproximación a la comprensión de la expresión de dos de las isoformas detectadas en células de sangre periférica (completa y sin exón 3). Bajo esta premisa, los datos obtenidos para la expresión de las variantes corta y completa debe entenderse como una parte de la expresión de SERPING1 detectada en el primer objetivo (apartado 7).

10.3. Efecto del tratamiento en la expresión de *SERPING1* en pacientes con AEH-C1INH.

El efecto del tratamiento con andrógenos atenuados y/o antifibrinolíticos se cuantifica comparando individuos tratados y no tratados, portadores todos ellos, de una misma mutación. Los pacientes de nuestra serie con la misma mutación de codón de parada prematura (c.1480C>T) mostraron niveles mayores de expresión de *SERPING1* si estaban tratados en el momento de la extracción de la muestra (niveles de expresión cercanos a los controles). En cambio, los pacientes con la mutación c.1480C>T no tratados no superaron el 10% de expresión respecto al grupo control. En los análisis se observa que los niveles de expresión en los pacientes con AEH-C1INH son significativamente dependientes del tratamiento.

Diferentes abordajes ya han demostrado que la administración de andrógenos atenuados aumenta la expresión de ARN mensajero de *SERPING1* en PBMCs de pacientes AEH-C1INH. Pappalardo y colaboradores en 2003 realizaron un seguimiento en dos pacientes sometidos a 400 mg por día de danazol durante un mes que perrmitió comprobar un aumento de hasta el 91% en los niveles de mensajero de estos pacientes (Pappalardo et al., 2003). Aunque no se ha demostrado la existencia de receptores de andrógenos en monocitos circulantes, sí se ha observado que la administración de danazol disminuye la expresión de receptores estrogénicos en PBMCs (Pappalardo et al., 2003). Con estos resultados, Pappalardo postuló un posible efecto negativo de los estrógenos sobre la expresión de *SERPING1*. Este efecto podría ser contrarrestado por la administración de danazol, el cual reduciría la síntesis de receptores estrogénicos en los monocitos aumentando la síntesis local del ARN mensajero de *SERPING1*.

10.4. Expresión de *SERPING1* dependiente de tipo celular.

La población de monocitos, dentro de las células blancas, es un subconjunto con posibilidad de diferenciarse a macrófagos y a células dendríticas específicas de tejido

(Shi and Pamer, 2011). En el laboratorio, cuando una población monocítica se cultiva durante 7 días en presencia de suero humano, se diferencia a macrófago (Andreesen and Kreutz, 1994). El estadio de macrófagos es el elegido por la mayoría de estudios de expresión de *SERPING1* bajo entorno inflamatorio con monocitos en cultivo *in vitro* (Lotz and Zuraw, 1987, Duponchel et al., 2006, Bensa et al., 1983).

En nuestro laboratorio se pretendió estudiar la respuesta a IFN-γ de dos variantes alternativas de *splicing* en la población monocítica previa a su diferenciación a macrófago. Para realizar el análisis se estudió la expresión de *SERPING1* en cultivos de monocitos de donantes sanos aislados 24 horas antes del comienzo del estímulo inflamatorio.

Nuestros estudios muestran que, en un entorno inflamatorio, la población monocítica aislada mediante separación inmunomagnética presenta un aumento de expresión de mensajero suficientemente detectable tras cinco horas de estimulación. Este aumento perduró hasta la finalización del ensayo de inflamación a las 24 horas. Además, en individuos sanos, el IFN-γ induce en mayor grado la expresión de la forma completa frente a la forma sin exón 3 (Figura 17). Este patrón esta invertido respecto a la situación basal, de tal modo que se favorece la producción y secreción del inhibidor de C1 funcional por estas células.

En la separación por citometría de flujo, tanto la población de monocitos y el co-cultivo de monocitos-plaquetas mostraron un aumento de los niveles de expresión de *SERPING1* cuando el estímulo permanecía durante 24 y/o 48 horas. Estas poblaciones fueron las únicas donde se detectó leve secreción de proteína mediante la técnica de ELISA. Es posible que la concentración de IFN-γ (10 ng/ml) y/o los tiempos de exposición a los que se sometieron las poblaciones aisladas fuesen demasiado cortos como para alcanzar una concentración de proteína detectable por estas técnicas.

El aumento de la transcripción de *SERPING1* en monocitos, como en plaquetas y micropartículas de plaquetas en respuesta a IFN-γ ha sido previamente descrito (Lappin et al., 1992, Lotz and Zuraw, 1987, Prada et al., 1998, Zahedi et al., 1993, Zahedi et al., 1994, Yin et al., 2008). El IFN‑γ actúa como interruptor para la diferenciación de monocitos a macrófagos en los estadios tempranos de la respuesta inmune (Delneste et al., 2003). A nivel local, esta diferenciación tiene gran importancia, ya que favorece la fagocitosis y la presentación de antígenos a los linfocitos T.

Como se observa en la Figura 21, la población monocítica no fue la única que respondió al estímulo con IFN-γ. A una dosis de 10 ng/ml, la población de *Natural*

Killer (NK, con marcadores de superficie CD14-/CD19-/CD3-/CD16+/CD56+) mostró un ligero aumento de la producción del mensajero de *SERPING1* tras las primeras 24 horas de estímulo inflamatorio. Los estudios mediante RT-PCR a tiempo final realizados por otros grupos hasta el momento habían concluido que los monocitos eran los únicos productores de C1INH en respuesta a inflamación en PBMCs (Randazzo et al., 1985, Lotz and Zuraw, 1987, Lappin et al., 1992). La RT-PCR a tiempo final es una técnica semicuantitiva y no es capaz de detectar pequeñas variaciones. Es, posiblemente, el uso de una técnica más sensible que RT-PCR a tiempo final lo que nos ha permitido detectar respuesta a estímulo por IFN-γ en la población de células NK. En 2010, la utilización de la técnica de arrays de expresión en el análisis transcripcional de las poblaciones celulares de PBMCs (linfocitos T $CD4^+$ y $CD8^+$, linfocitos B, células NK y monocitos) tratadas con IFN-γ, detectó un aumento de expresión de mensajero de *SERPING1* en poblaciones celulares de sangre periférica distintas de monocitos (Waddell et al., 2010).

Las células NK son linfocitos multicompetentes con capacidad de regular las respuestas inmunes de forma adaptativa e innata. La subpoblación conocida como NKT comparte marcadores de superficie con la población linfocitaria CD3+ (Poli et al., 2009, Vivier et al., 2008). Por eso, al compartir ambas poblaciones marcadores en superficie, es posible que en los primeros abordajes de enriquecimiento celular por *microbeads*, la población NKT fuese incluida como población de linfocitos T.

Las células NK humanas están subdividas en diferentes poblaciones en función de la presencia de los marcadores de superficie CD56 y CD16. Las poblaciones mayoritarias de este tipo celular son $CD56^{Bright}$ $CD16^-$ y $CD56^{dim}$ $CD16^+$. Se ha observado que las células NK $CD56^{bright}$ tiene capacidad de expresar proteínas reguladoras del complemento como CD55 y CD59 en elevadas cantidades (Poli et al., 2009). De la misma forma que se liberan estos reguladores, se podría estar liberando el mayor regulador de la activación de la vía clásica en las etapas tempranas de respuesta a inflamación. Las células $CD56^{Bright}$ colonizan preferentemente los órganos linfoides secundarios, mientras que la población $CD56^{dim}$ migra hacia lugares de ataque inflamatorio agudo. Durante el proceso de migración a los tejidos y órganos de destino, ambas coexisten en el torrente sanguíneo, pero diferentes estudios han mostrado que el 90% de la población de NK circulante está formado por el fenotipo $CD56^{dim}$ (Lünemann et al., 2011). Los datos obtenidos de la población de NK aisladas de sangre periférica, donde la producción de ARN mensajero de *SERPING1* por parte de la población NK se

produce a tiempos cortos, podrían indicar un cambio de fenotipo en esta población. Para comprobar esta hipótesis se requiere un estudio de caracterización fenotípica más detallado que permita una caracterización de ambas poblaciones tanto pre-estimulación como post-estimulación

En nuestro laboratorio se ha realizado *Western blot* y ELISA para detectar proteína en sobrenadantes y lisados celulares estimulados con 10 ng/ml de la citoquina, sin detectarse C1INH en ninguno los dos abordajes. Lappin, en 1992, realizó estudios de expresión inducida con IFN-γ (100 ng/ml) en diferentes tipos celulares entre los que incluyó monocitos. La concentración de IFN-γ debe ser un punto a tener en cuenta para futuros ensayos donde el objetivo sea la detección de proteína.

Estudios de expresión de mensajero de *SERPING1* como los realizados en los controles deberían realizarse en pacientes para comprobar si la población NK responde de igual forma a un estímulo de 24 horas con γ-IFN.

Por último, el hecho de detectar expresión de *SERPING1* en dos poblaciones de sangre periférica (monocitos y NK) que se presentan en proporciones muy variables puede explicar la enorme dispersión de los datos observados en las dos series de pacientes analizadas en este trabajo y las de otros grupos. Nuestros datos sugieren que los estudios posteriores deben tener en cuenta la proporción de ambas poblaciones en cada medición.

Conclusiones

1. En pacientes AEH-C1INH tipo I, los individuos heterocigotos manifiestan la patología porque el alelo sano es incapaz de producir suficiente expresión de *SERPING1*; ya que la presencia de un alelo mutado ejerce dominancia negativa sobre la expresión del ARN mensajero total del gen.

2. En pacientes con AEH-C1INH tipo I y en ausencia de señales proinflamatorias, la localización de la mutación determina el patrón de expresión de las dos variantes de mensajero estudiadas: si la mutación se localiza en el interior del dominio serpina, la variante con mayor expresión es la forma completa; mientras que si la mutación ocurre en el dominio no serpina o en los extremos del dominio serpina, se mantiene el mismo patrón que el observado en los controles (mayor expresión de la variante corta que de la variante completa)

3. Los pacientes con AEH-C1INH tipo II de nuestra serie mostraron una expresión de mensajero total superior al 50% respecto a controles, de lo que se deduce que la presencia de una mutación en las inmediaciones del centro activo de la proteína no ejerce dominancia negativa sobre la transcripción del gen.

4. En pacientes con AEH-C1INH tipo II y en ausencia de estímulo proinflamatorio, la producción de las variantes de *splicing* estudiadas es similar o mayor que en controles, y sigue el mismo patrón en los dos grupos de individuos. Este comportamiento indica que en estos pacientes la transcripción de *SERPING*1 puede estar aumentada.

5. De las cuatro poblaciones aisladas en los donantes sanos por la metodología de separación inmunomagnética (monocitos, linfocitos T, linfocitos B y células NK), sólo la población de monocitos y la de células NK respondieron a la estimulación con IFN-γ durante 24 horas produciendo mensajero de *SERPING1*.

6. En dos donantes sanos, el co-cultivo de monocitos y plaquetas mostró niveles de ARN mensajero para *SERPING1* mayores que los observados en cultivos aislados de monocitos. Este dato es relevante, ya que el aporte de las plaquetas deberá ser tenido en cuenta para el diseño y análisis de resultados de futuros experimentos de expresión de *SERPING1*.

7. En células NK de dos donantes sanos aisladas por citometría de flujo se observó expresión de *SERPING1* tras un estímulo con IFN-γ a las 24 horas. Parece necesario caracterizar la población de células NK post estímulo para descartar un posible cambio de fenotipo en esta población.

8. Este estudio ha sido desarrollado en donantes sanos, pero sería necesario realizar un ensayo con estímulo con IFN-γ en pacientes con AEH-C1INH para conocer el patrón de expresión de ambas variantes (completa y corta) en respuesta a inflamación.

Bibliografía

Abramowitz, N., Schechter, I. and Berger, A. (1967) 'On the size of the active site in proteases. II. Carboxypeptidase-A', *Biochem Biophys Res Commun,* 29(6), pp. 862-7.

Agostoni, A., Aygören-Pürsün, E., Binkley, K. E., Blanch, A., Bork, K., Bouillet, L., Bucher, C., Castaldo, A. J., Cicardi, M., Davis, A. E., De Carolis, C., Drouet, C., Duponchel, C., Farkas, H., Fáy, K., Fekete, B., Fischer, B., Fontana, L., Füst, G., Giacomelli, R., Gröner, A., Hack, C. E., Harmat, G., Jakenfelds, J., Juers, M., Kalmár, L., Kaposi, P. N., Karádi, I., Kitzinger, A., Kollár, T., Kreuz, W., Lakatos, P., Longhurst, H. J., Lopez-Trascasa, M., Martinez-Saguer, I., Monnier, N., Nagy, I., Németh, E., Nielsen, E. W., Nuijens, J. H., O'grady, C., Pappalardo, E., Penna, V., Perricone, C., Perricone, R., Rauch, U., Roche, O., Rusicke, E., Späth, P. J., Szendei, G., Takács, E., Tordai, A., Truedsson, L., Varga, L., Visy, B., Williams, K., Zanichelli, A. and Zingale, L. (2004) 'Hereditary and acquired angioedema: problems and progress: proceedings of the third C1 esterase inhibitor deficiency workshop and beyond', *J Allergy Clin Immunol,* 114(3 Suppl), pp. S51-131.

Agostoni, A., Bergamaschini, L., Martignoni, G., Cicardi, M. and Marasini, B. (1980a) 'Treatment of acute attacks of hereditary angioedema with C1-inhibitor concentrate', *Ann Allergy,* 44(5), pp. 299-301.

Agostoni, A. and Cicardi, M. (1992) 'Hereditary and acquired C1-inhibitor deficiency: biological and clinical characteristics in 235 patients', *Medicine (Baltimore),* 71(4), pp. 206-15.

Agostoni, A., Cicardi, M., Martignoni, G. C., Bergamaschini, L. and Marasini, B. (1980b) 'Danazol and stanozolol in long-term prophylactic treatment of hereditary angioedema', *J Allergy Clin Immunol,* 65(1), pp. 75-9.

Andreesen, R. and Kreutz, M. (1994) 'Differentiation of Human Monocytes In Vitro: A Model of Macrophage Ontogeny', in Graf, N.E.F.H. (ed.) *Cell Culture in Pharmaceutical Research.* Ernst Schering Research Foundation Workshop ed, pp. pp 9-27

Ariga, T., Carter, P. E. and Davis, A. E. (1990) 'Recombinations between Alu repeat sequences that result in partial deletions within the C1 inhibitor gene', *Genomics,* 8(4), pp. 607-13.

Bafunno, V., Divella, C., Sessa, F., Tiscia, G. L., Castellano, G., Gesualdo, L., Margaglione, M. and Montinaro, V. (2013) 'De novo homozygous mutation of the C1 inhibitor gene in a patient with hereditary angioedema', *J Allergy Clin Immunol,* 132(3), pp. 748-750.e3.

Bensa, J. C., Reboul, A. and Colomb, M. G. (1983) 'Biosynthesis in vitro of complement subcomponents C1q, C1s and C1 inhibitor by resting and stimulated human monocytes', *Biochem J,* 216(2), pp. 385-92.

Bergamaschini, L., Miedico, A., Cicardi, M., Coppola, R., Faioni, E. N. and Agostoni, A. (1999) 'Consumption of C4b-binding protein (C4BP) during in vivo activation of the classical complement pathway', *Clin Exp Immunol,* 116(2), pp. 220-4.

Berzins, S. P., Uldrich, A. P., Pellicci, D. G., McNab, F., Hayakawa, Y., Smyth, M. J. and Godfrey, D. I. (2004) 'Parallels and distinctions between T and NKT cell development in the thymus', *Immunol Cell Biol,* 82(3), pp. 269-75.

Bhoola, K. D., Figueroa, C. D. and Worthy, K. (1992) 'Bioregulation of kinins: kallikreins, kininogens, and kininases', *Pharmacol Rev,* 44(1), pp. 1-80.

Binkley, K. E. and Davis, A. (2000) 'Clinical, biochemical, and genetic characterization of a novel estrogen-dependent inherited form of angioedema', *J Allergy Clin Immunol,* 106(3), pp. 546-50.

Blair, P. and Flaumenhaft, R. (2009) 'Platelet alpha-granules: basic biology and clinical correlates', *Blood Rev,* 23(4), pp. 177-89.

Blanch, A., Roche, O., Urrutia, I., Gamboa, P., Fontán, G. and López-Trascasa, M. (2006) 'First case of homozygous C1 inhibitor deficiency', *J Allergy Clin Immunol,* 118(6), pp. 1330-5.

Bork, K. and Barnstedt, S. E. (2001) 'Treatment of 193 episodes of laryngeal edema with C1 inhibitor concentrate in patients with hereditary angioedema', *Arch Intern Med,* 161(5), pp. 714-8.

Bork, K., Barnstedt, S. E., Koch, P. and Traupe, H. (2000) 'Hereditary angioedema with normal C1-inhibitor activity in women', *Lancet,* 356(9225), pp. 213-7.

Bork, K., Wulff, K., Hardt, J., Witzke, G. and Staubach, P. (2009) 'Hereditary angioedema caused by missense mutations in the factor XII gene: clinical features, trigger factors, and therapy', *J Allergy Clin Immunol,* 124(1), pp. 129-34.

Bos, I. G., Lubbers, Y. T., Roem, D., Abrahams, J. P., Hack, C. E. and Eldering, E. (2003) 'The functional integrity of the serpin domain of C1-inhibitor depends on the unique N-terminal domain, as revealed by a pathological mutant', *J Biol Chem,* 278(32), pp. 29463-70.

Bucher, P. and Trifonov, E. N. (1986) 'Compilation and analysis of eukaryotic POL II promoter sequences', *Nucleic Acids Res,* 14(24), pp. 10009-26.

Bustin, S. A., Benes, V., Garson, J. A., Hellemans, J., Huggett, J., Kubista, M., Mueller, R., Nolan, T., Pfaffl, M. W., Shipley, G. L., Vandesompele, J. and Wittwer, C. T. (2009) 'The MIQE guidelines: minimum information for publication of quantitative real-time PCR experiments', *Clin Chem,* 55(4), pp. 611-22.

Büyüköztürk, S., Eroğlu, B. K., Gelincik, A., Uzümcü, A., Ozşeker, F., Colakoğlu, B., Dal, M. and Uyguner, Z. O. (2009) 'A Turkish family with a novel mutation in the promoter region of the C1 inhibitor gene', *J Allergy Clin Immunol,* 123(4), pp. 962-4.

Caballero, T., Farkas, H., Bouillet, L., Bowen, T., Gompel, A., Fagerberg, C., Bjökander, J., Bork, K., Bygum, A., Cicardi, M., de Carolis, C., Frank, M., Gooi, J. H., Longhurst, H., Martínez-Saguer, I., Nielsen, E. W., Obtulowitz, K., Perricone, R., Prior, N. and Group, C.-.-I. D. W. (2012) 'International consensus and practical guidelines on the gynecologic and obstetric management of female patients with hereditary angioedema caused by C1 inhibitor deficiency', *J Allergy Clin Immunol,* 129(2), pp. 308-20.

Caldwell, J., Ruddy, S., Schur, P. and Austen, K. 1972. Acquired C1 inhibitor deficiency in lymphosarcoma Clin Immunol Immunopathol.

Caliezi, C., Wuillemin, W. A., Zeerleder, S., Redondo, M., Eisele, B. and Hack, C. E. (2000) 'C1-Esterase inhibitor: an anti-inflammatory agent and its potential use in the treatment of diseases other than hereditary angioedema', *Pharmacol Rev,* 52(1), pp. 91-112.

Carter, P. E., Duponchel, C., Tosi, M. and Fothergill, J. E. (1991) 'Complete nucleotide sequence of the gene for human C1 inhibitor with an unusually high density of Alu elements', *Eur J Biochem,* 197(2), pp. 301-8.

Cerletti, C., Tamburrelli, C., Izzi, B., Gianfagna, F. and de Gaetano, G. (2012) 'Platelet-leukocyte interactions in thrombosis', *Thromb Res,* 129(3), pp. 263-6.

Chomczynski, P. (1993) 'A reagent for the single-step simultaneous isolation of RNA, DNA and proteins from cell and tissue samples', *Biotechniques,* 15(3), pp. 532-4, 536-7.

Chomczynski, P. and Sacchi, N. (1987) 'Single-step method of RNA isolation by acid guanidinium thiocyanate-phenol-chloroform extraction', *Anal Biochem,* 162(1), pp. 156-9.

Chomczynski, P. and Sacchi, N. (2006) 'The single-step method of RNA isolation by acid guanidinium thiocyanate-phenol-chloroform extraction: twenty-something years on', *Nat Protoc,* 1(2), pp. 581-5.

Cicardi, M., Aberer, W., Banerji, A., Bas, M., Bernstein, J. A., Bork, K., Caballero, T., Farkas, H., Grumach, A., Kaplan, A. P., Riedl, M. A., Triggiani, M., Zanichelli, A., Zuraw, B. and Immunology), H. u. t. p. o. E. E. A. o. A. a. C. (2014) 'Classification, diagnosis, and approach to treatment for angioedema: consensus report from the Hereditary Angioedema International Working Group', *Allergy,* 69(5), pp. 602-16.

Cicardi, M., Bork, K., Caballero, T., Craig, T., Li, H. H., Longhurst, H., Reshef, A., Zuraw, B. and Group), H. H. A. I. W. (2012) 'Evidence-based recommendations for the therapeutic management of angioedema owing to hereditary C1 inhibitor deficiency: consensus report of an International Working Group', *Allergy,* 67(2), pp. 147-57.

Cichon, S., Martin, L., Hennies, H. C., Müller, F., Van Driessche, K., Karpushova, A., Stevens, W., Colombo, R., Renné, T., Drouet, C., Bork, K. and Nöthen, M. M. (2006) 'Increased activity of coagulation factor XII (Hageman factor) causes hereditary angioedema type III', *Am J Hum Genet,* 79(6), pp. 1098-104.

Colman, R. W. (1999) 'Biologic activities of the contact factors in vivo--potentiation of hypotension, inflammation, and fibrinolysis, and inhibition of cell adhesion, angiogenesis and thrombosis', *Thromb Haemost,* 82(6), pp. 1568-77.

Colman, R. W., White, J. V., Scovell, S., Stadnicki, A. and Sartor, R. B. (1999) 'Kininogens are antithrombotic proteins In vivo', *Arterioscler Thromb Vasc Biol,* 19(9), pp. 2245-50.

Colobran, R., Lois, S., de la Cruz, X., Pujol-Borrell, R., Hernández-González, M. and Guilarte, M. (2014) 'Identification and characterization of a novel splice site mutation in the SERPING1 gene in a family with hereditary angioedema', *Clin Immunol,* 150(2), pp. 143-8.

Coppola, L., Guastafierro, S., Verrazzo, G., Coppola, A., De Lucia, D. and Tirelli, A. (2002) 'C1 inhibitor infusion modifies platelet activity in hereditary angioedema patients', *Arch Pathol Lab Med,* 126(7), pp. 842-5.

Cugno, M., Cicardi, M., Coppola, R. and Agostoni, A. (1996) 'Activation of factor XII and cleavage of high molecular weight kininogen during acute attacks in hereditary and acquired C1-inhibitor deficiencies', *Immunopharmacology,* 33(1-3), pp. 361-4.

Cumming, S. A., Halsall, D. J., Ewan, P. W. and Lomas, D. A. (2003) 'The effect of sequence variations within the coding region of the C1 inhibitor gene on disease expression and protein function in families with hereditary angio-oedema', *J Med Genet,* 40(10), pp. e114.

Davis, A. E. (2005) 'The pathophysiology of hereditary angioedema', *Clin Immunol,* 114(1), pp. 3-9.

Davis, T. L., Firulli, A. B. and Kinniburgh, A. J. (1989) 'Ribonucleoprotein and protein factors bind to an H-DNA-forming c-myc DNA element: possible regulators of the c-myc gene', *Proc Natl Acad Sci U S A,* 86(24), pp. 9682-6.

de la Cruz, R. M., López-Lera, A. and López-Trascasa, M. (2012) 'Analysis of SERPING1 expression on hereditary angioedema patients: quantitative analysis of full-length and exon 3 splicing variants', *Immunol Lett,* 141(2), pp. 158-64.

Delneste, Y., Charbonnier, P., Herbault, N., Magistrelli, G., Caron, G., Bonnefoy, J. Y. and Jeannin, P. (2003) 'Interferon-gamma switches monocyte differentiation from dendritic cells to macrophages', *Blood,* 101(1), pp. 143-50.

Donaldson, V. H. and Evans, R. R. (1963) 'A biochemichal Abnormality in hereditary angioneurotic edema:absence of serum of C´1-esterase.', *Am J Med,* 35, pp. 37-44.

Donaldson, V. H. and Rosen, F. S. (1964) 'Action of complement in hereditary angioneurotic edema: The role of C´1-esterase.', *J Clin Invest,* 43, pp. 2204-13.

Donaldson, V. H. and Rosen, F. S. (1966) 'Hereditary angioneurotic edema: a clinical survey', *Pediatrics,* 37(6), pp. 1017-27.

Duponchel, C., Djenouhat, K., Frémeaux-Bacchi, V., Monnier, N., Drouet, C. and Tosi, M. (2006) 'Functional analysis of splicing mutations and of an exon 2 polymorphic variant of SERPING1/C1NH', *Hum Mutat,* 27(3), pp. 295-6.

Egidio Fabiani, J., Squiquera, L., Leoni, J., Simkin, G. and Casala, A. (1987) '[Hereditary angioedema: changes in serum levels of C4 in response to danazol]', *Med Cutan Ibero Lat Am,* 15(6), pp. 461-7.

Fabiani, J. E., Paulin, P., Simkin, G., Leoni, J., Palombarani, S. and Squiquera, L. (1989) '[Hereditary angioedema. Effect of danazol on C4 and functional C1INH]', *Rev Alerg Mex,* 36(3), pp. 99-104.

Fabiani, J. E., Paulin, P., Simkin, G., Leoni, J., Palombarani, S. and Squiquera, L. (1990) 'Hereditary angioedema: therapeutic effect of danazol on C4 and C1 esterase inhibitors', *Ann Allergy,* 64(4), pp. 388-92.

Falus, A. (1990) 'Regulation of complement biosynthesis by tissue-specific and hormonal factors', *Immunol Lett,* 24(4), pp. 227-30; discussion 231-2.

Falus, A., Fehér, K. G., Walcz, E., Brozik, M., Füst, G., Hidvégi, T., Fehér, T. and Merétey, K. (1990a) 'Hormonal regulation of complement biosynthesis in human cell lines--I. Androgens and gamma-interferon stimulate the biosynthesis and gene expression of C1 inhibitor in human cell lines U937 and HepG2', *Mol Immunol,* 27(2), pp. 191-5.

Falus, A., Rokita, H., Walcz, E., Brozik, M., Hidvégi, T. and Merétey, K. (1990b) 'Hormonal regulation of complement biosynthesis in human cell lines--II. Upregulation of the biosynthesis of complement components C3, factor B and C1 inhibitor by interleukin-6 and interleukin-1 in human hepatoma cell line', *Mol Immunol,* 27(2), pp. 197-201.

Farkas, H., Gyeney, L., Gidófalvy, E., Füst, G. and Varga, L. (1999) 'The efficacy of short-term danazol prophylaxis in hereditary angioedema patients undergoing maxillofacial and dental procedures', *J Oral Maxillofac Surg,* 57(4), pp. 404-8.

Frank, M. M., Gelfand, J. A. and Atkinson, J. P. (1976) 'Hereditary angioedema: the clinical syndrome and its management', *Ann Intern Med,* 84(5), pp. 580-93.

Fu, X. D. and Ares, M. (2014) 'Context-dependent control of alternative splicing by RNA-binding proteins', *Nat Rev Genet,* 15(10), pp. 689-701.

Gaboriaud, C., Thielens, N. M., Gregory, L. A., Rossi, V., Fontecilla-Camps, J. C. and Arlaud, G. J. (2004) 'Structure and activation of the C1 complex of complement: unraveling the puzzle', *Trends Immunol,* 25(7), pp. 368-73.

Geffner, J. and Fainboim, L. (2008) 'Introducción a la inmunología humana', *Inmunidad mediada por células T.* 5 ed. Buenos Aires: Editorial Médica Panamericana, pp. 242-250.

Gelfand, J. A., Sherins, R. J., Alling, D. W. and Frank, M. M. (1976) 'Treatment of hereditary angioedema with danazol. Reversal of clinical and biochemical abnormalities', *N Engl J Med,* 295(26), pp. 1444-8.

Gompels, M. M., Lock, R. J., Abinun, M., Bethune, C. A., Davies, G., Grattan, C., Fay, A. C., Longhurst, H. J., Morrison, L., Price, A., Price, M. and Watters, D. (2005) 'C1 inhibitor deficiency: consensus document', *Clin Exp Immunol,* 139(3), pp. 379-94.

Gower, R. G., Busse, P. J., Aygören-Pürsün, E., Barakat, A. J., Caballero, T., Davis-Lorton, M., Farkas, H., Hurewitz, D. S., Jacobs, J. S., Johnston, D. T., Lumry, W. and Maurer, M. (2011) 'Hereditary angioedema caused by c1-esterase inhibitor deficiency: a literature-based analysis and clinical commentary on prophylaxis treatment strategies', *World Allergy Organ J,* 4(2 Suppl), pp. S9-S21.

Hamad, O. A., Bäck, J., Nilsson, P. H., Nilsson, B. and Ekdahl, K. N. (2012) 'Platelets, complement, and contact activation: partners in inflammation and thrombosis', *Adv Exp Med Biol,* 946, pp. 185-205.

Hamilton, A. O., Jones, L., Morrison, L. and Whaley, K. (1987) 'Modulation of monocyte complement synthesis by interferons', *Biochem J,* 242(3), pp. 809-15.

Han, E. D., MacFarlane, R. C., Mulligan, A. N., Scafidi, J. and Davis, A. E. (2002) 'Increased vascular permeability in C1 inhibitor-deficient mice mediated by the bradykinin type 2 receptor', *J Clin Invest,* 109(8), pp. 1057-63.

Harrison, P. and Cramer, E. M. (1993) 'Platelet alpha-granules', *Blood Rev,* 7(1), pp. 52-62.

Hattori, M., Abraham, L. J., Northemann, W. and Fey, G. H. (1990) 'Acute-phase reaction induces a specific complex between hepatic nuclear proteins and the interleukin 6 response element of the rat alpha 2-macroglobulin gene', *Proc Natl Acad Sci U S A,* 87(6), pp. 2364-8.

Heda, G. D., Mardente, S., Weiner, L. and Schmaier, A. H. (1990) 'Interferon gamma increases in vitro and in vivo expression of C1 inhibitor', *Blood,* 75(12), pp. 2401-7.

Hummon, A. B., Lim, S. R., Difilippantonio, M. J. and Ried, T. (2007) 'Isolation and solubilization of proteins after TRIzol extraction of RNA and DNA from patient material following prolonged storage', *Biotechniques,* 42(4), pp. 467-70, 472.

Huntington, J. A. (2011) 'Serpin structure, function and dysfunction', *J Thromb Haemost,* 9 Suppl 1, pp. 26-34.

Irving, J. A., Pike, R. N., Lesk, A. M. and Whisstock, J. C. (2000) 'Phylogeny of the serpin superfamily: implications of patterns of amino acid conservation for structure and function', *Genome Res,* 10(12), pp. 1845-64.

Jelinek, W. R. and Schmid, C. W. (1982) 'Repetitive sequences in eukaryotic DNA and their expression', *Annu Rev Biochem,* 51, pp. 813-44.

Johnson, A. M., Alper, C. A., Rosen, F. S. and Craig, J. M. (1971) 'C1 inhibitor: evidence for decreased hepatic synthesis in hereditary angioneurotic edema', *Science,* 173(3996), pp. 553-4.

Kaslik, G., Kardos, J., Szabó, E., Szilágyi, L., Závodszky, P., Westler, W. M., Markley, J. L. and Gráf, L. (1997) 'Effects of serpin binding on the target proteinase: global stabilization, localized increased structural flexibility, and conserved hydrogen bonding at the active site', *Biochemistry,* 36(18), pp. 5455-64.

Katz, Y. and Strunk, R. C. (1989) 'Synthesis and regulation of C1 inhibitor in human skin fibroblasts', *J Immunol,* 142(6), pp. 2041-5.

Keren, H., Lev-Maor, G. and Ast, G. (2010) 'Alternative splicing and evolution: diversification, exon definition and function', *Nat Rev Genet,* 11(5), pp. 345-55.

Kramer, J., Rosen, F. S., Colten, H. R., Rajczy, K. and Strunk, R. C. (1993) 'Transinhibition of C1 inhibitor synthesis in type I hereditary angioneurotic edema', *J Clin Invest,* 91(3), pp. 1258-62.

Langton, D., Weiner, J. and Fary, W. (1994) 'C1-esterase inhibitor concentrate prevents upper airway obstruction in hereditary angio-oedema', *Med J Aust,* 160(6), pp. 383-4.

Lappin, D. F., Birnie, G. D. and Whaley, K. (1990a) 'Interferon-mediated transcriptional and post-transcriptional modulation of complement gene expression in human monocytes', *Eur J Biochem,* 194(1), pp. 177-84.

Lappin, D. F., Birnie, G. D. and Whaley, K. (1990b) 'Modulation by interferons of the expression of monocyte complement genes', *Biochem J,* 268(2), pp. 387-92.

Lappin, D. F., Guc, D., Hill, A., McShane, T. and Whaley, K. (1992) 'Effect of interferon-gamma on complement gene expression in different cell types', *Biochem J,* 281 (Pt 2), pp. 437-42.

Laurell, A. B., Mårtensson, U. and Sjöholm, A. G. (1990) 'Trimer and tetramer complexes containing C1 esterase inhibitor, C1r and C1s, in serum and synovial fluid of patients with rheumatic disease', *J Immunol Methods,* 129(1), pp. 55-61.

Lin, R. Y., Cannon, A. G. and Teitel, A. D. (2005) 'Pattern of hospitalizations for angioedema in New York between 1990 and 2003', *Ann Allergy Asthma Immunol,* 95(2), pp. 159-66.

Lodish, H., Berk, A. and Zipursky, S. (2000) 'Regulation of mRNA Processing', in Freeman, W.H. (ed.) *Molecular Cell Biology*. New York.

Lotz, M. and Zuraw, B. L. (1987) 'Interferon-gamma is a major regulator of C1-inhibitor synthesis by human blood monocytes', *J Immunol,* 139(10), pp. 3382-7.

López-Lera, A., Favier, B., de la Cruz, R. M., Garrido, S., Drouet, C. and López-Trascasa, M. (2010) 'A new case of homozygous C1-inhibitor deficiency suggests a role for Arg378 in the control of kinin pathway activation', *J Allergy Clin Immunol,* 126(6), pp. 1307-10.e3.

López-Lera, A., Garrido, S., Roche, O. and López-Trascasa, M. (2011) 'SERPING1 mutations in 59 families with hereditary angioedema', *Mol Immunol,* 49(1-2), pp. 18-27.

López-Lera, A., Pernia, O., López-Trascasa, M. and Ibanez de Caceres, I. (2014) 'Expression of the SERPING1 gene is not regulated by promoter hypermethylation in peripheral blood mononuclear cells from patients with hereditary angioedema due to C1-inhibitor deficiency', *Orphanet J Rare Dis,* 9, pp. 103.

Lünemann, A., Tackenberg, B., DeAngelis, T., da Silva, R. B., Messmer, B., Vanoaica, L. D., Miller, A., Apatoff, B., Lublin, F. D., Lünemann, J. D. and Münz, C. (2011) 'Impaired IFN-γ production and proliferation of NK cells in multiple sclerosis', *Int Immunol,* 23(2), pp. 139-48.

Maurer, M., Aberer, W., Bouillet, L., Caballero, T., Fabien, V., Kanny, G., Kaplan, A., Longhurst, H., Zanichelli, A. and Investigators, I. O. S. (2013) 'Hereditary angioedema attacks resolve faster and are shorter after early icatibant treatment', *PLoS One,* 8(2), pp. e53773.

Montalvillo, E., Garrote, J. A., Bernardo, D. and Arranz, E. (2014) 'Células linfoides innatas y células T natural killer en el sistema

inmune del tracto gastrointestinal', *Revista Española de Enfermedades Digestivas,* 106(5), pp. 334-345.

Moore, G. P., Hurley, W. T. and Pace, S. A. (1988) 'Hereditary angioedema', *Ann Emerg Med*, 17(10), pp. 1082-6.

Morgan, B. P. and Gasque, P. (1997) 'Extrahepatic complement biosynthesis: where, when and why?', *Clin Exp Immunol*, 107(1), pp. 1-7.

Navarro Ruiz, A. 2013. Algoritmo de diagnóstico y tratamiento del angioedema hereditario como herramienta para su manejo. *In:* Crespo Diz, C., Poveda Andrés, J.L. & Cebollero de Torres , A. (eds.). Farm Hosp.

Pappalardo, E., Cicardi, M., Duponchel, C., Carugati, A., Choquet, S., Agostoni, A. and Tosi, M. (2000) 'Frequent de novo mutations and exon deletions in the C1inhibitor gene of patients with angioedema', *J Allergy Clin Immunol*, 106(6), pp. 1147-54.

Pappalardo, E., Zingale, L. C. and Cicardi, M. (2003) 'Increased expression of C1-inhibitor mRNA in patients with hereditary angioedema treated with Danazol', *Immunol Lett*, 86(3), pp. 271-6.

Pappalardo, E., Zingale, L. C. and Cicardi, M. (2004) 'C1 inhibitor gene expression in patients with hereditary angioedema: quantitative evaluation by means of real-time RT-PCR', *J Allergy Clin Immunol*, 114(3), pp. 638-44.

Poli, A., Michel, T., Thérésine, M., Andrès, E., Hentges, F. and Zimmer, J. (2009) 'CD56bright natural killer (NK) cells: an important NK cell subset', *Immunology*, 126(4), pp. 458-65.

Prada, A. E., Zahedi, K. and Davis, A. E. (1998) 'Regulation of C1 inhibitor synthesis', *Immunobiology*, 199(2), pp. 377-88.

Randazzo, B. P., Dattwyler, R. J., Kaplan, A. P. and Ghebrehiwet, B. (1985) 'Synthesis of C1 inhibitor (C1-INA) by a human monocyte-like cell line, U937', *J Immunol*, 135(2), pp. 1313-9.

Roche, O., Blanch, A., Caballero, T., Sastre, N., Callejo, D. and López-Trascasa, M. (2005a) 'Hereditary angioedema due to C1 inhibitor deficiency: patient registry and approach to the prevalence in Spain', *Ann Allergy Asthma Immunol*, 94(4), pp. 498-503.

Roche, O., Blanch, A., Duponchel, C., Fontán, G., Tosi, M. and López-Trascasa, M. (2005b) 'Hereditary angioedema: the mutation spectrum of SERPING1/C1NH in a large Spanish cohort', *Hum Mutat*, 26(2), pp. 135-44.

Schmaier, A. H. (2008) 'Assembly, activation, and physiologic influence of the plasma kallikrein/kinin system', *Int Immunopharmacol*, 8(2), pp. 161-5.

Schmaier, A. H., Amenta, S., Xiong, T., Heda, G. D. and Gewirtz, A. M. (1993) 'Expression of platelet C1 inhibitor', *Blood*, 82(2), pp. 465-74.

Schmaier, A. H., Murray, S. C., Heda, G. D., Farber, A., Kuo, A., McCrae, K. and Cines, D. B. (1989) 'Synthesis and expression of C1 inhibitor by human umbilical vein endothelial cells', *J Biol Chem*, 264(30), pp. 18173-9.

Sheffer, A. L., Fearon, D. T. and Austen, K. F. (1987) 'Hereditary angioedema: a decade of management with stanozolol', *J Allergy Clin Immunol*, 80(6), pp. 855-60.

Sheffer, A. L., Fearon, D. T., Austen, K. F. and Rosen, F. S. (1977) 'Tranexamic acid: preoperative prophylactic therapy for patients with hereditary angioneurotic edema', *J Allergy Clin Immunol*, 60(1), pp. 38-40.

Shi, C. and Pamer, E. G. (2011) 'Monocyte recruitment during infection and inflammation', *Nat Rev Immunol*, 11(11), pp. 762-74.

Shoemaker, C. J. and Green, R. (2012) 'Translation drives mRNA quality control', *Nat Struct Mol Biol*, 19(6), pp. 594-601.

Silverman, G. A., Bird, P. I., Carrell, R. W., Church, F. C., Coughlin, P. B., Gettins, P. G., Irving, J. A., Lomas, D. A., Luke, C. J., Moyer, R. W., Pemberton, P. A.,

Remold-O'Donnell, E., Salvesen, G. S., Travis, J. and Whisstock, J. C. (2001) 'The serpins are an expanding superfamily of structurally similar but functionally diverse proteins. Evolution, mechanism of inhibition, novel functions, and a revised nomenclature', *J Biol Chem,* 276(36), pp. 33293-6.

Sim, R. B. and Tsiftsoglou, S. A. (2004) 'Proteases of the complement system', *Biochem Soc Trans,* 32(Pt 1), pp. 21-7.

Simonovic, I. and Patston, P. A. (2000) 'The native metastable fold of C1-inhibitor is stabilized by disulfide bonds', *Biochim Biophys Acta,* 1481(1), pp. 97-102.

Stein, P. E. and Carrell, R. W. (1995) 'What do dysfunctional serpins tell us about molecular mobility and disease?', *Nat Struct Biol,* 2(2), pp. 96-113.

Stenson, P. D., Ball, E. V., Mort, M., Phillips, A. D., Shiel, J. A., Thomas, N. S., Abeysinghe, S., Krawczak, M. and Cooper, D. N. (2003) 'Human Gene Mutation Database (HGMD): 2003 update', *Hum Mutat,* 21(6), pp. 577-81.

Stoppa-Lyonnet, D., Carter, P. E., Meo, T. and Tosi, M. (1990) 'Clusters of intragenic Alu repeats predispose the human C1 inhibitor locus to deleterious rearrangements', *Proc Natl Acad Sci U S A,* 87(4), pp. 1551-5.

Stray-Pedersen, A., Abrahamsen, T. G. and Frøland, S. S. (2000) 'Primary immunodeficiency diseases in Norway', *J Clin Immunol,* 20(6), pp. 477-85.

Tappeiner, G., Hintner, H., Glatzl, J. and Wolff, K. (1979) 'Hereditary angio-oedema: treatment with danazol. Report of a case', *Br J Dermatol,* 100(2), pp. 207-12.

Tarzi, M. D., Hickey, A., Förster, T., Mohammadi, M. and Longhurst, H. J. (2007) 'An evaluation of tests used for the diagnosis and monitoring of C1 inhibitor deficiency: normal serum C4 does not exclude hereditary angio-oedema', *Clin Exp Immunol,* 149(3), pp. 513-6.

Tempel, S. (2012) 'Using and understanding RepeatMasker', *Methods Mol Biol,* 859, pp. 29-51.

Trabold, R., Erös, C., Zweckberger, K., Relton, J., Beck, H., Nussberger, J., Müller-Esterl, W., Bader, M., Whalley, E. and Plesnila, N. (2010) 'The role of bradykinin B(1) and B(2) receptors for secondary brain damage after traumatic brain injury in mice', *J Cereb Blood Flow Metab,* 30(1), pp. 130-9.

Verpy, E., Biasotto, M., Brai, M., Misiano, G., Meo, T. and Tosi, M. (1996) 'Exhaustive mutation scanning by fluorescence-assisted mismatch analysis discloses new genotype-phenotype correlations in angiodema', *Am J Hum Genet,* 59(2), pp. 308-19.

Vinci, G., Lynch, N. J., Duponchel, C., Lebastard, T. M., Milon, G., Stover, C., Schwaeble, W. and Tosi, M. (2002) 'In vivo biosynthesis of endogenous and of human C1 inhibitor in transgenic mice: tissue distribution and colocalization of their expression', *J Immunol,* 169(10), pp. 5948-54.

Vivier, E., Tomasello, E., Baratin, M., Walzer, T. and Ugolini, S. (2008) 'Functions of natural killer cells', *Nat Immunol,* 9(5), pp. 503-10.

Waddell, S. J., Popper, S. J., Rubins, K. H., Griffiths, M. J., Brown, P. O., Levin, M. and Relman, D. A. (2010) 'Dissecting interferon-induced transcriptional programs in human peripheral blood cells', *PLoS One,* 5(3), pp. e9753.

Wagenaar-Bos, I. G., Drouet, C., Aygören-Pursun, E., Bork, K., Bucher, C., Bygum, A., Farkas, H., Fust, G., Gregorek, H., Hack, C. E., Hickey, A., Joller-Jemelka, H. I., Kapusta, M., Kreuz, W., Longhurst, H., Lopez-Trascasa, M., Madalinski, K., Naskalski, J., Nieuwenhuys, E., Ponard, D., Truedsson, L., Varga, L., Nielsen, E. W., Wagner, E., Zingale, L., Cicardi, M. and van Ham, S. M. (2008) 'Functional C1-inhibitor diagnostics in hereditary angioedema: assay evaluation and recommendations', *J Immunol Methods,* 338(1-2), pp. 14-20.

Walker, D. G., Yasuhara, O., Patston, P. A., McGeer, E. G. and McGeer, P. L. (1995) 'Complement C1 inhibitor is produced by brain tissue and is cleaved in Alzheimer disease', *Brain Res,* 675(1-2), pp. 75-82.

Wall, R. T., Frank, M. and Hahn, M. (1989) 'A review of 25 patients with hereditary angioedema requiring surgery', *Anesthesiology,* 71(2), pp. 309-11.

Ward, A. J. and Cooper, T. A. (2010) 'The pathobiology of splicing', *J Pathol,* 220(2), pp. 152-63.

Weis, L. and Reinberg, D. (1992) 'Transcription by RNA polymerase II: initiator-directed formation of transcription-competent complexes', *FASEB J,* 6(14), pp. 3300-9.

Ye, S., Cech, A. L., Belmares, R., Bergstrom, R. C., Tong, Y., Corey, D. R., Kanost, M. R. and Goldsmith, E. J. (2001) 'The structure of a Michaelis serpin-protease complex', *Nat Struct Biol,* 8(11), pp. 979-83.

Yin, W., Ghebrehiwet, B. and Peerschke, E. I. (2008) 'Expression of complement components and inhibitors on platelet microparticles', *Platelets,* 19(3), pp. 225-33.

Zahedi, K., Prada, A. E. and Davis, A. E. (1993) 'Structure and regulation of the C1 inhibitor gene', *Behring Inst Mitt,* (93), pp. 115-9.

Zahedi, K., Prada, A. E. and Davis, A. E. (1994) 'Transcriptional regulation of the C1 inhibitor gene by gamma-interferon', *J Biol Chem,* 269(13), pp. 9669-74.

Zhao, Y., Qiu, Q., Mahdi, F., Shariat-Madar, Z., Røjkjaer, R. and Schmaier, A. H. (2001) 'Assembly and activation of HK-PK complex on endothelial cells results in bradykinin liberation and NO formation', *Am J Physiol Heart Circ Physiol,* 280(4), pp. H1821-9.

Ziccardi, R. J. (1981) 'Activation of the early components of the classical complement pathway under physiologic conditions', *J Immunol,* 126(5), pp. 1769-73.

Zuraw, B. L. and Lotz, M. (1990) 'Regulation of the hepatic synthesis of C1 inhibitor by the hepatocyte stimulating factors interleukin 6 and interferon gamma', *J Biol Chem,* 265(21), pp. 12664-70.

Anexos

Anexo A:

Artículos publicados relacionados con el trabajo.

Immunology Letters 141 (2011) 158–164

Contents lists available at SciVerse ScienceDirect

Immunology Letters

journal homepage: www.elsevier.com/locate/immlet

Analysis of *SERPING1* expression on hereditary angioedema patients: Quantitative analysis of full-length and exon 3 splicing variants

Rocío Mena de la Cruz[a,b,1], Alberto López-Lera[a,b,1], Margarita López-Trascasa[a,b,*]

[a] Unidad de Inmunología, Hospital Universitario La Paz, Paseo de la Castellana, 261, 28046 Madrid, Spain
[b] Centro de Investigación Biomédica en Red sobre Enfermedades Raras (CIBERER), idiPAZ, Spain

ARTICLE INFO

Article history:
Received 7 April 2011
Received in revised form 17 June 2011
Accepted 7 July 2011
Available online 4 October 2011

Keywords:
C1 inhibitor
Hereditary angioedema
Alternative splicing
RT-qPCR

ABSTRACT

Hereditary angioedema (HAE) due to C1-inhibitor (C1-Inh) deficiency is an autosomal dominant disease caused by mutations in the *SERPING1* locus. According to protein levels in plasma, two HAE phenotypes have been described: Type I, with low circulating protein levels in plasma, and Type II, where the protein is present but dysfunctional.

Although more than 200 mutations have been described to date, studies on the molecular basis of this autosomic dominant trait are scarce. Previous studies demonstrated that C1-Inh mRNA expression was decreased in HAE patients. Herein, we have confirmed these findings in a large series of Spanish patients. Moreover, when our data were analyzed taking into account the type of mutation carried by the patient (i.e., missense, frameshift,...), significant differences were amongst the control, nonsense and splicing mutations groups ($P < 0.05$). By opposite, no differences in C1-Inh mRNA expression were found between the control and HAE Type II groups, nor between treated and untreated patients groups, although a significant difference was observed between controls and untreated HAE Type I patients.

An alternative splicing event has been described in the *SERPING1* locus resulting in two different transcripts: the full-length and a shorter variant with skipping of exon 3. In order to investigate a possible role for this splicing in HAE, we quantified both mRNA variants in a series of 28 patients. No statistical differences were found in the expression of both variants between controls and patients when compared. However, a separate analysis considering each type of mutation evidenced a significant decrease (P: 0.0156) in the expression of the exon 3 skipping variant in those HAE Type I patients carrying nonsense mutations. Besides, median of the full variant's copy number was statistically decreased on the splicing group when compared with either stop and/or missense groups.

The results of these studies provide new data about C1 inhibitor expression in HAE patients and shed more light on the transcriptional regulation of the *SERPING1* locus. Quantitative analysis of splicing variants could help to determine the eventual variations of these two transcripts and their possible role under inflammatory stimuli.

1. Introduction

Hereditary angioedema (HAE; MIM#106100) is an autosomal disease due to alterations in the gene of C1 inhibitor (C1NH or SERPING1), which produces a C1 inhibitor (C1-Inh) deficiency. HAE is a rare but life-threatening disease that manifests as acute attacks of submucosal swelling affecting any body location that can extend for several days and cause suffocation if the upper airways are affected. Patients with HAE Type I, approximately 85%, have low antigenic and functional C1-Inh levels (less than 40% of control values), while patients with HAE Type II (the remaining 15% of patients) have normal or elevated antigenic levels but low C1-Inh function [1,2].

C1-Inh belongs to the superfamily of serpin-type protease inhibitors in plasma. Serpins (serine protease inhibitors) act as pseudo-substrates of serine/cysteine proteases with a highly conserved structure throughout evolution. The C1-Inh protein consists of two distinct domains: a C-terminal serpin domain and a poorly conserved, highly glycosylated amino-terminal domain that is dispensable for protease inhibition. C1-Inh plays a key role in the control of the classical and lectin pathways of complement. Complement activation is initiated by the pattern recognition molecules C1q and mannose-binding lectin (MBL), which typically recognize antigen–antibody complexes or foreign polysaccharides, respectively. The associated proteases (C1r, C1s, MASP-1 and MASP-2) then activate the complement system. C1-Inh blocks the activity

Abbreviations: C1-Inh, C1 inhibitor; HAE, hereditary angioedema.

* Corresponding author at: Unidad de Inmunología, Paseo de la Castellana, 261, 28046 Madrid, Spain. Tel.: +34 912071463; fax: +34 917277095.
E-mail address: mlopeztrascasa.hulp@salud.madrid.org (M. López-Trascasa).

[1] Both authors contributed equally to this work.

0165-2478/$ – see front matter © 2011 Elsevier B.V. All rights reserved.
doi:10.1016/j.imlet.2011.07.011

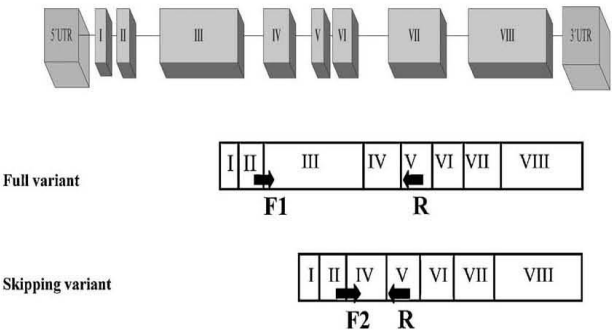

Fig. 1. Scheme of the two splicing variants of C1 inhibitor in exon 3. Arrows show the oligo positions in order to generate the two mRNA variants. Left arrows (➡) indicate the hybridation region for forward specific-sequence-primers (F1 and F2). Right arrows (⬅) indicate the hybridation region for reverse primers (R).

The relative mRNA copy number of *C1NH* for each patient was calculated as the ratio *C1NH/GAPDH* and the results were transformed (by multiplying them by 10^6) for an easier data analysis.

2.3.3. Analysis of exon 3 splicing variants

The expression of the two *C1NH* splicing variants was quantified in a group of 28 HAE patients (15 were under androgen therapy and 13 did not receive any treatment); 24 with Type I and 4 with Type II. Type I patients carry different kinds of mutations: frameshift (5), missense (6), splicing (6) and nonsense (7). Eighteen healthy donors were included as controls.

We designed primers for the amplification of the two transcripts resulting from alternative splicing in exon 3 (see the schema in Fig. 1). GAPDH mRNA expression was used for normalization procedures, as described above for *C1NH* total mRNA quantification (see Table 1). Table 2(a and b) shows the primer sequences and PCR conditions employed, respectively. Real time RT-PCR conditions and relative expression calculation were performed as described above for the *C1NH* total mRNA measurement.

2.3.4. Statistical analysis

Data analysis was performed with the SPSS 9.0 program (SPSS Inc.) and introducing a logarithmic transformation of the results. We studied the reliability of three responses with the Intraclass Correlation Coefficient (ICC), which is a measure of consistency or conformity for a dataset composed of multiple groups. Intra-assay variation was calculated as the ICC of two replicate measures in each sample. Inter-assay variation was calculated for all samples as the ICC between the responses of the first measure and a second measure in a different experiment. Data were expressed as median and range, according to tests.

Statistical analyses of the datasets were developed. Mann–Whitney's test has been used for the comparison of the medians on mRNA expression between controls and patients. When multiple variables had been assessed, we used Kruskal–Wallis (K–W) with a post-hoc Dunn's test and the Wilcoson's test was applied for non-parametric values in paired groups. The statistical probes were considered significant with a value of $P < 0.05$.

Table 3
Novel mutations in HAE Type I patients.

Family code	Exon	cDNA numbering	Predicted effect on protein
FJ	3	c.473C>G	Ser136STOP
FU	3	c.267del A	Gln 67fs
FF	4	c.614G>C	Cys183Ser
GE	4	c.669_670 del GA	Gln201fs
GI4	8	c.1340T>C	Leu425Pro
GO	7	c.1048T>C	Ser328Pro

3. Results

3.1. Molecular studies in HAE patients

In all cases, the mutations were detected by PCR and sequencing. Some of the patients included in this work are carriers of non-previously described mutations (see Table 3) and they will be reported elsewhere [16].

Table 2
Primers and PCR conditions for the analysis of the splicing variants.

		Position	Ref. sequence (accession number)
(a)			
Full variant	5′-GCTGGGGATAGAGCCTCCT-3′	237–255	NM_000062
	5′-GGGGCTGCTGCTGTACAGGG-3′	916–935	
Skipping variant	5′-TGGCTGGGGGGCTGGGGAGAA-3′	235–242/742–754	NM_000062
	5′-GGGGCTGCTGCTGTACAGGG-3′	916–935	
GAPDH	5′-TCCTGCACCACCAACTGCTTA-3	553–573	NM_002046.3
	5′-ACCACCCTGTTGCTGTAGCC-3′	1057–1076	

Amplification fragment	Activation	Desnat.	Annealing	Extension	Acquisition	Cycles	Melting point analysis
(b)							
Full variant	95 °C, 10 min.	95 °C, 10 s	63 °C, 10 s	72 °C, 10 s	72 °C, 10 s	40	65–95 °C
Skipping variant	95 °C, 10 min.	95 °C, 10 s	71 °C, 10 s	72 °C, 10 s	79 °C, 10 s	40	65–95 °C
mRNA GAPDH	95 °C, 10 min.	95 °C, 10 s	63 °C, 10 s	72 °C, 10 s	79 °C, 10 s	40	65–95 °C

(a) Primers used for the analysis expression of full-length, skipping variant and the reference house keeping gene and (b) PCR conditions.

Table 4a
Total mRNA C1-Inh levels in controls and patients.

Group	Cases	No. copies Median [range]	Stat. significance Mann Whitney test
Controls	19	230.6 [35.02–762.9]	
Patients	24	108.3 [3.845–288.8]	$P = 0.0025$

3.2. Expression of C1NH mRNA in peripheral blood mononuclear cells (PBMCs)

C1NH mRNA measurement in PBMCs was expressed as relative copy number and calculated for each individual (controls and patients) after normalization with GAPDH. Statistical analysis of the results showed a significant reduction in the mRNA levels of HAE patients when compared to the control group (Table 4a); patients' median: 108.3 (3.845–288.8), controls' median: 230.6 (35.02–762.9) ($P = 0.0025$, Mann–Whitney test). These results are in agreement with previous findings by other authors [13]. The statistical significance was maintained when controls were compared with the untreated patients but not with the treated patients group (Table 4b). This result dissents from previous reports on literature [17] and it could be related with the number of treated patients in the present cohort (n: 6).

When data analysis was performed separately considering HAE Types I and II, significant differences were also found amongst the three groups (controls, Type I and Type II, Kruskall–Wallis P: 0.0009). A by-pair comparison evidenced that this statistical difference was attributable to the low values measured in the Type I patients (control's median 230.6 (35.02–762.9), Type I patient's median 67.14 (3.845–277.8); see Table 5a). Moreover, this statistical significance was maintained when medians from control individuals were compared with those from untreated HAE Type I patients (Table 5b). Expression levels of the HAE Type II group were not statistically different to those of the control group (Type II patient's median 172.4 (104.1–288.8)). These results are similar but not identical to those reported previously. In the cohort studied by Pappalardo and colleagues, the amount of C1 Inh mRNA in HAE patients was also significantly reduced in comparison with healthy controls (40% in patients with Type I HAE and 47% in patients with Type II HAE), but the difference between the two types of HAE was not significant [13]. This disparity with the literature may be due to the small number of Type II patients analyzed.

Considering that patients with HAE Type I carry different types of mutations, a more detailed analysis was developed to compare mRNA expression amongst controls and each mutation subgroup. Dunn's test uncovered statistical differences ($P < 0.05$) in mRNA expression amongst the controls (230.6 (35.02–762.9)) and patients carrying splicing (67.14 (7.85–158)) and nonsense (20.80 (3.85–37.75)) mutations (Fig. 2).

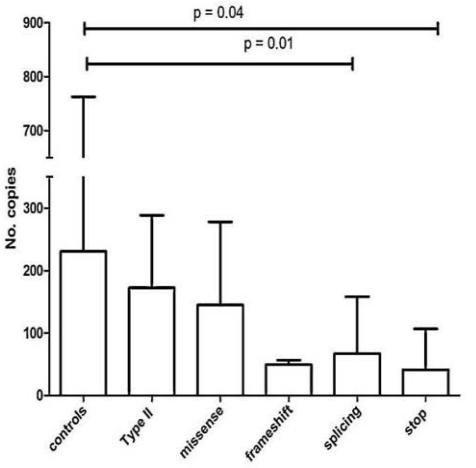

Fig. 2. Comparison of total C1-Inh mRNA expression amongst controls and patients with different kinds of mutations.

3.3. Transcripts expression in peripheral blood from patients

Two facts motivated these experiments. First, previous RT-PCR analysis of mRNA samples from five unrelated patients with mutations affecting the 3′ end of exon 3 (c.550G>C, c.550G>A, and c. 550+5 G>A) performed by our group, showed an additional transcript lacking exon 3. Second, the semi-quantitative comparison of the expression of both variants in controls and patients on agarose gels, revealed an apparently higher expression of the exon 3 skipped variant in these patients than in controls [14]. Fig. 3 shows the patterns of both transcripts in controls and patients bearing different types of mutations as seen on agarose gel. This novel splicing variant has also been observed by other authors in peripheral blood cells from healthy controls but it was reported to be absent in hepatocytes from either patients and controls, indicating that its expression is restricted to monocytes [15].

Table 4b
Effect of treatment with androgens. mRNA levels in controls, treated and untreated patients.

Group	Cases	No. copies Median [range]	Stat. significance Kruskal–Wallis	Stat. significance Dunn's test
Controls	19	230.6 [35.02–762.9]		
Untreated patients	18	105 [3.85–288.8]	$P = 0.0142$	**$P < 0.05$ vs. controls**
Treated patients	6	146 [56.6–277.8]		$P > 0.05$ vs. controls

Table 5a
Total mRNA C1-Inh levels by type of HAE.

Group	Cases	No. copies Median [range]	Stat. significance K–W	Stat. significance Dunn's test
Controls	19	230.6 [35.02–762.9]		
HAE Type I	18	67.14 [3.845–277.8]	$P = 0.0009$	**$P < 0.05$ vs. controls**
HAE Type II	6	172.4 [104.1–288.8]		$P > 0.05$ vs. controls

Table 5b
Total mRNA C1-Inh levels in treated and untreated HAE Type I patients.

Group	Cases	No. copies Median [range]	Stat. significance K–W	Stat. significance Dunn's test
Controls	19	230.6 [35.02–762.9]		
Untreated HAE Type I patients	13	77.21 [3.845–158.0]	$P = 0.0032$	**$P < 0.05$ vs. controls**
Treated HAE Type I patients	5	144.6 [56.58–277.8]		$P > 0.05$ vs. controls

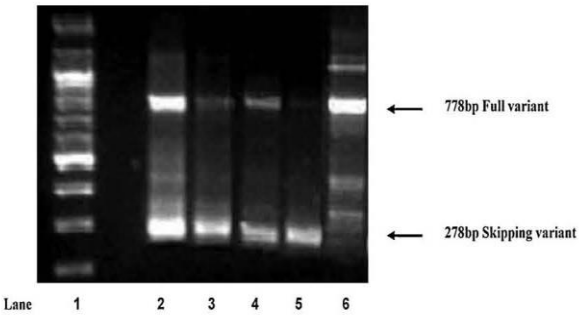

Fig. 3. Qualitative analysis of the splicing variants in patients with various mutations. Total cDNA was generated from 1 μg of total mRNA and the splicing variants were generated as described in Section 2, the final products were analyzed on 2% agarose gel. Lane 1: 100 bp DNA leader; lane 2: control sample (C65); lane 3: Y patient (c.550+5G>A splicing mutation); lane 4: GO patient (c.1048T>C missense mutation); lane 5: BI patient (c. 550G>A splicing mutation); lane 6: DT5 patient (c.1396C>T, Type II).

A more accurate measurement of the distribution of each variant in peripheral blood cells was performed in a series of 28 patients by RT-qPCR with transcript-specific primers.

The relative copy number of each splicing variant (full-length and exon 3-skipping) was calculated for each individual and normalized with GAPDH as described above for the total mRNA measurement. Table 6 shows the medians in controls and patients groups. In the control group, the expression of the full variant (179.9 (25.08–512.7)) was slightly higher than that of the alternative spliced isoform (165.5 (20.92–512.2)) but the differences were not statistically different.

When the same analysis was applied for the patients group data, similar values were obtained for both the full-length (154.7 (7.922–717)) and the exon 3-skipped variants (115.7 (8.24–801.8)). Treatment intake had a minor, non significant effect on the expression of both variants (data not shown).

These analyses were also performed by considering the two subtypes of HAE. In HAE Type I patients, the pattern of expression of both variants was very similar to that observed in the control group, with a modest but not significant increase in the expression of the full length variant (see Table 7a). When the different types of mutations present in the HAE Type I subgroup were considered for the analysis, we did find a significant increase in the expression of the full-length variant (403.3 (128.0–717.0)) compared to that of the alternative transcript (51.23 (8.24–164.3) (P: 0.0156)) in the patients bearing nonsense mutations. By contrast, the opposite tendency was observed in the HAE Type II subgroup, although in this case the P value did not reach significance: exon 3-skipped variant: 317.9 (108.7–547.9); full variant: 138.5 (56.8–327.8). Moreover, Dunn's test evidenced that the median for the full variant copy number was statistically lower in the splicing group compared with either stop and/or missense groups (Table 7b).

In order to study the effect of androgen treatment on the expression of the C1nh splicing variants, we analyzed treatment effect on HAE Type I patients carrying different types of mutations. This analysis could only be performed in patients with missense and splicing defects due to the small number of untreated individuals in the remaining groups. Overall, our results show that HAE Type I patients carrying missense and splicing mutations undergo a significant increase in the expression of both the full-length and exon-3 skipping variants in response to androgens (Figs. 4 and 5).

4. Discussion

Hereditary angioedema (HAE) caused by C1 inhibitor deficiency is associated to mutations in the *C1NH* locus. Hundreds of different

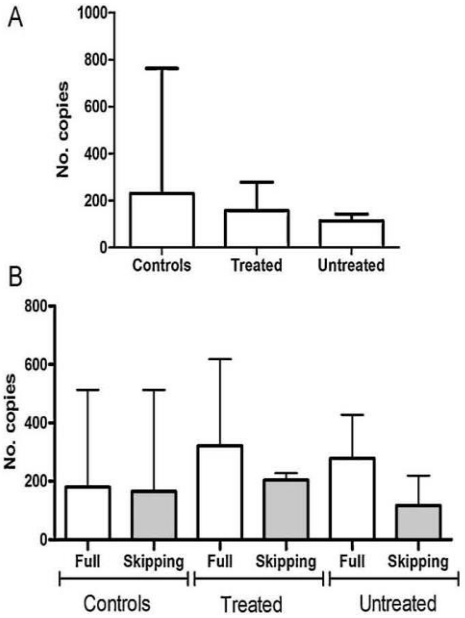

Fig. 4. Effect of the androgens treatment in patients with missense mutations. (a) Total mRNA copy numbers in controls (n: 19) and patients (four treated and two untreated). (b) RNA copy number of splicing variants in controls (n: 18) and three treated and three untreated patients.

Table 6
Expression levels of C1 inhibitor splicing variants in controls and patients.

Group	Cases	Full variant No. copies Median [range]	Skipping variant No. copies Median [range]	Stat. significance Wilcoxon test's
Controls	18	179.9 [25.08–512.7]	165.5 [20.92–512.2]	$P = 0.7275$
Patients	28	154.7 [7.922–717.0]	115.7 [8.24–801.8]	$P = 0.5164$
Stat. significance U-Mann Whitney		$P = 0.931$	$P = 0.6607$	

Table 7a
Analysis of splicing variants.

	Cases	No. copies Median [range]		Stat. significance Wilcoxon test's
		Full variant	Skipping variant	
Controls	18	179.9 [25.08–512.7]	165.5 [20.92–512.2]	$P = 0.7275$
HAE Type I	24	154.7 [7.92–717.0]	106.0 [8.24–801.8]	$P = 0.1840$
HAE Type II	4	138.5[56.80–327.8]	317.9 [108.7–547.9]	$P = 0.1250$
Stat. significance Kruskal–Wallis		$P = 0.9766$	$P = 0.1208$	

Table 7b
Analysis of splicing variants by mutation type.

	Cases	No. copies Median [range]		Stat. significance Wilcoxon test's
		Full variant	Skipping variant	
Controls	18	179.9 [25.08–512.7]	165.5 [20.92–512.2]	$P = 0.7275$
- Missense	6	[a] 300.0[64.53–618.8]	160.9[83.49–227.9]	$P = 0.0938$
- Stop	7	[a] 403.3 [128.0–717.0]	51.23 [8.24–164.3]	$P =$ **0.0156**
- Frameshift	5	59.36[28.25–256.7]	197.0[31.53–322.2]	$P = 0.3125$
- Splicing	6	[a] 63.9[7.92–174.6]	94.65[39.83–801.8]	$P = 0.0625$
HAE Type II	4	138.5[56.80–327.8]	317.9 [108.7–547.9]	$P = 0.1250$
Stat. significance Kruskal–Wallis		$P = 0.0082$ [a]	$P = 0.1324$	

[a] Dunn's test evidenced that medians for full variant transcripts were statistically different when splicing was compared with either stop and missense groups ($P < 0.05$).

heterozygous mutations have been described in this gene, although little is known about the molecular mechanisms involved in the disease. Particularly, the precise events regulating *C1NH* transcription and, those leading to the negative dominance in protein expression and functionality (less than 40% of control values) that characterize HAE.

Previous studies on the expression of the *C1NH* gene by RT-qPCR showed that mRNA levels were lower in patients than controls [13]. The quantitative study of a Spanish cohort presented here confirms these results. In addition, the comparison of mRNA levels between controls and HAE Type I patients carrying different types of mutations revealed statistically significant differences amongst controls, nonsense and splicing subgroups (Fig. 2).

Fig. 5. Effect of the androgens treatment in patients with mutations affecting splicing of exon 3. RNA copy number of splicing variants in controls (n: 18) and two treated and two untreated patients.

Moreover, in all cases, patients carrying Type I mutations showed mRNA expression levels below 50% when compared to controls, which might indicate the trans-inhibition of the normal allele by the mutant one, as previously described [11–13].

In addition, RT-PCR studies developed by Roche [14], evidenced the existence of an alternative splicing variant lacking exon 3. This alternative splicing event seems to be specific of PBMCs, since it was not found in hepatocytes [15], which are the major source of serum C1-Inh.

Qualitative analysis of the expression of both transcripts shows different patterns in controls and patients (see Fig. 3). In order to accurately analyze this result, we performed a quantitative study by means of RT-qPCR with transcript-specific primers. The results did not show statistically significant differences in the expression levels of both variants, neither if we analyzed patients versus controls groups globally, nor in the case that we separately considered treated and untreated patients.

Regarding HAE Type I patients, only those bearing nonsense mutations show significant differences in the expression levels of the two transcripts. In this subgroup, the median of expression of the full length isoform is increased by a 3-fold factor compared to that of the exon 3-skipped splicing variant (Table 7b). In this patients, the presence of a premature termination codon introduced by the mutation could trigger a process of Nonsense-Mediated Decay, leading to the degradation of the

mutant transcript prior to its translation. NMD is a translation-coupled mechanism that eliminates mRNAs containing premature termination codons. In mammalian cells, NMD is also linked to pre-mRNA splicing. Termination codons are generally considered premature if they occur more than 50–55 nucleotides upstream from an splice site recognized by the exon junction complex [18]. We speculate that in those patients with nonsense mutations, this process could in turn modify transcription and/or splicing at the *C1NH* locus in a positive feedback manner. Such a mechanism would be unproductive in terms of protein expression (as additional mechanisms exist that efficiently target truncated peptides in the secretory pathway), but would explain our observations at the mRNA level. Alternatively, it is possible that the marked reduction in the levels of the exon 3-skipped splicing variant is due to a higher susceptibility to the NMD process when its triggered by the mutant allele carrying a premature termination codon.

The biological significance of this splicing variant is unknown as no evidence exists of its expression at the protein level. Bos and colleagues described a mutation in a HAE Dutch pedigree which involved the in frame-deletion of 165 bp in exon 3, yet conserving the N-terminal signal peptide [19]. The authors observed the simultaneous presence of a 66-kDa non-functional protein and high molecular weight multimers in the patient's plasma. These facts evidence that the lost of this region does not impede protein synthesis although leading to a multimerization phenotype [19].

Furthermore, a cDNA corresponding to an exon 3-skipped variant of C1Inh has been recently deposited in the databases (ENST00000531133). This transcript, that is compatible in size with the splicing variant studied by us, has been manually annotated as a nonsense mediated decay (NMD) transcript on a case-by-case basis. NMD not only eliminates abnormal transcripts, but also controls transcript levels through a global system known as RUST (Regulated Unproductive Splicing and Translation) [20]. Several recent studies have demonstrated that the role of alternative splicing in gene regulation has been largely underestimated and have shown that this process is involved in homeostatic regulation and pathogenesis [21]. In the context of the present report and assuming the exon 3 skipping variant to be NMD-targeted, the presence of the exon 3-skipped transcript in the control individuals would suggest that such a regulatory system is operating in the control of C1Inh expression in health and disease. However, the fact that the levels of this splicing variant are not statistically different in controls and patients seems to discard this possibility at least in the basal (non inflammatory) situations tested.

Alternative splicing is a major mechanism of functional regulation in the human genome and it has been detected by genomic studies in 40–60% of human genes [22]. Mutations that alter the splicing process have been associated with variable phenotypes in different diseases (for a revision, see [23]). Moreover, an increasing number of human pathologies are being associated to splicing deregulation resulting in changes in the relative levels of alternatively spliced isoforms. Examples can be found especially in several types of cancer [24] but also in other disorders [25,26], including some inflammatory diseases [27].

In conclusion, our results lead us to speculate an additional role for this exon 3-skipped variant that is not related with the regulation of *C1NH* expression, at least in the conditions tested here. Studies are in progress to evaluate its ultimate role in local inflammation models.

Acknowledgments

The skilful technical help of Sofía Garrido and Inmaculada Rueda was much appreciated. We also thank Elía Pérez Sánchez for her help with the statistical analysis. We would like to thank also to Dr. Luis Álvarez-García for his critical reading of the manuscript.

This work was performed with the financial support of Ministerio de Ciencia e Innovación (PI 09/00122) to Margarita López Trascasa and from CIBERER (INTRA/09/758,2).

References

[1] Agostoni A, Aygören-Pürsün E, Binkley KE, Blanch A, Bork K, Bouillet L, et al. Hereditary and acquired angioedema: problems and progress: proceedings of the third C1 esterase inhibitor deficiency workshop and beyond. J Allergy Clin Immunol 2004;114(September (3 Suppl.)):S51–131.
[2] Papadopoulou-Alataki E. Upper airway considerations in hereditary angioedema. Curr Opin Allergy Clin Immunol 2010;10(1):20–5.
[3] Beinrohr L, Dobó J, Závodszky P, Gál P. C1 MBL-MASPs and C1-inhibitor: novel approaches for targeting complement-mediated inflammation. Trends Mol Med 2008;14(12):511–21.
[4] Cugno M, Nussberger J, Cicardi M, Agostoni A. Bradykinin and the pathophysiology of angioedema. Int Immunopharmacol 2003;3(3):311–7.
[5] Davis 3rd AE, Mejia P, Lu F. Biological activities of C1 inhibitor. Mol Immunol 2008;45(16):4057–63. Review.
[6] Bos IG, Hack CE, Abrahams JP. Structural and functional aspects of C1-inhibitor. Immunobiology 2002;205(4–5):518–33.
[7] Bissler JJ, Aulak KS, Donaldson VH, Rosen FS, Cicardi M, Harrison RA, et al. Molecular defects in hereditary angioneurotic edema. Proc Assoc Am Phys 1997;109(2):164–73.
[8] Blanch A, Roche O, López-Granados E, Fontán G, López-Trascasa M. Detection of C1 inhibitor (SERPING1/C1NH) mutations in exon 8 in patients with hereditary angioedema: evidence for 10 novel mutations. Hum Mutat 2002. Mutation in Brief #544, Online.
[9] Roche O, Blanch A, Duponchel C, Fontán G, Tosi M, López-Trascasa M. Hereditary angioedema: the mutation spectrum of SERPING1/C1NH in a large Spanish cohort. Hum Mutat 2005;26(2):135–44.
[10] Pappalardo E, Caccia S, Suffritti C, Tordai A, Zingale LC, Cicardi M. Mutation screening of C1 inhibitor gene in 108 unrelated families with hereditary angioedema: functional and structural correlates. Mol Immunol 2008;45(13):3536–44.
[11] Kramer J, Rosen FS, Colten HR, Rajczy K, Strunk RC. Transinhibition of C1 inhibitor synthesis in Type I hereditary angioneurotic edema. J Clin Invest 1993;91(March (3)):1258–62.
[12] Verpy E, Couture-Tosi E, Tosi M. C1 inhibitor mutations which affect intracellular transport and secretion in Type I hereditary angioedema. Behring Inst Mitt 1993:120–4.
[13] Pappalardo E, Zingale LC, Cicardi M. C1 inhibitor gene expression in patients with hereditary angioedema: quantitative evaluation by means of real-time RT-PCR. J Allergy Clin Immunol 2004;114(3):638–44.
[14] Roche O. Angioedema hereditario: Mutaciones puntuales de los exones 1 al 7 en el gen del C1-inhibidor, Registro español de la enfermedad. PhD Thesis. Universidad Autónoma de Madrid; 2005.
[15] Duponchel C, Djenouhat K, Frémeaux-Bacchi V, Monnier N, Drouet C, Tosi M. Functional analysis of splicing mutations and of an exon 2 polymorphic variant of SERPING1/C1NH. Hum Mutat 2006;27(3):295–6.
[16] López-Lera A, Garrido S, Roche O, López-Trascasa M. SERPING1 mutations in 59 families with hereditary angioedema. Mol Immunol 2011, doi:10.1016/j.molimm.2011.07.010.
[17] Pappalardo E, Zingale LC, Cicardi M. Increased expression of C1-inhibitor mRNA in patients with hereditary angioedema treated with Danazol. Immunol Lett 2003;86:271–6.
[18] Brogna S, Wen J. Nonsense-mediated mRNA decay (NMD) mechanisms. Nat Struct Mol Biol 2009 Feb;16(2):107–13.
[19] Bos IGA, Lubbers YTP, Roem D, Abrahams JP, Hack CE, Eldering E. The functional integrity of the serpin domain of C1-inhibitor depends on the unique N-terminal domain, as revealed by a pathological mutant. J Biol Chem 2003;278(32):29463–70.
[20] Lareau LF, Brooks AN, Soergel DA, Meng Q, Brenner SE. The coupling of alternative splicing and nonsense-mediated mRNA decay. Adv Exp Med Biol 2007;623:190–211.
[21] Nissim-Rafinia M, Kerem B. The splicing machinery is a genetic modifier of disease severity. Trends Genet 2005;21(9):480–3.
[22] Modrek B, Lee CA. Genomic view of alternative splicing. Nat Genet 2002;30(1):13–9.
[23] Hammond SM, Wood MJ. Genetic therapies for RNA mis-splicing diseases. Trends Genet 2011;27(5):196–205.
[24] Venables JP. Unbalanced alternative splicing and its significance in cancer. Bioessays 2006;28(4):378–86.
[25] Cáceres JF, Kornblihtt AR. Alternative splicing: multiple control mechanisms and involvement in human disease. Trends Genet 2002;18(4): 186–93.
[26] Chen M, Manley JL. Mechanisms of alternative splicing regulation: insights from molecular and genomics approaches. Nat Rev Mol Cell Biol 2009;10(11):741–54.
[27] Häsler R, Kerick M, Mah N, Hultschig C, Richter G, Bretz F, et al. Alterations of pre-mRNA splicing in human inflammatory bowel disease. Eur J Cell Biol 2011;90(6–7):603–11.

Anexo B: ¨

Artículos en los que se ha participado producto de colaboraciones

Molecular Immunology 46 (2009) 2340–2347

Contents lists available at ScienceDirect

Molecular Immunology

journal homepage: www.elsevier.com/locate/molimm

Molecular characterization of three new mutations causing C5 deficiency in two non-related families☆

Alberto López-Lera, Sofía Garrido, Rocío Mena de la Cruz, Gumersindo Fontán, Margarita López-Trascasa*

Unidad de Inmunología, Centro de Investigación Biomédica en Red de Enfermedades Raras (CIBERER) U 754, Hospital Universitario "La Paz", Paseo de la Castellana, 261, 28046 Madrid, Spain

ARTICLE INFO

Article history:
Received 25 February 2009
Received in revised form 27 March 2009
Accepted 27 March 2009
Available online 2 May 2009

Keywords:
Complement deficiency
C5
de novo mutation
Splicing enhancer
Immunodeficiency
Meningitis

ABSTRACT

Deficiencies in complement components are rare diseases whose diagnosis is often underestimated. In addition, in only a few cases molecular studies have been carried out for the characterization of the underlying genetic defects. To date, studies involving C5-deficient patients are scarce.

The aim of the present report is to characterize the biochemical and molecular complement deficiency in two non-related families with one or more members showing no detectable hemolytic complement activity (CH50 < 50 U/ml) and reporting a history of several episodes of meningitis. Protein deficiency was assessed by means of hemolytic assays, bi-dimensional double immunodiffusion, ELISA and Western blot of patients' sera. Molecular studies were carried out by PCR and RT-PCR of DNA and RNA, respectively, both extracted from fresh blood samples of each family member. In Family A, only the *propositus* had complete C5 deficiency. Molecular studies showed that he was heterozygous for two changes in the C5 gene. One of the mutations was also carried by the father (c.1883_1884AG < CTCT) and the second (c.2536T > C, Y846H) was a *de novo* mutation. In Family B, the two C5-deficient members share the homozygous nonsense mutation c.892C > T (Q298X) in exon 9.

The characterization of these new mutations is interesting in order to elucidate structure–function relationships in the C5 gene and it also helps to understand the molecular basis of this uncommon deficiency. Moreover, this report highlights the importance of complement screening in cases of repeated meningococcal infections in order to establish its involvement and to consider adequate clinical recommendations such as prophylactic antibiotics or meningococcal vaccines.

1. Introduction

The complement system is a set of soluble and membrane-bound proteins that take part both in the innate and adaptative immunity of vertebrates. Proteolytic activation of the complement cascade triggers a wide range of cellular responses, from apoptosis to opsonization.

Under physiological conditions, complement promotes the clearance of immune complexes, an important means of removing antibody-coated bacteria. Complement defects increase susceptibility to infection and are frequently associated with autoimmune disorders. The complement system is closely linked to adaptative immunity through its activation and recognition of specific receptors on several cell types' surfaces. Moreover, a normally functioning complement system is also required for physiological tissue regeneration and repair (Ross and Densen, 1984; Figueroa and Densen, 1991; Mastellos et al., 2001).

Three different pathways are implicated in complement activation: the classical pathway (activated by the recognition of immunocomplexes by C1q), the alternative pathway (based on spontaneous activation of C3 on the pathogen surface lacking inhibitory factors) and the lectin pathway (homologous to the classical pathway, but using lectins and ficolins instead of C1q). These three phylogenetically related proteolytic systems converge in C3, which initiates the so-called terminal pathway (C5–9) by cleaving C5.

Human complement component C5 is a plasma glycoprotein (Mr: 196 kDa) composed of two disulfide-bound polypeptide chains (C5α and C5β, 115 and 75 kDa, respectively). This component is mainly synthesized in the liver, monocytes and lymphocytes as an intracellular single chain precursor of 1976aa, including a leader peptide and an arginine-rich linker region (RPRR) connecting the α and β chains (Ooi and Colten, 1979; Carney et al., 1991).

☆ Supported by Ministerio de Educación y Ciencia (SAF2006-02948) and Ministerio de Sanidad (Centro de Investigación Biomédica en Red. CIBERER).

* Corresponding author. Tel.: +34 912071463; fax: +34 917277095.
E-mail address: mlopeztrascasa.hulp@salud.madrid.org (M. López-Trascasa).

0161-5890/$ – see front matter © 2009 Elsevier Ltd. All rights reserved.
doi: 10.1016/j.molimm.2009.03.026

Upon activation by the classical/lectin or alternative pathways' convertases, the precursor form of C5 is cleaved to yield two proteolytic fragments:

- C5a is the N-terminal fragment of the alpha chain. It is a potent anaphylotoxin that induces smooth muscle contraction, increases vascular permeability, basophil and mastocyte degranulation and lymphocyte recruitment to the site of infection (Gerard and Gerard, 1994). Moreover, C5a modulates the acute phase of the hepatic response and globally increases the immune response by inducing the synthesis of tumor necrosis factor (TNF) and interleukins (IL) 1β, IL-6 and IL-8 in certain cell types (Lambris et al., 1998).
- C5b, containing the binding site for C6, initiates the lytic pathway upon binding of the late complement components, leading to lysis of the pathogen (Ware and Kolb, 1981).

C5 proteolytic fragments have been implicated in inflammatory processes such as sepsis (Riedemann et al., 2003) and fetal injury in antiphospholipid syndrome (Girardi et al., 2003). Besides, several candidate gene searches and genome-wide analyses have identified polymorphisms in the TRAF1-C5 genomic region as a relevant modifier of susceptibility to and severity of rheumatoid arthritis (Atkinson, 2003; Plenge et al., 2007).

The C5 coding gene (NC_000009.10) is located on chromosome 9q34.1 and spans a genomic region of 79 kb. Its open reading frame, composed of 41 exons, codes for C5α (exons 1–16) and C5β (exons 17–41) and gives rise to a 6 kb mRNA (NM_001735.2) translated into a pre-C5 protein (in β–α orientation) which is proteolyticaly processed into the mature, two-chain C5 form by the removal of the RPRR region. In addition, two truncated transcripts using alternative splicing and polyadenylation signals have been reported (Haviland et al., 1991).

C5 deficiency (C5D, MIM#120900) is a rare autosomal recessive disease that has previously been reported in several families from different ethnic origins. It is commonly associated with severe and recurrent Gram-negative infections, particularly meningitis and extragenital gonorrhoea by *Neisseriae* species (Peter et al., 1981). Furthermore, studies in C5-deficient mice have demonstrated a significant genetic link between C5 deficiency and elevated airway hyper-responsiveness in experimental asthma. This suggests that C5 plays an important protective role in allergic lung disease by suppressing inflammatory responses and Th2 effector functions (Karp et al., 2000; Drouin et al., 2004). From a clinical point of view, as with other complement terminal components deficiencies, meningococcal vaccination and prophylactic antibiotics should be considered for the treatment of C5-deficient patients.

To date, only four mutations resulting in C5 deficiency in humans have been described at the molecular level (Wang et al., 1995; Delgado-Cerviño et al., 2004; Pfarr et al., 2005) and in every case, the affected members belonged to consanguineous families. In two of these families, the responsible mutation was found to be heterozygote, and a second, uncharacterized molecular defect accounting for the complete C5 deficiency was speculated (Wang et al., 1995). Pfarr et al. (2005) suggested the association between this deficiency and mRNA alterations were caused by the disruption of an exonic splicing enhancer (ESE) in exon 10. Previous studies in our group allowed us to characterize the first homozygous mutation in a C5-deficient family (Delgado-Cerviño et al., 2004).

The aim of the present work was to characterize the molecular defects underlying the complete C5 deficiency in two non-related families with several members showing undetectable hemolytic complement activity.

2. Materials and methods

2.1. Patients

Family A: The propositus (AP.1), his parents (AP.2, father; AP.3, mother) and brothers (AP.4 and AP.5) were referred to Hospital Universitario La Paz, with suspected complement deficiency. There was no family history of consanguinity.

AP.1 had a clinical history of repetitive meningococcal infections from infancy. During the last episode, his cerebrospinal liquid cultures revealed *Neisseria meningitidis* group B infection. Neither parents nor brothers suffered from meningococcal infections.

Family B: Three members from an Italian family, the propositus (BP.1), his sister (BP.2), and his brother (BP.3), were remitted to Hospital Universitario La Paz. Both BP.1 and BP.2 had a clinical history of meningococcal infections from infancy, whereas BP.3 remained healthy. Their parents were deceased and had a consanguineous relationship.

Blood samples from all available members of both families were obtained for serological and molecular studies and stored at −80 °C until used. All signed an informed consent form for these studies.

2.2. DNA and RNA extraction

DNA and RNA samples were obtained from peripheral blood mononuclear cells using Gentra Puregene BloodCore (Gentra systems, Minneapolis, MN) and RNeasy Midi (Qiagen, Valencia, CA) kits, respectively, and following the manufacturer's instructions.

2.3. Complement studies

Serum levels of C3 and C4 were measured by nephelometry. Classical pathway function was evaluated by hemolytic assay (CH50) as described by Phimister and Whaley (1990). The presence of each complement component was assessed by Ouchterlony double immunodiffusion with polyclonal antibodies.

2.4. C5 measurement and functional studies

C5 levels were determined by means of an ELISA sandwich method as previously described (Delgado-Cerviño et al., 2004). The presence of C5 in serum was analyzed by Western blot. Briefly, 5 μl of 1:10 diluted serum samples from all family members, a pool of normal human sera, a commercial human serum with known C5 concentration, (Complement Std. Serum, DadeBehring), purified normal C5 and molecular weight markers (Rainbow, Amersham, UK) were run on a 8% SDS-PAGE gels under non-reducing conditions. After electrophoresis, samples were transferred onto a nitrocellulose membrane and probed with a murine anti-C5 mAb (Quidel) diluted 1:5000. A biotinylated antimouse IgG (Dako) diluted 1:2000 was used as secondary antibody. Later, the membrane was incubated with alkaline phosphatase labelled-streptavidin (Sigma) and the reaction was developed with NBT/BCIP (nitroblue tetrazolium/5-bromo-4chloro-3-indolylphosphate). In addition and following the protocols described in Delgado-Cerviño et al. (2004), functional C5 in serum was analyzed using a C5 specific hemolytic assay.

2.5. Molecular study of the C5 gene

Genetic study of all family members was approached by RT-PCR amplification of six overlapping fragments of the C5 mRNA (Fig. 1), following a protocol modified from Delgado-Cerviño et al. (2004). Briefly, total cDNA from patients and controls was synthesized from 1 μg of total RNA in 20 μl reactions with 0.5 μg Oligo$(dT)_{12-18}$, 0.2 mM dNTPs, 1 mM $MgCl_2$ and 50 units of

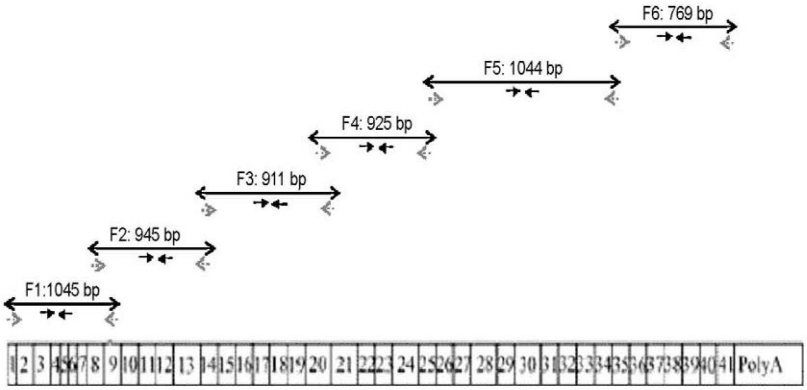

Fig. 1. mRNA analysis. Strategy for the generation of overlapping cDNA fragments. Sequences of the primers used in each case are described in Table 1. Grey thick arrows (➔) denote external primers (F1–F6) and black thin (➔) arrows represent internal primers (F1i–6i).

Table 1
Primers list.

Fragment	Sense	Antisense
RT-PCR external primers		
1	ctacctccaaccatgggcc	tgccaggtatttctgcctcttc
2	catctggagtgac ggtgctgg	cattccagttgccatattaagag
3	atgtggcaaccagctccagg	ctttcc gaagtgcagattcc
4	gaactgtttacaactatagg	tccaatcacagtaaaggctg
5	tcaaccaataaaattacaggg	gaaatcactggagggaatcg
6	agacttaaaagcccttgtgg	caacaggagtccataagtgc
RT-PCR internal primers		
1i	atgacgacttgaagccagcc	ctaccatgtcaacttctgatcc
2i	cactggagtgac ggtgctgg	ttgctcggtaaccttccctg
3i	gcgttaataatgatgaaacc	acacaacattcagtgaaagc
4i	gtaggtgagatcttgtctgc	agctccgcctctgcactcc
5i	gatataaattatgttaaccc	tggcattgatggtgtcctgg
6i	gcgtgcaagtgtgtagaagc	ctgcagagattgtcagatcc
Genomic primers		
Exon 9	tccgaaataactcctccttttttc	cacacacacacacacacacact
Intron 14A	agtccaaagaggagccaaaa	tggctgaagacttgtttgga
Intron 14B	tcgaggcttgaatgtctttg	ccacagcccagatcactctt
Exon 15	catctccaatgtgctcaac	ggcaaatgatcaatgggatt
Exon 20	gcttccactttgggctga	tcagaaaaccagagaatgtttcc

External (F1–F6) and internal (F1i–2i–F5i–6i) primers used for cDNA synthesis of the six overlapping fragments; genomic DNA primers employed for the analysis of the regions containing mutations.

SuperScript II RT, included in the SuperScript™ First-Strand kit (Invitrogen, Barcelona, Spain) as recommended by the manufacturer. The 6 fragments, ranging from 750 to 1050 bp in length, were amplified from the total cDNA using 0.25 pg of each fragment-specific primer pair, 1.5 mM $MgCl_2$, 0.2 mM dNTPs and 2.5 units of AmpliTaq Gold® DNA Polymerase (Applied Biosystems, Madrid, Spain). PCR reactions were started with 12′ at 94 °C, followed by 35 cycles of 15″ at 94 °C, 30″ at 50 °C and 1′40″ at 72 °C and a final extension of 10′ at 72 °C. The nucleotide sequence of each primer pair used is detailed in Table 1.

Amplified fragments were purified from 1% agarose gels using the Gel Extraction Kit (Qiagen, Madrid, Spain) and sequenced with two pairs of specific primers for each fragment (internal and external primers) using BigDye® Terminator v3.1 (Applied Biosystems, Madrid, Spain). Sequencing products were analyzed in an automated 3130XL Genetic Analyzer (Applied Biosystems).

A sequence tagged site (STS) analysis was carried out for polymorphic regions flanking the C5 gene. For this purpose, primer pairs D9S103-S: 5′-ATAGACTTCCAGACAGA TAG-3′/D9S103-AS: 5′-CCTCTCTCATTCCTGGTACT-3′ and D9S1823-S: 5′-AA CTACCA-TTGACATTATTATGTGC-3′/D9S1823AS: 5′-GTTGGATTCATCTTGGAT-TC-3′ were used. PCRs were developed as described above and with an annealing temperature of 59 °C.

Exonic splicing enhancer motifs were analyzed using Rescue ESE (http://genes.mit.edu/burgelab/rescue-ese/) algorithms.

2.6. Molecular modeling

A protein structural model of the Y846H mutant was obtained by side chain substitution using Deep View Swiss-PDB viewer (http://expasy.org/spdbv/) upon PDB accession 3cu7 and visualized using PyMOL software (DeLano, 2002).

3. Results

3.1. Complement studies

Classical pathway activity, measured as CH50, was undetectable in AP.1, BP.1 and BP.2 sera and was within the normal ranged in all their relatives. A qualitative screening for any complement component deficiency by double immunodiffusion revealed the absence of C5 in AP.1 (Fig. 2x), BP.1 and BP.2 (data not shown). The deficiency was exclusively found in these patients, as ascertained by means of ELISA and Western blot of both family members' sera (Fig. 3). Furthermore, C5-specific hemolytic activity was undetectable in AP.1, BP.1 and BP.2 and could be restored to normal levels by adding purified C5 (data not shown). Besides, components C3 and C4 were normal in all of the screened individuals (Fig. 3, bottom).

3.2. Molecular study of the C5 gene

Family A: A first RT-PCR analysis gave the expected sizes for all cDNA fragments except AP.1 and AP.2's fragment 3 (F3), where a

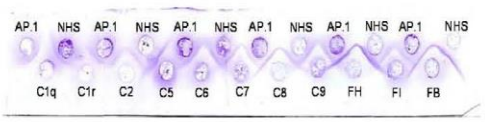

Fig. 2. Ouchterlony double immunodiffusion. Upper row: AP.1: propositus; NHS: normal human serum; lower row: antisera used to detect each complement component.

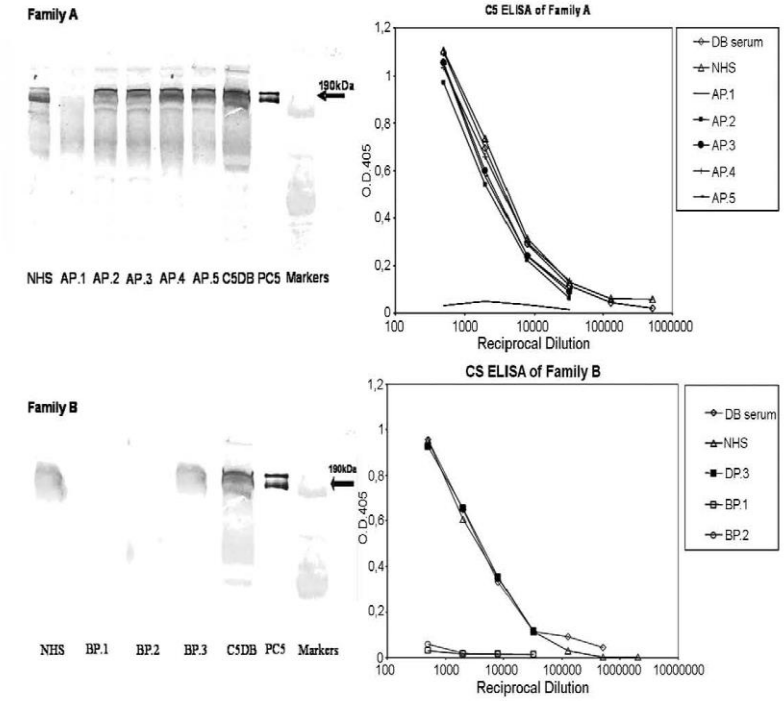

Complement Profile

	C3 (mg/dl)	C4 (mg/dl)	CH50 (AU)	C5HA (AU)
NHS	75-135	16-60	150-350	1250-3250
AP.1	117	33.5	**<50**	**0.0***
AP.2	125	24	239	2100
AP.3	112	33.1	176	2400
AP.4	121	21.9	240	1500
AP.5	99	23.3	265	1900
BP.1	158	29.2	**<50**	**0.0***
BP.2	140	24	**<50**	**0.0***
BP.3	102	19.3	288	2800

Fig. 3. Analysis of C5 in serum of families A and B. Western blot, ELISA and complement profile of each family member are shown. NHS: normal human serum; PC5: purified C5 (Calbiochem); C5DB: C5 calibrated serum (Dade Behring). In C5-deficient subjects, * denotes undetectable complement hemolytic activity only restored by the addition of purified C5 (data not shown).

double band was observed (see Fig. 4). Besides the 911 bp expected band, a second amplification product of 780 bp was found, suggesting the presence of a genomic DNA deletion or a splicing defect in both family members. By comparing the sizes obtained in AP.1 and AP.2 for the overlapping fragments F3, extending over exons 14–21 (double band) and F3i–4i, spanning from exons 17 to 24 (a single band of the expected 925 bp), it was inferred that the responsible molecular defect must be located in the 5′ region of F3 (Fig. 4). In addition, direct sequencing of the 780 bp cDNA fragment revealed the absence of exon 15, whereas the 911 bp band sequence was normal. By means of sequencing the corresponding genomic region, the heterozygous substitution c.1883_1884AG > CTCT was found in AP.1 and AP.2's exon 15, while any other mutation in canonical splicing sequences (exon–intron boundaries and intron 14 branch point and polypyrimidine tract) was ruled out. These results suggested that the mutation was affecting a non-canonical splicing sequence. We used the Rescue ESE program to evaluate whether the substitution could be affecting an exonic splicing enhancer sequence. Four overlapping hexamers (GAAGAG, AGAAGA, GAGAAG and AGAGAA) were identified as putative ESEs in the region altered by the mutation. Moreover, no candidate ESE was detected on the mutated sequence, supporting the idea that c.1883_1884AG > CTCT substitution was disrupting an exonic splicing regulator. The lack of exon 15 in the resulting mRNA alters the reading frame and leads to the generation of a truncated transcript lacking the whole alpha chain coding sequence. The corresponding truncated peptide could not be detected in carriers' sera. A second heterozygous mutation located in exon 20, the missense change c.2536T > C (Y846H), was found exclusively in AP.1 (Fig. 5). This substitution could not be detected in 50 normal individuals with the same ethnic background.

Sequence tagged site analysis of C5 gene flanking markers D9S103 and D9S1823 showed normal segregation in AP.1, AP.2 and AP.3 (data not shown).

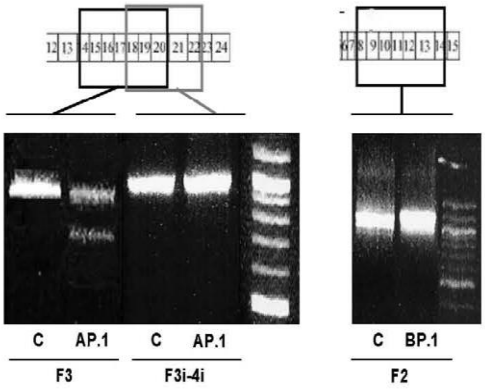

Fig. 4. Analysis in 2% agarose gel of the relevant fragments in each family. Left panel shows fragments 3 (F3, black box in the schematic view) and F3i and F4i (grey box in the schematic view) after RT-PCR in AP.1 and controls (C). Right panel shows fragment 2 (F2, black coloured box in the scheme) after RT-PCR of BP.1 and controls (C).

Family B: RT-PCR analyses gave the expected sizes for the six cDNA fragments (Fig. 4). Fragment 2 sequencing showed the homozygous change c.892C>T in exon 9 of BP.1 and BP.2, not being present in BP.3 nor in the 50 controls screened (Fig. 5).

3.3. Molecular modeling

The structure of C5 has recently been resolved by X-ray diffraction (Fredslund et al., 2008) and that allows us to interpret the effects of mutations on protein structure and function. For this purpose, the Y846H mutant protein model was generated upon PDB accession 3cu7. Residue Y846 is located in the α-chain of the protein, inside the α-2-macroglobulin domain and close to residues Y254, F255 and Y256 of the β-chain. The Y846H mutation seen in our patient does not seem to have any significant effect on global folding of the polypeptide backbone nor in the relative distances with the three closest residues mentioned above (Fig. 6). Moreover, global electrostatic charge of the mutant protein is identical to that of the wild type. Taking these facts into account, we can conclude that Y846H mutation does not lead to perturbation of the protein structure.

4. Discussion

Deficiencies in the terminal components of the complement pathway are known to increase susceptibility to Gram-negative infections, particularly to those of *Neisseriae* species (Peter et al., 1981). C5 deficiency, whose prevalence in the population is unknown, is a clear example of this kind of molecular defect. C5 is essential not only for the innate immune response, as it initiates the assembly of the membrane attack complex, but it is also responsible, through the fragments generated upon its activation, for a wide range of proinflamatory, chemotactic and anaphylactic responses, which are necessary for correct adaptive immunity modulation (Walport, 2001a,b).

The substitution c.1883_1884AG>CTCT, found in exon 15 of AP.1 and AP.2, disrupts the sequence of a putative exonic splicing enhancer (ESE). This alteration in a non-canonical splicing regulator produces exon 15 skipping in the mature mRNA of both family members, and changes the reading frame of this transcript leading to the introduction of a premature stop codon in exon 16. The resulting protein, lacking the whole α chain, seems to be unstable and susceptible to intracellular degradation, as no C5 protein is observed in the propositus' serum. In order to rule out any other mutation causing exon 15 skipping, full intron 14 was sequenced and no alteration was found. As stated in recent reviews, point mutations in non-consensus splicing sequences are a potentially disease-causing molecular defect that is generally underestimated (Cartegni et al., 2002). ESEs are regulatory elements located in coding sequences that seem to be essential for the maintenance of correct splicing patterns. They act as binding sites for sequence specific serine–arginine rich (SR) proteins, promoting the inclusion of the ESE-harbouring exons in mature mRNA (Ryther et al., 2003). Pfarr et al. (2005) previously characterized a C5 deficiency due to the homozygous disruption of an ESE located in exon 10. The presence of several ESEs in the same gene seems to be quite frequent. Actually, there is evidence that suggests the presence of ESEs in the majority of human exons (Fairbrother et al., 2002) and that ESE-affecting mutations can cause disease by generating truncated transcripts or proteins lacking functional domains (Blencowe, 2002). As reported in previously characterized C5 mutations, the heterozygous carriers show significantly reduced C5 serum levels. In the case of the c.1883_1884AG>CTCT heterozygous carrier (AP.2), C5 serum concentration is about 60% of that of the control population. That slight deviation from the expected 50% value, in addition to the fact that the homozygous patient shows a markedly reduced, but detectable expression level (3–6% of control individuals) as shown in Fig. 3, suggests that the allele bearing the c.1883_1884AG>CTCT splicing mutation maintains residual levels of expression. This is in agreement with the findings by Pfarr et al. (2005), where the homozygous carriers of the ESE-disrupting mutation in exon 10 of C5, also showed very low, but detectable protein levels.

No test of anaphylactic, chemotactic or proinflamatory functionality has been performed, so we cannot rule out that these C5 non-lytic activities could be affected in heterozygous carriers. However, the absence of disease in AP.2 and his normal lytic activity are in accordance with the hypothesis that these functions remain unaltered.

The second mutation described in Family A, present only in the *propositus*' maternal allele, the missense substitution c.2536T>C (Y846H), affects the a2M domain, located in the (chain of the protein. This domain, also found in components C3 and C4 of the classical pathway, belongs to the I39 protease inhibitor family. As this nucleotide change had not been previously described and no other obvious mutation was found within the family, a STS analysis was carried out in the *propositus* and his parents. The results of this analysis showed normal segregation, therefore an anomalous chromosomal segregation or non-homologous recombination can be discounted as the cause of the deficiency.

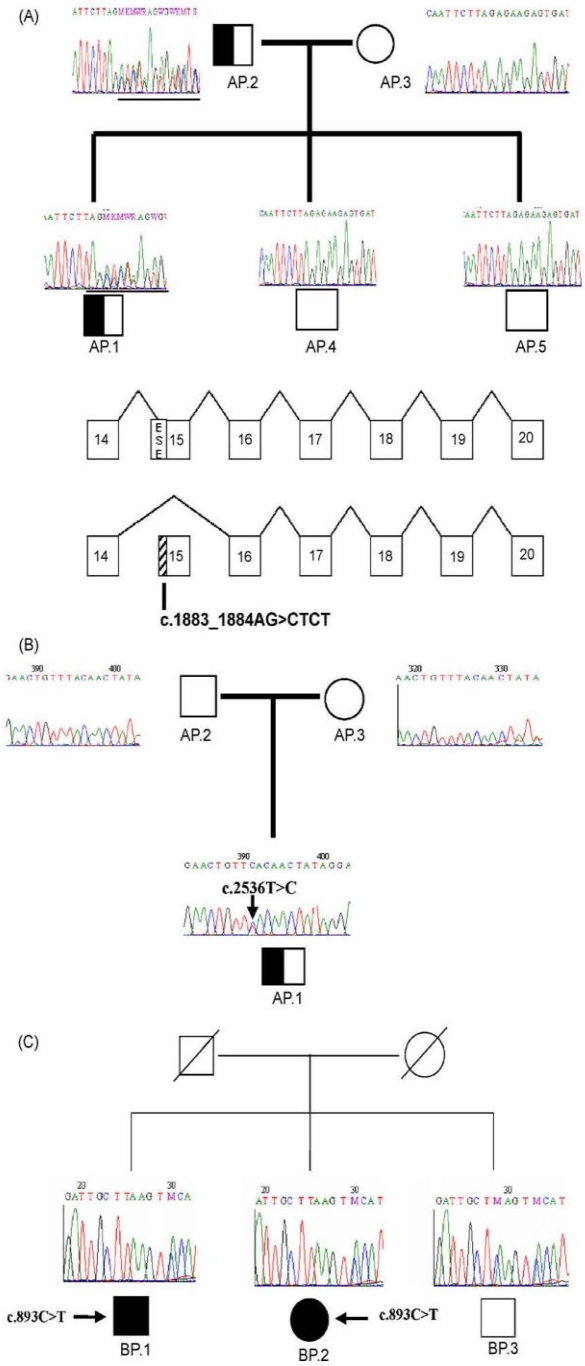

Fig. 5. Familial trees showing the segregation of each mutation in the two families. In Family A, the heterozygous substitution c.1883_1884AG > CTCT is carried by the propositus (AP.1) and his father (AP.2), and generates a mRNA lacking exon 15 due to an ESE sequence alteration, as schematically shown in the at the bottom (A). The missense mutation c.2536T > C is exclusively found in AP.1 (B). In Family B, the homozygous nonsense mutation c.892C > T is present both in BP.1 and BP.2 (C).

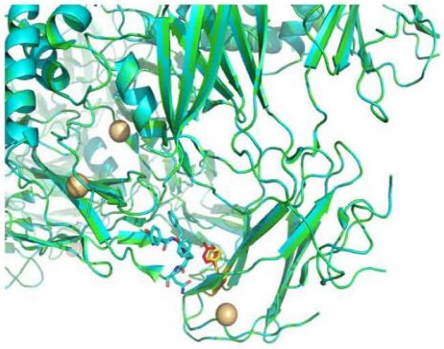

Fig. 6. *In silico* structural models of the mutant protein. No obvious structural constraint can be detected at the model's resolution. The aminoacid change caused by the Y846H substitution does not generate nor disrupt any structural contact at a resolution of 4A. Wild type Tyr residue is shown in red; mutant His residue is shown in yellow. Closest residues (Y254, F255 and Y256) are also labelled in blue. Brown spheres represent Cadmium ions added as chemical ligands.

The total absence of C5 in AP.1 serum suggests that Y846H substitution blocks protein production, either pre- or post-translationally. Structural models for the mutant protein were developed based on PDB accession 3cu7 and no obvious structural change was observed at the model's resolution (Fig. 6). The closest residues to position 846 (Y254, F255 and Y256) were identified and their distances to that position remain unaltered in the mutant model. Moreover, the global charge of the region surrounding the mutation was almost identical in the wild type and mutant protein models, therefore structural or folding defects leading to protein degradation are not likely to cause the C5 deficiency. We cannot rule out, however, alterations in the mutant protein secretory pathway or the RNA harbouring c.2536T>C substitution to be unstable or susceptible to nuclease degradation.

The mutation found in Family B, the substitution c.892C>T (Q298X) located in exon 9, disrupts the transcript's reading frame by introducing a stop codon, thus explaining the complete lack of C5 protein in the homozygous carriers (BP.1 and BP.2).

5. Conclusion

In conclusion, we have described three non-previously characterized mutations causing C5 deficiency. Two of them, affecting Family A, are present in heterozygosis: c.1883_1884AG>CTCT is associated with the disruption of a putative exonic splicing enhancer and c.2536T>C (Y846H) is the first *de novo* mutation identified in the C5 gene. The other mutation presented here, the change c.892C>T (Q298X), found in homozygosis in Family B C5-deficient members, is a nonsense mutation that is expected to give rise to a truncated transcript.

These results are in accordance with the high heterogeneity that characterizes this disorder, with four different mutations found in the four deficiencies studied at the molecular level to date. Further systematic studies will be required to know the real prevalence of this deficiency in the population and to deepen knowledge of the mechanisms underlying its clinical implications.

Acknowledgements

We would like to thank Drs. José Manuel Ramos (Medicina Interna; Hospital Universitari d'Elx, Alicante, Spain) and Paolo Airo (Servizio di Immunologia Clinica; Spedali Civili, Università di Brescia, Brescia, Italy) for sending us the biological samples as well as Drs. Ana Rojas-Mendoza and Osvaldo Graña (from the Structural Bioinformatics Group of Centro Nacional de Investigaciones Oncológicas,CNIO, Madrid, Spain) for their technical support in the development of the mutant protein models. Last but not least, we are grateful to Dr. Pablo Lapunzina (Unidad de Genética Médica; Hospital Universitario La Paz, Madrid, Spain) for his constant support and his helpful discussions on the genetic analysis.

References

Atkinson, J.P., 2003. Complement system on the attack in autoimmunity. J. Clin. Invest. 112, 1639–1641.
Blencowe, B.J., 2002. Exonic splicing enhancers: mechanism of action, diversity and role in human genetic diseases. Trends Biochem. Sci. 25, 106–110.
Carney, D.F., Haviland, D.L., Noack, D., Wetsel, R.A., Vik, D.P., Tack, B.F., 1991. Structural aspects of the human C5 gene. Intron/exon organization, 5′ flanking region features, and characterization of two truncated cDNA clones. J. Biol. Chem. 266, 18786–18791.
Cartegni, L., Chef, S.L., Krainer, A.R., 2002. Listening to silence and understanding nonsense: exonic mutations that affect splicing. Nat. Rev. Genet. 3 (4), 285–298.
DeLano, W.L., 2002. The PyMOL Molecular Graphics System. DeLano Scientific, Palo Alto, CA, USA.
Delgado-Cerviño, E., Fontán, G., López-Trascasa, M., 2004. C5 complement deficiency in a Spanish family. Molecular characterization of the double mutation responsible for the defect. Mol. Immunol. 42, 105–111.
Drouin, S.M., Corry, D.B., Wetsel, R.A., 2004. Increased inflammation and airway hyperresponsiveness in C5-deficient mice reveal opposite roles for C3a and C5a in mediating Th2 effector functions in experimental asthma. Mol. Immunol. 41, 225–226.
Fairbrother, W.G., Yeh, R.F., Sharp, P.A., Burge, C.B., 2002. Predictive identification of exonic splicing enhancers in human genes. Science 297 (5583), 1007–1013.
Figueroa, J.E., Densen, P., 1991. Infectious diseases associated with complement deficiencies. Clin. Microbiol. Rev. 4, 359–395.
Fredslund, F., Laursen, N.S., Roversi, P., Jenner, L., Oliveira, C.L.P., Pedersen, J.S., Nunn, M.A., Lea, S.M., Discipio, R., Sottrup-Jensen, L., Andersen, G.R., 2008. Structure of and influence of a tick complement inhibitor on human complement component 5. Nat. Immunol. 9, 753–760.
Gerard, C., Gerard, N.P., 1994. C5a anaphylotoxin and its seven transmembrane-segment receptor. Ann. Rev. Immunol. 12, 775–808.
Girardi, G., Berman, J., Redecha, P., Spruce, L., Thurman, J.M., Kraus, D., Hollmann, T.J., Casali, P., Caroll, M.C., Wetsel, R.A., Lambris, J.D., Holers, V.M., Salmon, J.E., 2003. Complement C5a receptors and neutrophils mediate fetal injury in the antiphospholipid syndrome. J. Clin. Invest. 112, 1644–1654.
Haviland, D.L., Haviland, J.C., Fleischer, D.T., Hunt, A., Westel, R.A., 1991. Complete cDNA sequence of human complement pro-C5. Evidence of truncated transcripts derived from a single copy gen. J. Immunol. 146, 362–368.
Karp, C.L., Grupe, A., Schadt, E., Ewart, S.L., Keane-Moore, M., Cuomo, P.J., Kohl, J., Wahl, L., Kuperman, D., Germer, S., 2000. Identification of complement factor 5 as a susceptibility locus for experimental allergic asthma. Nat. Immunol. 1, 221–226.
Lambris, J.D., Sahu, A., Wetsel, R.A., 1998. The chemistry and biology of C3, C4 and C5. In: Volanakis, J.E., Frank, M.F. (Eds.), The Human Complement System in Health and Disease. Marcel Decker, New York, pp. 83–118.
Mastellos, D., Papadimitriou, J.C., Franchini, S., Tsonis, P.A., Lambris, J.D., 2001. A novel role of complement: mice deficient in the fifth component of complement (C5) exhibit impaired liver regeneration. J. Immunol. 166, 2479–2486.
Ooi, Y.M., Colten, H.R., 1979. Biosynthesis and post-synthetic modification of a precursor (Pro-C5) of the fifth component of mouse complement (C5). J. Immunol. 123, 2494–2498.
Peter, G., Weigert, M.B., Bissel, A.R., Gold, R., Kreutzer, D., Mclean, R.H., 1981. Meningoccocal meningitis in familial deficiency of the fifth component of complement. Pediatrics 67, 882–886.
Pfarr, N., Prawitt, D., Kirschfink, M., Schroff, C., Knuf, M., Habermehl, P., Mannhardt, W., Zepp, F., Fairbrother, W., Loos, M., Burge, C.B., Pohlenz, J., 2005. Linking C5 deficiency to an exonic splicing enhancer mutation. J. Immunol. 174, 4172–4177.
Phimister, G.M., Whaley, K., 1990. Measurement of complement. In: Gooi, H.C., Chapel, H. (Eds.), Clinical Immunology: A Practical Approach. Oxford University Press, Oxford, pp. 81–109.
Plenge, R.M., Seielstad, M., Padyukov, L., Lee, A.T., Remmers, E.F., Ding, B., Liew, A., Khalili, H., Chandrasekaran, A., Davies, L.R., Li, W., Tan, A.K., Bonnard, C., Ong, R.T., Thalamuthu, A., Pettersson, S., Liu, C., Tian, C., Chen, W.V., Carulli, J.P., Beckman, E.M., Altshuler, D., Alfredsson, L., Criswell, L.A., Amos, C.I., Seldin, M.F., Kastner, D.L., Klareskog, L., Gregersen, P.K., 2007 Sep 20. TRAF1-C5 as a risk locus for rheumatoid arthritis: a genomewide study. N. Engl. J. Med. 357 (12), 1250–1251.
Riedemann, N.C., Guo, R.F., Ward, P.A., 2003. The enigma of sepsis. J. Clin. Invest. 112, 460–467.
Ross, S.C., Densen, P., 1984. Complement deficiency states and infection: epidemiology, pathogenesis and consequences of Neisserial and other infections in an immune deficiency. Medicine (Baltimore) 63, 243–273.
Ryther, R.C., McGuinness, L.M., Phillips III, J.A., Moseley, C.T., Magoulas, C.B., Robinson, I.C., Patton, J.G., 2003. Disruption of exón definition produces a dominant-negative growth hormone isoform that causes somatotroph death and IGHD II. Hum. Genet. 113, 140–148.
Walport, M.J., 2001a. Complement. First of two parts. N. Engl. J. Med. 344, 1058–1066.

Walport, M.J., 2001b. Complement. Second of two parts. N. Engl. J. Med. 344, 1140–1144.
Wang, X., Fleischer, D.T., Whitehead, W.T., Haviland, D.L., Rosenfeld, S., Leddy, I., Snyderman, J.P., Wetsel, R.A., 1995. Inherited human complement C5 deficiency. Nonsense mutations in exons 1 (Gln1 to stop) and (Arg1458 to stop) and compound heterozygosity in three African–American families. J. Immunol. 154, 5464–5471.
Ware, C.F., Kolb, W.P., 1981. Assembly of the functional membrane attack complex of human complement: formation of disulfide-linked C9 dimers. Proc. Natl. Acad. Sci. U.S.A. 78 (10), 6426–6430.

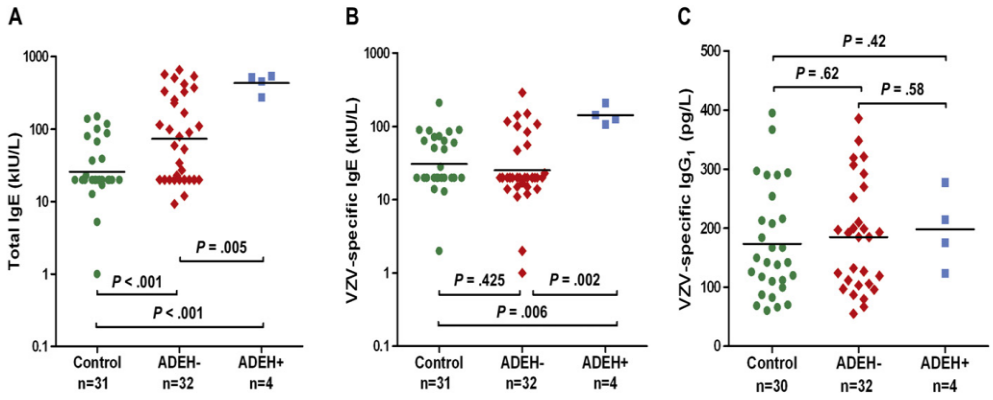

Note: Horizontal lines in dot plots represent geometric means (A and B) and mean values (C).

FIG 2. Total IgE level **(A)**, VZV-specific IgE **(B)**, and VZV-specific IgG **(C)** in control subjects and subjects with AD without a history of EH (ADEH−) and with a history of EH (ADEH+).

high rates of local side effects were found.[8,9] Our current data raise the possibility that virus-specific IgE could result in adverse responses to future vaccinations or exposures. Of note, in the Atopic Dermatitis Vaccinia Network Registry, ADEH+ subjects reported more adverse effects from primary VZV infection or vaccination than nonatopic subjects (unpublished data, Zaccaro, Atopic Dermatitis Vaccinia Network, May 2010).

Subjects with AD have an increased susceptibility to viral skin infections, and we anticipated that cell-mediated immunity to VZV vaccine would be reduced in subjects with moderate to severe AD. However, we found that the control subjects and subjects with AD had similar cellular responses. Future studies of varicella may yield larger differences by enrolling more ADEH+ patients. We were surprised to see the wide variation in cellular responses in both groups and the effect of the timing of the blood draw after VZV vaccination.

In summary, controls and subjects with AD had similar cell-mediated responses to the VZV vaccine. However, ADEH+ subjects demonstrated higher VZV-specific IgE, a possible risk factor for adverse effects to booster doses of vaccine or to wild-type VZV exposure.

We thank the supervising study coordinator, Irene Borras-Coughlin, and administrative assistant, Jeanne Testa, at Children's Hospital Boston and the pediatric offices that referred subjects including Longwood Pediatrics and the Children's Hospital Primary Care Center in Boston, Mass.

Lynda Schneider, MD[a]
Adriana Weinberg, MD[b]
Mark Boguniewicz, MD[b,c]
Patricia Taylor, NP[c]
Hans Oettgen, MD, PhD[a]
Lisa Heughan, BS[a]
Daniel Zaccaro, MS[d]
Brian Armstrong, MPH[d]
Aaron Holliday, BS[d]
Donald Y. M. Leung, MD, PhD[b,c]

From [a]Children's Hospital Boston, Mass; [b]the University of Colorado, Denver, Colo; [c]National Jewish Health, Denver, Colo; and [d]Rho Inc, Chapel Hill, NC. E-mail: lynda.schneider@childrens.harvard.edu.

Supported by federal funds from the National Institute of Allergy and Infectious Diseases, National Institutes of Health, Department of Health and Human Services, under contract nos. N01 AI40029 and N01 AI40033, as well as the Clinical Translational Scientific Award UL1 RR025780 (National Jewish) and UL1 RR025758-01 from the National Center for Research Resources, National Institutes of Health, to the Harvard Catalyst Clinical and Translational Science Center (Harvard Catalyst).

Disclosure of potential conflict of interest: L. Schneider has received research support from the NIH/NIAID Atopic Dermatitis Vacinnia Network. A. Weinberg has received grants and consulting fees from Merck & Co. H. Oettgen is a consultant and scientific advisor for Schering Plough, is a consultant for Genentech, and has received research support from Novartis. The rest of the authors have declared that they have no conflict of interest.

REFERENCES

1. Boguniewicz M, Leung DYM. Recent insights into atopic dermatitis and implications for management of infectious complications. J Allergy Clin Immunol 2010;125:4-13.
2. Beck LA, Boguniewicz M, Hata T, Schneider LC, Hanifin J, Gallo R, et al. Phenotype of atopic dermatitis subjects with a history of eczema herpeticum. J Allergy Clin Immunol 2009;124:260-9.
3. Gao PS, Rafaels NM, Hand T, Murray T, Boguniewicz M, Hata T, et al. Filaggrin mutations that confer risk of atopic dermatitis confer greater risk for eczema herpeticum. J Allergy Clin Immunol 2009;124:507-13.
4. Gao PS, Rafaels NM, Mu D, Hand T, Murrau T, Boguniewicz M, et al. Genetic variants in thymic stromal lymphopoietin are associated with atopic dermatitis and eczema herpeticum. J Allergy Clin Immunol 2010;125:1403-7.
5. Kreth HW, Hoeger PH. Members of the VZV-AD Study Group. Safety, reactogenicity and immunogenicity of the live attenuated varicella vaccine in children between 1 and 9 years of age with atopic dermatitis. Eur J Pediatr 2006;165:677-83.
6. Smith JG, Liu X, Kaufhold RM, Clair J, Caulfield MJ. Development and validation of a gamma interferon ELISPOT assay for quantitation of cellular immune responses to varicella-zoster virus. Clin Diagn Lab Immunol 2001;8:871-9.
7. Kumar A, Grayson MH. The role of viruses in the development and exacerbation of atopic disease. Ann Allergy Asthma Immunol 2009;103:181-6.
8. Nagel JE, Whie C, Lin MS, Fireman P. IgE synthesis in man, II: comparison of tetanus and diphtheria igE antibody in allergic and nonallergic children. J Allergy Clin Immunol 1979;63:308-14.
9. Mark A, Bjorksten B, Granstrom M. Immunoglobulin IgE responses to diphtheria and tetanus toxoids after booster with aluminium-adsorbed and fluid DT-vaccines. Vaccine 1995;13:669-73.

Available online October 2, 2010.
doi:10.1016/j.jaci.2010.08.010

A new case of homozygous C1-inhibitor deficiency suggests a role for Arg378 in the control of kinin pathway activation

To the Editor:

Hereditary angioedema (HAE) caused by C1-inhibitor (C1-Inh) deficiency is a rare disease with an autosomal dominant pattern of

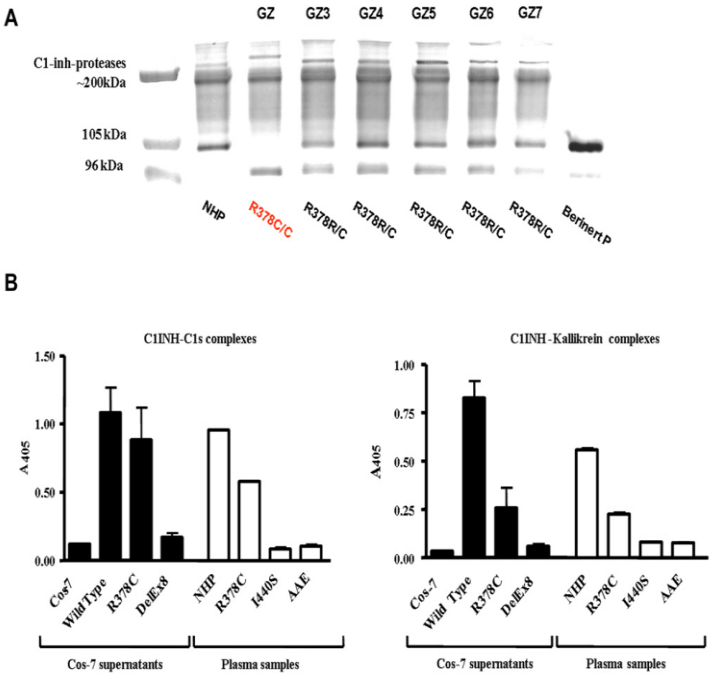

FIG 1. Biochemical and functional studies on the R378C mutant: Western blot of fresh plasma samples of the family members showing the native (105 kd) and cleaved/latent (96 kd) forms of C1-Inh. Equal plasma volumes were loaded in each lane. Normal human plasma *(NHP)* and purified C1-Inh *(Berinert P)* are shown as reference **(A)**. C1-Inh's interaction with C1s protease and kallikrein was examined by means of ELISA of Cos-7 cell supernatants (20 ng of protein per lane) and plasma samples **(B)**.

inheritance. Clinically, HAE is characterized by episodes of localized swelling in the limbs, face, gut, or upper respiratory tract.[1] Those affected are generally heterozygous for mutations in the C1-inhibitor gene *(C1NH)*, which result in either low levels of circulating C1-Inh (HAE type I) or normal or increased levels of a nonfunctional C1-Inh (HAE type II). Acquired forms of angioedema (AAE) caused by accelerated C1-Inh consumption associated with lymphoproliferative disorders or anti–C1-Inh autoantibodies have also been described.[2] HAE and AAE clinical manifestations are almost identical, but distinctive biochemical traits of patients with AAE include low amounts of C1q, C1r, and C1s proteins in serum.

C1-Inh is a serum glycoprotein belonging to the serpin superfamily of protease inhibitors, the main function of which is to prevent the activation of the classical pathway of complement, as well as the activation of kinin generation, coagulation, and fibrinolytic cascades.[3]

Serpins are globular proteins with a conserved structure of 9 α-helices and 3 β-pleated sheets.

Their reactive center is located in an exposed flexible loop referred to as the reactive center loop (RCL). They act on their target proteases by means of a suicide-substrate mechanism involving the cleavage of the RCL and its insertion into β-sheet A. As a result, conformational changes take place in the serpins that ultimately trap and inactivate the targeted protease. Nonphysiological conformations involving RCL insertion and leading to latent states, multimeric states, or both have been attributed to several naturally occurring mutations.[4]

Although more than 200 different heterozygous mutations leading to HAE have been described, only 2 homozygous C1-Inh–deficient subjects, 2 siblings of consanguineous origin carrying the I440S missense mutation, have been identified. Those patients produced a nonfunctional protein and exhibited an unusual disease phenotype, with mild symptomatology and complement consumption. Moreover, they had a total absence of circulating C1q, thus resembling AAE.[5]

Herein we describe a new case of homozygous C1-Inh deficiency in a patient with severe angioedema lacking circulating C1q. Genetic and functional characterization of the patient showed that he carries an R378C substitution and that this is a unique alteration resulting in partial inability of C1-Inh to control kallikrein activation.

The patient is a 33-year-old man who, for the last 10 years, has experienced attacks of angioedema involving the face and extremities. He has had several episodes of laryngeal edema with ventilatory compromise. Biochemical study of the complement proteins (C1-Inh, C4, and C3 antigenic levels) was performed by means of nephelometry, C1-Inh function was determined by a specific colorimetric assay (Berichrom; Siemens, Berlin, Germany), and C1q was measured by means of radial immunodiffusion (The Binding Site, Birmingham, United Kingdom). Complement profile in the propositus revealed values concordant with a C1-Inh deficiency (C1-Inh, 4.38 mg/dL; C1-Inh function, 11%; C4, 1.44 mg/dL) and undetectable C1q, suggesting consumption of the classical pathway of complement. No lymphoproliferative disorder or anti–C1-Inh or anti-C1q

J ALLERGY CLIN IMMUNOL
VOLUME 126, NUMBER 6

autoantibodies were detected. Five additional relatives (all of them asymptomatic) were recruited for this study. Four of them had values consistent with HAE type II, and only 1 relative (GZ7; III.1), a 3-year-old girl, had C1-Inh levels and function within the normal range (see Fig E1 in this article's Online Repository at www.jacionline.org).

Once a diagnosis of HAE was established, the propositus started prophylactic treatment with the attenuated androgen stanozolol (12 mg/12 hours). Clinical examination was performed, and blood samples were obtained before treatment and at 21 and 28 months after treatment.

After written informed consent was obtained, genetic studies of the *C1NH* locus were performed in all the family members, as previously described.[5] Sequence analysis revealed the homozygous substitution c.1198C>T (R378C) in exon 7 of the propositus. All of his relatives were heterozygous for the mutation (see Fig E1). Data from multiplex ligation-dependent probe amplification of the propositus ruled out a possible genomic deletion affecting the *C1NH* gene and confirmed homozygosity (data not shown).

Biochemical characterization of the patient's C1-Inh was done by means of Western blotting of fresh plasma samples. Under nonreducing conditions, native (105 kd) and inactive (cleaved or latent, 96 kd) forms of C1-Inh can be resolved. Interestingly, in the present R378C homozygote, and as reported for the other 2 previously described I440S missense homozygotes,[5] plasma C1-Inh circulates almost exclusively in its cleaved or latent state. All the heterozygous relatives studied had both forms of circulating C1-Inh (Fig 1).

We studied the functionality of the R378C C1-Inh mutant by measuring complex formation with biotinylated C1s and kallikrein proteases by means of ELISA of plasma samples and supernatants of stably transfected Cos-7 cells. For the plasma assays, samples from an I440S homozygote and a patient with AAE were also analyzed. C1-Inh constructs for the Cos-7 experiments were built on the previously described C1-Inh minigene.[6] A mutant clone lacking exon 8 (DelEx8) was used as a negative control for all the transfection assays.

The R378C mutant protein binds C1s normally but exhibits a strongly decreased capacity to associate with kallikrein both in plasma and Cos-7 supernatants. No complexes between C1-Inh and target proteases could be detected in the I440S, AAE, and DelEx8 samples (Fig 1).

This unexpected result prompted us to analyze the conformational alterations in the R378C mutant. Cleaved and latent forms of C1-Inh can be distinguished, taking advantage of the previously described, conformational-specific mAbs KII and KOK12 (kindly provided by Dr Diana Wouters, Sanquin Research, Amsterdam, The Netherlands). KII specifically recognizes cleaved inactivated C1-Inh, whereas KOK12 reacts with cleaved C1-Inh, complexed/latent C1-Inh, or both.[7] KII signal in the homozygous R378C patient's plasma was higher than in normal human plasma and comparable with that obtained in the I440S homozygote (an HAE type II mutation) and AAE samples. Similar detection patterns were obtained for both mutant proteins when screened with the KOK12 antibody (data not shown).

The results of the I440S homozygote are consistent with complete lack of functionality because of reactive-site cleavage. In the case of the R378C homozygote and considering its normal binding to C1s, the detection of this protein by both the KII and KOK12 antibodies suggests that the R378C mutation creates a latent-like epitope recognizable by these 2 antibodies. Because only the 96-kd band was detected in this patient by means of Western blotting, we hypothesize that the C1-Inh mutant might undergo a partial insertion of the RCL into β-sheet A.

One striking similarity among both the R378C and I440S families is the absence of HAE-related symptomatology in the heterozygous subjects. However, unlike the I440S homozygotes, who only reported mild clinical manifestations, the R378C homozygous patient described here did have recurrent and severe attacks of angioedema before treatment. Yet on prophylactic treatment with stanozolol, a decrease in the frequency and severity of symptoms was achieved in the R378C homozygote. This clinical amelioration coincided with a partial recovery of the patient's complement profile. Specifically, C1-Inh, C4, and C2 concentrations were recovered to normal levels in the 2 samples analyzed after attenuated androgen therapy (posttreatment samples 1 and 2). C1q concentrations remained undetectable in posttreatment sample 1 and were only restored to normal values (10.3 mg/dL) in the second posttreatment sample (see Fig E2 in this article's Online Repository at www.jacionline.org). A broader discussion can be found in Appendix E1 in this article's Online Repository at www.jacionline.org.

Our results further characterize the complement profile associated with homozygous mutations in the *C1NH* gene and suggest that suspicion of homozygous deficiency cannot rely on the presence of mild symptomatology. Additionally, we provide insights on the biochemical function of the R378C mutation, a substitution that induces a latent-like conformation of C1-Inh that specifically inhibits kallikrein binding, suggesting that the Arginine 378 position is of strategic importance for C1-Inh control of kinin formation.

We thank Dr Ángeles Rico Díaz (Hospital Juan Canalejo, A Coruña, Spain) and Dr Gabriel Barderas (Centro de Salud Collado Villalba, Madrid, Spain) for referring the patients and Dr Diana Wouters (Department of Immunopathology, Sanquin Research, Amsterdam, The Netherlands) for providing the KII and KOK12 mAbs.

Alberto López-Lera, MS[a,b,c]
Bertrand Favier, PhD[d]
Rocío Mena de la Cruz, MS[a,b,c]
Sofía Garrido, BS[a,c]
Christian Drouet, PhD[d]
Margarita López-Trascasa, PhD[a,b,c]

From [a]the Immunology Unit, Hospital Universitario La Paz, Madrid, Spain; [b]Centro de Investigaciones Biomédicas en Red (CIBERER, Madrid, Spain) U-754; [c]Hospital La Paz Health Research Institute (IdiPAZ, Madrid, Spain); and [d]GREPI/TIMC-IMAG CNRS UMR 5525, Université J. Fourier and Unité d'Exploration de l'Angioedème, CHU Grenoble, France. E-mail: a_lopezlera@yahoo.es.

Supported by Ministerio de Educación y Ciencia SAF2006-02948 and CIBERER Intra 09758.2.

Disclosure of potential conflict of interest: A. López-Lera receives research support from the Biomedical Network Research Center on Rare Diseases and the Ministry of Education and Science. R. Mena de la Cruz receives research support from the Biomedical Network Research Center on Rare Diseases. M. López-Trascasa receives research support from the Biomedical Network Research Center on Rare Diseases and the Ministry of Education and Science. The rest of the authors have declared that they have no conflict of interest.

REFERENCES

1. Grigoriadou S, Longhurst HJ. Clinical immunology review series: an approach to the patient with angio-oedema. Clin Exp Immunol 2009;155:367-77.
2. Cugno M, Castelli R, Cicardi M. Angioedema due to acquired C1-Inhibitor deficiency: a bridging condition between autoimmunity and lymphoproliferation. Autoimmun Rev 2008;8:156-9.

3. Cugno M, Zanichelli A, Foieni F, Caccia S, Cicardi M. C1-inhibitor deficiency and angioedema: molecular mechanisms and clinical progress. Trends Mol Med 2009; 15:69-78.
4. Eldering E, Verpy E, Roem D, Meo T, Tosi M. COOH-terminal substitutions in the serpin C1 inhibitor that cause loop overinsertion and subsequent multimerization. J Biol Chem 1995;270:2579-87.
5. Blanch A, Roche O, Urrutia I, Gamboa P, Fontán G, López-Trascasa M. First case of homozygous C1 inhibitor deficiency [published erratum in J Allergy Clin Immunol 2007;119:745]. J Allergy Clin Immunol 2006;118:1330-5.
6. Vinci G, Lynch NJ, Duponchel C, Lebastard TM, Milon G, Stover C, et al. In vivo biosynthesis of endogenous and of human C1 inhibitor in transgenic mice: tissue distribution and colocalization of their expression. J Immunol 2002;169: 5948-54.
7. Nuijens JH, Huijbregts CC, van Mierlo GM, Hack CE. Inactivation of C1-inhibitor by proteases: demonstration by a monoclonal antibody of a neodeterminant on inactivated, non-complexed C1-inhibitor. Immunology 1987;61:387-9.

Available online September 23, 2010.
doi:10.1016/j.jaci.2010.07.037

Lymphoid neogenesis in the giant papillae of patients with chronic allergic conjunctivitis

To the Editor:

Lymphoid neogenesis (tertiary lymphoid organ [TLO]) resembles a secondary lymphoid organ (eg, the lymph node) and is observed in patients with chronic inflammatory diseases.[1] TLOs play roles in immune responses against persistent antigens; however, they can also induce severe tissue damage.[1] It has also been reported that the germinal centers and follicular dendritic cell (FDC) networks in TLOs relate to class-switch recombination.[2] In this study we examined the lymphoid neogenesis and lymphatic vessel formation in patients with atopic keratoconjunctivitis (AKC) and vernal keratoconjunctivitis (VKC),[3] severe chronic forms of allergic conjunctivitis. AKC and VKC are often accompanied by giant papillae formation in tarsal conjunctivae and/or marked inflammatory cell infiltration in the limbal region, with prominent T_H2 cytokine profiles.[3] We found various degrees of lymphoid neogenesis in the giant papillae with B-cell clusters, FDCs, and a marginal T-cell zone essential for TLO formation.[1]

The IgE class of immunoglobulin is produced by B cells and plasma cells through class-switch recombination in the germinal center of lymphoid tissues.[2] Preferential expression of the FcεRI β-chain protein, an amplifier of allergic responses, has been observed in the giant papillae of patients with AKC/VKC.[4] These findings suggested the role of an IgE–FcεRI β cascade in the pathophysiology of severe chronic allergic conjunctivitis. The IgE might originate from tears[5] or from blood flow; however, local IgE class-switch recombination in the giant papillae itself, as well as in the nasal polyps,[6] might also be possible. Regional IgE expression at the mast cells, dendritic cells, and Langerhans cells of the giant papillae was reported previously.[7] Therefore it is important to clarify the origin of IgE production in patients with AKC/VKC because anti-IgE antibody therapy has recently been introduced for the treatment of severe atopic asthma, and it might also be effective for AKC/VKC.

Ten giant papillae obtained from patients with AKC/VKC were resected for a therapeutic purpose, as previously described.[4] The clinical information of the patients is summarized in Table I. All the patients had chronic allergic conjunctivitis and were treated with topical dexamethasone eye drops for at least 4 weeks before surgery. Total IgE concentrations and specific IgE titers against 26 common antigens were measured by SRL, Inc (Tokyo, Japan),

TABLE I. Clinical information of the patients and summary of the results

Patient no.	Age (y)	Sex	Total IgE (IU/mL)	Specific IgE	Diagnosis*	$CD20^+$ cell cluster†	FDC
1	16	F	509	Positive	VKC	Large clusters	+
2	22	M	89	Positive	VKC	Diffuse	+
3	13	M	2,319	Positive	VKC	Large clusters	+
4	18	M	375	Positive	AKC	Diffuse and large clusters	+
5	17	M	17,260	Positive	AKC	Large clusters	+
6	21	M	1,904	Positive	AKC	Small clusters	+
7	16	M	3,763	Positive	AKC	Large clusters	+
8	34	M	22,800	Positive	AKC	Large clusters	+
9	45	F	28	Negative	AKC	Small clusters	+
10	29	M	56	Positive	VKC	Small clusters	+

*AKC was defined as a bilateral chronic inflammation of the conjunctiva and lids associated with atopic dermatitis. VKC was defined as a bilateral, chronic, conjunctival inflammatory condition of the conjuctiva found in subjects predisposed by their atopic background. Patients who had atopic dermatitis or corneal stromal neovascularization were excluded from the VKC diagnosis.
†Large lymphocyte clusters were defined as those having more than 10 lymphocytes in length/diameter.

TABLE II. List of antibodies used in this study

Antigen	Class	Dilution	Supplier
Anti–LYVE-1	Rabbit polyclonal	1:400	RELIATech, Wolfenbüttel, Germany
Anti-CD3	Murine monoclonal	1:100	DAKO, Glostrup, Denmark
Anti-CD20	Rabbit monoclonal	1:200	Epitomics, South San Francisco, Calif
Anti-CD35	Murine monoclonal	1:50	Dako
Anti-PNAd	Rat monoclonal (IgM)	1:25	Becton Dickinson, Franklin Lakes, NJ
Alexa 488–anti-mouse IgG	Donkey polyclonal	1:1,000	Invitrogen, Carlsbad, Calif
Alexa 594–anti-rabbit IgG	Donkey polyclonal	1:1,000	Invitrogen
Alexa 488–anti-rabbit IgG	Goat polyclonal	1:1,000	Invitrogen
Alexa 594–anti-rat IgM	Goat polyclonal	1:1,000	Invitrogen

J ALLERGY CLIN IMMUNOL
VOLUME 126, NUMBER 6

APPENDIX E1

The results in the present work are in agreement with previous reports concerning attenuated androgen treatment in patients with HAE. Androgens are known to increase C1-Inh and C4 antigenic levels in plasma of heterozygous patients with HAE.[E1] Moreover, it has been shown that androgen treatment increases C1-Inh mRNA expression in PBMCs.[E2] Increased levels and function of C1-Inh might restore local homeostasis between the inhibitor and its target proteases, thus controlling the activation of the classical pathway of complement in the focus of edema. Nevertheless, clinical and laboratory experience regarding androgen use in patients with HAE is restricted to heterozygous situations, in which the wild-type allele can be driven to increment C1-Inh production. To date, reports on the prophylactic intake of androgens in homozygous patients with HAE are lacking.

Of note, the homozygous R378C substitution markedly reduces but does not completely suppress C1-Inh synthesis and secretion. This basal expression of the R378C allele provides a source for the low but detectable levels of C1-Inh in the patient before treatment and makes the mutant allele susceptible to androgen upregulation, explaining the patient's good response to attenuated androgen therapy.

To our knowledge, the R378C substitution described here is the first mutation outside of the RCL reported to alter C1-Inh specificity. The R378 residue is located in the gate region, in the turn between 2C helix and the S6A strand of β-sheet A (Protein Data Bank accession 2OAY). The importance of this region is highlighted by studies on the model serpin α-1-antitrypsin (A1AT), in which, on interaction with proteases, the RCL inserts into β-sheet A and is stabilized by a salt bridge formed between amino acids K290 and E342. The disruption of this salt bridge in the Z variant of A1AT (carrying the E342K mutation) reduces the stability of the molecule and induces its intracellular multimerization by means of a loop-sheet insertion mechanism.[E3] Based on structural models of C1-Inh, it is predictable that R378 also forms a salt bridge with E429. In the R378C mutant the positively charged arginine (homologous to K290 in A1AT) is replaced by the neutral cysteine at position 378 and probably prevents salt bridge formation with subsequent alteration of the protein conformation.

The specific impairment in kallikrein activation control found in the R378C mutant sheds more light on the pathogenesis of HAE. The situation seems to be opposite to that of the family reported by Wisnieski et al,[E4] in which an Ala443Val substitution in C1-Inh prevented C1r binding but maintained full inhibitory capacity to kallikrein and coagulation factor XII.[E5,E6] Although the R378C homozygous patient has had recurrent episodes of edema, no family member with the Ala443Val mutation, all of whom also had complement system activation, ever had symptoms of HAE, suggesting that classical complement activation alone does not result in angioedema.

REFERENCES

E1. Gelfand JA, Sherins RJ, Alling DW, Frank MM. Treatment of hereditary angioedema with danazol. Reversal of clinical and biochemical abnormalities. N Engl J Med 1976;295:1444-8.

E2. Pappalardo E, Zingale LC, Cicardi M. Increased expression of C1-inhibitor mRNA in patients with hereditary angioedema treated with danazol. Immunol Lett 2003; 86:271-6.

E3. Janciauskiene S, Eriksson S, Callea F, Mallya M, Zhou A, Seyama K, et al. Differential detection of PAS-positive inclusions formed by the Z, Siiyama, and Mmalton variants of alpha1-antitrypsin. Hepatology 2004;40:1203-10.

E4. Wisnieski JJ, Knauss TC, Yike I, Dearborn DG, Narvy RL, Naff GB. Unique C1 inhibitor dysfunction in a kindred without angioedema, I: a mutant C1 INH that inhibits C1-s but not C1-r. J Immunol 1994;152:3199-209.

E5. Zahedi R, Bissler JJ, Davis AE 3rd, Andreadis C, Wisnieski JJ. Unique C1 inhibitor dysfunction in a kindred without angioedema. II. Identification of an Ala443→Val substitution and functional analysis of the recombinant mutant protein. J Clin Invest 1995;95:1299-305.

E6. Zahedi R, Wisnieski JJ, Davis AE 3rd. Role of the P2 residue of complement 1 inhibitor (Ala443) in determination of target protease specificity: inhibition of complement and contact system proteases. J Immunol 1997;159:983-8.

Patient Code	Age (y.o.)	C4 (14-47 mg/dl)	C3 (77-120 mg/dl)	C2 (45.23 A.U.)	C1-Inh (14-35 mg/dl)	C1-Inh Function (70-130%)	C1q (10-30 mg/dl)	Genotype	HAE Type
GZ	33	1.44	141	ND	4.38	11	ND	R378C/C	I
GZ3	28	21.70	119	39.7	24.90	44	12	R378R/C	II
GZ4	27	14.50	125	52.25	19.70	34	14.2	R378R/C	II
GZ5	37	15	119	61.89	14.70	52	13.8	R378R/C	II
GZ6	6	16.40	125	54.73	23.50	36	14.6	R378R/C	II
GZ7	3	12	97	41.19	18.9	100	12	R378R/C	-

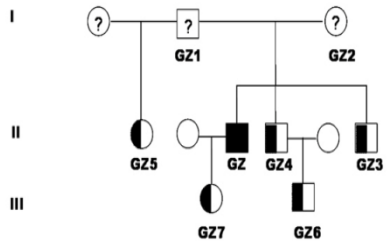

FIG E1. Complement profile and family tree. The reference values were obtained from a series of healthy donors. The first generation was not available for the study. *ND,* Not detectable.

J ALLERGY CLIN IMMUNOL
VOLUME 126, NUMBER 6

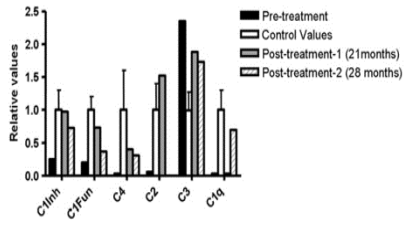

FIG E2. Follow-up of complement profile after treatment with stanozolol. C1-Inh levels and function and C4 and C2 levels were markedly increased in plasma of the R378C homozygote after treatment with stanozolol. C1q increased to normal levels only in the second posttreatment sample 28 months after the beginning of stanozolol intake. All the measures are expressed as a percentage of the reference values in each case.

RESEARCH ARTICLE

AMERICAN JOURNAL OF medical genetics PART A

CDKN1C ($p57^{Kip2}$) Analysis in Beckwith–Wiedemann Syndrome (BWS) Patients: Genotype–Phenotype Correlations, Novel Mutations, and Polymorphisms

Valeria Romanelli,[1,2] Alberta Belinchón,[1,2] Sara Benito-Sanz,[1,2] Victor Martínez-Glez,[1,2] Ricardo Gracia-Bouthelier,[3,4] Karen E. Heath,[1,2] Angel Campos-Barros,[1,2] Sixto García-Miñaur,[1,2] Luís Fernandez,[1,2] Heloisa Meneses,[1,2] Juan Pedro López-Siguero,[5] Encarna Guillén-Navarro,[6] Paulino Gómez-Puertas,[7] Jan-Jaap Wesselink,[7,8] Graciela Mercado,[9] Victoria Esteban-Marfil,[10] Rebeca Palomo,[1,2] Rocío Mena,[1,2,11] Aurora Sánchez,[2,12] Miguel del Campo,[2,13] and Pablo Lapunzina[1,2,4]*

[1]INGEMM, Instituto de Genética Médica y Molecular, IdiPAZ-Hospital Universitario La Paz, Universidad Autónoma de Madrid, Madrid, Spain

[2]CIBERER, Centro de Investigación Biomédica en Red de Enfermedades Raras, Madrid, Spain

[3]Servicio de Endocrinología Infantil, Hospital Universitario La Paz, Universidad Autónoma de Madrid, Madrid, Spain

[4]RESSC, Registro Español de Síndromes de Sobrecrecimiento, Madrid, Spain

[5]Servicio de Endocrinología Infantil, Hospital Carlos Haya, Málaga, Spain

[6]Unidad de Genética Médica, Servicio de Pediatría, Hospital Universitario Virgen de la Arrixaca, Murcia, Spain

[7]Centro de Biología Molecular "Severo Ochoa" (CSIC-UAM), Madrid, Spain

[8]Biomol-Informatics S.L., Parque Científico de Madrid, Madrid, Spain

[9]CENAGEM, Centro Nacional de Genética Médica, Buenos Aires, Argentina

[10]Servicio de Pediatría, Hospital de Jaén, Jaén, Spain

[11]Unidad de Secuenciación Automática, Hospital Universitario La Paz, Madrid, Spain

[12]Secció de Citogenètica i Genètica Clínica, Servei de Bioquímica i Genètica Molecular, Hospital Clínic, Barcelona, Spain

[13]Unitat de Genética, Hospital Vall d'Hebrón, Barcelona, Spain

Received 27 November 2009; Accepted 5 March 2010

Beckwith–Wiedemann syndrome (BWS) is an overgrowth syndrome characterized by macroglossia, macrosomia, and abdominal wall defects. It is a multigenic disorder caused in most patients by alterations in growth regulatory genes. A small number of individuals with BWS (5–10%) have mutations in *CDKN1C*, a cyclin-dependent kinase inhibitor of G1 cyclin complexes that functions as a negative regulator of cellular growth and proliferation. Here, we report on eight patients with

How to Cite this Article:
Romanelli V, Belinchón A, Benito-Sanz S, Martínez-Glez V, Gracia-Bouthelier R, Heath KE, Campos-Barros A, García-Miñaur S, Fernandez L, Meneses H, López-Siguero JP, Guillén-Navarro E, Gómez-Puertas P, Wesselink J-J, Mercado G, Esteban-Marfil V, Palomo R, Mena R, Sánchez A, del Campo M, Lapunzina P. 2010. *CDKN1C* ($p57^{Kip2}$) analysis in Beckwith–Wiedemann syndrome (BWS) patients: Genotype–phenotype correlations, novel mutations, and polymorphisms.
Am J Med Genet Part A 152A:1390–1397.

Grant sponsor: Fondo de Investigación Sanitaria (FIS); Grant number: PI08/1360.
*Correspondence to:
Pablo Lapunzina, M.D., Ph.D., INGEMM Instituto de Genética Médica y Molecular, CIBERER, Centro de Investigación Biomédica en Red de Enfermedades Raras, Madrid, Spain; IdiPaz-Hospital Universitario La Paz; Paseo de la Castellana 261, 28046 Madrid, Spain.
E-mail: plapunzina.hulp@salud.madrid.org
Published online 14 May 2010 in Wiley InterScience (www.interscience.wiley.com)
DOI 10.1002/ajmg.a.33453

BWS and *CDKN1C* mutations and review previous reported cases. We analyzed 72 patients (50 BWS, 17 with isolated hemihyperplasia (IH), three with omphalocele, and two with macroglossia) for *CDKN1C* defects with the aim to search for new mutations and to define genotype–phenotype correlations. Our findings suggest that BWS patients with *CDKN1C* mutations have a different pattern of clinical malformations than those with other molecular defects. Polydactyly, genital abnormalities, extra nipple, and cleft palate are more frequently observed in BWS with mutations in *CDKN1C*. The clinical observation of these malformations may help to decide which genetic characterization should be undertaken (i.e., *CDKN1C* screening), thus optimizing the laboratory evaluation for BWS.

Key words: overgrowth syndrome; mutations; cleft palate; omphalocele; polydactyly; extra nipple

INTRODUCTION

Beckwith–Wiedemann syndrome [BWS (OMIM 130650)] is a phenotypically variable and genotypically heterogeneous overgrowth syndrome characterized by somatic overgrowth, macroglossia and abdominal wall defects. Other findings include hemihyperplasia, embryonal tumors, adrenocortical cytomegaly, ear anomalies, visceromegaly, renal abnormalities, neonatal hypoglycemia, and occasionally cleft palate, polydactyly and a positive family history [Beckwith, 1963; Wiedemann, 1964; Pettenati et al., 1986; Elliott and Maher, 1994; Elliott et al., 1994; Weng et al., 1995; Engstrom et al., 1998]. BWS is a complex, multigenic disorder caused in up to 90% of patients by an alteration in growth regulatory genes located on chromosome 11p15 [Li et al., 1997, 1998]. Several molecular abnormalities are associated with BWS. Chromosomal rearrangements are relatively rare (~2–3% of cases) and comprise translocations or inversions (typically maternally inherited), and paternal duplications. The largest molecular subgroup (~60–70% of cases) is represented by patients carrying an epigenetic error in one or more genes on 11p15 [Maher and Reik, 2000; Cooper et al., 2005; Weksberg et al., 2005; Enklaar et al., 2006]. This region spans approximately 1 Mb and includes two differentially-methylated imprinted domains that control imprinting of genes in this cluster [Weksberg et al., 2003]. Patients (~15%) may also have paternal uniparental disomy, two paternally derived copies of 11p15 and no maternal contribution for that region [Henry et al., 1991]. Finally, a small number of individuals with BWS carry point mutations in *CDKN1C* (also known as $p57^{kip2}$; OMIM 600856). These mutations have been found in 5–10% of sporadic BWS cases [Lee et al., 1997; Li et al., 2001] and in approximately 40% of cases with a positive family history [O'Keefe et al., 1997].

CDKN1C maps centromeric to the region 11p15 and it is paternally imprinted in humans with preferential expression of the maternal allele [Hatada and Mukai, 1995]. It encodes a Cyclin-dependent Kinase (CdK) that functions as a potent tight-binding inhibitor of several G1 Cyclin/CdK complexes, thus acting as a negative regulator of cellular proliferation [Lee et al., 1995]. Alterations of genes involved in cell cycle regulation are tightly linked to tumorigenesis, which led us to consider *CDKN1C* as a putative tumor suppressor gene. Despite this, and the fact that BWS patients have a 1,000-fold increased risk of embryonal tumors, including Wilms tumor, hepatoblastoma, and rhabdomyosarcoma [Wiedemann, 1983], there is no conclusive evidence that BWS patients with *CDKN1C* mutations have this increased risk of neoplasia.

CDKN1C (ENST00000414822) contains three exons (two coding) and two GC-rich introns of 535 and 83 bp (Fig. 1). Alternative splicing generates the heterogeneity in the translational initiations [Tokino et al., 1996]. The CDKN1C protein has 316 amino acids and is expressed in the heart, brain, lung, skeletal muscle, kidney, pancreas and testis. In addition, high levels are seen in placenta, and this fact may have importance in the pathophysiology of preeclampsia/HELLP syndrome [Romanelli et al., 2009]. The protein consists of three structurally distinct domains: (i) the N-terminal domain (aa 1–110) which is significantly similar to the CdK-inhibitors p21Cip1 and $p27^{Kip1}$ and has been shown to be necessary for CdK inhibition; (ii) a central highly polymorphic hexanucleotide repeat encoding a proline-alanine series of repeats, PAPA-repeats (aa 156–213), and (iii) a highly conserved C-terminal region (QT domain) that presents homology with $p27^{Kip1}$ (Fig. 1) [Lee et al., 1995; Matsuoka et al., 1995].

In this investigation we analyzed *CDKN1C* by direct bidirectional sequencing in a series of BWS patients who did not have chromosomal or epigenetic abnormalities at the 11p15 locus. The aim of this work was to look for new mutations, review reported *CDKN1C* aberrations and to evaluate genotype–phenotype correlations. We also performed *CDKN1C* mutational analysis in a series of patients with isolated hemihyperplasia, macroglossia or omphalocele, since these manifestations are frequent features of BWS and theoretically, mutations in *CDKN1C* might be present in patients with mild symptoms of the disorder.

We identified several novel mutations and polymorphisms of *CDKN1C*. We also carried out a genotype–phenotype correlation in our patients and found useful clinical findings that may aid in the laboratory workflow for diagnosis [Percesepe et al., 2008]. Nucleotide c.845 appears to be a mutation hotspot as 4 patients had an alteration at this position.

PATIENTS AND METHODS

Patients

To date we have collected a total of 149 patients (127 BWS, 17 IH, 3 omphalocele, 2 macroglossia) which are included in the Spanish Overgrowth Syndrome Registry. We analyzed *CDKN1C* in 50 patients with BWS and 17 with IH who were negative for chromosomal or epigenetic alterations in 11p15. We also included 5 patients with isolated omphalocele (3 patients), and isolated macroglossia (2 patients). Data documented were: clinical and family history, biochemical analysis, X-rays and follow-up information. The institutional research board at Hospital Universitario La Paz approved this investigation and consent was obtained from all cases or their parents.

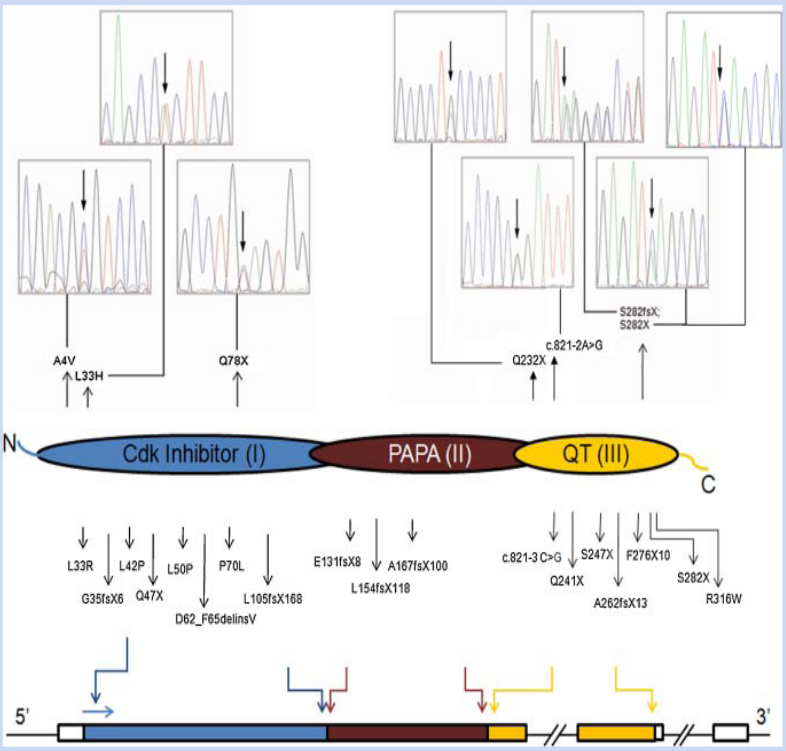

FIG. 1. Schematic representation of *CDKN1C* and mutations identified. Chromatograms of the eight novel mutations identified in this study are shown above the protein structure, while the previously reported mutations are shown below the protein. At the bottom, schematic representation of the gene; rectangles denote the three exons, and the broken lines represent the two introns. [Color figure can be viewed in the online issue, which is available at www.interscience.wiley.com.]

PCR Amplification and Sequencing of *CDKN1C*

DNA samples were obtained from peripheral blood leukocytes using Puregene Blood Core Kit B (Qiagen, Hilden, Germany) according to the manufacturer's instructions.

Primers for the amplification of *CDKN1C* were designed with the help of the OLIGO 6 software (Molecular Biology Insights, Inc., Cascade, CO). The following set of primers was used to obtain a single amplicon (1,675 bp) that comprises the entire coding region of *CDKN1C*: sense primer, 5′-cgccctctcctcctctctttccccttc-3′ and antisense primer: 5′-tcggggctctttgggctctaaact-3′. The PCR reaction mixture consisted of: 10× PCR buffer HotStartTaq QIAGEN (containing 15 mM $MgCl_2$), 0.4 mM dNTPs, 0.4 μM of each primer, 10% DMSO, 100 ng DNA, 2 units HotStart Taq polymerase (Qiagen) in a final volume of 25 μL. A Tetrad2 thermocycler (Bio-Rad Laboratories, Inc., Hercules, California) was used for PCR; PCR conditions were a touchdown PCR consisting of an activation step at 95°C for 15 min; followed by 15 cycles of 95°C for 1 min 30 sec, 68°C for 1 min (with a touchdown of 0.5°C every cycle) and 72°C for 2 min and subsequently 23 cycles of 95°C for 1 min 30 sec, 60°C for 1 min and 72°C for 2 min and a final primer extension step for 72°C for 10 min. PCR fragments were purified by ExoSAP-IT (USB) and sequenced by BigDye Terminator Cycle Sequencing Kit (Applied Biosystems, Foster City, California). Due to the high polymorphic structure of the PAPA domain, sequencing of *CDKN1C* was performed with the help of eight different primers (Table I). Finally, sequences were precipitated by CleanSEQ (Agencourt) and sequenced on an ABI 3130 automatic sequencer.

TABLE I. Primers Used for Sequencing of *CDKN1C*

	Primer for sequencing	Exons
1F	5′-ctcctttccccttcttctcg-3′	1
2F	5′-tggaccgaagtggacagcga-3′	1
3R	5′-cctgcaccgtctcgcggtag-3′	1
4F	5′-ccggagcagctgcctagtgtc-3′	1
5R	5′-ggggccaggaccgcgacc-3′	1
6R	5′-gggaggaggcgggaaccctgcga-3′	1
7F	5′-cggcgacgtaaacaaagctgac-3′	2
8R	5′-tcggggctctttgggctctaaact-3′	2

3D Structure Modeling

Structural model of the CdK-inhibitor domain of human CDKN1C protein (UniProtKB/Swiss-Prot code P49918, aa 26–96) bound to cyclin A-CDK2 complex was constructed by standard comparative modeling methods and the software DeepView [Guex and Peitsch, 1997], using the structure of $p27^{kip1}$/cyclin a/CdK2 complex deposited in the Protein Data Bank (PDB) [Berman et al., 2000] with code 1JSU [Russo et al., 1996] as template. Sequence identity between p27 and CDKN1C modeled domain was 47%, with a Blast e-value of 1.4×10^{-14}. The quality of the model was checked using the analysis programs (Anolea, Gromos and Verify3D) provided by the SWISS-MODEL server [Peitsch, 1996; Guex et al., 1999; Schwede et al., 2003].

RESULTS

Patients with either a complete phenotype of BWS (n = 50) or IH, omphalocele or macroglossia (n = 22) were studied. We found mutations in 8 BWS patients; all were novel, 6 of 7 were inherited from the mother, 1 was a de novo mutation and in 1 (patient 8) the inheritance is not known. Five of 8 mutations were nonsense mutations (Table II, Fig. 1). We also identified 6 synonymous non-described variants in our series (Table III). Novel mutations and clinical findings are listed in Tables II and IV.

DISCUSSION

To date, 25 different mutations have been reported in *CDKN1C* including the 7 novel mutations reported here. Among these, we found a novel splice mutation in intron 1 (c.821-2 A>G) which may lead to either inclusion of the intron 1 or exon-skipping of exon 2. Only two amino acids were affected in more than one patient; Leu33 (in two patients, L33H and L33R) and Ser282 (in four patients, S282X and S282fsX) (Table II). These residues comprise 23% of reported mutations and may well behave as mutation hot spots. Using homology-based modeling, we constructed a 3D structural model of the CdK-inhibitor domain of CDKN1C bound to cyclin A -CdK2 (Fig. 2). The model suggested that the pair of CDKN1C residues (Leu33 and Phe34) conforms to a small hydrophobic patch in close contact with a hydrophobic groove composed by cyclin A residues Met210, Ile213, Leu214, Trp217, and Leu253. The introduction of a positively charged His at residue 33 (L33H) probably affects the stabilization of the complex (as suggested in the L33R mutant [Engel et al., 2000]) and may modify the local protein-protein interaction, which may result in a loss of binding affinity.

We searched for putative Exonic Splicing Enhancer (ESE) sequences in the CDS of *CDKN1C* using ESEfinder [Cartegni et al., 2003; Smith et al., 2006], RESCU-ESE [Fairbrother et al., 2002] and the Regulatory Sequence Database of the ASD Project [Stamm et al., 2006]. ESEs are short sequences found within coding exons that are

TABLE II. *CDKN1C* Mutations Identified to Date in BWS Patients*

Nucleotide change	Amino acid change	Protein domain	Inheritance	References
c.11 C>T	p. A4V	I	Maternal	Novel
c.98 T>A	p. L33H	I	Maternal	Novel
c.98 T>G	p. L33R	I		Engel et al. [2000]
c.105delG	p. G35fsX6	I		Lee et al. [1997]
c.125 T>C	p. L42P	I		Li et al. [2001]
c.139 C>T	p. Q47X	I		Hatada et al. [1996]
c 149 T>C	p. L50P	I		Li et al. [2001]
c.185_193delATTACGACT	p. D62_F65delinsV	I		O'Keefe et al. [1997]
c.209 C>T	p. P70L	I		Lam et al. [1999]
c.232 C>T	p. Q78X	I	De novo	Novel
c.310_311delCTinsG	p. L105fsX168	I		Hatada et al. [1997]
c.391_392insT	p. E131fsX8	I/II		Engel et al. [2000]
c.461delT	p. L154fsX118	I/II		Lee et al. [1997]
c.499_514delGCTCCGGTCGCGGCTC	p. A167fsX100	II		Lam et al. [1999]
c.694 C>T	p. Q232X	III	Maternal	Novel
c.721 C>T	p. Q241X	III		Li et al. [2001]
c.740 C>A	p. S247X	III		Hatada et al. [1996]
c.784_785delGC	p. A262fsX13	III		Li et al. [2001]
c.821-2 A>G	Splice mutation		Maternal	Novel
c 821-3 C>G	Splice mutation			Lam et al. [1999]
c.826delTinsAG	p. F276fsX10	III		Hatada et al. [1996]
c.845 C>G	p. S282X	III		Lam et al. [1999], current paper
c.845 C>A	p. S282X	III	Maternal	Novel
c.845delC	p. S282fsX	III	Maternal	Novel
c.946 C>T	p. R316W	III		Lam et al. [1999]

#Mutations affecting the same residues as previously reported mutation [Lam et al., 1999; Engel et al., 2000].

*Mutations are numbered according to ensembl ENST00000414822.

TABLE III. Reported and Novel *CDKN1C* Variants*

Number and percentage of patients (n = 72)	Nucleotide change	Amino acid residue	Protein domain	References
11 (15.3)	c.1–84 G>A			Lam et al. [1999]
1 (1.4)	c.1–83 G>A			Lam et al. [1999]
1 (1.4)	c.456 G>A	p. V152V	I/I I	Current paper
1 (1.4)	c.504 G>A	p. P168P	II	Current paper
32 (44.4)	c.511_522delGCTCCGGTCGCG	p. A171_A174del	II	Tokino et al. [1996]
3 (4.2)	c.528 G>C	p. A176A	II	Current paper
26 (36.1)	c.555 T>C	p. A185A	II	Tokino et al. [1996]
2 (4.2)	c.598_609delCCAGCCCCGGCC	p. P200_A203del	II	Tokino et al. [1996]
2 (2.8)	c.599 A>G	p. P200P	II	Current paper
3 (4.2)	c.612 G>A	p. P205P	II	Current paper
1 (1.4)	c.616_627delCCGGCCCCGGCC	p. P206_A209del	II	Tokino et al. [1996]
1 (1.4)	C.708 G>A	p. E236E	III	rs3741341
45 (62.5)	c.951 + 29_951 + 30insG			rs34289096
1 (1.4)	c.951 + 29_951 + 30insGG			Current paper

*Mutations are numbered according to ensembl transcript ENST00000414822.

often predicted to be binding sites for splicing factors. ESEs are required for efficient splicing and may influence splice site recognition during both constitutive and alternative splicing [Blencowe, 2000]. We analyzed all known and novel missense mutations to find possible alterations in ESE sequences. ESEfinder identified a putative SRp40 element that is disrupted by the cytosine to thymine substitution at position 139 (c.139 C>T, Q47X; from score 3.04 to score 0). Both RESCU-ESE and the ASD-Regulatory Sequence Database identified a putative ESE sequence that is disrupted by the deletion at position 185 (c.185_193delATACGACT, D62-_F65delinsV). RESCU-ESE identified a putative ESE sequence that is disrupted by the thymine insertion at position 391 (c.391_392insT, E131fsX8). These findings suggest that these mutations (Q47X, D62_F65delinsV and E131fsX8), apart from leading to the synthesis of a truncated protein, may also affect the splicing of the *CDKN1C* pre-mRNA. However, experimental evidence is necessary to confirm that these mutations disrupt ESE motifs. Finally, we also observed known and novel non-described variants not only SNPs but also the 12 bp ins/del polymorphism in the PAPA domain.

CDKN1C mutations were identified in 8 of 50 patients with BWS and in none of the patients with isolated omphalocele, hemihyperplasia or macroglossia. The absence of mutations in these three other malformations was expected due to the small number of cases evaluated and to the observation that no mutations in *CDKN1C* have previously been reported in these patients with isolated findings. The percentage of cases presenting with *CDKN1C* mutations in our series is in agreement with previously reports (8/127 = 6.2%) [Lee et al., 1997; Li et al., 2001]. In most BWS cases (6/7) the mutation was inherited from apparently asymptomatic mothers, who either inherited the change from their fathers or had de novo mutations in the paternal chromosome. Three of these mothers developed preeclampsia/HELLP syndrome during pregnancy [Romanelli et al., 2009]. In one adult case, the pattern of inheritance could not be evaluated due to lack of parental samples.

Most patients with BWS had omphalocele or umbilical herniae and three displayed cleft palate, which is considered as a major finding but is not frequently reported in BWS cases [Weksberg et al., 2010]. The *cdkn1c −/−* mice have cleft palate, which suggests the possibility of an increased frequency of this malformation in BWS caused by *CDKN1C* mutations [Takahashi et al., 2000]. Among the 126 patients with BWS present in our cohort only three had cleft palate, all with *CDKN1C* mutations located in the QT domain of the protein. However, previously reported patients with mutations affecting domain III did not show cleft palate [Hatada et al., 1996; Lam et al., 1999; Li et al., 2001] indicating that our finding may be merely coincidental or caused by unknown factors. Interestingly, of the 26 mutations reported, 15 were mutations that altered or lacked the QT domain, which would leave the cyclin/CdK binding and inhibitory region of the protein intact [Matsuoka et al., 1995]. Therefore, the QT domain seems to have a regulatory function for the $p57^{kip2}$ protein.

Furthermore, two patients had polydactyly and two had extra nipples. Lam et al. [1999] reported a high frequency of omphalocele in patients with *CDKN1C* mutations, but found no cases with polydactyly, extra nipple, or cleft palate. One patient with polydactyly and an accessory nipple was previously reported, but his affected sister had neither polydactyly nor polythelia [Hatada et al., 1996]. Finally, one patient had hypospadias and another cryptorchidism. Genital anomalies have been recently noted as important clinical findings in adults and they seem to be more frequent than initially reported [Greer et al., 2008].

Altogether, these findings suggest that BWS with *CDKN1C* mutations may sometimes exhibit a different, heterogeneous pattern of clinical malformations than those with epigenetic/chromosomal abnormalities. These anomalies include polydactyly, extra nipple, genital anomalies and cleft palate. Identifying those characteristics may be useful to focus the molecular analysis undertaken.

BWS patients have a 5–7% risk of neoplasia [Lapunzina, 2005]. *CDKN1C* has been implicated in several types of human cancer such

TABLE IV. Clinical Findings of Eight BWS Patients With *CDKN1C* Mutations

	Patient							
	1	2	3	4	5	6	7	8
Sex	Male	Female	Male	Female	Male	Male	Male	Male
Age	1 y 6 m	3 y 6 m	11 y 3 m	2 y 10 m	6 y ? m	1 y ? m	? y ? m	32 y
Nucleotide change	c.11 C>T	c.98 T>A	c.232 C>T	c.694 C>T	IVS2- 2A>G	c.845delC	c.845 C>A	c.845 C>G
Amino acid change	p. A4V	p. L33H	p. Q78X	p. Q232X	Splicing mutation	p. S282fsX	p. S282X	p. S282X
Overgrowth	Generalized	Generalized	Generalized	Generalized	Generalized	Generalized	Generalized	Generalized
Birth weight (g)	4,240	4,830	2,890 (33 ws)	4,700	3,650 (36 ws)	1,940 (29 ws)	2,440 (34 ws)	—
Craneofacial	Macroglosia; posterior ear pits	Macroglosia; ear pits; glabellar flat vascular malformations	Macroglosia; ear creases; nevus flammeus	Macroglosia; cleft palate; flat vascular malformation	Mild macroglosia; flat vascular malformation in glabella	Macroglossia; cleft palate; ear creases; nevus flammeus	Macroglossia; cleft palate; ear creases; nevus flammeus	Macroglossia; ear creases
Cardiovascular	—	—	—	—	—	—	VSD-PDA	—
Abdomen	Bilateral nephromegaly; hepatomegaly; splenomegaly	Large umbilical hernia	Umbilical hernia; inguinal hernia	Omphalocele	Omphalocele; inguinal hernia	Omphalocele; inguinal hernia; renal cystis	Omphalocele; hepatomegaly	Omphalocele
Neurologic (CNS)	—	—	—	—	—	Hypotonia	—	—
Limbs	Polydactyly	—	—	Polydactyly (postminimi)	—	—	—	—
Skin	—	Extra nipple	—	—	—	Capillary malformation	Extra nipple	Psoriasis
Genital	—	—	—	—	—	Hypospadias	—	Cryptorchidism
Other	Apneas	—	Hypoglycaemia	Hypoglycaemia	—	—	—	Hypoglycaemia; strabismus

y, year; m, month.

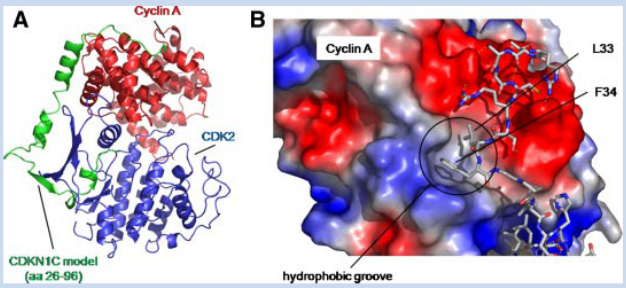

FIG. 2. 3D structural model of the CDK-inhibitor domain of CDKN1C. A: Ribbon-plot representation of 3D model for CDKN1C/cyclin A-CDK2 complex interaction. Model for CDKN1C includes only CDK-inhibitor domain [aa 26–96]. B: Detail of the interaction of CDKN1C Leu33 residue with Cyclin A surface, colored according to electrostatic properties (Red: negative, Blue: positive). The pair of hydrophobic residues L33 and F34 are located in a hydrophobic groove of Cyclin A. Plots were generated using PyMOL (W.L. DeLano (2002) DeLano Scientific, San Carlos, CA). [Color figure can be viewed in the online issue, which is available at www.interscience.wiley.com.]

as colorectal, lymphohematologic and breast cancer, and it has been suggested as a putative breast cancer tumor suppressor [Larson et al., 2008]. To date, none of our eight patients with *CDKN1C* mutations developed neoplasia and as far as we know, only one patient has been previously described with neuroblastoma [Lee et al., 1997]. Follow-up of these patients was carried out until the age of 10 years as recommended [Lapunzina, 2005], though some patients have not yet reached this age. In summary, no patient had Wilms tumor, hepatoblastoma, or rhabdomyosarcoma, which are the commonest neoplasms observed in BWS patients with aberrant methylation and/or paternal UPD. While the total number of cases is small we suggested that familial and sporadic cases with *CDKN1C* mutations seem not to have an increased risk of Wilms tumor or other neoplasias [Cooper et al., 2005].

Simpson–Golabi–Behmel syndrome (OMIM 312870) has overlapping findings with BWS with *CDKN1C* mutations [Romanelli et al., 2007; Romanelli et al., 2009], mainly cleft palate, polydactyly, abnormal genitalia, and extra nipple. It is tempting to speculate that there may be a common pathway between CDKN1C protein and the *MYOD1/CIB2/p73*-dependent pathway. In contrast, no patient with isolated IH, macroglosia or omphalocele had mutations in *CDKN1C* suggesting that these malformations alone are not observed in association with *CDKN1C* mutations. However, further cases are needed to confirm this.

Finally, we suggest that this gene should be analyzed first, not only in BWS with cleft palate (as previously described) but also in BWS patients presenting with polydactyly, extra nipple and/or genital anomalies.

ACKNOWLEDGMENTS

This work was supported by grants from the "Fondo de Investigación Sanitaria" (FIS; PI08/1360). Valeria Romanelli was a recipient of a PhD fellowship from FIS and currently is supported by Fundación Mutua Madrileña. Alberta Belinchón was supported by CIBERER Lanzadera PhD fellowship. Biomol-Informatics SL is partially supported by Torres-Quevedo funds from Ministerio de Ciencia e Innovación.

REFERENCES

Beckwith JB. 1963. Extreme cytomegaly of the adrenal fetal cortex, omphalocele, hyperplasia of kidneys and pancreas, and Leydig-cell hyperplasia: Another syndrome? Western Soc Pediat Res. Los Angeles, Nov 11, 1963.

Berman HM, Westbrook J, Feng Z, Gilliland G, Bhat TN, Weissig H, Shindyalov IN, Bourne PE. 2000. The Protein Data Bank. Nucleic Acids Res 28:235–242.

Blencowe BJ. 2000. Exonic splicing enhancers: Mechanism of action, diversity and role in human genetic diseases. Trends Biochem Sci 25:106–110.

Cartegni L, Wang J, Zhu Z, Zhang MQ, Krainer AR. 2003. ESEfinder: A web resource to identify exonic splicing enhancers. Nucleic Acids Res 31:3568–3571.

Cooper WN, Luharia A, Evans GA, Raza H, Haire AC, Grundy R, Bowdin SC, Riccio A, Sebastio G, Bliek J, Schofield PN, Reik W, Macdonald F, Maher ER. 2005. Molecular subtypes and phenotypic expression of Beckwith-Wiedemann syndrome. Eur J Hum Genet 13:1025–1032.

Elliott M, Maher ER. 1994. Beckwith-Wiedemann syndrome. J Med Genet 31:560–564.

Elliott M, Bayly R, Cole T, Temple IK, Maher ER. 1994. Clinical features and natural history of Beckwith-Wiedemann syndrome: Presentation of 74 new cases. Clin Genet 46:168–174.

Engel JR, Smallwood A, Harper A, Higgins MJ, Oshimura M, Reik W, Schofield PN, Maher ER. 2000. Epigenotype-phenotype correlations in Beckwith-Wiedemann syndrome. J Med Genet 37:921–926.

Engstrom W, Lindham S, Schofield P. 1998. Beckwith-Wiedemann syndrome. Eur J Pediatr 147(5):450–457.

Enklaar T, Zabel BU, Prawitt D. 2006. Beckwith-Wiedemann syndrome: Multiple molecular mechanisms. Expert Rev Mol Med 8:1–19.

Fairbrother WG, Yeh RF, Sharp PA, Burge CB. 2002. Predictive identification of exonic splicing enhancers in human genes. Science 297:1007–1013.

Greer KJ, Kirkpatrick SJ, Weksberg R, Pauli RM. 2008. Beckwith-Wiedemann syndrome in adults: Observations from one family and recommendations for care. Am J Med Genet Part A 146A:1707–1712.

Guex N, Peitsch MC. 1997. SWISS-MODEL and the Swiss-PdbViewer: An environment for comparative protein modeling. Electrophoresis 18:2714–2723.

Guex N, Diemand A, Peitsch MC. 1999. Protein modelling for all. Trends Biochem Sci 24:364–367.

Hatada I, Mukai T. 1995. Genomic imprinting of p57KIP2, a cyclin-dependent kinase inhibitor, in mouse. Nat Genet 11:204–206.

Hatada I, Ohashi H, Fukushima Y, Kaneko Y, Inoue M, Komoto Y, Okada A, Ohishi S, Nabetani A, Morisaki H, Nakayama M, Niikawa N, Mukai T. 1996. An imprinted gene p57KIP2 is mutated in Beckwith-Wiedemann syndrome. Nat Genet 14:171–173.

Henry I, Bonaiti-Pellie C, Chehensse V, Beldjord C, Schwartz C, Utermann G, Junien C. 1991. Uniparental paternal disomy in a genetic cancer-predisposing syndrome. Nature 351:665–667.

Lam WW, Hatada I, Ohishi S, Mukai T, Joyce JA, Cole TR, Donnai D, Reik W, Schofield PN, Maher ER. 1999. Analysis of germline CDKN1C (p57KIP2) mutations in familial and sporadic Beckwith-Wiedemann syndrome (BWS) provides a novel genotype-phenotype correlation. J Med Genet 36:518–523.

Lapunzina P. 2005. Risk of tumorigenesis in overgrowth syndromes: A comprehensive review. Am J Med Genet Part C 137C:53–71.

Larson PS, Schlechter BL, King CL, Yang Q, Glass CN, Mack C, Pistey R, de Las MA, Rosenberg CL. 2008. CDKN1C/p57kip2 is a candidate tumor suppressor gene in human breast cancer. BMC Cancer 8:68.

Lee MH, Reynisdottir I, Massague J. 1995. Cloning of p57KIP2, a cyclin-dependent kinase inhibitor with unique domain structure and tissue distribution. Genes Dev 9:639–649.

Lee MP, DeBaun M, Randhawa G, Reichard BA, Elledge SJ, Feinberg AP. 1997. Low frequency of p57KIP2 mutation in Beckwith-Wiedemann syndrome. Am J Hum Genet 61:304–309.

Li M, Squire JA, Weksberg R. 1997. Molecular genetics of Beckwith-Wiedemann syndrome. Curr Opin Pediatr 9:623–629.

Li M, Squire JA, Weksberg R. 1998. Molecular genetics of Wiedemann-Beckwith syndrome. Am J Med Genet 79:253–259.

Li M, Squire J, Shuman C, Fei YL, Atkin J, Pauli R, Smith A, Nishikawa J, Chitayat D, Weksberg R. 2001. Imprinting status of 11p15 genes in Beckwith-Wiedemann syndrome patients with CDKN1C mutations. Genomics 74:370–376.

Maher ER, Reik W. 2000. Beckwith-Wiedemann syndrome: Imprinting in clusters revisited. J Clin Invest 105:247–252.

Matsuoka S, Edwards MC, Bai C, Parker S, Zhang P, Baldini A, Harper JW, Elledge SJ. 1995. p57KIP2, a structurally distinct member of the p21CIP1 Cdk inhibitor family, is a candidate tumor suppressor gene. Genes Dev 9:650–662.

O'Keefe D, Dao D, Zhao L, Sanderson R, Warburton D, Weiss L, Anyane-Yeboa K, Tycko B. 1997. Coding mutations in p57KIP2 are present in some cases of Beckwith-Wiedemann syndrome but are rare or absent in Wilms tumors. Am J Hum Genet 61:295–303.

Peitsch MC. 1996. ProMod and Swiss-Model: Internet-based tools for automated comparative protein modelling. Biochem Soc Trans 24: 274–279.

Percesepe A, Bertucci E, Ferrari P, Lugli L, Ferrari F, Mazza V, Forabosco A. 2008. Familial Beckwith-Wiedemann syndrome due to CDKN1C mutation manifesting with recurring omphalocele. Prenat Diagn 28:447–449.

Pettenati MJ, Haines JL, Higgins RR, Wappner RS, Palmer CG, Weaver DD. 1986. Wiedemann-Beckwith syndrome: Presentation of clinical and cytogenetic data on 22 new cases and review of the literature. Hum Genet 74:143–154.

Romanelli V, Magano L, Segovia M, Cosentino V, González-Meneses A, del Campo M, Pérez Jurado LA, Giovannucci Uzielli ML, Soler V, Sanchis A, Arias P, Incera I, Gracia-Bouthelier R, Lapunzina P. 2008. The *OFD1* (*CXORF5*) gene at Xp22 is not mutated in a subset of Simpson-Golabi-Behmel syndrome patients. Curr Top Genet. 3:45–47.

Romanelli V, Arroyo I, Rodriguez JI, Magano L, Arias P, Incera I, Gracia-Bouthelier R, Lapunzina P. 2007. Germinal mosaicism in Simpson-Golabi-Behmel syndrome. Clin Genet 72:384–386.

Romanelli V, Belinchon A, Campos-Barros A, Heath KE, Garcia-Minaur S, Martinez-Glez V, Palomo R, Mercado G, Gracia R, Lapunzina P. 2009. CDKN1C mutations in HELLP/preeclamptic mothers of Beckwith-Wiedemann Syndrome (BWS) patients. Placenta 30:551–554.

Russo AA, Jeffrey PD, Patten AK, Massague J, Pavletich NP. 1996. Crystal structure of the p27Kip1 cyclin-dependent-kinase inhibitor bound to the cyclin A-Cdk2 complex. Nature 382:325–331.

Schwede T, Kopp J, Guex N, Peitsch MC. 2003. SWISS-MODEL: An automated protein homology-modeling server. Nucleic Acids Res 31:3381–3385.

Smith PJ, Zhang C, Wang J, Chew SL, Zhang MQ, Krainer AR. 2006. An increased specificity score matrix for the prediction of SF2/ASF-specific exonic splicing enhancers. Hum Mol Genet 15:2490–2508.

Stamm S, Riethoven J-JM, Le Texier V, Gopalakrishnan C, Kumanduri V, Tang Y, Barbosa-Morais NL, Thanaraj TA. 2006. ASD: A bioinformatics resource on alternative splicing. Nucleic Acids Res 34:D46–D55.

Takahashi K, Nakayama K, Nakayama K. 2000. Mice lacking a CDK inhibitor, p57Kip2, exhibit skeletal abnormalities and growth retardation. J Biochem 127:73–83.

Tokino T, Urano T, Furuhata T, Matsushima M, Miyatsu T, Sasaki S, Nakamura Y. 1996. Characterization of the human p57KIP2 gene: Alternative splicing, insertion/deletion polymorphisms in VNTR sequences in the coding region, and mutational analysis. Hum Genet 97:625–631.

Weksberg R, Smith AC, Squire J, Sadowski P. 2003. Beckwith-Wiedemann syndrome demonstrates a role for epigenetic control of normal development. Hum Mol Genet 12 Spec No. 1:R61–R68.

Weksberg R, Shuman C, Smith AC. 2005. Beckwith-Wiedemann syndrome. Am J Med Genet Part C 137:12–23.

Weksberg R, Shuman C, Beckwith JB. 2010. Beckwith-Wiedemann syndrome. Eur J Hum Genet 18:8–14.

Weng EY, Moeschler JB, Graham JM Jr. 1995. Longitudinal observations on 15 children with Wiedemann-Beckwith syndrome. Am J Med Genet 56:366–373.

Wiedemann H-R. 1964. Familal malformation complex with umbilical hernia and macroglossia: A "new syndrome"? J Genet Hum 13:223–232.

Wiedemann H-R. 1983. Tumours and hemihypertrophy associated with Beckwith-Wiedemann syndrome. Eur J Pediatr 129.

Genetics and Molecular Biology, 37, 1 (suppl), 210-219 (2014)

www.sbg.org.br

Review Article

New microdeletion and microduplication syndromes: A comprehensive review

Julián Nevado[1,2]*, Rafaella Mergener[3]*, María Palomares-Bralo[1,2], Karen Regina Souza[3], Elena Vallespín[1,2], Rocío Mena[1,2], Víctor Martínez-Glez[1,2], María Ángeles Mori[1,2], Fernando Santos[1,4], Sixto García-Miñaur[1,4], Fé García-Santiago[1,5], Elena Mansilla[1,5], Luis Fernández[1,6], María Luisa de Torres[1,5], Mariluce Riegel[3,7]$ and Pablo Lapunzina[1,4,8]$

[1]*Centro de Investigación Biomédica en Red de Enfermedades Raras, Instituto de Salud Carlos III, Madrid, Spain.*
[2]*Section of Functional and Structural Genomics, Instituto de Genética Médica y Molecular, Hospital Universitario la Paz, Madrid, Spain.*
[3]*Programa de Pós-graduação em Genética e Biologia Molecular, Universidade Federal do Rio Grande do Sul, Porto Alegre,RS, Brazil.*
[4]*Section of Clinical Genetics, Instituto de Genética Médica y Molecular, Hospital Universitario la Paz, Madrid, Spain.*
[5]*Section of Cytogenetics, Instituto de Genética Médica y Molecular, Hospital Universitario la Paz, Madrid, Spain.*
[6]*Section of Preanalytics, Instituto de Genética Médica y Molecular, Hospital Universitario la Paz, Madrid, Spain.*
[7]*Serviço de Genética Médica, Hospital de Clínicas de Porto Alegre, Porto Alegre ,RS, Brazil.*
[8]*Section of Molecular Endocrinology, Overgrowth Disordes Laboratory, Instituto de Genética Médica y Molecular, Hospital Universitario la Paz, Madrid, Spain.*

Abstract

Several new microdeletion and microduplication syndromes are emerging as disorders that have been proven to cause multisystem pathologies frequently associated with intellectual disability (ID), multiple congenital anomalies (MCA), autistic spectrum disorders (ASD) and other phenotypic findings. In this paper, we review the "new" and emergent microdeletion and microduplication syndromes that have been described and recognized in recent years with the aim of summarizing their main characteristics and chromosomal regions involved. We decided to group them by genomic region and within these groupings have classified them into those that include ID, MCA, ASD or other findings. This review does not intend to be exhaustive but is rather a quick guide to help pediatricians, clinical geneticists, cytogeneticists and/or molecular geneticists.

Keywords: microdeletion, microduplication, chromosome rearrangement, novel deletions, novel duplications.

Introduction

Alteration of gene dosage due to gains or deletions of large genomic regions causes many genetic disorders that are frequently associated with intellectual disability (ID), multiple congenital anomalies (MCA), autistic spectrum disorders (ASD) and other phenotypic findings (Lupski and Stankiewicz, 2005) The advances in the use of microarrays for diagnosis and research in genomic disorders has permitted the discovery of infrequent genomic rearrangements in a variety of diseases and the report of several microdeletion and microduplication syndromes (Deak *et al.*, 2011; Rafati *et al.*, 2012; Vissers and Stankiewicz , 2012;.Weise *et al.*, 2012).

The identification of novel syndromes is based on consistent, clinically recognizable features associated with a common chromosomal region; however, for some copy number variations (CNVs), variability in expression and penetrance of clinical manifestations have complicated the establishment of their clinical significance. Currently, the delineation of novel syndromes may start with the identifi-

Send correspondence to Pablo Lapunzina. Instituto de Genética Médica y Molecular, Hospital Universitario la Paz, Paseo de la Castellana 261-28046, Madrid, Spain. E-mail: plapunzina.hulp@salud.madrid.org.
*These authors contributed equally to this work.
$These authors contributed equally to this work.

cation of overlapping genotypes, that is, a 'genotype-first' approach, in which patients are characterized by a similar genomic aberration before a common clinical presentation is delineated. This is referred to as "reverse genetics". This approach has proven to be successful considering the growing list of microdeletion/microduplication syndromes that have been described in the past five years. Furthermore, the collection of clinical and genetic information in databases such as DECIPHER, ISCA, ECARUCA and other free databases has been crucial for discriminating between patients with rare aberrations and those with new microdeletion/duplication syndromes.

In this paper, we systematically review the novel microdeletion and microduplication syndromes described in the past five years. We grouped these disorders by chromosome, with the intention of serving as a quick guide for clinicians and researchers.

Chromosome 1

1p34.2-p34.3 Deletion. This deletion is characterized by microcephaly, ID and ASD. The deletion spans approximately 3.3 Mb and involves approximately 43 genes, including RIMS3, which is the main candidate gene for this phenotype.

1p31.3-p32.2 Deletion. There are approximately 7 cases described to date. In five of these cases with an *NFIA* deletion, the patients show central nervous system (CNS) malformations (hypoplasia of the corpus callosum, macrocephaly, ventriculomegaly) and urinary tract defects.

1q21.1 Deletion/Duplication. Patients have a phenotype similar to 22q11.2 deletion syndrome (velocardiofacial syndrome-like phenotypic findings). They may have congenital heart disease, schizophrenia and ID. The microduplication of approximately 212 kb could be responsible for congenital heart disease in at least 2 patients. The phenotype of dup1q21.1 is variable due to incomplete penetrance and variable expression levels. Therefore, this microduplication is also observed in asymptomatic individuals. Patients with deletions (1.4-1.65 Mb) may also have microcephaly, epilepsy, ataxic gait, severe dysmorphic features of the face and ID. This deleted region comprises approximately 30 coding genes, including the cluster of genes encoding the ephrins (*EFNA1, EFNA3* and *EFNA4*), which are tyrosine kinase receptors.

1q24-q25 Deletion. This deletion is characterized by growth retardation, microcephaly, small hands and feet (with brachydactyly), dysmorphic facies, small ears, micrognathia, short nose with bulbous tip and severe ID. The deleted region is approximately 1.9 Mb (chr1: 170135865-172099327 coordinates hg18) and contains 13 genes including *DNM3* and *CENPL*, which encodes a protein essential for centromeric function, mitotic progression and synaptic reaction.

1q32.2-q32.3 Deletion. Patients exhibit dysmorphic features and facial clefts due to deletion of the *IRF6* gene, which is responsible for the Van der Woude syndrome (VWS). The deletion is approximately 2.98 Mb and includes 25 genes.

1q41-q42.12 Deletion. This deletion is characterized by moderate to severe ID, seizures, Pelger-Huet anomaly (leukocyte alteration), cleft lip and palate and agenesis of the corpus callosum. Patients may also have hypoglycemia, 13 pairs of ribs and a micropenis. *DISP1,* in the sonic hedgehog pathway, has been proposed as the gene responsible for the alterations of the midline observed in this deletion. The deletions have a size of 777 kb to 6.87 Mb. It has been proposed that this would represent a locus for Fryns syndrome, a Fryns syndrome phenocopy, or congenital diaphragmatic hernia (CDH). It has also been observed in patients with the isolated 1q42 deletion (together with agenesis of the corpus callosum) or within a contiguous deletion, 1q41q42 syndrome (Filges *et al.*, 2010).

1q43-q44 Deletion. Microcephaly, abnormalities of the corpus callosum, seizures, ID and speech disorder are observed in patients with this deletion. Deletion of the *AKT3* gene appears to be correlated with microcephaly and alteration of the other 3 genes (*FAM36A, C1ORF199* and *HNRNPU*) correlates with the epileptic phenotype.

Chromosome 2

2p14-p15 Deletion. This deletion is associated with ID, speech disorder, mild dysmorphic features, hearing loss and relative microcephaly. The deletion is approximately 2.23-2.84 Mb, with a minimal overlapping region of 10 genes.

2p15-q16.1 Deletion. This deletion is associated with ID, ASD and dysmorphic features. Eight patients described by three different groups have this deletion. The *OTX1* and *XPO1* genes have been associated with ASD. It has also been observed in patients with prenatal and postnatal growth retardation, ptosis of both eyelids and microcephaly. The deletions range from 2.6 Mb to 3.2 Mb.

2q13 Deletion. Patients with this deletion have CNS disorders and present with cortical disruption and Joubert syndrome. These phenotypes are associated with the deletion of the *NPHP1* gene.

2q23.1 Deletion/Duplication. Seizures, speech disturbances, ataxia, short stature, ID and dysmorphic features (brachycephaly, proximal implementation of the hair, short nose, hypertelorism, everted lower lip, thick tongue, brachytelephalangy, clinodactyly and hypertrichosis) are observed. This deletion includes the *MBD5* gene, which is implicated in the pathophysiology of seizures. Stereotyped behaviors are also present and these are similar to Rett syndrome or Angelman syndrome. Microduplications in this region present with ID, hypotonia, ASD and include the following genes: *MBD5, ACVR2A, ORC4L, EPC2, KIF5C, MIR1978, LYPD6B* and *LYPD6*. (Jaillard *et al.*, ,2009).

2q31.1-q31.2. Deletion. This deletion is characterized by monodctylous hands, ectrodactyly, brachydactyly

and clinodactyly with or without duplication of both halluces. This deletion is of the *HOXD* cluster. Mutations in *HOXD13* and *HOXD10* are associated with malformations of the limbs. Some patients may have ID, microcephaly and growth retardation.

2q32-33.1 Deletion. Patients with this deletion have ID, learning disabilities, growth retardation, thin and sparse hair, feeding difficulties, cleft lip/palate and multiple dysmorphic features. *SATB2* haploinsufficiency has been suggested to be responsible for most of these findings. The deletions are between 35 kb to 10.4 Mb (Rosenfeld *et al.*, 2009)].

2q37 Deletion. This deletion shows the Albright phenotype (hereditary osteodystrophy: brachydactyly, ID and short stature).

Chromosome 3

3p21.31 Deletion. Patients present with cortical blindness, CNS abnormalities, cleft lip and ID. The deletions are approximately 3.1 Mb, including approximately 80 genes.

3p25 interstitial Deletion. Patients present with low birth weight, mental retardation, telecanthus, ptosis and micrognathia and congenital heart disease, typically atrioventricular septal defect. *SRGAP3* is the major determinant of ID.

3p11.2-p12.1 Deletion. This deletion includes *POU1F1*, *CHMP2B* and *VGLL3*. Patients have abnormalities in pituitary hormones similar to the hypothalamic Laron syndrome but are unresponsive to GH treatment.

3q13.31 Deletion. ID, postnatal overgrowth, hypoplastic genitalia (in men) and recognizable facial features (short philtrum and protruding lips) are observed in these patients. The deletion is 580 kb and includes *DRD3* and *ZBTB20* as candidate genes.

3q22.1-q25.2 Deletion. Patients with this deletion have multiple congenital anomalies and peculiar facial appearance. In particular, the phenotypes result from the variable combination of three recognizable patterns: Dandy-Walker malformation, BPES syndrome and Wisconsin syndrome.

3q27.3 Deletion. Patients shared a recognizable facial dysmorphism and Marfanoid habitus associated with psychosis and mild to severe ID. Most of these patients have severely impaired adaptive skills.

3q29 Deletion/Duplication. Facial dysmorphism, ASD, psychiatric disorders (bipolar disease), ID and MCA (cleft palate, congenital heart disease) are all associated with deletions in this region. There are reports of patients with deletions and parents with mosaic deletions. The microduplication is characterized by mild ID, microcephaly, dysmorphic features and musculoskeletal abnormalities. The minimum size of the rearrangement is 1.6 Mb (Figure 1A).

Chromosome 4

4q21 Deletion. Growth retardation, ID and absence of language are found in patients with this deletion. The smallest region of overlap in deletions is 1.37 Mb and contains five genes: *PRKG2*, *RASGEF1B*, *HNRNPD*, *HNRPDL* and *ENOPH1*. It has been suggested that PRKG2 and RASGEF1B are the genes responsible for this clinical phenotype.

4q21.3 Deletion. Patients present ID, dysmorphic facial features, hypotonia and short stature.

4q34.1-q35.2 Deletion. The phenotype is somewhat similar to the 22q11.2 deletion syndrome.

Chromosome 5

5q14.3-q15 Deletion. ID (late Honest), epilepsy, hypotonia and dimples in the jugular region are found in patients with this deletion. Patients present with atypical clinical Rett syndrome features. The gene involved is *MEF2C*.

5q35.2-q35.3 Deletion/Duplication. The deletion is 1.63 Mb and sometimes includes *NSD1*, the gene responsible for Sotos syndrome. Patients also have the Sotos phenotype, cleft palate, language delay, ID and macrocephaly. Microduplication of the Sotos syndrome region, which contains *NSD1*, has been associated with microcephaly, short stature and development delay.

Chromosome 6

6p25 Deletion. Patients present with white matter abnormalities, hypotonia, ID, a dysmorphic face, hypoacusis, short stature, Axenfeld-Rieger anomaly and a bicuspid aortic valve.

6q13-q14 Deletion. ID and connective tissue abnormalities are found in patients with this deletion. The deletion is 3.7 Mb and affects 16 genes, including *COL12A1*, a good candidate for the anomaly in the connective tissue.

6q14.1-q15 Deletion. Obesity, ID and atypical facial phenotypic traits are observed among these patients. This deletion syndrome partly phenocopies patients with Prader-Willi syndrome. The haploinsufficiency of *SIM1* is suggested to be responsible for the phenotype.

6q16.1 Deletion. Patients present with ID and characteristic facies. The deletion includes the haploinsufficiency of one gene (ephrin receptor 7; *EPHA7*) that has implications in cortical development.

6q25 Deletion. Patients usually show ID. Olfactory bulb aplasia and anosmia may also be observed. The syndrome is due to the haploinsufficiency of *ARID1B*, a member of the SWI/SNF chromatin-remodeling complex. Some patients with ID have point mutations in this gene.

6q25.2-q25.3 Deletion. Microcephaly, ID, hypoacusis and dysmorphic features are observed in patients with this deletion. The smallest region of overlap of the deletion in 4 patients is 3.52 Mb in size.

Chromosome 7

7p14.1 Deletion. This deletion is characterized by polysyndactyly, hypertelorism and microcephaly, having a phenotype similar to Greig syndrome.

7p22.1 Duplication. Speech delay and recognizable facial features are observed in these patients. The duplication is approximately 1.7 Mb. Macrocephaly, ocular hypertelorism and low-set ears can also occur. Fifteen genes are involved in the duplicated segment.

7q11.23 Duplication. It is the reciprocal duplication of the deletion observed in Williams Syndrome. Patients present with speech delay, epilepsy, ID, straight and thick eyebrows and ASD.

7q11.23 Deletion. This is the distal deletion of the Williams-Beuren region. The deletions are recurrent, 1.2 Mb in size and include the Huntingtin-interacting protein 1 (*HIP1*) and tyrosine 3-monooxygenase/tryptophan 5-monooxygenase activation protein gamma (*YWHAG*) genes. The deletion of *HIP1* seems to be sufficient to cause ID.

7q21.3 Deletion. Myoclonus, dystonia, ID and psychosis have been observed in these patients. Two regions of 455 and 496 kb are critical for ID, which is where the gene *LOC253012* (*HEPACAM2*) is located.

7q22.2-q22.3 Deletion. Overgrowth, delayed bone age, epilepsy, ID, unusual face, hypoplasia of the corpus callosum and cerebellar hypoplasia are observed in patients with this deletion. The deletion spans 3.2 Mb and includes four of 15 genes involved in cell cycle (*SRPK2, MLL5, RINT1* and *LHFPL3*).

7q33-q35 Deletion. Patients with this deletion present with speech delay and ID. The deletion includes *CNTNAP2*, a gene that has previously been found in children with speech disorders.

Chromosome 8

8p21 Deletion. ID and behavior disorder, with some features of autistic spectrum disorder occur in patients with this deletion.

8p23.1 Duplication. This duplication leads to a variable phenotype that may include one or more of the following: congenital heart disease (CHD), ID and mild dysmorphism with prominent forehead and arched eyebrows. The critical region is a duplication of 3.68 Mb that contains 31 genes and microRNAs, of which only *GATA4*, *TNKS*, *SOX7* and *XKR6* are likely to be dosage-sensitive genes. Of the microRNAs, *MIR124-1* and *MIR598* have been implicated in neurocognitive phenotypes. A combination of the duplication of *GATA4*, *SOX7* and related genes may account for the variable penetrance of CHD.

8q12 Duplication. This duplication includes *CHD7*. Patients present with hypotonia, ID, failure to thrive, Duane anomaly, Mondini malformation, hearing loss, malformations of the ear canal and atrial septal defects.

8q21.11 Deletion. ID, round face with full cheeks, eyelid ptosis, ocular malformations, hypoplastic nose, abnormal philtrum and vermillion and minimal hand anomalies (camptodactyly, syndactyly) are all observed in these patients. The smallest region of overlap is 539.7 kb, which includes three genes, including Zinc Finger Homeobox 4 (*ZFHX4*)(Figure 1B).

8q22.1 Deletion. The phenotype of this deletion is similar to that of the Nablus mask syndrome, symptoms include ID, speech disorder and typical dysmorphic features. The deletion is approximately 1.6 Mb.

8q22.2 Deletion. Patients with this deletion have characteristic facial features, ID, absent speech, seizures, growth retardation and diaphragmatic hernia in some cases. The smallest region of deletion is 3.87 Mb (100.69 to 104.56 Mb, hg18), comprising at least 25 genes.

Chromosome 9

9p13.3-p13.1 interstitial Deletion. Patients with a 9p13 deletion have mild to moderate ID, social and interactive personality and behavioral problems, such as attention deficit-hyperactivity disorder. Short stature, prominent antihelices, hypoplastic nails and precocious/early puberty are also present (Figure 1C).

9q22.3 Deletion. ID, dysarthria, metopic craniosynostosis, hydrocephalus, macrosomia and seizures are associated with this deletion. Patients with a 9q22.3 microdeletion have the clinical findings of the Gorlin syndrome. The 9q22.3 microdeletions (352 kb to 20.5 Mb in size) include *PTCH1*, the gene that is mutated in Gorlin syndrome (nevoid basal cell carcinoma syndrome).

9q31.1-q31.3 Deletion Patients have a distinct clinical phenotype characterized by mild ID, short stature with high body mass index, thick hair, arched eyebrows, flat profile with broad chin, mild prognathism, broad and slightly overhanging tip of the nose and short neck with cervical gibbus.

9q34.3 Deletion (Kleefstra syndrome). Patients have ID, behavior anomalies, hypotonia, epilepsy, congenital heart defect and renal anomalies. The highly recognizable facial features are hypertelorism, midface hypoplasia, prognathism, prominent eyebrows, cupid bow or tented upper lip and everted lower lip. The syndrome is either caused by a submicroscopic deletion in the chromosomal region 9q34.3 or an intragenic mutation of the *EHMT1* gene causing haploinsufficiency of *EHMT1*. There are some communications of mosaicism in parents of affected patients (Figure 1D).

Chromosome 10

10q22-q23 Deletion. The overlap of neuropathological phenotypes among patients described suggests that this region harbors genes important for function and neurodevelopment (*NRG3, GRD1D1,* BMPR1A, SNCG). In-

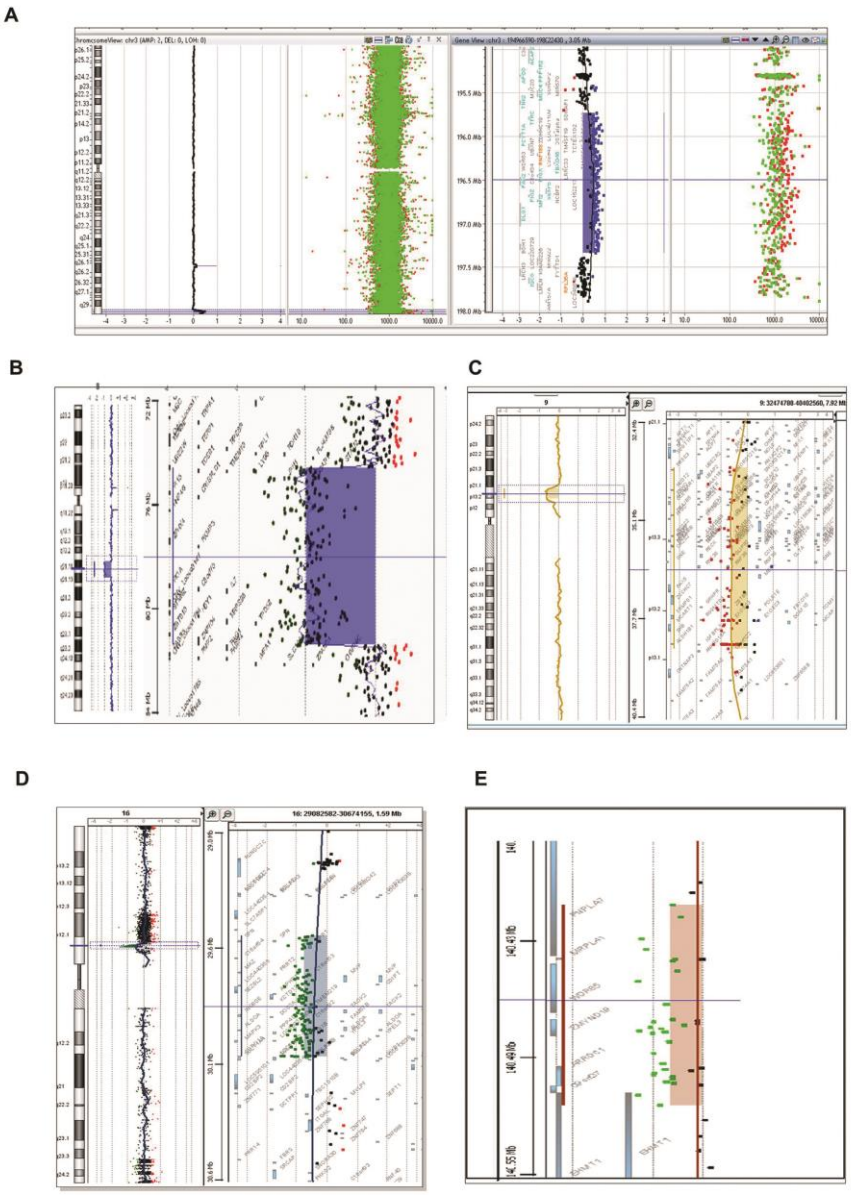

Figure 1 - Chromosome microduplications and microdeletions. A: 3q29 microduplication. B: 8q21 microdeletion. C: Chromosome 9 profile showing a 9p13 microdeletion. D: Atypical microdeletion of 9q34. E: Partial aCGH in a patient with a 16p11.2 microdeletion.

deed, several genes in this region are candidates for neuropsychiatric disorders. *NRG3 and GRD1D1* have been described as candidate genes associated with schizophrenia.

Chromosome 11

11q13.1 Deletion. Speech delay, autistic spectrum disorder, dysmorphic features, such as wide halluces and firsts digits and pancreatic gastrinoma. The deletion is 0.57 Mb.

Chromosome 12

12q13.11 Deletion. Severe ID, cleft palate and severe myopia. The deleted region contains 16 genes. It is hypothesized that haploinsufficiency of *AMIGO2* is responsible for the ID and haploinsufficiency of *COL2A1* in cleft palate and myopia.

12q13 Duplication. This syndrome may represent a phenocopy of the Wolf Hirschhorn syndrome (Bertioli *et al.*, 2013)

12q14 Deletion. Microcephaly, short stature with similar clinical findings to the Russell Silver syndrome. Patients may have osteopoikilosis, low weight, failure to thrive and learning problems. The *HMGA2* gene is involved in the growth deficiency.

12q24.31 Deletion. Hypoglycemia, macroglossia and overgrowth (similar to the Beckwith-Wiedemann syndrome at birth). The deleted region contains the gene *HNF1* homeobox A (HNF1A) and others.

Chromosome 14

14q12-q22.1 Deletion. Patients present ID, failure to thrive, microcephaly and recognizable facial features (hypertelorism, epicanthic folds, peculiar eyebrows, depressed nose, receding forehead, CNS disorders, seizures, apnea, myoclonus and infection proneness).

14q32.2 Deletion. ID and many phenotypic abnormalities in two unrelated patients with identical deletions. The deletions are mediated by repetitions (TGG) (n)

14q32.33 Deletion. ID and minimal dysmorphic features. The deletion affects a small fragment of 0.3 Mb with 6 genes, including *NUDT14, BRF1, BTBD6, PACS2, MTA1* and *TEX22*. A 250-kb region critical for certain features of terminal 14q deletion syndrome has been proposed. Amongst them three potential candidate genes for intellectual disability: *CRIP2, MTA1* and *TMEM121* (Engels *et al.*, 2012).

Chromosome 15

15q11.2 Deletion. ID, speech delay, behavioral problems, seizures and ASD. The deletion is between the *BP1* and *BP2* regions of the proximal portion of chromosome 15 that contains four genes (*TUBGCP5, NIPA1, NIPA2* and *CYFIP1*) not subjected to imprinting.

15q11-q13 Duplication. ASD, mild facial dysmorphism, sleep problems and unusual electroencephalogram findings (Urraca *et al.*, 2013).

15q13.2-q13.3 Deletion. Phenotypic findings similar to the Angelman syndrome, with ASD, epilepsy and behavioral problems.

15q13.3 Deletion. Epilepsy, ID, psychiatric disorders (bipolar disorder), severe hypotonia and EEG abnormalities. Locus with incomplete penetrance for autism; may show retinal dysfunction and encephalopathy. One gene appears to be involved (*CHRNA7*) (Shinawi *et al.*, 2009).

15q14 Deletion. Dandy-Walker malformation, ID, macrocephaly, myopia and brachytelephalangy.

15q21.1-q21.2 Deletion. Clinical features similar to Marfan syndrome and with ID. The deletions involve the *FBN1* gene.

15q24 Deletion/Duplication. Growth delay, ID, facial features (long face, anterior hairline, epicanthic folds, hypertelorism, long philtrum and thick lower lip). Other findings include ASD, hypotonia, behavioral problems, hearing loss, hernias and GH deficiency. Most deletions have breakpoints in five LCRs (LCR15q24A, -B, -C, -D and -E) and the minimum region of overlap is 1.2 Mb between LCR15q24B and LCR15q24C. Candidate genes within this deletion are *CYP11A1, SEMA7A, CPLX3, ARID3B, Stra6, Sin3A* and *CSK*. The duplication cases described share similar clinical features with the 15q24 deletion.

15q24.1 Deletion. Multiple cysts of the corpus callosum, ID, micropenis and strabismus. The deletion is approximately 3.1 Mb. The sizes of the deleted regions range from 1.7 Mb to 6.1 Mb. Most of the reported cases are male. Male genital abnormalities are frequently observed in 15q24 microdeletion patients. One candidate gene is *CYP11A1*, which is highly expressed in the adrenal gland.

15q24.3- q25.2 Deletion. Cleft palate with or without cleft lip and hypotonia.

15q26 Deletion. Patients have mainly short stature due to haploinsufficiency of the *IGF1R* gene.

15q26.1 Deletion. Intractable epilepsy, ID and short stature.

Chromosome 16

16p11.2 Deletion/Duplication. The deletion is characterized by ID, ASD, epilepsy and other less common findings, such as obesity, microphthalmia, coloboma of the optic nerve, kidney and urinary tract abnormalities, Hirschsprung disease, endocardial fibroelastosis and hemivertebrae. Duplication is associated with autism, ID, CNS disorders and schizophrenia (Rosenfeld *et al.*, 2010). A 600-kb 16p11.2 deletion containing 29 genes has been associated with several neurocognitive disorders, including autism, diabetes-independent obesity and microcephaly,

whereas duplication of the same region is associated with autism, schizophrenia, anorexia and microcephaly. The 16p11.2 deletion is associated with increased head size, whereas 16p11.2 duplication is associated with decreased head size (Golzio *et al.*, 2012) (Figure 1E).

16p11.2-p12.2 Deletion/Duplication. Minimal facial abnormalities, speech disorder, frequent ear infections and ID. It should be distinguished from the proximal deletion (see immediately above). Patients with duplications have severe ID, ASD and dysmorphic features (Figure 2A and B).

16p12.1 Deletion. ID and abnormal behavioral phenotype with behavioral disorders. It is a 520-kb deletion.

16q12-q13 Deletion. The phenotypic spectrum of microdeletions in 16q12-q13 region is broad with variable degrees of ID, craniofacial dysmorphic features, congenital brain abnormalities and limb and congenital heart disease.

16q22.1 Deletion/Duplication. Deletion presents ID and lobular breast cancer. The deletion is 0.24 MB and affects 3 genes (*ZFP90, CDH3* and *CDH1*). *ZFP90* is expressed in the brain and is responsible for ID, while *CDH1* may be responsible for cancer. Duplication is characterized by epilepsy and learning disabilities.

16q24.1 Deletion. Typically present persistent pulmonary hypertension in the newborn and sometimes atrioventricular canal, ureteral stenosis and annular pancreas. *FOXF1* alterations would be responsible for alveolar capillary dysplasia and other alveolar malformations.

16q24.3 Deletion. ID, ASD, short stature and minimal facial anomalies. Deletions involve the *ANKRD11* gene and cause KBG-like syndrome.

Chromosome 17

17p13.1 Deletion. ID, hypotonia and anomalies of the hands and feet but not cancer. Microdeletions affect the *TP53* gene.

17p13.3 Deletion/Duplication. Short stature, ID and abnormal facial features. The microduplication includes autism and affects a region of 72 kb that includes a single gene (*YWHAE*). The microdeletion sometimes includes *CRK*, sometimes *YWHAE* and / or *TUSC5* (Figure 2C and 2D).

17q11.2 Deletion/Duplication. The deletion and duplication affects the *NF1* region. ID, facial dysmorphic features and seizures.

17q12 Deletion/Duplication. The deletion presents congenital diaphragmatic hernias and pulmonary and renal cysts. A case of Mayer-Rokitansky-Kuster-Hauser syndrome has been described with this deletion. The deletion is 1.4 Mb and affects 17 genes, including *AATF, ACACA, DDX52, DUSP14, GGNBP2, HNF- 1B, Lhx1, PIGW, SYNRG, TADA2A* and *ZNHIT3*. Duplication is characterized by ASD (Figure 2E).

17q21.31 Deletion/Duplication. Deletions are associated with macrocephaly, ID, epilepsy, congenital anomalies and dysmorphic facial alterations of the pituitary. The skin lesions are characterized by nevi, abnormal skin pigmentation similar to cardiofaciocutaneous syndrome. Other findings include dilation of the aortic root, joint subluxation, hearing loss, recurrent otitis media and persistent digital pads. At least 6 genes are affected, including *MAPT* and *STH*.

17q22-q23.2 Deletion. Microcephaly, thyroid duct cyst, sensorineural hearing loss and pulmonary hypertension. Includes the loss of *TBX2* and *TBX4* but not *NOG*.

17q23.1-q23.2 Deletion/Duplication. Duplication has been associated with pes cavus familiar. Duplication affects *PITX1* and *TBX4*. The deletion has congenital heart disease and limb abnormalities.

17q23.2 Deletion. Bilateral sensorineural hearing loss in two isolated patients.

17q24.2-q24.3 Deletion/Duplication. Duplication presents generalized hypertrichosis with gingival hyperplasia and deletions in general have less gingival hyperplasia.

Chromosome 18

18q12.3 Deletion. The deletion is 372 kb in size with haploinsufficiency of *SETBP1*. The clinical findings include ID and speech disorder. Missense heterozygous mutations in this gene cause Schinzel-Giedion syndrome (SGS). However, the phenotype of individual with partial chromosome 18q deletions does not resemble SGS.

Chromosome 19

19p13.11 Deletion. One patient presented with pontocerebellar hypoplasia and ID and haploinsufficiency of the helicase *DDX39*. Another patient with a deletion in this region showed a deletion of 1.1 Mb involving *EPS15L1*. The patient showed short stature, ID, severe hypotonia, ataxia, premature pubarche and dysmorphic features.

19p13.12 Deletion. Defects of the branchial arches (preauricular tags, ear canal stenosis), mild hearing loss and mild ID are due to the deletion of a region of 0.8 Mb of genomic DNA. The deletion extends 15300338-16064271 (hg18, NCBI build 36.1). One patient presented with ID, obesity and hypertrichosis.

19p13.13 Deletion/Duplication. The deletion is characterized by macrocephaly, overgrowth and ophthalmologic and gastrointestinal disturbances. Duplication has short stature and microcephaly. The smallest region of overlap is 311-340 Kb and has 16 genes including *MAST1, NFIX* and *CALR*.

19p13.2 Deletion. Patients present with ID, mild facial features, febrile seizures. The deletion is 834.2 kb in size and includes 32 genes.

19p13.3 Terminal Duplication. Patients' phenotypes include severe psychomotor DD, skeletal malformations and a distinctive facial appearance.

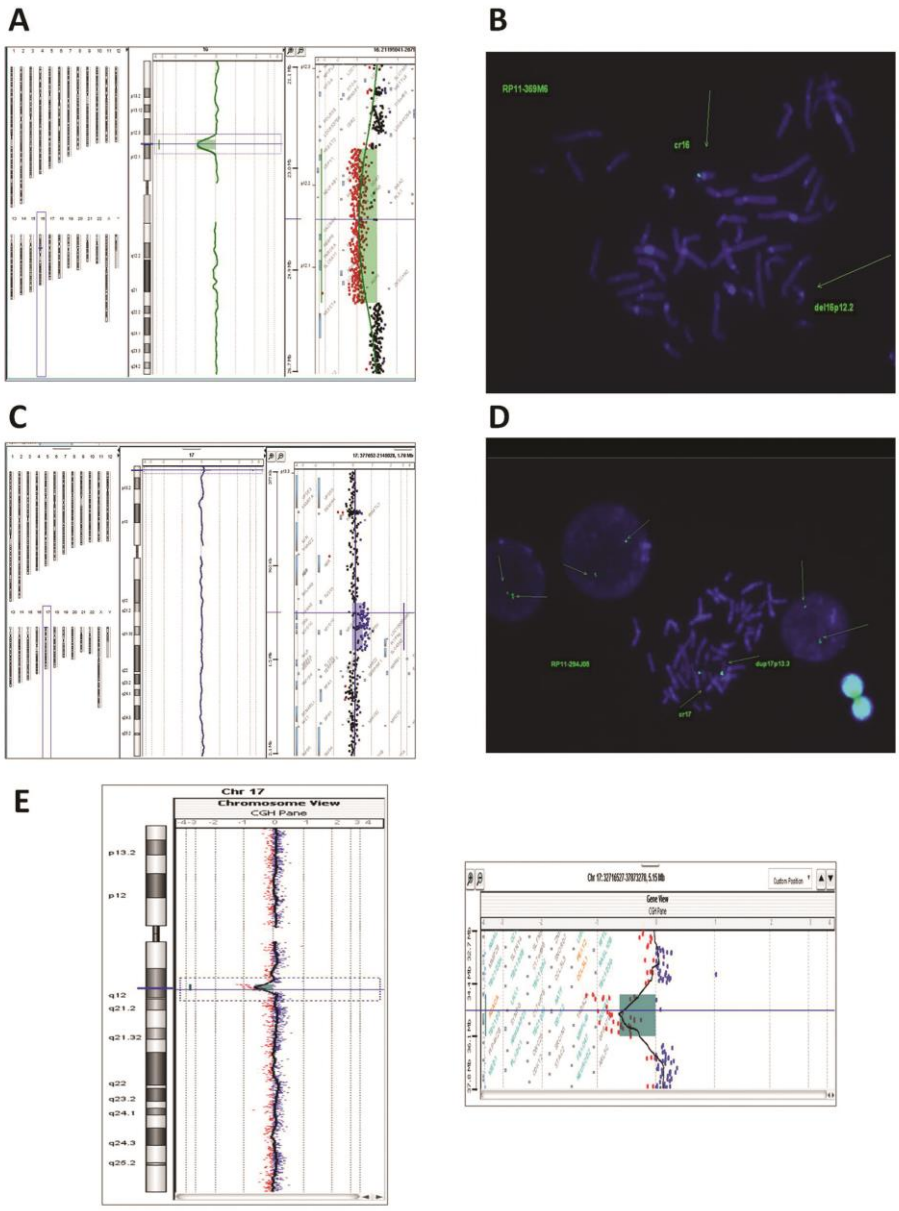

Figure 2 - A: 16p12.2 deletion (array-cgh) and B: (FISH). C: 17p13.3 duplication (array-cgh) and D (FISH). E: 17q12 deletion (array-cgh).

19q13.2 Deletion. Patients present branchial arch defects. The critical region is approximately 0.8 Mb

19q12-q13.2 Duplication. It is an obesity-related syndrome, with ID and minor facial findings.

19q13.11 Deletion. Patients present a Diamond-Blackfan syndrome, pre and postnatal growth deficiency, tall stature, microcephaly, hypospadias, signs of ectodermal dysplasia and aplasia cutis vertex. The critical region is defined to 750 kb and is due to haploinsufficiency of *RPS19* (Malan *et al.*, 2009).

Chromosome 20

20p12.3 Deletion. Cleft palate / cleft lip, Pierre-Robin sequence. The deletion involves the *BMP2* gene and has been implicated in Wolff-Parkinson-White (WPW) syndrome with neurocognitive deficits and with Alagille syndrome when the deletion includes the neighboring *JAG1* gene in addition to *BMP2*.

20p13 Deletion. Dysmorphic features, ID, epilepsy and brachydactyly. *SOX12* and *NRSN2* are the candidate genes that may be involved in the developmental defects.

20q13.33 Deletion. Severe limb malformations, skeletal abnormalities, ID, speech delay, seizures and other minimal dysmorphic features. The *ARFGAP1, CHRNA4* and *KCNQ2* genes have been associated with neurological deficits.

Chromosome 21

21q22 Deletion. Two patients with similar phenotype and overlapping deletions of the 21q22 region were observed. They had behavioral problems, no speech, microcephaly, feeding problems, regurgitation, obesity dysplastic ears and pointed chin. They also present with cerebral atrophy, thinned corpus callosum, epilepsy and ventricular septal defect. Another patient had microcephaly, ID, hypospadias and corneal opacity. Patients with chromosomal deletions of 21q show a variation in size and usually include the 21q22.12 region. The deleted region in most of these patients included, among other deleted genes, the *RUNX1* gene (21q22.12), which is related with thrombocytopenia and platelet function and a predisposition to develop myeloid leukemia.

Chromosome X

Xq11.11 Deletion. Patients with this deletion have ID, epilepsy, macrosomia, macrocephaly, tall stature and dysmorphic features. The 1.3 Mb deletion includes *ARHGEF9,* which is proposed to have a role in the cognitive development.

Conclusions

The extensive use of high-resolution microarrays and the "genotype-first" experimental approach taken by ge-

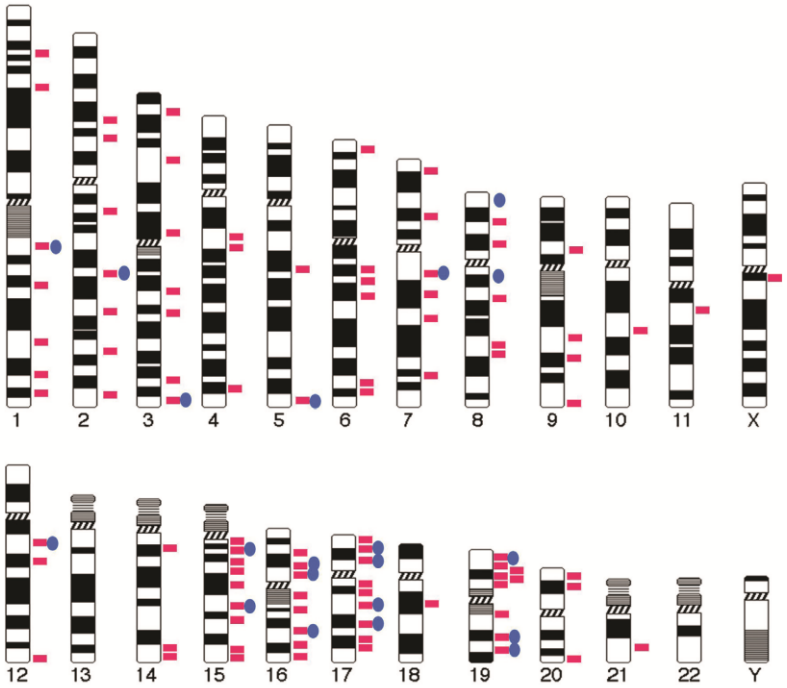

Figure 3 - New microdeletion and microduplication syndromes discovered over the last three to five years. Red squares indicate reported microdeletions; blue circles indicate reported microduplications.

netic laboratories have allowed for the recognition and description of an important and growing number of new microdeletion and microduplication syndromes over the last three to five years (Figure 3). Interestingly, most of these syndromes have phenotypic features that are similar to and overlapping with other previously described genetic syndromes. This review may be considered a quick guide to help pediatricians, clinical geneticists, cytogeneticists and/or molecular geneticists and emphasizes the necessity of a strong collaboration between clinical (pediatricians, geneticists) and molecular geneticists to assure new phenotype recognitions for these genomic aberrations.

References

Bertoli M, Alesi V, Gullotta F, Zampatti S, Abate MR, Palmieri C, Novelli A, Frontali M and Nardone AM (2013) Another patient with 12q13 microduplication. Am J Med Genet A 161A:2004-2008.

Deak KL, Horn SR and Rehder CW (2011) The evolving picture of microdeletion/microduplication syndromes in the age of microarray analysis: Variable expressivity and genomic complexity. Clin Lab Med 31:543-564.

Engels H, Schüler HM, Zink AM, Wohlleber E, Brockschmidt A, Hoischen A, Drechsler M, Lee JA, Ludwig KU, Kubisch C, *et al.* (2012) A phenotype map for 14q32.3 terminal deletions. Am J Med Genet A.158A:695-706.

Filges I, Röthlisberger B, Boesch N, Weber P, Wenzel F, Huber AR, Heinimann K and Miny P (2010) Interstitial deletion 1q42 in a patient with agenesis of corpus callosum: Phenotype-genotype comparison to the 1q41q42 microdeletion suggests a contiguous 1q4 syndrome. Am J Med Genet A 152A:987-993.

Jaillard S, Dubourg C, Gérard-Blanluet M, Delahaye A, Pasquier L, Dupont C, Henry C, Tabet AC, Lucas J, Aboura A, *et al.* (2009) 2q23.1 microdeletion identified by array comparative genomic hybridisation: An emerging phenotype with Angelman-like features? J Med Genet 46:847-855.

Golzio C, Willer J, Talkowski ME, Oh EC, Taniguchi Y, Jacquemont S, Reymond A, Sun M, Sawa A, Gusella JF, *et al.* (2012) KCTD13 is a major driver of mirrored neuroanatomical phenotypes of the 16p11.2 copy number variant. Nature.485:363-367.

Lupski, J and Stankiewicz, P (2005) Genomic disorders: Molecular mechanism for rearrangements and conveyed phenotypes. PLoS Genetics 1:e-49.

Malan V, Raoul O, Firth HV, Royer G, Turleau C, Bernheim A, Willatt L, Munnich A, Vekemans M, Lyonnet S, *et al.* (2009) 19q13.11 deletion syndrome: A novel clinically recognisable genetic condition identified by array comparative genomic hybridisation. J Med Genet 46:635-640.

Rafati M, Seyyedabouttorabi E, Ghadirzadeh MR, Heshmati Y, Adibi H, Keihanidoust Z, Eshraghian MR, Javadi GR, Dastan J, Mosavi-Jarrahi A, *et al.* (2012) "Familial" *vs.* "Sporadic" intellectual disability: Contribution of common microdeletion and microduplication syndromes. Mol Cytogenet 5:9.

Rosenfeld JA, Ballif BC, Lucas A, Spence EJ, Powell C, Aylsworth AS, Torchia BA and Shaffer LG (2009) Small deletions of SATB2 cause some of the clinical features of the 2q33.1 microdeletion syndrome. PLoS One 4:e6568.

Rosenfeld JA, Coppinger J, Bejjani BA, Girirajan S, Eichler EE, Shaffer LG and Ballif BC (2010) Speech delays and behavioral problems are the predominant features in individuals with developmental delays and 16p11.2 microdeletions and microduplications J Neurodev Disord 2:26-38.

Shinawi M, Schaaf CP, Bhatt SS, Xia Z, Patel A, Cheung SW, Lanpher B, Nagl S, Herding HS, Nevinny-Stickel C, *et al.* (2009) A small recurrent deletion within 15q13.3 is associated with a range of neurodevelopmental phenotypes. Nat Genet 41:1269-1271.

Urraca N, Cleary J, Brewer V, Pivnick EK, McVicar K, Thibert RL, Schanen NC, Esmer C, Lamport D and Reiter LT (2013) The interstitial duplication 15q11.2-q13 syndrome includes autism, mild facial anomalies and a characteristic EEG signature. Autism Res 6:268-279.

Vissers LE and Stankiewicz P (2012) Microdeletion and microduplication syndromes. Methods Mol Biol 838:29-75.

Weise A, Mrasek K, Klein E, Mulatinho MV, Llerena JC Jr, Hardekopf D, Pekova S, Bhatt S, Kosyakova N and Liehr T (2012) Microdeletion and Microduplication Syndromes. J Histochem Cytochem 60:346-358.

BRIEF REPORT

Human Mutation

OFFICIAL JOURNAL HGVS HUMAN GENOME VARIATION SOCIETY www.hgvs.org

A New Overgrowth Syndrome is due to Mutations in *RNF125*

Jair Tenorio,[1,2] Alicia Mansilla,[3] María Valencia,[1,4] Víctor Martínez-Glez,[1,5] Valeria Romanelli,[1] Pedro Arias,[1,2] Nerea Castrejón,[6] Fernando Poletta,[7] Encarna Guillén-Navarro,[1,8] Gema Gordo,[2] Elena Mansilla,[1,9] Fé García-Santiago,[1,9] Isabel González-Casado,[10] Elena Vallespín,[1,5] María Palomares,[1,5] María A. Mori,[1,5] Fernando Santos-Simarro,[1,11] Sixto García-Miñaur,[1,11] Luis Fernández,[1,12] Rocío Mena,[1,5] Sara Benito-Sanz,[1,13] Ángela del Pozo,[14] Juan Carlos Silla,[14] Kristina Ibañez,[14] Eduardo López-Granados,[15] Alex Martín-Trujillo,[16] David Montaner,[1,17] The SOGRI Consortium,[18] Karen E. Heath,[1,13] Ángel Campos-Barros,[1,13] Joaquín Dopazo,[1,17] Julián Nevado,[1,5] David Monk,[16] Víctor L. Ruiz-Pérez,[1,4] and Pablo Lapunzina[1,2,11]*

[1]*CIBERER, Centro de Investigación Biomédica en Red de Enfermedades Raras, ISCIII, Madrid, Spain;* [2]*Molecular Endocrinology Unit - Overgrowth Syndromes Laboratory, INGEMM, Instituto de Genética Médica y Molecular, IdiPAZ, Hospital Universitario La Paz, Universidad Autónoma de Madrid (UAM), Madrid, Spain;* [3]*Instituto Cajal, CSIC, Madrid, Spain;* [4]*Instituto de Investigaciones Biológicas, IIB, Universidad Autónoma de Madrid, Madrid, Spain;* [5]*Functional and Structural Genomics Unit, INGEMM, Instituto de Genética Médica y Molecular, IdiPAZ, Hospital Universitario La Paz-UAM, Madrid, Spain;* [6]*Developmental Cancer Group, Hospital San Juan de Dios, Barcelona, Spain;* [7]*ECLAMC, Estudio Colaborativo Latinoamericano de Malformaciones Congénitas at CEMIC, Buenos Aires, Argentina;* [8]*Medical Genetics Service, Hospital Virgen de la Arrixaca, Murcia, Spain;* [9]*Cytogenetics Unit, INGEMM, IdiPAZ, Hospital Universitario La Paz-UAM, Madrid, Spain;* [10]*Pediatric Endocrinology Unit, Hospital Universitario La Paz, Madrid, Spain;* [11]*Clinical Genetics Unit, INGEMM, IdiPAZ, Hospital Universitario La Paz-UAM, Madrid, Spain;* [12]*Preanalytics Unit, INGEMM, IdiPAZ, Hospital Universitario La Paz-UAM, Madrid, Spain;* [13]*Molecular Endocrinology Unit, INGEMM, IdiPAZ, Hospital Universitario La Paz-UAM, Madrid, Spain;* [14]*Bioinformatics Unit, INGEMM, IdiPAZ, Hospital Universitario La Paz, Madrid, Spain;* [15]*Department of Immunology, IdiPAZ, Hospital Universitario La Paz, Madrid, Spain;* [16]*Laboratory of Epigenetics, Cancer Epigenetics and Biology Program, Idibell, Barcelona, Spain;* [17]*Bioinformatics Unit, Centro de Investigación Príncipe Felipe, Valencia, Spain;* [18]*SOGRI Consortium (Spanish OverGrowth Registry Initiative) Consortium at INGEMM, IdiPAZ, Hospital Universitario La Paz-UAM, Madrid, Spain*

Communicated by Iain McIntosh

Received 4 June 2014; accepted revised manuscript 26 August 2014.
Published online 6 September 2014 in Wiley Online Library (www.wiley.com/humanmutation). DOI: 10.1002/humu.22689

ABSTRACT: Overgrowth syndromes (OGS) are a group of disorders in which all parameters of growth and physical development are above the mean for age and sex. We evaluated a series of 270 families from the Spanish Overgrowth Syndrome Registry with no known OGS. We identified one *de novo* deletion and three missense mutations in *RNF125* in six patients from four families with overgrowth, macrocephaly, intellectual disability, mild hydrocephaly, hypoglycemia, and inflammatory diseases resembling Sjögren syndrome. *RNF125* encodes an E3 ubiquitin ligase and is a novel gene of OGS. Our studies of the RNF125 pathway point to upregulation of RIG-I-IPS1-MDA5 and/or disruption of the PI3K-AKT and interferon signaling pathways as the putative final effectors.

Hum Mutat 35:1436–1441, 2014. © 2014 Wiley Periodicals, Inc.

KEY WORDS: overgrowth; macrocephaly; autoimmune disorder; intellectual disability; RNF125

Additional Supporting Information may be found in the online version of this article.

*Correspondence to: Pablo Lapunzina, IdiPAZ - Instituto de Investigación Sanitaria del Hospital Universitario La Paz- Universidad Autónoma de Madrid-CIBERER- Centro de Investigación Biomédica en Red de Enfermedades Raras, ISCIII, Madrid, Spain; Paseo de la Castellana, 261-28046 Madrid, Spain. E-mail: pablo.lapunzina@salud.madrid.org

Contract grant sponsors: Fondo de Investigación Sanitaria (ISCIII [FIS 11/2491]); ENDOSCREEN (S2010/BMD-2396); The Marató-TV3; the EUCID-COST Project (BM1208); The Dravet Syndrome Foundation grant through the BBK-KutxaBank; The Spanish Sotos Syndrome Association.

Generalized overgrowth syndromes (OGS) include the classic overgrowth disorders in which all of most parameters of growth and physical development are above the mean for age and sex [Lapunzina et al., 2002; Lapunzina, 2005]. Partial, localized, or regional OGS are those disorders in which excessive growth is confined to one or a few regions of the body. Macrocephaly is usually part of the clinical features observed in many OGS such as the Sotos (MIM #117550), Weaver (MIM #277590), Simpson–Golabi–Behmel (MIM #312870), Bannayan–Riley–Rubalcava (MIM #153480), Primrose (MIM #259050) [Cordeddu et al., 2014], and the 17q11.2 deletion (van Asperen syndrome; MIM #613675) [van Asperen et al., 1998] as well as in hemimegalencephaly-capillary malformation (MIM #602501) and CLAPO association (MIM #613089) [Lopez-Gutierrez and Lapunzina, 2008]. In 2007, Douglas et al. identified mutations in *RNF135* (an ubiquitin E3 ligase also known as Riplet mapping in the 17q11.2 deletion interval) in six families with a phenotype similar to the van Asperen syndrome but without neurofibromata [Douglas et al., 2007]. The authors demonstrated that haploinsufficiency of a RING finger gene was responsible for this OGS. All patients had macrocephaly (ranging from +2 to +4.1 SD), most were tall and heavy and some of them had relatives with mutations and similar clinical features. This clinical entity shares many clinical features with the van Asperen syndrome and has been recently renamed as macrocephaly–macrosomia–facial dysmorphism syndrome (MMFD; MIM #614192).

Ubiquitin-proteasome degradation is one of the major post-transcriptional processes regulating the levels and function of proteins. The ubiquitin pathway includes the activity of at least three different enzymes: an ubiquitin-activating enzyme or E1, a conjugating enzyme or E2, and a ligase enzyme or E3. More than 600 E3 ubiquitin ligases are expressed in the human genome, allowing for the specificity of the ubiquitination system. However, the implication of the ubiquitin-proteasome pathway in OGS is not well known. E3 ubiquitin-ligases are involved, among others, in the phosphoinositide 3-kinase (PI3K) pathway. PI3K enzymes generate 3-phosphorylated phosphoinositides that act as second messengers downstream of numerous cellular receptors implicated in the regulation of cell growth, proliferation, survival, differentiation, and cytoskeletal changes. One of the best characterized targets of PI3K lipid products are the protein kinases AKT (v-AKT murine thymoma viral oncogene). The PI3K-AKT pathway has been implicated in the pathophysiology of several OGS such as the Proteus (MIM #176920), hemihyperplasia–hypoglycemia (240900), CLOVES (MIM #612918), and hemimegalencephaly-capillary malformation (MIM #602501) syndromes due to mutations in *AKT1, AKT2, AKT3, PI3KCA*, and/or *PI3KR2* [Lindhurst et al., 2011; Lindhurst et al., 2012; Riviere et al., 2012]. In this article, we report six patients from four families with overgrowth, macrocephaly and other findings, in whom we have found mutations in another RING finger gene, *RNF125* which encodes an E3 ligase. Similarly to RNF135, RNF125 is upstream of RIG-I (retinoic acid-inducible gene) and MDA5 (melanoma differentiation-associated gene 5), two proteins implicated in a variety of biological pathways including the interferons and the PI3K-AKT signaling pathways.

We selected a subset of 270 patients out of a total of 1,632 individuals registered at the Spanish Overgrowth Syndrome Registry with non-syndromic overgrowth (as defined by Neri in 2001) [Cohen et al., 2001]. We included all individuals with OGS who were negative for *NSD1, EZH2, GPC3*, and 11p methylation defects. We performed in all of them karyotypes and in most of them array CGH or SNP arrays (Supp. Materials and Methods). On SNP-array screening, one patient (patient 1, Fig. 1A and C, Supp. Table S1) showed a *de novo* 9 Mb deletion at chromosome 18 (chr18:24658770-34038769) encompassing candidate genes, including *RNF125*, *RNF138* and many other RefSeq genes (Supp. Table S2). This finding led us to redirect our investigations in the subset, by screening *RNF125* and *RNF138* in all 270 individuals using multiplex ligation probe amplification), high-resolution melting, Sanger sequencing, and pyrosequencing (Supp. Materials and Methods).

Three variants were identified in *RNF125* (c.336G>A [p.M112I], c.488C>T [p.S163L], and c.520C>T [p.R174C] (Fig. 1D and E) which were predicted, by in silico analysis, to be pathogenic (Supp. Table S3). In one of the patients, the mutation was *de novo* and in the other two patients the mutations were also observed in their affected mothers (patients 4 and 6, respectively) (Supp. Table S1, Fig. 1A and F). Pyrosequencing of *RNF125* in patients 2–6 confirmed that heterozygous point mutations were 1:1 in dosage and that there was no evidence of mosaicism (Fig. 1E). No pathogenic mutation in *RNF138* was found in any of the 270 patients. Clinical features and a summary of the studies performed in the four patients are listed in Supp. Table S1. The three missense mutations in *RNF125* were absent in 600 chromosomes from Spanish healthy controls and in 350 exomes of Spanish controls. We also explored the 1000 genome database (http://browser.1000genomes.org) and the Exome Variant Server (EVS) (http://evs.gs.washington.edu/EVS/). None of the three variants were reported in the 1000 genomes. In the EVS, we found that c.336G>A (p.M112I) was absent, whereas the other two variants were reported in 1/13005 chromosomes (0.0077%, Supp. Table S3). Predictions using the Polyphen2, Mut Pred, and Mutation Taster software suggest that all three changes are pathogenic or damaging (Supp. Table S3). Furthermore, methionine 112 and serine 163 residues are both highly conserved in mammals, whereas arginine 174 is conserved in almost all but a few mammals (Supp. Fig. S1). Protein modeling using Phyre2 predicted moderate to severe changes in the mutant proteins (Supp. Fig. S2).

To test other possible genetic or epigenetic alterations, we performed whole expression and whole methylation analysis (Supp. Figs. S3 and S4). We retrospectively also applied whole exome sequencing of DNA samples from blood of patients 2 and 5, to exclude the presence of other pathogenic overgrowth-causing mutations (Supp. Materials and Methods). After filtering for common variants, known polymorphisms and comparison with Spanish databases of exomes, bioinformatic analysis demonstrated that they shared variants in *RNF125* and seven other genes (Supp. Table S4). Segregation analysis in two affected mothers strongly suggested *RNF125* as the unique candidate gene (Fig. 1F). In all patients, we also applied whole-genome expression arrays and subsequently RT-qPCR confirmation in the three main pathways, RIG-I-IPS1, PI3K-AKT, and interferon signaling pathways, in which RNF125 participates. Clear differences were observed between patients and controls. The mRNA levels of *RNF125* were low in all patients (Fig. 2A) compared with controls, whereas *RNF135* levels were similar in the two groups (data not shown). In the RIG I-IPS1 pathway, some transcripts (*RIG-I, LGP2, MDA5*, and *IPS1*) were upregulated in patients compared to age and sex-matched controls (Fig. 2A). Other genes downstream of *RNF125* showed a non-homogeneous behavior: *DUBA, TRAF3*, and *TRAF6* were downregulated, *IRF3* and *TRADD* were upregulated and *TRAF2* was equal to controls (Supp. Fig. S4A). Similar results were obtained after the analysis of genes implicated in the PI3K-AKT pathway. Levels of *mTOR, PIK3R2, BTK, ILK, MYD88, PAK1, EIF4G1, HSPB1, PTEN*, and *TLR4* (Fig. 2A and Supp. Fig. S4B) were upregulated in patients compared with controls whilst *ATK2, AKT3, EIF4B, EIF4E, PIK3CA, PIK3R1*, and *RPS6KB1* were downregulated (Supp. Fig. S4B). Finally, analysis of 15 genes of the interferon pathway showed that only two genes, *IFNA8* and *IFNA14* were down-regulated (Supp. Fig. S4C), whereas the remaining 13 genes showed no differences in their expression profile pattern between patients and controls. These results confirm that mutations in *RNF125* lead to transcriptional downregulation of the gene and that haploinsufficiency of *RNF125* leads to upregulation of *RIG-I, IPS1*, and *MDA5* and misregulation of at least three main pathways (RIG-I-IPS1, PI3K-AKT, and Interferon). We tested whether expression of RIG-I protein is dysregulated in patients with *RNF125* mutations and found that basal RIG-I levels were not significantly different in B-lymphocytes cells of patients 1 and 2 compared with controls (data not shown). However, after treatment with poly (I:C), which acts as a double strand RNA-activator of the RIG-I signaling pathway, RIG-I induction levels were doubled in patients compared to controls (Fig. 2B and C). In order to demonstrate that RNF125 haploinsufficiency slows RIG-I degradation, we monitored the degradation kinetics of RIG-I after blocking translation with cycloheximide, a standard approach used to assay proteasome-mediated degradation. When protein synthesis was blocked, the turnover of endogenous RIG-I was slower in patient cells than in controls (Fig. 2D). After 12 hr post-cycloheximide treatment, patient-derived cells retained ~50% of the amount of RIG-I, whereas RIG-I was almost fully degraded in control cells (Fig. 2D–E).

Overgrowth, macrocephaly and intellectual disability (ID) are observed in a relatively small number of disorders [Lapunzina, 2005]. We here report six individuals from four families with mutations in *RNF125* and macrocephaly, overgrowth, enlarged ventricles, a

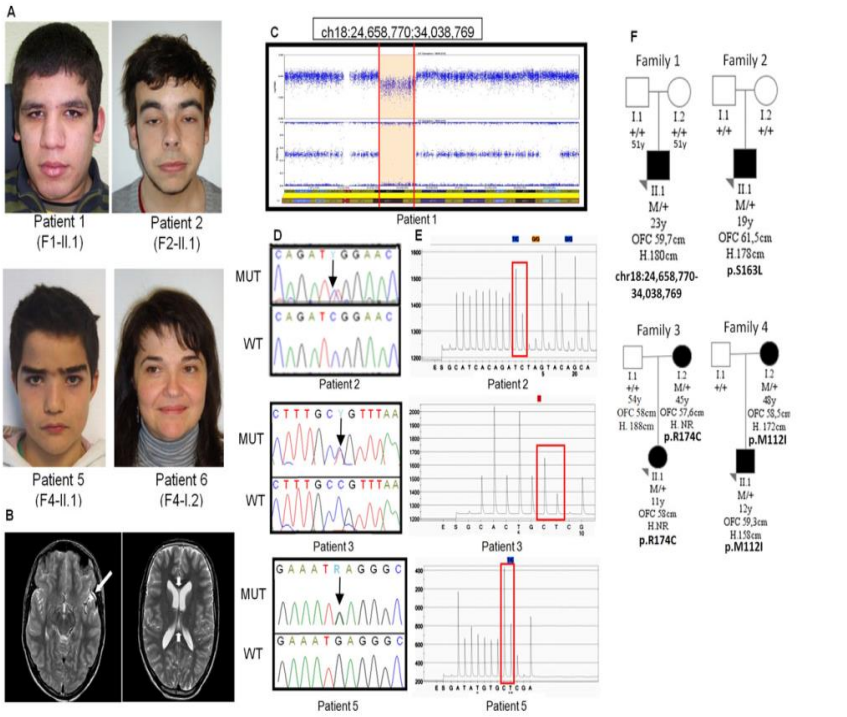

Figure 1. **A:** Facial phenotypes of patients 1, 2, 5, and 6. Correlation among the individuals and their position in the pedigree is in brackets. Note macrocephaly and large forehead in all patients and in some of them, a broad nose and synophrys. Patient 1 also presents a large mouth and a squared face, patient 2 has fleshy lips and upturned nose and patients 5 and 6 non-curved eyebrows and deep-set eyes. **B:** MRI of patient 2. Arrow indicates the anomaly of the Galenous' vein; note mild hydrocephalus and septum cavum pellucidum (white arrow). **C:** SNP-array of patient 1; the deleted region is shaded. The upper panel represents the log2 ratio score (dosage) and the lower panel shows the haplotype plot showing loss of heterozygosity (LOH) in the deleted region. The deletion coordinates are in hg19. **D:** Comparison of the mutant and wild type chromatograms showing the *RNF125* mutations in the three probands (RefSeq NM_017831.3; data submitted to http://www.lovd.nl/RNF125). **E:** Pyrosequencing confirmation of each mutation showing a 1:1 ratio. F: Pedigrees of the four families showing cosegregation of the mutation with the phenotype in families 3 and 4. The pedigrees also include: genotype (+ = wt; M = mutant); y: (years), OFC: occipitofrontal circumference; H: height; and mutation detected for each case. NR: not recorded.

variable degree of intellectual disability and in some, hypoglycemia and recurrent inflammatory disease resembling Sjögren syndrome. Two patients inherited the mutations from their affected mothers and in the other two the mutations were *de novo*. The p.M112I and p.R174C mutations cosegregated with the phenotypes of their affected mothers. In silico analysis of the amino acid changes in RNF125 indicates that they occurred in protein domains with important biological functions: p.M112I and p.R174C directly affect the first (C2HC) and third (C2H2) zinc finger domains of the protein, respectively (Supp. Fig. S1). The p.S163L mutation is located between the second and the third (C2H2) zinc finger domains, thus potentially affecting the intramolecular folding and the interactions among these zinc fingers [Giannini et al., 2008]. The introduction of a cysteine instead of an arginine at the third zinc finger disrupts the balance of the finger domain from C2H2 to C3H2 and potentially may also impair its function. In addition, in silico 3D analysis of the mutant proteins also suggest that the mutations may potentially alter the tertiary structure (Supp. Fig. S2), thus, affecting their functions. Finally, and very importantly, expression studies confirmed that all analyzed patients showed decreased *RNF125* RNA levels.

All our patients with *RNF125* mutations that resulted in downregulation of *RNF125* were shown to have upregulation of *RIG-I, MDA5* and *IPS1* (Fig. 2A). RNF125 functions as a negative regulator of RIG-I and MDA5 signaling and a positive T cell regulator [Arimoto et al., 2007]. Dysregulation of RIG-I has been implicated in several infectious diseases and disorders of the immune system [Giannini et al., 2008]. Further, gain of function mutations of *IFIH1* (*MDA5*) have been recently described in patients with Aicardi-Goutieres syndrome (MIM #225750) featuring CNS anomalies and autoinflammatory diseases, as observed in our patients [Rice et al., 2014]. In accordance with our findings, Rice et al. (2014) proposed that mutations in *IFIH1* (*MDA5*) cause a gain of function of the protein leading to an increase in its binding with the RNA in the innate immune response. Similarly, haploinsufficiency of *RNF125* (which is upstream in the same pathway and regulates both RIG-1 and MDA5) (Supp. Fig. S5) would lead to an increase of MDA5 levels resulting in a gain of function of it and potentially dysregulating the immune response. In the interferon pathway, both *IFNA8* and *IFNA14* were also downregulated. Transcriptional upregulation and increased protein levels of RIG-I and/or IPS1 have been reported to play a role in the pathophysiology of autoinflammation [Britto et al., 2013]. Interestingly, some patients reported herein suffered from recurrent inflammation with a chronic pattern (Supp. Table S1). Patient 2 had several episodes of Raynaud phenomena, dry conjunctivitis and recurrent aphthous stomatitis and patient 4 suffered from continuous episodes

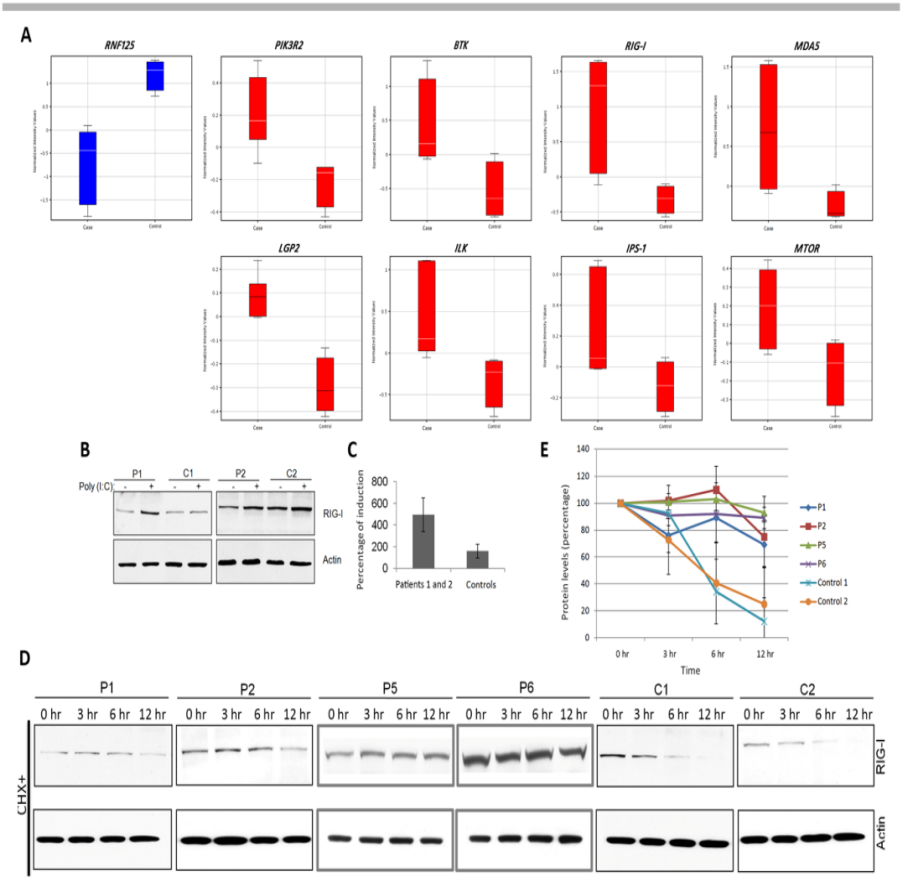

Figure 2. Functional analysis of RNF125. **A:** Expression arrays showing dysregulation of the RIG-I and PI3K-AKT pathways. Boxplot of mRNA expression of different genes included in the RIG-I and PI3K-AKT signaling pathways: *RNF125*; *RIG-I* (*DDX58*); *IPS-1*; *MTOR*; *PIK3R2*; *BTK*; *ILK*; and *LGP2*. Case = average of normalized mRNA levels of patients (P1: Patient 1; P2: Patient 2; P5: Patient 5) Control = average of normalized mRNA levels of controls. For each patient one age and sex matched control were use. The color range indicates the lowest (blue) to highest (red) expression. **B–E:** Western blot analysis of mutations in RNF125. RIG-I degradation is impaired in *RNF125* haploinsufficiency derived cells. **B:** RIG-I levels were examined by Western blot of untreated cells from each patients (1 and 2) or the corresponding controls (C) and compared with cells treated with 100 μg/ml poly (I:C) for 16 hr. **C:** Densitometry was undertaken for three independent experiments, as in Figure 2B. The percentage of RIG-I induction was plotted in a graph, after values were corrected for actin expression. Patient cells showed a major percentage of induction compared to control cells. **D:** Patients' cells (patients 1, 2, 5, and 6) were treated with poly (I:C) followed by addition of cycloheximide (CHX). Cells were harvested at the indicated times after addition of CHX and RIG-I levels analyzed by Western blot. **E:** Degradation kinetic plots of for patients 1, 2, 5, and 6 versus controls showed a significance difference between the kinetic of the patients and controls.

of keratitis, conjunctivitis, limbitis, serous otitis, and pneumonia findings that are usually observed in the Sjögren syndrome (MIM #270150), a common autoimmune disease. We observed transcriptional upregulation of RIG-I and IPS1 at the RNA and protein level in our patients. Three E3 ubiquitin ligases, RNF125, RNF135, and TRIM25 target RIG-I for ubiquitination [Arimoto et al., 2007; Gack et al., 2007; Oshiumi et al., 2010] allowing RIG-I, and the three RIG I-like receptors, namely MDA5 [*IFIH1*], LGP2 (or DEXH box polypeptide 58 [*DHX58*], (MIM #608588) and IPS1 to interact in a very complex cascade of downstream activations (Supp. Fig. S5). IPS1 is activated by RIG-I and MDA5 which in turn both interacts with RNF125, RNF135 and TRIM25 [Oshiumi et al., 2010] (Supp. Fig. S5). The interaction between RIG-I and IPS1 is induced by TRIM25-mediated Lys63-linked polyubiquitination at Lys 172 of the RIG-I CARDs (caspase activation and recruitment domains) [Gack et al., 2007]. Previous studies demonstrated that RNF125 binds IPS1 as well as MDA-5 and was also ubiquitinately conjugated [Arimoto et al., 2007] confirming that RNF125 has activity against RIG-I, MDA5, LGP2, and IPS1. These findings were also confirmed by the fact that the concentrations of MDA5 and IPS1 were reduced in cells overexpressing RNF125 ectopically and by a suppression of conjugation of ubiquitin to these proteins was observed by treatment with siRNA specific to RNF125 [Arimoto et al., 2007].

Shared features in our patients were overgrowth, macrocephaly with prominent and large forehead and some degree of ID; however, some other features were not observed in all individuals (Supp. Table S1). Our patients have phenotypic similarities with individuals with van Asperen syndrome (chromosome 17q11.2 deletion; MIM #613675) and MMFD (MIM #614192) due to mutations in *RNF135* [Douglas et al., 2007]. Although *RNF135* haploinsufficiency either to deletion or mutations leads to disease in humans, knockout of the mouse homolog, *rnf135*, does not cause any apparent developmental defects but rather severely reduced type I interferon, and abrogates

the activation of RIG-I and RIG-I C-terminal domain polyubiquitination [Oshiumi et al., 2010]. In addition, *rig-i* deficient mice are usually embryonic lethal, but interestingly, a few mice were born alive and died within 3 weeks after birth showing growth retardation (the reverse phenotype of overgrowth) [Kato et al., 2005]. Thus, mutations in *RNF125* and *RNF135* could lead to the same biological effect: haploinsufficiency of *RNF125* would prevent RIG-I binding thus, impairing IPS1 function while haploinsufficiency of *RNF135* would prevent activation of RIG-I and IPS1; similarly (Supp. Fig. S5). Despite not knowing the precise mechanism through which RNF125 and RNF135 haploinsufficiency results in the dysregulation of the RIG-I-IPS1 pathway, we have clearly demonstrated that the patients with RNF125 mutations result in dysregulation of the two main activators of this pathway.

We have also observed transcriptional activation of some of the phosphatases of the PI3K pathway in patients with *RNF125* haploinsufficiency. There is considerable experimental evidence for the dysregulation of E3 ligases, PI3K signaling abnormalities, and altered growth. Abnormal E3 ligases and growth retardation is reported in Angelman (MIM #105830), Johanson–Blizzard (MIM #243800) and Kaufman oculocerebrofacial (MIM #615057) syndromes, among others. Additionally, some conditions with overgrowth have E3 ligases dysregulation. Firstly, synaptic overgrowth was observed in the absence of the E3 ubiquitin ligase "*highwire*" together with an increased PI3K signaling in motor neurons [Mozer and Sandstrom, 2012]. Secondly, a Ring Finger E3 responsible of Ecdysone receptor (a steroid hormone) degradation in *Drosophila melanogaster* acts at high concentrations as a developmental timer and at basal levels contributes to the inhibition of tissue growth [Gradilla et al., 2011]. Thirdly, another E3 ligase complex associated to akt (SCF^{slimb}) inhibits neuroblast overgrowth in *drosophila* brains [Li et al., 2014]. Fourthly, the Big Brother (*bb*) gene, encoding an E3 ubiquitin ligase, represents a central regulator of organ size and growth in *Arabidopsis*. Plants lacking *bb* activity form larger organs; whereas conversely, plants expressing higher levels of *bb* produce smaller organs, indicating that *bb* acts as a negative regulator for organ size [Breuninger and Lenhard, 2012]. RNF125 has a 46% (20/45) positive identity at the zinc finger domains with bb (amino acids 197–241). Exact amino acid identity between RNF125 and BB occurs at the eight conserved cysteines and histidines of the zinc finger domains. Fifthly, individuals with haploinsufficiency of *NSD1* (a gene whose protein has several zinc fingers) develop Sotos syndrome (MIM #117550), an overgrowth/macrocephaly disorder. Thus, haploinsufficiency of E3 ubiquitin ligases in plants (*Arabidopsis*) and *D. melanogaster* leads to overgrowth and in humans, haploinsufficiency of *RNF135* [Douglas et al., 2007] and now in this study, *RNF125*, leads to overgrowth, macrocephaly and intellectual disability. Finally, firm evidence of the implication of the PI3K-AKT pathways in overgrowth-macrocephaly syndromes and links among the PI3K and the RIG-I/interferon pathway have recently been communicated. Mutations in *PIK3CA*, *PIK3R2* and *AKT3* are observed in the megalencephaly-capillary malformation [Riviere et al., 2012], in *AKT1* in Proteus syndrome [Lindhurst et al., 2011] and in *AKT2* in hemihypertrophy–hypoglycemia [Lindhurst et al., 2012]. In addition, PI3K has been defined as one of the main factors activated through RIG-I mediated anti-pathogen response to enhance expression of type I interferons. Other features observed in some of our patients were intellectual disability, mild hydrocephaly, and hypoglycemia. Intellectual disability and hydrocephaly are also observed in patients with *AKT3*, *PI3KR2*, and *PI3KCA* mutations, whereas hypoglycemia has been observed in individuals with *AKT2* mutations [Lindhurst et al., 2011; Lindhurst et al., 2012; Riviere et al., 2012]. Intellectual disability has been also described in patients with mutations in other RING finger genes such as *RNF133* and *RNF148* [Bonora. et al., 2012].

In summary, we have identified six affected individuals from four OGS families with mutations in *RNF125*. We have demonstrated that mutations in *RNF125* result in a loss of function of *RNF125* and dysregulation of the RIG-I-IPS1, PI3K-AKT, and interferon pathways. The exact mechanism/s by which haploinsufficiency of *RNF125* results in overgrowth, macrocephaly and in some patients intellectual disability, hypoglycemia, and Sjögren-like syndrome remains elusive. Though the complex pathways linking E3 ubiquitin ligases, RING fingers, CARD/CARD-like proteins and the RIG I-IPS1, PI3K-AKT and interferon pathways need further investigations, this article demonstrates the connections among these proteins and their implication in a novel disorder of growth, development and autoimmunity.

Acknowledgments

The SOGRI (Spanish OverGrowth Registry Initiative) Consortium is constituted by the following researchers: A. Plasencia, Alberto L. Rosa, Aleixandre Blanquer, Alfredo García-Alix, Alfredo Santana, Alicia Delicado, Almudena Alonso, Amaya Rodriguez, Amparo Sanchis, Ana Moreno, Ana Patiño García, Ana Vega, Analía Bredani, Andrea Paula Solari, Andrea Villavicencio, Angelina Acosta, Anibal Nieto, Anna Maria Cueto González, Antonio Baldellón, Antonio González Meneses, Antonio Martinez Carrascal, Aranzazu Díaz de Bustamante, Arteche Ocasar, Blanca Gener, Blasco González, Boris Groisman, Bradford Coffee, Carlos Alcalde Martín, Carmen Aragon Fernandez, Carmen Benito, Carmen Martin Seisdedos, Carmen Roche, Claudia Arberas, Claudia Perandones, Claudio Contessotto, Cristina Olivas, Daniel Armenta, Denise Cavalcanti, Dolores Elorza, Eduardo Castilla, Elena Zamora, Elisa Zambrano, Elisabeth Steichen, Enrique Caro Cruz, Enrique Galán Gómez, Enriqueta Román, Ernesto Goldschmidt, Esteban Marfil, Esther Gean, Eugenia Antolín, F. Javier Gascón Jiménez, Feliciano Ramos, Fermina López Grondona, Fernández Córdoba, Fernando Regla Vargas, Francisco Martinez, J. Miguel García Vegada, Giovannucci Uzielli, Gloria Gacio, Carmen González Armengod, Graciela Mercado, Hamilton Cassinelli, Ieda Orioli, Ignacio Arroyo, Ignacio Díez López, Ignacio Onsurbe Ramírez, Ignacio Pascual Castroviejo, Ignacio Pascual Pascual, Ignacio Vázquez Rio, Inés Bueno, Isabel Espejo Portero, Isabel Lorda Sánchez, Jaime Sánchez del Pozo, Jaume Campistol, Javier Arcas, Javier Fernández, Javier García Planells, Javier López Pisón, Jesús Barreiro, Jesús del Valle Núñez, María José Jiménez Liria, Joaquín Fernández Toral, Joaquín Ramírez, Jordi Rosell, Jorge Vilaplana, José Carlos Cabral de Almeida, José Ignacio Labarta, José L. Herranz, José Luis Fernández Luna, José Luis Fuster, José M. Díaz, Jose M. Gairi, José Miguel García Sagredo, Juan A. Piñero, Juan Carlos López Gutiérrez, Juan Manuel Fernández, Juan P. López Siguero, Juan Tovar, Judith Armstrong, Julián Lara, Leonor Arranz, Laura Rodríguez, Leandro Soriano, Leila Cardoso, Liliana De Alba, Loreta Cimbalistiene, Loreto Martorell, Luis González Gutiérrez Solana, Luis Pérez Jurado, M Asunción López Ariztegui, M. Antonia Molina, M. Cruz García, M. Ferrer Lozano, M. Jesús Alija Merillas, M. Luisa Martínez-Frías, María L. Martínez Fernández, M. Rocío Jadraque, Mª Asunción García Pérez, Mª Montserrat Rodríguez Pedreira, Mª Pilar Ribate, Mª Teresa González López, Mª Teresa Moral Pumarega, Mabel Segovia, Macarena Lizama, Manuel Pombo, Margarita Martínez, Margarita Tabernero, María Antonia Ramos, Maria Ballesta, María Belar, María Jesús Lautre, Marta Cruz, M. Nieves Martínez Guardia, F. Javier Martínez Sarries, Mercedes Artigas, Mercedes Villanueva, Meritxell Torrabías, Miguel del Campo, Miguel Tomás Vila, Miguel Urioste, Mónica Rosello, Nik Kantaputra, Pablo Prieto Matos, Paloma Dorao, Paula Casano, Paula Lalaguna Mallada, Pedro Olivares, Raquel Perez Delgado, Priscila Bernardi, Rafael Camino León, Ramón Cañete, Ramón Gaztañaga, Ramón Velazquez, Ramón Vidal Samahuja, Raquel Sáez Villaverde, Ricardo Gracia, Richard Scott, Rita Valdez, Rosa Arteaga, Rosa Cedeño, Rosario Cazorla, Rosario Marín Iglesias, Rubén Bronberg, Salvador Climent, Santiago Conde Barreiro, Seema Kapoor, Soledad Kleppe, Sonia Santillán, Trinidad García Lopez, Teresa Calvo, Teresa Vendrell, Pilar Tirado, Claudia Toledo Pacheco, Alicia Ureta Huertos, Vanesa Lopez, Vanesa Lotersztein, Vanesa Méndez,

Selma Vázquez Martín, Verónica Seidel, Vicente Albiach, Víctor M. Navas López, Virgina Soler, and Viviana Cosentino. We also thank the CIBERER BioBank for the support and all participating families.

References

Arimoto K, Takahashi H, Hishiki T, Konishi H, Fujita T, Shimotohno K. 2007. Negative regulation of the RIG-I signaling by the ubiquitin ligase RNF125. Proc Natl Acad Sci USA 104:7500–7505.

Bonora E, Wischmeijer A, Minopoli F, Tabarroni C, Vidone M, Seri M, Graziano C, Romeo G. 2012. Analysis of ring finger proteins RNF133 and RNF148 in intellectual disability. Eur J Hum Genet 20:Suppl. 1–78.

Breuninger H, Lenhard M. 2012. Expression of the central growth regulator BIG BROTHER is regulated by multiple cis-elements. BMC Plant Biol 12:41.

Britto AM, Amoedo ND, Pezzuto P, Afonso AO, Martinez AM, Silveira J, Sion FS, Machado ES, Soares MA, Giannini AL. 2013. Expression levels of the innate response gene RIG-I and its regulators RNF125 and TRIM25 in HIV-1-infected adult and pediatric individuals. AIDS 27:1879–1885.

Cohen MM, Neri G, Weksberg R. 2001. *Overgrowth syndromes*. Oxford University Press, New York, NY, USA.

Cordeddu V, Redeker B, Stellacci E, Jongejan A, Fragale A, Bradley TE, Anselmi M, Ciolfi A, Cecchetti S, Muto V, Bernardini L, Azage M, et al. 2014. Mutations in ZBTB20 cause Primrose syndrome. Nat Genet 46:815–817.

Douglas J, Cilliers D, Coleman K, Tatton-Brown K, Barker K, Bernhard B, Burn J, Huson S, Josifova D, Lacombe D, Malik M, Mansour S, et al. 2007. Mutations in RNF135, a gene within the NF1 microdeletion region, cause phenotypic abnormalities including overgrowth. Nat Genet 39:963–965.

Gack MU, Shin YC, Joo CH, Urano T, Liang C, Sun L, Takeuchi O, Akira S, Chen Z, Inoue S, and Jung JU et al. 2007. TRIM25 RING-finger E3 ubiquitin ligase is essential for RIG-I-mediated antiviral activity. Nature 446: 916–920.

Giannini AL, Gao Y, Bijlmakers MJ. 2008. T-cell regulator RNF125/TRAC-1 belongs to a novel family of ubiquitin ligases with zinc fingers and a ubiquitin-binding domain. Biochem J 410:101–111.

Gradilla AC, Mansilla A, Ferrus A. 2011. Isoform-specific regulation of a steroid hormone nuclear receptor by an E3 ubiquitin ligase in *Drosophila melanogaster*. Genetics 189:871–883.

Kato H, Sato S, Yoneyama M, Yamamoto M, Uematsu S, Matsui K, Tsujimura T, Takeda K, Fujita T, Takeuchi O, and Akira S. et al. 2005. Cell type-specific involvement of RIG-I in antiviral response. Immunity 23:19–28.

Lapunzina P. 2005. Risk of tumorigenesis in overgrowth syndromes: a comprehensive review. Am J Med Genet C Semin Med Genet 137C:53–71.

Lapunzina P, Camelo JS, Rittler M, Castilla EE. 2002. Risks of congenital anomalies in large for gestational age infants. J Pediatr 140:200–204.

Li S, Wang C, Sandanaraj E, Aw SS, Koe CT, Wong JJ, Yu F, Ang BT, Tang C, Wang H. 2014. The SCFSlimb E3 ligase complex regulates asymmetric division to inhibit neuroblast overgrowth. EMBO Rep 15:165–174.

Lindhurst MJ, Parker VE, Payne F, Sapp JC, Rudge S, Harris J, Witkowski AM, Zhang Q, Groeneveld MP, Scott CE, Daly A, Huson SM, et al. 2012. Mosaic overgrowth with fibroadipose hyperplasia is caused by somatic activating mutations in PIK3CA. Nat Genet 44:928–933.

Lindhurst MJ, Sapp JC, Teer JK, Johnston JJ, Finn EM, Peters K, Turner J, Cannons JL, Bick D, Blakemore L, Blumhorst C, Brockmann K, et al. 2011. A mosaic activating mutation in AKT1 associated with the Proteus syndrome. N Engl J Med 365:611–619.

Lopez-Gutierrez JC, Lapunzina P. 2008. Capillary malformation of the lower lip, lymphatic malformation of the face and neck, asymmetry and partial/generalized overgrowth (CLAPO): report of six cases of a new syndrome/association. Am J Med Genet A 146A:2583–2588.

Mozer BA, Sandstrom DJ. 2012. Drosophila neuroligin 1 regulates synaptic growth and function in response to activity and phosphoinositide-3-kinase. Mol Cell Neurosci 51:89–100.

Oshiumi H, Miyashita M, Inoue N, Okabe M, Matsumoto M, Seya T. 2010. The ubiquitin ligase Riplet is essential for RIG-I-dependent innate immune responses to RNA virus infection. Cell Host Microbe 8:496–509.

Rice GI, del Toro Duany Y, Jenkinson EM, Forte GM, Anderson BH, Ariaudo G, Bader-Meunier B, Baildam EM, Battini R, Beresford MW, Casarano M, Chouchane M, et al. 2014. Gain-of-function mutations in IFIH1 cause a spectrum of human disease phenotypes associated with upregulated type I interferon signaling. Nat Genet 46:503–509.

Riviere JB, Mirzaa GM, O'Roak BJ, Beddaoui M, Alcantara D, Conway RL, St-Onge J, Schwartzentruber JA, Gripp KW, Nikkel SM, Worthylake T, Sullivan CT, et al. 2012. De novo germline and postzygotic mutations in AKT3, PIK3R2 and PIK3CA cause a spectrum of related megalencephaly syndromes. Nat Genet 44:934–940.

van Asperen CJ, Overweg-Plandsoen WC, Cnossen MH, van Tijn DA, Hennekam RC. 1998. Familial neurofibromatosis type 1 associated with an overgrowth syndrome resembling Weaver syndrome. J Med Genet 35:323–327.

European Journal of Human Genetics (2015) 23, 1615–1626

www.nature.com/ejhg

ARTICLE

PIAS4 is associated with macro/microcephaly in the novel interstitial 19p13.3 microdeletion/ microduplication syndrome

Julián Nevado*[,1,2], Jill A Rosenfeld[3], Rocío Mena[1], María Palomares-Bralo[1,2], Elena Vallespín[1,2], María Ángeles Mori[1,2], Jair A Tenorio[1], Karen W Gripp[4], Elizabeth Denenberg[4], Miguel del Campo[5], Alberto Plaja[5], Rubén Martín-Arenas[1], Fernando Santos-Simarro[6], Lluis Armengol[7], Gordon Gowans[8], María Orera[9], M Carmen Sanchez-Hombre[9], Esther Corbacho-Fernández[9], Alberto Fernández-Jaén[10], Chad Haldeman-Englert[11], Sulagna Saitta[12], Holly Dubbs[13], Duban B Bénédicte[14], Xia Li[15], Lani Devaney[16], Mary Beth Dinulos[17], Stephanie Vallee[17], M Carmen Crespo[1], Blanca Fernández[18], Victoria E Fernández-Montaño[1], Inmaculada Rueda-Arenas[1], María Luisa de Torres[2,18], Jay W Ellison[19], Salmo Raskin[20], Carlos A Venegas-Vega[21,22], Fernando Fernández-Ramírez[21], Alicia Delicado[2,18], Sixto García-Miñaúr[2,6] and Pablo Lapunzina[2,6]

Array comparative genomic hybridization (aCGH) is a powerful genetic tool that has enabled the identification of novel imbalances in individuals with intellectual disability (ID), autistic disorders and congenital malformations. Here we report a 'genotype first' approach using aCGH on 13 unrelated patients with 19p13.3 submicroscopic rearrangement (11 deletions and 2 duplications) and review cases in the literature and in public databases. Shared phenotypic features suggest that these patients represent an interstitial microdeletion/microduplication syndrome at 19p13.3. Common features consist of abnormal head circumference in most patients (macrocephaly with the deletions and microcephaly with the duplications), ID with developmental delay (DD), hypotonia, speech delay and common dysmorphic features. The phenotype is associated with at least a ~0.113 Mb critical region harboring three strong candidate genes probably associated with DD, ID, speech delay and other dysmorphic features: *MAP2K2*, *ZBTB7A* and *PIAS4*, an E3 ubiquitin ligase involved in the ubiquitin signaling pathways, which we hypothesize for the first time to be associated with head size in humans.

European Journal of Human Genetics (2015) **23,** 1615–1626; doi:10.1038/ejhg.2015.51; published online 8 April 2015

INTRODUCTION

Chromosome 19 has the highest gene density of the human chromosomes.[1] However, only a few disease-associated microdeletion/duplication regions have been described.[2–11] On the short arm, microdeletion/duplication syndromes have been proposed for 19p13.13,[2] 19p13.12[3] and terminal 19p13.3 microdeletions.[4] Pure terminal 19p13.3 duplications[7] have also been described as syndromic entities.

High-resolution microarray comparative genomic hybridization (aCGH) is a powerful genetic tool implemented as a first-tier test for diagnosis of genomic imbalances.[12,13] A 'genotype first' approach, in which patients are characterized by a similar genomic rearrangement before a common clinical presentation is observed, has proven to be successful in characterizing the growing list of microdeletion/duplication syndromes. In fact, using this experimental approach, we and others recently described new microdeletion or microduplication syndromes.[14–17]

Here we report 13 new patients with proximal 19p13.3 submicroscopic rearrangements (11 deletions and 2 duplications) and review patients from the literature (14 cases; 13 deletions and 1 duplication) [18–22] and public genomic databases such as DECIPHER and ISCA Consortium (10 cases; 6 deletions and 4 duplications) for a total of 37 cases. We describe the phenotypic findings and suggest that these patients represent a new microdeletion/duplication syndrome at 19p13.3, with a 113.5 Kb critical region harboring three genes: *ZBTB7A*, *MAP2K2* and *PIAS4*, the latter being a candidate gene for abnormal head size.

[1]Section of Functional and Structural Genomics Instituto de Genética Médica y Molecular (INGEMM)-IdiPAZ, Hospital Universitario La Paz, Madrid, Spain; [2]CIBERER, Centro de Investigación Biomédica en Red de Enfermedades Raras, ISCIII, Madrid, Spain; [3]Signature Genomic Laboratories, PerkinElmer Inc., Spokane, WA, USA; [4]AI DuPont Hospital for Children, Wilmington, DE, USA; [5]Hospital Vall D'Hebron, Barcelona, Spain; [6]Section of Clinical Genetics, INGEMM-IdiPAZ, Hospital Universitario La Paz, Madrid, Spain; [7]Q-Genomics Laboratory, Barcelona, Spain; [8]University of Louisville, Kentucky, USA; [9]CGC-Genetics, Madrid, Spain; [10]Hospital Quirón de Madrid, Madrid, Spain; [11]Wake Forest University, Winston-Salem, NC, USA; [12]Medical Genetics Institute, Cedars Sinai Medical Center, Los Angeles, CA, USA; [13]The Children's Hospital of Philadelphia, Philadelphia, PA, USA; [14]Hospital Saint Vincent de Paul, Lille, France; [15]Ameripath Northeast, Shelton, CT, USA; [16]Henry Ford Health System, Sterling Heights, Michigan, USA; [17]Dartmouth-Hitchcock Medical Center, Lebanon, NH, USA; [18]Section Cytogenetics, INGEMM-IdiPAZ, Hospital Universitario La Paz, Madrid, Spain; [19]Kaiser Permanente, San Francisco, CA, USA; [20]Center for Health and Biological Sciences, Pontifícia Universidade Católica do Paraná (PUC-PR), Curitiba, Brazil; [21]Genetic Unit Hospital General de México, México, México; [22]School of Medicine. Universidad Autónoma de México, México, México
*Correspondence: Dr J Nevado, Section of Functional and Structural Genomics, Instituto de Genética Médica y Molecular (INGEMM), IdiPAZ; Hospital Universitario La Paz, Paseo de la Castellana 261, Madrid 28046, Spain. Tel: +34 91 7277217; Fax: +34 91 2071040; E-mail: jnevado@salud.madrid.org
Received 12 October 2014; revised 23 December 2014; accepted 17 February 2015; published online 8 April 2015

MATERIALS AND METHODS

Individuals

Patients 1–4 were referred for genetic assessment and patients 5–9 and 12–13 for a customized aCGH analysis to the Institute of Medical and Molecular Genetics at the University Hospital La Paz in Madrid (Madrid, Spain). Patients 5, 7 and 9–13 were originally ascertained following referral for clinical aCGH testing to Signature Genomics, Spokane, WA, USA. The clinical investigations were performed according to the guidelines in the Declaration of Helsinki. Informed consent was obtained from all family members and specific permission to publish photographs was obtained. The studies were approved by the IRB of both institutions. All data reporting variants/phenotypes linked to all rearrangements described herein have been submitted to DECIPHER public data base.

aCGH, fluorescence *in situ* hybridization and parent-of-origin analysis with short tandem repeats

The aCGH experiments were performed using previously described methods.[23–26] Details on the used arrays and specific techniques are given in Supplementary Materials. FISH studies[27] and microsatellites analyses were performed following standard procedures.

Detection of breakpoints and junction fragment analysis with long-range PCR and Sanger sequencing

To determine the sequence at the breakpoints for some 19p13.3 deletions (patients 1–7, 9, 12 and 13), we designed a different set of primers (available upon request); according to our custom 19p13.3 aCGH results and followed previously described methods.[16]

RESULTS

Clinical data

Clinical and phenotypic findings of all 13 individuals are listed in Table 1, and the facial phenotypes of some patients are shown in Figure 1 (patients 1, 3–6 and 13). Table 1 also analyzes the frequency of several phenotypic features, and compares with previously reported cases (reviewed in Table 2 and references[18–22]). Among them, developmental delay (DD), abnormal head size, speech delay, intellectual disability (ID), feeding problems, hypotonia and other dysmorphic features were the most prevalent, present in most deletion cases. Individuals with duplications share many of these main phenotypic features. Unique traits only reported with microdeletion include ophthalmologic alterations, gastroesophageal reflux, sleep disorders, congenital heart disease, and in a lower incidence, behavioral disorders such as autism or aggressive behavior. Distinct recognizable facial features, including a short philtrum, thin upper lip, abnormal ears, wide nasal bridge, depressed nose and root, downslanting palpebral fissures and hypertelorism were apparent in many patients (see Figure 1 and Tables 1 and 2). Ocular anomalies included strabismus, amblyopia, astigmatism and myopia. Congenital heart disease, such as atrial septal defect (the most frequent), dilated aorta, tetralogy of Fallot, bicuspid aortic valve, prominent aortic root and patent ductus arteriosus were observed. In addition, six out of nine patients, including both individuals with duplication, showed proportionate short stature, and three others had a postnatal growth pattern above the mean. In total, 9/13 showed some height alteration. Interestingly, head circumference was abnormal in all but two patients (patients 6 and 10). Head circumference had an almost complete phenotype–genotype correlation among our and previously reported patients: 21/24 patients with deletion have macrocephaly and 2/3 patients with duplication have microcephaly. In fact, macrocephaly (OFC>97th centile) or microcephaly (OFC<3rd centile) was observed at birth in patients with 19p13.3 genomic rearrangements and remained a medical concern throughout their lives.

Additional cases (without full clinical information available) with genomic rearrangements at this region and published in public databases, such as DECIPHER and ISCA consortium, were summarized in Supplementary data (Supplementary Table S1).

aCGH studies

Genomic rearrangements within 19p13.3 were demonstrated by aCGH in 13 patients (see Supplementary Figure S1 and Table 3 for genomic coordinates in hg19; NCBI build 37). Eleven had deletions, ranging in size from 151 kb (patient 11) to 1.70 Mb (patient 7), and two had duplications, 1.48 Mb (patient 10) and 2.39 Mb (patient 8). In all but three (patients 6, 9 and 13), the 19p13.3 deletion was the sole significant aberration (Table 3). In patient 6 we also observed a *de novo* 0.226 Mb deletion at 19q13.2, and patients 9 and 13 showed two genomic rearrangements within 19p13.3 separated by a normal region (see supplementary data Supplementary Figure S3). FISH and/or other aCGH assays confirmed the initial aCGH results (data not shown). Most of the deletions/duplications have different breakpoints, although the breakpoints in some cases are in close proximity (Figure 2 and Supplementary Figure S1 and Table 3). When parental samples were available, the rearrangements were found to be *de novo* (by means of either FISH or aCGH, see supplementary data).

Among individuals with interstitial 19p13.3 rearrangements (sharing characteristic features of abnormal head size, DD, speech delay, hypotonia and dysmorphic features) the shortest region of overlap (SRO) in our series is delineated distally and proximally by patient 11 with estimated breakpoints at genomic positions chr19:3979568-4131259; hg19; NCBI build 37 (~150 kb; Figure 3a). This SRO is shared by 11 of 13 patients (excluding patient 6 partially and patient 10 totally, both of whom have normal head size) and by 13/14 patients in previously reported cases.[18–22] This segment of ~150 kb includes one microRNA (*SNORD37*) and four RefSeq genes: *PIAS4*, *ZBTB7A*, *MAP2K2* and partially *EEF2*. Review of additional cases included in the literature and public databases such as DECIPHER and ISCA Consortium (with full clinical data) allowed us to narrow this SRO to a 113.5 kb segment (chr19:3979568–4093035; hg19; NCBI build 37) and excluded *EEF2* (Figure 2). Thus, 31/37 individuals shared this SRO and others overlapped it partially (case 4 in reference,[22] patient 6 in our series and DECIPHER case 271675; Figure 2). On the other hand, three cases did not share the SRO (patient 10 in our series and DECIPHER cases 259222, 255689), although they shared some clinical findings, such as ID, wide nasal bridge, narrow forehead or vesicoureteral reflux, with the SRO's patients.

Characterization of mechanisms underlying interstitial 19p13.3 genomic rearrangements

We initially designed a custom aCGH with a significant coverage of 19p13.3 (chr19:1477536–6653608, hg19). Further, long-range PCR and automated sequencing were performed to precisely define the breakpoints in some cases (patients 1–7 and 12, Figure 3; patients 9 and 13, data not shown), followed by bioinformatic analysis in both breakpoints through several web tools showing that those lay next to highly homologous repetitive sequences of SINE or LINE elements, which could mediate those rearrangements directly. Results of repeat element analyses, breakpoints and sequences involved are summarized in Table 4, and showed in detail in supplementary data (Supplementary Figure S2). In addition, we also showed analysis of known repeat and genomic architectural elements, such as palindromic DNA or stem-loop structures within the deleted breakpoints that may also modulate in those non-recurrent genomic rearrangements (Supplementary Tables S2 and S3).

Table 1 Patients reported herein with 19p13.3 rearrangements

Patients	*Patient 1*	*Patient 2*	*Patient 3*	*Patient 4*	*Patient 5*	*Patient 6*	*Patient 7*	*Patient 8*	*Patient 9*	*Patient 10*	*Patient 11*	*Patient 12*	*Patient 13*	*Subtotal*	*Frequency, all cases*[a]	*Total (%)*
Type of rearrangement	Deletion	Deletion	Deletion	Deletion	Deletion	Deletion	Deletion	Duplication	Deletion	Duplication	Deletion	Deletion	Deletion	11del/2dup	24del/3dup	
Included in our SRO	Y	Y	Y	Y	Y	±	Y	Y	Y	N	Y	Y	Y	11/13	24/27	**88.88**
Includes *PIAS4*	Y	Y	Y	Y	Y	N	Y	Y	Y	N	Y	Y	Y	11/13	24/27	**88.88**
Gender	F	F	M	F	M	M	M	F	F	F	M	F	F	8F/5M	15F/12M	1.25:1 (F:M)
Age diagnosis	7 yr	9 yr	10 yr	5 yr	3 yr	5 yr	NB (current 5 yr)	6 yr	10 yr	NB (current 3 yr)	6 yr	20 mo	5 yr, 6 mo	NB to 10 yrs	NB to 23 yrs	
Growth and develop																
Psychom develop delay	+	+	+	+	+	+	Mild	++	+	+	+	+	+	**13/13**	**27/27**	**100**
Intellectual disability	Mild	+	Mild	Mild	+	+	+	+	Mild	Mild	+	+	+	**13/13**	**26/26**	**100**
Speech delay	+	+	+	+	++	++	+	+/Basic sentences		+		NA	+	**10/10**	**19/19**	**100**
Macro-/microcephaly	+ p>97	+ p>97	+ p>97	Macro relative	+ p>97	Normo	+ p>97	-4.4SD	+ p>97	Normo	+ p>97	+ p>97	+ p>97	**11/13**	**25/27**	**92.59**
Overgrowth synd testing	–	+	–	–	+	–	–	–	–	–	–	–	+At birth	3/13	4/14	28.57
Proportionate short stature	+	–	+	+	–	+	–	+	–	+	–	–		6/09	8/11	**72.72**
Face									++							
Hypertelorism	+	+	+	+	+	+		–	+	+			+	**9/10**	**17/18**	**94.44**
Downslanting palpebral fissures	–	–	+	–	+	+		–	–	Upslant				3/9 down 1/9 up	12/20 down 2/20 up	60.00
Short palpebral fissures				–	–	–								0/3	2/5	40.00
Ptosis	–	–	–	–	–	+		–	–	–				1/9	4/12	33.33
Epicanthal folds	+	+	–	–	–	+		–	–	Mild				3/9	5/11	45.45
Wide nasal bridge	+	+	+	+	+	+	+	+		+			+	**10/10**	**19/19**	**100**
Depressed nose and root	+	+	+	–	–	+	+			+			+	7/10	9/13	69.23
Philtrum anomalies	Short	Short	–	Short	Short	–		Short	–	–				5/9	10/14	71.43
Thin upper lip	+	+	+	+	+	+		+	–	–				**7/9**	**16/19**	**84.21**
Ear anomalies	+	+	+	+	+	+		–	–	+			+	**8/10**	**17/19**	**89.47**
High or prom forehead	+	+	+	+	+	+	+	+	Mild	+			+	**11/11**	**24/24**	**100**
Neurology																
Hypotonia	+	+	+	+	+	+	+	+		Mild	+	+	+	**12/12**	**21/25**	**84.00**
Behavior	Timid	–	–	–	–	Aggressive/ hyperactive		Deficit of attention	Abnormal		Abnormal			5/9	6/10	60.00
Hearing problems	–	–	–	–	–	–	–	–	–	–	–	–	+	1/13	4/17	23.52
Others																
Cutis aplasia	–	–	–	–	–	–	–	–		–				0/9	3/22	13.64
Urinary reflux	+				+					-				2/4	3/5	60.00
Gastroesophageal reflux			+		+		+						+	**4/4**	**13/14**	**92.85**
Abnormal fingers/toes	Syndactyly		+	+				+		+			+	**6/6**	**13/15**	**86.67**
Feeding problems	+	–	+	+		–	+			+				6/9	14/22	63.63
Ophthalmologic abnormalities	+	+	+	+		–	+	–	–	+				6/9	7/10	70.00
Umbilical hernias			+		+		+						+	4/4	6/12	50.00
Sleeping disorders		–			+		+						+	**3/3**	**10/13**	**76.90**
Heart disease	–	–	+	–	+	+	+	–	+	+			+	7/11	15/24	62.50

Abbreviations: develop, development; F, female; M, male; Macro, macrocephaly; mo, months; N, no; NA, not applicable; NB, newborn; Normo, normocephaly; p, percentile; prom, prominent; psychom, psychomotor; synd, syndrome; Y, yes; yr, years.
A frequency over 75% is marked in bold. +, feature present; –, feature absent; ++, feature severe.
[a]Includes 14 cases from the literature (13 deletions and 1 duplication, Table 2).

DISCUSSION

We delineate, review and refine recently described overlapping interstitial deletions/duplications within proximal 19p13.3 (genomic coordinates: 2329320–4996928; genome assembly hg19, NCBI build 37), showing a consistent genotype–phenotype correlation of 13 novel patients, using a 'genotype first approach'. Thus, we propose a novel interstitial microdeletion/duplication syndrome at 19p13.3, centromeric to the 19p13.3 terminal microdeletions and microduplications.[6,7]

Both deletions and duplications of this region result in some common, non-specific features present in many other microdeletion/duplication syndromes. Available clinical data presented here, together with cases in the literature[8–22] and databases, demonstrate several consistent phenotypic findings for this interstitial 19p13.3 deletion: macrocephaly, typically combined with prominent forehead and bitemporal narrowing; facial dysmorphic features such as hypertelorism, depressed nasal bridge and nasal root, short philtrum, thin upper lip and ear anomalies; and developmental and speech delay and ID. Similarly, all patients with duplications of the same region consistently showed microcephaly, dysmorphic facial features (wide nasal bridge, depressed nasal root and hypertelorism), feeding problems in infancy, DD and ID, although dysmorphic features and DD/ID were less severe than in the reciprocal deletions.

Genomic context, deletion size and genes implicated

The SRO for most cases (31 out of 37) presented here is a 113.5 kb region harboring three genes: *PIAS4*, *ZBTB7A* and *MAP2K2* (Figure 2). Although patient 6 (who partially shared the SRO), patient 10 and DECIPHER cases 255689 and 259222 did not share the SRO, they were included in this study because they share many clinical features with patients with deletion or duplication of the SRO. The three SRO genes are involved in diverse functions, including transcription, histone deacetylation and gene translation; *ZBTB7A* (zinc finger and BTB domain containing 7A) is a transcriptional repressor belonging to the POK (POZ/BTB) family involved in adipogenesis. *ZBTB7A* may have an important role in neuronal development;[28] thus deletion of *ZBTB7A* might contribute to the DD in our patients. In addition, other similar members of this protein family, such as *ZBTB20, ZBTB38* and *ZBTB18,* are strong candidates for the DD in a new microdeletion syndrome at 3q13[17] and have been associated with human height in GWAS studies[29] or with several features in 1q43-q44 microdeletion syndrome,[30] respectively. Dominant gain-of-function mutations of *MAP2K2* (mitogen-activated protein kinase kinase 2) cause cardiofaciocutaneous syndrome,[31] and recently, haploinsufficiency of *MAP2K2* has been suggested as a new model of RASopathy in a series of seven patients with deletions.[22] Finally, *PIAS4* (protein inhibitor of activated *STAT4*) encodes a RING finger (RNF) protein, which interacts with the androgen receptor (AR). PIAS4 is also an E3 ligase involved in ubiquitin signaling pathways.[32] Additional cases (showing almost the same phenotype) that either partially overlapped or did not include this 113.5 kb SRO region suggest that part of the phenotypic features could be explained by a 'position effect' or by additional genes close to this SRO (Figure 2). Therefore we hypothesize that the interval from *TLE2* to *CREB3L3* within 19p13.3, a highly conserved region among different species[33,34] with a rich content in haploinsufficient genes (with 16/55 with a high likelihood of being haploinsufficient),[35] as a critical region responsible for most clinical features. Additional genes that may contribute to clinical features are (from centromere to telomere): *EEF2, DAPK3, NMRK2, ATCAY* and *NFIC,* among others (Figure 2), which are involved in cognitive impairment,[36] regulation of myogenic differentiation,[37] apoptosis and transcriptional regulation of canonical Wnt/β-catenin signaling,[38] and autosomal recessive Cayman cerebrallar ataxia,[39] respectively. *NFIC* is a member of the nuclear factor I (NFI) gene family necessary for optimal cellular gene expression,[40] similar to

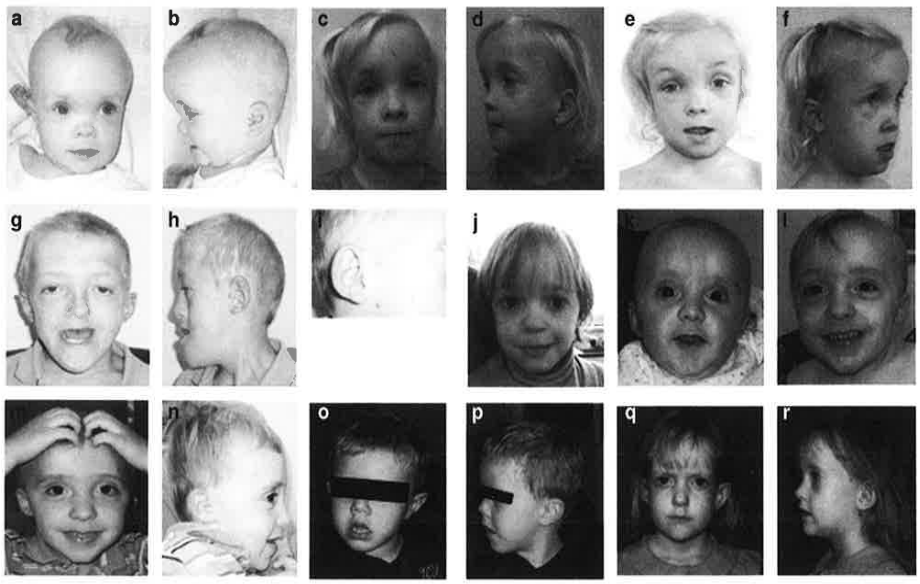

Figure 1 Facial photographs of individuals presented in this study. Patient 1 at age 8 months (**a**, **b**), 4 years (**c**, **d**) and 7 years (**e**, **f**); patient 3 at age of diagnosis, 10 yrs (**g**, **h**, **i**); patient 4 at age 5 years (**j**); patient 5 at age 7 months (**k**), 2 years (**l**) and 4 years (**m**, **n**); patient 6 at age 5 years (**o**, **p**); patient 13 at age 8 years (**q**, **r**).

Table 2 Patients reported in the literature with interstitial 19p13.3 rearrangements

Patients	*Al-Kateb et al* [18]	*De Smith et al,* [19]	*Siggberg et al* [21]	*Siggberg et al*[21]	*Risheg et al,*[20] *Pat1*	*Risheg et al,*[20] *Pat2*	*Risheg et al,*[20] *Pat3*	*Nowaczyk et al,*[22] *Pat1*	*Nowaczyk et al,*[22] *Pat2*	*Nowaczyk et al,*[22] *Pat3*	*Nowaczyk et al,*[22] *Pat4*	*Nowaczyk et al,*[22] *Pat5*	*Nowaczyk et al,*[22] *Pat6*	*Nowaczyk et al,*[22] *Pat7*	*Frequency*
Type of rearrangement	Deletion	Deletion	Deletion	Duplication	Deletion	Deletion	Deletion	Deletion	Deletion	Deletion	Deletion	Deletion	Deletion	Deletion	13del/1 dup
Included in our SRO	Y	Y	Y	Y	Y	Y	Y	Y	Y	Y	±	Y	Y	Y	14/14
Includes *PIAS4*	Y	Y	Y	Y	Y	Y	Y	Y	Y	Y	N	Y	Y	Y	13/14
Gender	F	F	M	M	F	F	M	M	F	M	F	F	M	M	7F/7M
Age at diagnosis	4 yr	17 yr	2 yr	9 yr	23 yr	2 yr	6 yr	10 yr	5.9 yr	3 yr	4 yr	6 yr	2 mo	5 yr	2 mo–23 yr
Growth and develop															
Psychom develop delay	+	Mild	+	+	+	+	+	+	+	+	+	+	+	+	14/14
Intellectual disability	+	+	+	Mild	+	+	+	+	+	Mild	Mild	++		++	13/13
Speech delay	+	+	+	+	+	+	+	++	+						9/9
Macro-/microcephaly	+3SD	+4.5SD	+3SD	Micro	Macro relative	+	Macro relative	+2.5SD	−3.5SD	−2.5SD	+3.5SD	+5.5SD	+1SD*	+3.5SD	14/14
Obesity		+													1/1
Proportionate short stature		−													0/1
Overgrowth synd testing		+													1/1
Face															
Hypertelorism	+			+				+	+	+	+	+	+		8/8
Downslanting palpebral fissures	+	Upslant	+	−				+	+	+	+	+	+	+	9/11down 1/11 up
Short palpebral fissures				+	+										2/2
Ptosis			Mild	+		+									3/3
Epicanthal folds	+			+											2/2
Wide nasal bridge	+	+		+				+		+	+	+	+	+	9/9
Depressed nose and root	−	−		+											1/3
Philtrum anomalies	Prominent	Short		Short	Hypoplastic		Flat								5/5
Thin upper lip	Tented	+		+				+	+	+	++	+	+	−	9/10
Ear anomalies	+	Dysplastic	+		+	+	+			+		+		+	9/9
High or prom forehead	+	+	+	+		+	+	++	++	+	+	+	+	+	13/13
Neurology															
Hypotonia	+	+	+	+		+	+	−	+	+	−	−	−	+Mild	9/13
Behavior		Self injury/ agressivity													1/1
Hearing problems	Mild loss	−	Minor problems				Moderate bilateral conductive								3/4

Table 2 (Continued)

Patients	Al-Kateb *et al* [18]	De Smith *et al*, [19]	Sigg*berg et al* [21]	Sigg*berg et al*[21]	Risheg *et al*,[20] Pat1	Risheg *et al*,[20] Pat2	Risheg *et al*,[20] Pat3	Nowaczyk *et al*,[22] Pat1	Nowaczyk *et al*,[22] Pat2	Nowaczyk *et al*,[22] Pat3	Nowaczyk *et al*,[22] Pat4	Nowaczyk *et al*,[22] Pat5	Nowaczyk *et al*,[22] Pat6	Nowaczyk *et al*,[22] Pat7	Frequency
Others															1/1
Cutis aplasia	+	−	+		−	−	−	−	+	−	−	−	−	−	3/13
Urinary reflux							+								1/1
Gastroesophagealreflux	+	−				+		+	+	+	+	+	+	+	9/10
Feeding problems	+	−	+					+	+	+	+	+	+	−	8/10
Abnormal fingers/toes															
Ophthalmologic abnormalities				+											1/1
Umbilical hernia	−							−	−	+	+	−	−	−	2/8
Sleeping disorders	−	−				+		+	+	+	−	+	+	+	7/10
Heart disease	+	−	+		+	+	+	+	−	−	+	+	−	−	8/13

Abbreviations: develop, development; dysplast, dysplastic; F, female; M, male; Macro, macrocephaly; Micro, microcephaly; mo, months; N, no; prom, prominent; psychom, psychomotor; SD, standard deviation; synd, syndrome; Y, yes; yr, years. +, feature present; ++, severe feature; −, feature absent. (*) this proband has born after 27 gestational weeks, showing low weight and height, but showed +1SD in OFC. Thus, is considered a relative macrocephaly.

NFIX, a strong candidate for many phenotypic findings similar to those reported here in the recently described 19p13.13 microdeletion/duplication syndrome (located ~9 Mb centromeric to our SRO).[2] *NFIX* has been also implicated in the autosomal dominant Marshall–Smith syndrome (MIM 602535) and in patients with Sotos-like syndrome (currently known as Sotos syndrome type 2; MIM 614753).[10] Interestingly, deletion of *NFIC* is observed in 22/37 of patients discussed here (Figure 2). Altogether, these genes appear to be involved in important pathways that could contribute to developmental abnormalities. Additional cases will be needed to refine genes directly implicated in the complete phenotype.

The potential relevance of this ~1.1 Mb interval from *TLE2* to *CREB3L3* (that includes the SRO) is supported by its highly conserved nature in all vertebrates, from fish to mammals.[33,34] Further support underlining the importance of this highly conserved region and its contribution to the clinical features in patients with 19p13.3 deletion/duplications is given by their haploinsuffiency (HI) score. HI score (defined by Huang and colleagues, 2010)[35] ranges from 0 to 100, where 0 means highly haploinsufficient and 100 not haploinsufficient. The region from *TLE2* to *CREB3L3* includes 16/55 potential HI genes with a score <50.[35]

Chromosomal architecture context and mechanisms of rearrangement

The deletions and duplications at 19p13.3 in patients reported here were not flanked by segmental duplications and mostly unique to each patient, though some are in close proximity (see Figure 2,Table 3). This fact combined with the absence of low copy repeats within or flanking deleted/duplicated regions makes non-allelic homologous recombination (NAHR) an unlikely causative mechanism. Several mechanisms have been proposed for the formation of copy number alterations with non-recurrent breakpoints, and in most microhomology at breakpoint junctions have been invoked. They can be grouped as non-replicative (NAHR and others such as non-homologous end joining (NHEJ) and microhomology-mediated end joining (MMEJ)) or replicative-based repair mechanisms (fork stalling and template switching (FoSTeS), serial replication slippage (SRS), break-induced SRS and microhomology-mediated break-induced replication).[41–44]

We hypothesize that most interstitial non-recurrent 19p13.3 rearrangements are a consequence of NHEJ and/or the alternative pathway MMEJ, although different patterns have been depicted. Indeed, although repetitive elements of the same family (SINE; Alu: patients 1, 4 and 5) or different family (DNA MER and LINE; patient 2) are present at both breakpoints, the level of sequence identity is probably too low for Alu/Alu-mediated NAHR. In addition, the 4bp, 3bp, 50 bp or 3bp of microhomology (patients 1, 2, 4 and 5, respectively) and/or some changes of nucleotides at the breakpoints (patients 2 and 5) may point to NHEJ or to MMEJ as mechanisms preferentially involved (Table 4,Supplementary Figure S2). In another group of patients, such as patients 6 and 7, only the distal breakpoint showed a repetitive element directly involved, although microhomology of 5- and 6 bp, respectively, and some nucleotide insertions observed at the junctions of these deletions, suggested also a MMEJ mechanism (Table 4, Supplementary Figure S2). Finally, a third group of patients (eg, patient 12) did not show any repetitive element directly involved, but close to them. In fact, breakpoints were flanked by AluJo and L1 (LIMB7) elements and the presence of 3 bp microhomology without any scar may point to NHEJ mechanism.

In silico genomic analysis of the breakpoints of the remaining patients (3, 9 and 13) revealed numerous highly repetitive sequences (SINEs/LINEs, see Table 4) that may be involved in the generation of such events. In fact, chromosome 19 contains 'Alus' in the highest

Table 3 Coordinates of imbalances at interstitial 19p13.3 region according to the HGVS and ISCN nomenclatures

Patient	*Genomic imbalance; inheritance*	*Size (Mb)*	*Type*	*CGH-array platforms and methods used*
01	chr19.hg19:g.(3,324,025_ 3,324,026)_(4,870,882_4,870,883)del ISCN:19p13.3 (3,324,026-4,870,882)x1 dn	1.546	Deletion	KaryoArray_v3.0 and custom 19p13.3 and Sanger sequencing
02	chr19.hg19:g.(3,874,599_3,874,600)_(4,183,343_4,183,344)del ISCN: arr[hg19] 19p13.3(3,874,600- 4,183,343)x1 dn	0.309	Deletion	KaryoArray_v3.0 and custom 19p13.3 and Sanger sequencing
03	chr19.hg19:g.(3,227,720_3,234,036)_(4,823,723_4,830,039)del ISCN: arr[hg19] 19p13.3 (3234036-4823723)x1 dn	1.491	Deletion	KaryoArray_v3.0 and custom 19p13.3
04	chr19.hg19:g.(3,932,784_3,932,785)_(4,523,183_4,523,184)del ISCN: arr[hg19] 19p13.3 (3,932,785-4,523,183)x1 dn	0.590	Deletion	KaryoArray_v3.0 and custom 19p13.3 and Sanger sequencing
05	chr19.hg19:g.(3,279,941_3,279,942)_(4,168,106_4,168,107)del ISCN: arr[hg19] 19p13.3 (3,279,942-4,168,106)x1 dn	0.888	Deletion	SignatureChipOS v2.0 12-plex, KaryoArray_v3.0, custom 19p13.3 and Sanger sequencing
06	chr19.hg19:g.(3,789,486_3,789,487)_(3,988,746_3,988,747)del ISCN: arr[hg19] 19p13.3 (3,789,487-3,988,746)x1 dn/ chr19.hg19:g.(46,121,111_4,6121,112)_(46,387,319-46,387,320)del ISCN: arr[hg19] 19q13.32 (46,121,112-46,387,319)x1 dn	0.199/0.266	Deletion/deletion	KaryoArray_v3.0 and custom 19p13.3 and Sanger sequencing
07	chr19.hg19:g.(3,295,067_3,295,068)_(4,996,928_4,996,929)del ISCN: arr[hg19] 19p13.3 (3,295,068-4,996,928)x1 dn	1.700	Deletion	SignatureChipWG v1.0.1; KaryoArray_v3.0 and custom 19p13.3 and Sanger sequencing
08	chr19.hg19:g.(2,362,767_2,487,767)_(4,882,351_5,007,351)dup ISCN: arr[hg19] 19p13.3 (2,487,767-4,882,351)x3 dn	2.395	Duplication	Qchip_v3.0
09	chr19.hg19:g.(3,184,457_3,190,773)_(3,448,532_3,454,848)del ISCN: arr[hg19] 19p13.3 (3,190,773-3,448,532)x1 chr19.hg19:g.(3,579,614_3,585,930)_(4,621,011_ 4,627,327)del ISCN: arr[hg19] 19p13.3 (3,585,930-4,621,011)x1 dn	0.257/1.035	Deletion/deletion	SignatureChipWG v1.0.1, and custom 19p13.3
10	chr19.hg19:g.(2,294,320_2,329,320)_(3,808,325_ 3,843,325)dup ISCN: arr[hg19] 19p13.3 (2,329,320-3,808,325)x3 dn	1.479	duplication	SignatureChipOS v2.0 12-plex
11	chr19.hg19:g.(3,944,568_3,979,568)_(4,131,259_ 4,166,259)del ISCN: arr[hg19] 19p13.3 (3,979,568-4,131,259)x1	0.151	Deletion	SignatureChipOS v2.0 12-plex
12	chr19.hg19:g.(3,451,210_3,451,211)_(4,600,362_4,600,363)del ISCN: arr[hg19] 19p13.3 (3,451,211-4,600,362)x1 dn	1.149	Deletion	SignatureChipOS Version 4.0 and custom 19p13.3 and Sanger sequencing
13	chr19.hg19:g.(3,397,174_3,403,490)_(3,405,207_3,411,524)dup ISCN: arr[hg19] 19p13.3 (3,403,490-3,405,207)x3 chr19.hg19:g.(3,406,937_3,413,253)_(4,195,610_4,201,926)del ISCN: arr[hg19] 19p13.3 (3,413,253-4,195,610)x1	0.00177/0.781	Duplication/deletion	SignatureChipOS Version 4.0 and custom 19p13.3

Abbreviations: dn, *de novo*; HGVS, Human Genome Variation Society; ISCN, International System for Human Cytogenetic Nomenclature. *Data are from* UCSC Genome Browser (February 2009 assembly, hg19, NCBI build 37).

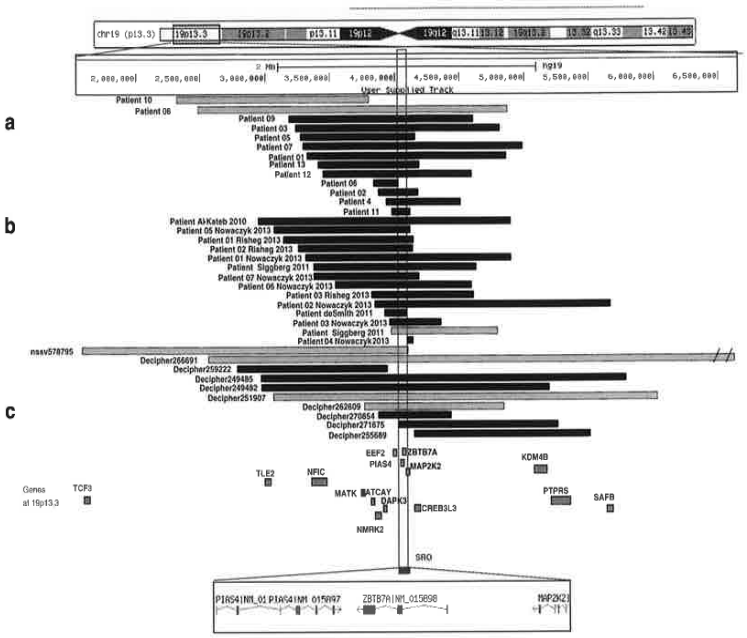

Figure 2 Graphical representation of interstitial 19p13.3 deletions and duplications; genes within the minimal region of overlap. SRO (chr19: 3979568–4093035; hg19; NCBI build 37). Patients are from our series (**a**); previous reports (**b**) and public databases, such as DECIPHER and ISCA consortium (**c**). Gray; duplications, Black; deletions.

density, comprising 27.2% of chromosome.[45] In patients 9 and 13 a replicative mechanism may be suggested by the complex genomic rearrangement observed (deletion-normality-deletion and duplication-normality-deletion, respectively; see Supplementary Figure S3). Additional cases must be analyzed for a more complete understanding of the mechanisms of deletion and whether genomic architecture in this region predisposes to genomic rearrangements, as previously suggested in other chromosomal regions.[46] In fact, additional analysis of sequence elements at both breakpoints revealed repetitive elements in all cases, sequences forming nonB-DNA conformations and sequence motifs that may lead to genomic instability and subsequently genomic rearrangements by promoting double strand breaks (DSBs) or by stalling the replication fork as we discussed for the *FOXL2* locus[47] (also see Supplementary Tables S2).

Clinical findings and genotype correlation with head circumference

Macrocephaly can be caused by disruption of a broad spectrum of genes and biological functions. There are a few microdeletion/duplication syndromes with macrocephaly listed in the DECIPHER database: the 1q21.1 microduplication, 8p23.1 duplication, 19p13.13 deletion and Sotos syndrome. In contrast, microcephaly is listed in 16 syndromes in the DECIPHER database. We add the interstitial 19p13.3 microdeletion/duplication syndrome to the differential diagnosis of macrocephaly or microcephaly, respectively. A similar phenomenon of 'mirror' head size phenotypes has been previously reported with genomic rearrangements such as the 19p13.13 microdeletion/duplication syndrome,[2] the 1q21.1 microdeletion/duplication syndrome,[48] and the Sotos syndrome/5q35 duplication syndrome.[49]

A comparative analysis of almost all deleted and duplicated patients pointed to *PIAS4* as a strong candidate for abnormal head size (see Figure 3, dashed line), as all patients but one with abnormal head size had deletion or duplication of this gene. In agreement with this, injection of high doses of *PIAS* into early frog embryos led to reduced head structures with a general and reduced embryonic body length.[34] In addition, most patients without rearrangements of *PIAS4* are normocephalic (Figure 3 panel b). Further support for *PIAS* genes' implication in head size in humans was obtained reviewing our own database for macrocephalic patients. Indeed, we found a patient with a 3.68 Mb 7p13-p12.3 deletion (43 511 010-47 209 011, genome assembly hg19, NCBI build 37), which included *ZMIZ2*, a PIAS-like family gene[50] (see Supplementary Figure S4), as well as that other patients with rearrangement at 7p13-p12.3; cases nssv578186 and nssv584525 and DECIPHER 1224, 1223, 1222, 1221, 1220 (deletions) and nssv579045 (duplication) also showed macrocephaly and microcephaly, respectively.

In contrast, other facts do not support *PIAS4*'s role in head size in humans. Heterozygous and homozygous knockout mice for *PIAS4* did not show phenotypic changes.[51] However, no brain weight measures were taken in the study (Dr Grossched's personal communication). In addition, normocephalic patients have *PIAS4* deletions or duplications; 11 of 48 patients in this review had a head size that did not correlate with *PIAS4* copy number changes (see Figure 3, mostly in normocephalic individuals in panel b; with asterisks). However, some were evaluated using low-resolution arrays (case 4 in reference[22] and DECIPHER 255689) or have additional (case 3 in reference[22]) or very large chromosomal rearrangements that extend toward the centromere (Figure 3 panel b). We speculate that very large deletions and

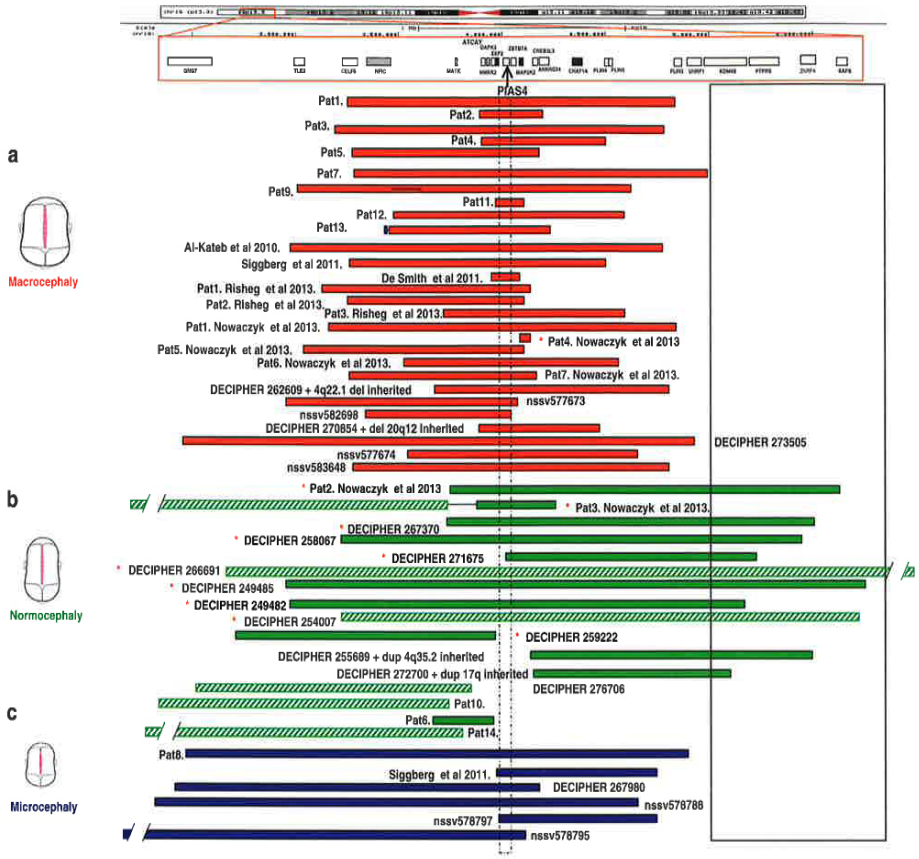

Figure 3 Graphic representation of the minimal region of overlap (SRO, dashed line) responsible for macro/microcephaly in interstitial 19p13.3 microdeletion/duplication syndrome (by means of aCGH). The SRO included only one gene, *PIAS4*. (**a**) Almost all patients with macrocephaly (including relative macrocephaly, red bars) have deletions affecting *PIAS4*. In contrast, all patients with microcephaly (blue bars) have duplications of *PIAS4* (**c**). Patients in panel **b**, with either deletions (full green bars) or duplications (striped green bars), are normocephalic. The majority of these CNAs either do not include *PIAS4* or extend further towards the centromere than the individuals with head size abnormalities. Cases where *PIAS4* deletion/duplication status does not correlate with head size (mainly in the normocephalic group) are illustrated by an asterisk (*). The solid black line outlines a putative region which may negate effects of *PIAS4* dosage changes. Pat, Patient; nssv, ISCA consortium patients.

duplications extending toward the centromere past genomic coordinate 5 000 000 (at 19p13.3 band; hg19, NCBI 37) may modify the head size phenotype of *PIAS4* dosage change owing to the existence of putative dominant-negative regulator genes within this area. *KDM4B*, *PTPRS* and *SAFB* are predicted haploinsufficient genes[35] that might be strong candidates for this effect. Mouse knockout studies reveal that these genes are involved in abnormal head morphology (*Kdm4b*), decreased brain size by weight (*Ptprs*), or in smaller fetal size (including head; *Safb*) compared with littermates (Mouse Genomic Informatic database, MGI; and Mouse Genome Database, MGD; web pages).

The specific mechanism of how PIAS4 or other RNF proteins may be involved in macro/microcephaly is unknown, but *PIAS4* is highly conserved from zebrafish to mammals.[33,34] One hypothesized mechanism is disruption of AR-mediated transcription, which is a common feature of PIAS-like proteins.[52] A second hypothesis is disruption of bone morphogenetic protein-signaling pathways, as the RING domain of PIAS4 is involved in its suppression.[53] Third, PIAS4 may be involved in the WNT signaling pathway through its interaction with several transcription factors,[32,54] and *WNT* is important for several aspects of facial morphogenesis. Fourth, PIAS4 is an E3 ubiquitin ligase, and haploinsufficiency of E3 ubiquitin ligases in plants and *Drosophila melanogaster*[55–57] leads to organ overgrowth. Interestingly, individuals with haploinsufficiency of *RNF135* or *RNF125*, which encode other RNF proteins, have been associated recently (via alteration of ubiquitin signaling pathways) by us and others with macrocephaly and overgrowth in patients with dysmorphic features and ID.[58,59] Thus, additional efforts will be necessary to definitively establish how PIAS4, PIAS-like or other RNF proteins, may be involved in regulation of human head size.

In summary, after identifying 13 unrelated patients and reviewing others previously reported, we further delineate a novel interstitial microdeletion/duplication syndrome at 19p13.3 (different from subtelomeric microdeletions) whose clinical features overlap many other known microdeletion/duplication syndromes, such as anomalies of head size (macrocephaly in deletions and microcephaly in duplications), pointing to *PIAS4* as a putative candidate. This study also provides detailed clinical information for geneticists to assist in the evaluation, diagnosis and management of individuals with similar genomic rearrangements.

Table 4 Detection of breakpoints and junction fragment analysis in some interstitial 19p13.3 deletion patients

Patient	Genomic rearrangement	Deletion size (Mb)	Micro-homology at the breakpoint	Change of the sequence at the breakpoint	Repetitive elements at the breakpoints distal/proximal	Most probable Mechanism
01	chr19.hg19:g.(3,324,025_ 3,324,026)_(4,870,882_4,870,883)del	1.546	TTTC	Not detected	AluJr/AluSp	NEHJ or MMEJ
02	chr19.hg19:g.(3,874,599_3,874,600)_(4,183,343_4,183,344)del	0.309	TGG	chr19.hg19:g.3874596delT	DNAMer82/L2b (LINE)	NEHJ or MMEJ
03[a]	chr19.hg19:g.(3,227,720_3,234,036)_(4,823,723_4,830,039)del	1.491			SINE/SINE	NEHJ or MMEJ
04	chr19.hg19:g.(3,932,784_3,932,785)_(4,523,183_4,523,184)del	0.590	CCGCCTCGGCCTCCCAA; AGTGCTGGGATTACAGG CGTGAG CCACTGTGCCC	Not detected	AluSx3/AluSx	MMEJ
05	chr19.hg19:g.(3,279,941_3,279,942)_(4,168,106_4,168,107)del	0.888	ATG	chr19.hg19:g.(3279937dupT; 3279938A>T)	AluSx/AluSq	NEHJ or MMEJ
06	chr19.hg19:g.(3,789,486_3,789,487)_(3,988,746_3,988,747)del	0.199	CCCAG	chr19.hg19:g.(3789465GGGGAAC-CAAGGTCTTGAG > TCCTAGCACCGGGCCTGTA; 3789485dupAT)	AluSc8/near to DNAMer113	MMEJ
07	chr19.hg19:g.(3,295,067_3,295,068)_(4,996,928_4,996,929)del	1.700	GCCCTG	chr19.hg19:g.4996938du pXCCTTCXTT	DNAMer20/-	MMEJ
09[a]	chr19.hg19:g.(3,184,457_3,190,773)_(3,448,532_3,454,848)del chr19.hg19:g.(3,579,614_3,585,930)_(4,621,011_4,627,327)del	0,257/1.035			Near toGC-rich/ between AluSX1 and MIR3/Near toC-rich/ AluSq2	Replicative –based repair mechanism
12	chr19.hg19:g.(3,451,210_3,45,1211)_(4,600,362_4,600,363)del	1.149	GCA	Not detected	near Limb7(LINE)/near to AluJo	NEHJ
13[a]	chr19.hg19:g.(3,397,174_3,403,490)_(3,405,207_3,411,524)dup chr19.hg19:g.(3,406,937_3,413,253)_(4,195,610_4,201,926)del	0.00177/0.781			MIR/near toMIRC near to AluSx/near to AluSx/AluSg	Replicative –based repair mechanism

[a]cases under *in silico* analysis.

CONFLICT OF INTEREST

The authors declare no conflict of interest.

ACKNOWLEDGEMENTS

We would like to thank Drs J Andrieux, N Van der Aa, L Bird, T Cole, K Neas, F Faletra, T de Ravel, N Morrison, four useful and additional information required for several patients in free Databases. This work was supported by a grant from REDES/FIBHULP08 of the Fundación para la Investigación Biomédica Hospital Universitario la Paz, the ENDOSCREEN project from Comunidad Autonóma de Madrid, FIS 011/2491 from ISCIII and the EUCID-COST Action BM-1208.

AUTHOR CONTRIBUTIONS

MAM, MPB, EV and JN performed the microarray analysis. JAT did the punctual mutational analysis of *PIAS4* gene. MLT, AD and BF did the cytogenetic and FISH studies. IRA and MVFM did Sanger sequencing analysis. IRA and RM did the detection of breakpoints and the junction fragment analysis. RMA and MCC performed the aCGH studies. JN, FSS, SGM, PDL, AD, MC, AP, LD, MO, MCSH, ECF, ASJ, GG, LA, CHE, SS, ED, XL, HD, DBB, SV, MBD, JWE, SR, CAVV, FFR did the clinical characterization of the patients described herein. JAR, KWG, PL and JN wrote the paper in consultation with all the other authors.

1 Grimwood J, Gordon LA, Olsen A *et al*: The DNA sequence and biology of human chromosome 19. *Nature* 2004; **428**: 529–535.
2 Dolan M, Mendelsohn NJ, Pierpont ME: A novel microdeletion/microduplication syndrome of 19p13.13. *Genet Med* 2010; **12**: 503–511.
3 Kosaki K, Saito H, Kosaki R, Torii C, Kishi K, Takahashi T: Branchial arch defects and 19p13.12 microdeletion: defining the critical region into a 0.8 M base interval. *Am J Med Genet A* 2011; **155A**: 2212–2214.
4 Archer HL, Gupta S, Enoch S *et al*: Distinct phenotype associated with a cryptic subtelomeric deletion of 19p13.3-pter. *Am J Med Genet A* 2005; **136**: 38–44.
5 Peddibhotla S, Kaslifa M, Probst FJ *et al*: Expanding the genotype-phenotype correlation in subtelomeric 19p13.3 microdeletions using resolution clinical chromosomal microarray analysis. *Am J Med Genet A* 2013; **161A**: 2953–2963.
6 Souza J, Faucz F, Sotomaior V, Filho AB, Rosenfeld J, Raskin S: Chromosome 19p13.3 deletion in a child with Peutz-Jeghers syndrome, congenital heart defect, high myopia, learning difficulties and dysmorphic features: Clinical and molecular characterization of a new contiguous gene syndrome. *Genet Mol Biol* 2011; **34**: 557–561.
7 Ishikawa A, Enomoto K, Tominaga M, Saito T, Nagai J, Furuya N, Ueno K, Ueda H, Masuno M, Kurosawa K: Pure duplication of 19p13.3. *Am J Med Genet A* 2013; **161**: 2300–2304.
8 Tentler D, Gustavsson P, Elinder G *et al*: A microdeletion in 19q13.2 associated with mental retardation, skeletal malformations, and Diamond-Blackfan anaemia suggests a novel contiguous gene syndrome. *J Med Genet* 2000; **3**: 128–131.
9 Zung A, Rienstein S, Rosensaft J, Aviram-Goldring A, Zadik Z: Proximal 19q trisomy: a new syndrome of morbid obesity and mental retardation. *Horm Res* 2007; **67**: 105–110.
10 Malan V, Raoul O, Firth HV: 19q13.11 deletion syndrome: a novel clinically recognisable genetic condition identified by array comparative genomic hybridisation. *J Med Genet* 2009; **46**: 635–640.
11 Chowdhury S, Bandholz AM, Parkash S *et al*: Phenotypic and molecular characterization of 19q12q13.1 deletions: a report of five patients. *Am J Med Genet A* 2013; **164A**: 62–69.
12 Miller DT, Adam MP, Aradhya S *et al*: Consensus statement: chromosomal microarray is a first-tier clinical diagnostic test for individuals with developmental disabilities or congenital anomalies. *Am J Hum Genet* 2010; **86**: 749–764.
13 Vermeesch JR, Brady PD, Santaville D, Kok K, Hastings RJ: Genome-wide arrays: quality criteria and platforms to be used in routine diagnostics. *Hum Mutat* 2012; **33**: 906–915.
14 Shaffer LG, Theisen A, Bejjani BA: The discovery of microdeletion syndromes in the post-genomic era: review of the methodology and characterization of a new 1q41q42 microdeletion syndrome. *Genet Med* 2007; **9**: 607–616.
15 Mefford HC, Sharp AJ, Baker C *et al*: Recurrent rearrangements of chromosome 1q21.1 and variable pediatric phenotypes. *N Engl J Med* 2008; **359**: 1685–1699.
16 Palomares M, Delicado A, Mansilla E *et al*: Characterization of a 8q21.11 microdeletion syndrome associated with intellectual disability and a recognizable phenotype. *Am J Hum Genet* 2011; **89**: 295–301.
17 Molin AM, Andrieux J, Koolen DA *et al*: A novel microdeletion syndrome at 3q13.31 characterised by developmental delay, postnatal overgrowth, hypoplastic male genitals, and characteristic facial features. *J Med Genet* 2012; **49**: 104–109.
18 Al-Kateb H, Hahn A, Gastier-Foster JM, Jeng L, McCandless SE, Curtis CA: Molecular characterization of a novel, de novo, cryptic interstitial deletion on 19p13.3 in a child with a cutis aplasia and multiple congenital anomalies. *Am J Med Genet A* 2010; **152A**: 3148–3153.
19 de Smith AJ, van Haelst MM, Ellis RJ: Chromosome 19p13.3 deletion in a patient with macrocephaly, obesity, mental retardation, and behavior problems. *Am J Med Genet A* 2011; **155A**: 1192–1195.
20 Risheg H, Pasion R, Sacharow S *et al*: Clinical comparison of overlapping deletions of 19p13.3. *Am J Med Genet A* 2013; **161A**: 1110–1116.
21 Siggberg L, Olsén P, Nänto-Salonen K, Knuutila S: 19p13.3 aberrations are associated with dysmorphic features and deviant psychomotor development. *Cytogenet Genome Res* 2011; **132**: 8–15.
22 Nowaczyk MJ, Thompson BA, Zeesman S *et al*: Deletion of MAP2K2/MEK2: a novel mechanism for a RASopathy? *Clin Genet* 2013; **85**: 138–146.
23 Vallespín E, Palomares Bralo M, Mori M *et al*: Customized high resolution CGH-array for clinical diagnosis reveals additional genomic imbalances in previous well-defined pathological samples. *Am J Med Genet A* 2013; **161A**: 1950–1960.
24 Bejjani BA, Theisen AP, Ballif BC, Shaffer LG: Array-based comparative genomic hybridization in clinical diagnosis. *Expert Rev Mol Diagn* 2005; **5**: 421–429.
25 Duker AL, Ballif BC, Bawle EV *et al*: Paternally inherited microdeletion at 15q11.2 confirms a significant role for the SNORD116 C/D box snoRNA cluster in Prader-Willi syndrome. *Eur J Hum Genet* 2010; **18**: 1196–1201.
26 Ballif BC, Theisen A, Coppinger J *et al*: Expanding the clinical phenotype of the 3q29 microdeletion syndrome and characterization of the reciprocal microduplication. *Mol Cytogenet* 2008; **1**: 8.
27 Traylor RN, Fan Z, Hudson B *et al*: Microdeletion of 6q16.1 encompassing EPHA7 in a child with mild neurological abnormalities and dysmorphic features: case report. *Mol Cytogenet* 2009; **2**: 17.
28 Artavanis-Tsakonas S, Matsuno K, Fortini ME: Notch signaling. *Science* 1995; **268**: 225–232.
29 Kim JJ, Park YM, Baik KH *et al*: Exome sequencing and subsequent association studies identify five amino acid-altering variants influencing human height. *Hum Genet* 2012; **131**: 471–478.
30 de Munnik SA, García-Miñaúr S, Hoischen A *et al*: A *de novo* non-sense mutation in ZBTB18 in a patient with features of the 1q43q4 microdeletion syndrome. *Eur J Hum Genet* 2013; **22**: 844–846.
31 Rodriguez-Viciana P, Tetsu O, Tidyman WE: Germline mutations in genes within the MAPK pathway cause cardio-facio-cutaneous syndrome. *Science* 2006; **311**: 1287–1290.
32 Ihara M, Yamamoto H, Kikuchi A: SUMO-1 modification of PIASy, an E3 ligase, is necessary for PIASy-dependent activation of Tcf-4. *Mol Cell Biol* 2005; **25**: 3506–3518.
33 Burn B, Brown S, Chang C: Regulation of early Xenopus development by the PIAS genes. *Dev Dyn* 2011; **240**: 2120–2126.
34 Xiong R, Nie L, Xiang LX, Shao JZ: Characterization of a PIAS4 homologue from zebrafish: insights into its conserved negative regulatory mechanism in the TRIF, MAVS, and IFN signaling pathways during vertebrate evolution. *J Immunol* 2012; **188**: 2653.
35 Huang N, Lee I, Marcotte EM, Hurles ME: Characterising and predicting haploinsufficiency in the human genome. *PLoS Genet* 2010; **6**: e1001154.
36 Verpelli C, Piccoli G, Zibetti C *et al*: Synaptic activity controls dendritic spine morphology by modulating eEF2-dependent BDNF synthesis. *J Neurosci* 2010; **30**: 5830–5842.
37 Li J, Rao H, Burkin D, Kaufman SJ, Wu C: The muscle integrin binding protein (MIBP) interacts with alpha7beta1 integrin and regulates cell adhesion and laminin matrix deposition. *Dev Biol* 2003; **261**: 209–219.
38 Togi S, Ikeda O, Kamitani S *et al*: Zipper-interacting protein kinase (ZIPK) modulates canonical Wnt/beta-catenin signaling through interaction with Nemo-like kinase and T-cell factor 4 (NLK/TCF4). *J Biol Chem* 2011; **286**: 19170–19177.
39 Bomar JM, Benke PJ, Slattery EL *et al*: Mutations in a novel gene encoding a CRAL-TRIO domain cause human Cayman ataxia and ataxia/dystonia in the jittery mouse. *Nat Genet* 2003; **35**: 264–269.
40 Mermod N, O'Neill EA, Kelly TJ, Tjian R: The proline-rich transcriptional activator of CTF/NF-I is distinct from the replication and DNA binding domain. *Cell* 1989; **58**: 741–753.
41 Hastings PJ, Ira G, Lupski JR: A microhomology-mediated break-induced replication model for the origin of human copy number variation. *PLoS Genet* 2009; **5**: e1000327.
42 Lee JA, Carvalho CM, Lupski JR: A DNA replication mechanism for generating nonrecurrent rearrangements associated with genomic disorders. *Cell* 2007; **131**: 1235–1247.
43 Shaw CJ, Lupski JR: Non-recurrent 17p11.2 deletions are generated by homologous and non-homologous mechanisms. *Hum Genet* 2005; **116**: 1–7.
44 Lieber MR: The mechanism of human nonhomologous DNA end joining. *J Biol Chem* 2008; **283**: 1–5.
45 Tae-Min K, Seung-Jin H, Mun-Gan R: Periodic explosive expansion of human retroelements associated with the evolution of the hominoid primate. *J Korean Med Sci* 2004; **19**: 177–185.
46 Auffray C, Caulfield T, Khoury MJ, Lupski JR, Schwab M, Veenstra T: Looking back at genomic medicine in 2011. *Genome Med* 2012; **4**: 9.
47 Verdin H, D'haene B, Beysen D *et al*: Microhomology-mediated mechanisms underlie non-recurrent disease-causing microdeletions of the foxl2 gene or its regulatory domain. *PLoS Genet* 2013; **9**: e1003358.
48 Brunetti-Pierri N, Berg JS, Scaglia F *et al*: Recurrent reciprocal 1q21.1 deletions and duplications associated with microcephaly or macrocephaly and developmental and behavioral abnormalities. *Nat Genet* 2008; **40**: 1466–1471.
49 Rosenfeld JA, Kim KH, Angle B *et al*: Further evidence of contrasting phenotypes caused by reciprocal deletions and duplications: duplication of nsd1 causes growth retardation and microcephaly. *Mol Syndromol* 2013; **3**: 247–254.

50 Beliakoff J, Sun Z: Zimp7 and Zimp10, two novel PIAS-like proteins, function as androgen receptor coregulators. *Nucl Recept Signal* 2006; **4**: e017.
51 Roth W, Sustmann C, Kieslinger M: PIASy-deficient mice display modest defects in IFN and Wnt signaling. *J Immunol* 2004; **173**: 6189–6199.
52 Peng Y, Lee J, Zhu C, Sun Z: A novel role for protein inhibitor of activated STAT (PIAS) proteins in modulating the activity of Zimp7, a novel PIAS-like protein, in androgen receptor-mediated transcription. *J Biol Chem* 2010; **285**: 11465–11475.
53 Imoto S, Sugiyama K, Yamamoto T, Matsuda T: The RING domain of PIASy is involved in the suppression of bone morphogenetic protein-signaling pathway. *Biochem Biophys Res Commun* 2004; **319**: 275–282.
54 Sachdev S, Bruhn L, Sieber H, Pichler A, Melchior F, Grosschedl R: PIASy, a nuclear matrix-associated SUMO E3 ligase, represses LEF1 activity by sequestration into nuclear bodies. *Genes Dev* 2001; **15**: 3088–3103.
55 Breuninger H, Lenhard M: Expression of the central growth regulator BIG BROTHER is regulated by multiple cis-elements. *BMC Plant Biol* 2012; **12**: 41.
56 Colombani J, Bianchini L, Layalle S *et al*: Antagonistic actions of ecdysone and insulins determine final size in Drosophila. *Science* 2005; **310**: 667–670.
57 Gradilla AC, Mansilla A, Ferrús A: Isoform-specific regulation of a steroid hormone nuclear receptor by an E3 ubiquitin ligase in Drosophila melanogaster. *Genetics* 2011; **189**: 871–883.
58 Douglas J, Cilliers D, Coleman K *et al*: Mutations in RNF135, a gene within the NF1 microdeletion region, cause phenotypic abnormalities including overgrowth. *Nat Genet* 2007; **39**: 963–965.
59 Tenorio J, Mansilla A, Valencia M *et al*: A New Overgrowth Syndrome is Due to Mutations in RNF125. *Hum Mutat* 2014; **35**: 1436–1441.

Supplementary Information accompanies this paper on European Journal of Human Genetics website (http://www.nature.com/ejhg)

CLINICAL GENETICS An International Journal of Genetics, Molecular and Personalized Medicine

Clin Genet 2015: 88: 579–583
Printed in Singapore. All rights reserved

CLINICAL GENETICS
doi: 10.1111/cge.12549

Short Report

A founder *EIF2AK4* mutation causes an aggressive form of pulmonary arterial hypertension in Iberian Gypsies

Tenorio J., Navas P., Barrios E., Fernández L., Nevado J., Quezada C.A., López-Meseguer M., Arias P., Mena R., Lobo J.L., Alvarez C., Heath K., Escribano-Subías P., Lapunzina P. A founder *EIF2AK4* mutation causes an aggressive form of pulmonary arterial hypertension in Iberian Gypsies. Clin Genet 2015: 88: 579–583. © John Wiley & Sons A/S. Published by John Wiley & Sons Ltd, 2014

Pulmonary arterial hypertension (PAH) is a pathological condition characterized by a persistent and progressive elevation of pulmonary vascular resistance with devastating consequences if untreated. In the past recent years, several genes have been related to PAH, however, the molecular defect remains unknown in a significant proportion of patients with familial PAH (~20%). During the past few years, we have observed that PAH shows a particular behavior in Iberian Gypsies, with more aggressive course and frequently affecting multiple members of the same family. We studied five Gypsy families in whom at least one individual from each family developed a severe form of PAH and in whom no mutation had been identified in the common genes. We applied SNP-array-based homozygosity mapping in three families and obtained, among others, one of which included the gene *EIF2AK4*, recently reported in patients with PAH from group-1' pulmonary veno-occlusive disease (PVOD) and pulmonary capillary hemangiomatosis (PCH). Subsequently, we sequenced *EIF2AK4* and found a homozygous mutation in all five families: c.3344C>T(p.P1115L). The majority of our patients required early lung transplantation. Hence, this mutation appeared with a more severe phenotype than previously reported for other *EIF2AK4* mutations. The finding of this novel mutation is important for genetic counseling and calculation of population recurrence risks.

Conflict of interest

The authors have declared no conflict of interest related to this article.

J. Tenorio[a,b,†], P. Navas[c,d,†], E. Barrios[e], L. Fernández[a,b], J. Nevado[a,b], C.A. Quezada[d], M. López-Meseguer[f,g,h], P. Arias[a,b], R. Mena[b], J.L. Lobo[i], C. Alvarez[j], K. Heath[a,b], P. Escribano-Subías[c,d,††] and P. Lapunzina[a,b,††]

[a]CIBERER, Centro de Investigación Biomédica en Red de Enfermedades Raras, ISCIII, 28029 Madrid, Spain, [b]INGEMM, Instituto de Genética Médica y Molecular, IdiPAZ, Hospital Universitario La Paz, Madrid, Spain, Universidad Autónoma de Madrid (UAM), 28046 Madrid, Spain, [c]RIC (Red de Investigación Cardiovascular), ISCIII, 28029 Madrid, Spain, [d]Unidad Multidisciplinar de Hipertensión Pulmonar, Servicio de Cardiología. Hospital Doce de Octubre, Madrid, Spain, [e]Unidad de Cardiología pediátrica, Hospital Universitario Ramón y Cajal, Madrid, Spain, [f]Servicio de Neumología, Hospital Universitario Vall d' Hebron, Barcelona, Spain, [g]Universitat Autònoma de Barcelona, Barcelonal, Spain, [h]CIBERES, Centro de Investigación Biomédica en Red de Enfermedades Respiratorias, ISCIII, 28029 Madrid, Spain, [i]Servicio de Neumología, Hospital Txagorritxu, Vitoria, Spain, and [j]Servicio de Neumología, Hospital Central de Asturias, Spain

[†]These two authors contributed equally to this work.

[††]These two authors contributed equally to this work.

Key words: autosomal recessive disease – c.3344C>T – *EIF2AK4* – Gypsies – pulmonary arterial hypertension – SNP-arrays

Corresponding author: Pablo Lapunzina, MD, PhD, Director and

Tenorio et al.

Coordinador, INGEMM, Instituto de Genética Médica y Molecular, IdiPAZ, Instituto de Investigación Sanitaria del Hospital Universitario La Paz, Madrid, Spain, Universidad Autónoma de Madrid (UAM), 28046 Madrid, Spain; CIBERER, Centro de Investigación Biomédica en Red de Enfermedades Raras, ISCIII, Madrid, Paseo de la Castellana, 261-28046 Madrid, Spain.
Tel.: 34 91 727 72 17;
fax: 34 91 207 10 40;
e-mail:
pablo.lapunzina@salud.madrid.org

Received 13 October 2014, revised and accepted for publication 13 December 2014

Pulmonary hypertension is an increase of blood pressure in the pulmonary artery, pulmonary vein, or pulmonary capillaries, together known as the lung vasculature, leading to shortness of breath, dizziness, fainting, leg swelling and other symptoms. Pulmonary hypertension is currently classified in five different groups (1). Group 1 comprises pulmonary arterial hypertension (PAH) (idiopathic and heritable) as well as pulmonary veno-occlusive disease (PVOD) and pulmonary capillary hemangiomatosis (PCH) as group 1', group 2 corresponds to pulmonary hypertension due to left heart disease, group 3 pulmonary hypertension due to lung diseases and/or hypoxia, group 4 chronic thromboembolic pulmonary hypertension and group 5 pulmonary hypertension with unclear multifactorial mechanisms (2).

PAH is a rare pathological condition defined by a persistent and progressive elevation of pulmonary vascular resistance due to a primary injury and subsequent remodeling of pulmonary arterioles and small pulmonary arteries, leading to respiratory insufficiency and right ventricular failure and death (3, 4). Reports of the REHAP Registry (Spanish Registry of PAH) (3, 4) indicate that PAH has an overall estimated prevalence of 16 cases per million adult inhabitants in Spain and a poor prognosis with survival rates of 87%, 75% and 54% at 1, 3 and 5 years, respectively.

For a long period of time, the only described gene associated to PAH was *BMPR2 (Bone morphogenetic protein receptor type II*, MIM 600799) and *ALK-1* or *ENG* when associated to Rendu-Osler disease, MIM 187300); however, a significant proportion of heritable PAH (~20%) had no detectable mutations in these genes (2, 5). Recently, additional genes (*SMAD9*, *KCNK3*, *CAV1*, *TBX4* and *TOPBP1*) (2, 6) have been showed to cause different forms of PAH (3, 6). The pathophysiology of PVOD and PCH (PAH group 1′) remained unknown for many years but recent studies have described autosomal recessive mutations in *EIF2AK4*, a gene unrelated to the transforming growth factor beta (TGF beta) family, in patients with PVOD and PCH (7, 8).

In our cohort of PAH patients, there appeared to be a distinct subgroup of individuals who developed an aggressive form of the disease with poorer outcomes. Interestingly, they were of Gypsy-Romani ethnicity and multiple affected members were present in each family, due to the high rate of consanguinity due to endogamy. The pathogenic mutation has yet to be identified. In this article, we investigated the molecular basis of this disorder in this group of Gypsy individuals with an aggressive form of PAH and identified a common mutation in *EIF2AK4*.

Material and methods

All clinical data of 136 patients with PAH [functional class, 6-min walk test (6MWT), right heart catheterization parameters, D_{LCO} (diffusing capacity of the lung for carbon monoxide) and survival] were obtained from medical records. The study was ethically approved by both participating hospitals, Hospital Universitario 12 de Octubre and Hospital Universitario La Paz, Madrid. All patients gave their informed consent to this study. DNA was extracted using the Chemagen® DNA isolation equipment (PerkinElmer, Germany). Mutations and deletions or duplications had been previously excluded in *BMPR2*, *KCNK3* and *TBX4*.

From our series of 136 PAH patients with molecular studies, we detected five Gypsy families (four from Spain, one from Portugal) with heritable PAH. All of them had more than one affected member in their families. Baseline evaluation depicted in most of them a high-risk profile with poor prognosis data, namely an early age at diagnosis, advanced functional class with low performance in the 6MWT and a severe pre-capillary pulmonary hypertension with low cardiac output. Interestingly, all of them presented a severely diminished carbon monoxide diffusing capacity. In addition, in two of them, there was a high clinical suspicion for PVOD. Clinical findings, hemodynamic and outcomes are listed in Table 1. Survival free from death or lung transplantation was 40%, with three out of the five patients (60%) requiring bilateral lung transplantation for end stage right ventricular failure at a medium time of 1.1 years from diagnosis, despite targeted PAH medical therapy.

Table 1. Baseline clinical findings and outcome of five Gypsy PAH probands

Proband ID	Origin country	Family number	Gender	Age[a]	Clinical diagnosis	NYHA[b]	6MWT[c]	CO[d]/CI	PVR	mPAP[e]	DLCO	Last treatment	Time to death/ lung transplant
1	Spain	1	M	34 years	HPAH	III	450	2,57/NA	14,78	42	28	Combination oral therapy + iloprost	No
2	Spain	2	M	15 years	Suspected familial PVOD	III	ND	2,75/1,62	NA	63	18	Sildenafil	0,18 years
3	Spain	3	M	18 years	HPAH	III	463	4,73/2,36	10,3	59	32	Combination oral therapy + sc treprostinil	1,78 years
4	Spain	4	F	29 years	Suspected familial PVOD	III	180	4,46/NA	9,8[f]	44[f]	32	Low dose epoprostenol ECMO[g]	1,31 years
5	Portugal	5	M	37 years	IPAH	II	465	6,8	5,6	47	NA	Sildenafil	No

Gender: F, Female; M, Male.

[a]age at diagnosis in years; HPAH, heritable pulmonary arterial hypertension; IPAH, idiopathic pulmonary arterial hypertension.

[b]NYHA, New York Heart Association Class at diagnosis.

[c]6MWT, 6-min walk test (in meters) at diagnosis.

[d]CO/CI, cardiac output/cardiac index at diagnosis; PVR, pulmonary vascular resistance

[e]mPAP, mean pulmonary artery pressure; DLCO, Carbon monoxide diffusing capacity; Time to dead/lung transplantation in years and NO for not lung transplantation.

[f]Measures obtained on inotropic support with dobutamine, intravenous diuretic and intravenous epoprostenol.

[g]ECMO, extracorporeal membrane of oxygenation; NA, not available.

SNP-arrays

For SNP-arrays, we applied the Illumina Cyto850K SNP array according to the manufacturer's specifications (Illumina, San Diego, CA) and analyzed the results using the Chromosome Viewer tool contained in Genome Studio (Illumina). Gencall scores < 0.15 at any locus were considered 'no calls'. The log *r* ratio was employed, which is the log (base 2) ratio of the observed normalized *r* value for an SNP divided by the expected normalized *r* value.

PCR and Sanger sequencing

We subsequently screened for mutations in the 39 exons and intron–exon boundaries of *EIF2AK4* (NM_001013703), by Sanger sequencing, in the five selected patients. PCR conditions were the following: initial denaturation at 94°C for 3 min; 30 cycles of: denaturation at 94°C for 45 s; annealing at 60°C for 30 s and final extension at 72°C for 45 s; Final extension were performed at 72°C for 7 min. Sequencing was undertaken using BigDye Terminator 3.1 (Life Technologies) according to manufacturer's procedures and performed on an ABI3730XL DNA Analyzer (Life Technologies). The sequences were analysed using Sequencher v4.1.4 (Gene Codes). We also performed haplotype analysis of the five patients using a panel of eight microsatellites (*D15S1012, D15S143, D15S146, D15S161, D15S214, D15S971, D15S994 and D15S1044*).

Results

Due to the consanguinity in the families and with the suspicion of an autosomal recessive form of PAH, we applied SNP-array-based homozygosity mapping in three families, looking for common blocks of homozygosity. We observed four large blocks of homozygosity, 1.42, 1.81, 0.8 and 11.8 Mb, shared by all individuals at chromosomes 1, 3, 14 and 15, respectively (Table S1, Supporting Information). At this stage of our investigations, two different groups reported the identification of homozygous or compound heterozygous *EIF2AK4* mutations in a series of patients with PCH and PVOD (7, 8). This gene maps to chromosome 15q15.1, and located within one of the homozygosity blocks, which led us to focus directly on this gene in these individuals. We sequenced the coding regions and intron–exon boundaries of this gene and identified a variant in exon 23 of *EIF2AK4* c.3344C>T (p.P1115L); Chr15:40,003,301C>T (GRCh38/hg38) in all five patients (Fig. 1). This variant co-segregated with the PAH in an autosomal recessive model of inheritance in the five families. This change is absent in the Exome Variant Server and 1000 Genomes control population databases and was not present in 350 exomes of Spanish control population (http://bioinfo.cipf.es/apps-beta/exome-server/1.0.6). Proline 1115 is conserved in all organisms from *Drosophila melanogaster* to humans (Table S2, Supporting Information). *In silico* analyses using sorting tolerant from intolerant (SIFT), Polyphen, MutationTaster, predicted that the variant was pathogenic. The haplotype analysis confirmed an ancestral block of homozygosity of 0.546 Mb shared in all five unrelated patients which includes *D15S146, D15S214* and *D15S994*.

Discussion

The Roma Gypsies are an ethnic group with a high incidence of consanguinity and consequently with an increased risk of autosomal recessive disorders (9, 10).

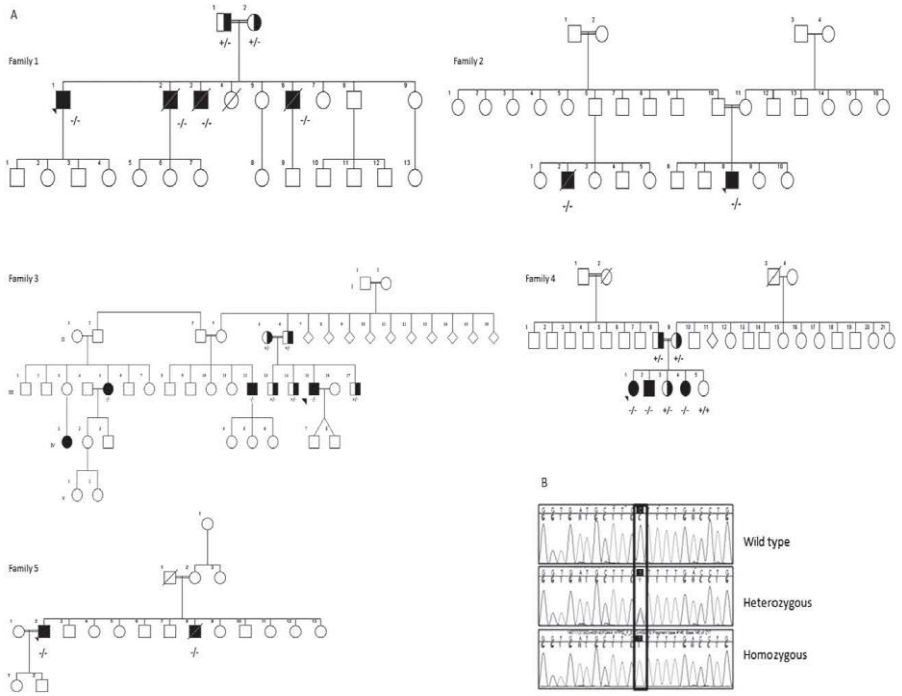

Fig. 1. (**a**) Pedigree of the five families (arrow indicates index patient) showing the segregation of the phenotype and the homozygous mutation c.3344C>T (p.P1115L) in *EIF2AK4* in affected individuals. +: 'wild type allele' −: 'mutated allele'. (**b**) Electropherograms of the three genotypes at position 3344 of the cDNA of *EIF2AK4*. The homozygous TT is the mutated genotype.

The population of European Gypsies is about 10 million; with more than 500,000 individuals in Spain, Slovakia, Hungary, Bulgaria and Romania (9). Many Mendelian disorders in European Gypsies are caused by private founder mutations (9) and specifically in Spain and Portugal, about a dozen genetic diseases are highly prevalent in this ethnic group (11–20). In this study, we detected a new founder mutation in *EIF2AK4* [c.3344C>T; (p.P1115L)] (Fig. 1) as a further autosomal recessive disorder with high prevalence in Iberian Gypsies with PAH and a severe clinical outcome.

EIF2AK4 (formerly known as *GCN2*) encodes a serine-threonine kinase that can induce changes in gene expression in response to amino acid deprivation and that phosphorylates and inactivates the alpha subunit of the eukaryotic initiation factor 2 (Eif2α) leading to preferential synthesis of stress proteins (8). The way by means bi-allelic loss of function mutations of *EIF2AK4* leads to remodeling of lung vessels, pulmonary capillary dilatation and vascular cell proliferation is unknown. However, transgenic mice with biallelic loss of function of *eif2ak4* show increase of metabolites typical of oxidative stress that may be important for the physiopathology of PAH (21) and also it appears to impair the ventricular adaptation to chronic pressure overload by reducing bcl-2 expression and increasing cardiomyocyte susceptibility to apoptotic stimuli (22).

At least 28 patients with mutations in *EIF2AK4* have been described to date in 21 different families with PAH (PCH and PVOD) (7, 8). In this study, we describe a founder mutation in five patients belonging to five Iberian Gypsy families with heritable PAH. The majority of affected presented with an early onset, aggressive form of the disease resulting in a very low survival rate post-lung transplantation (1.1 years). The latter data are very poor compared to data derived from the REHAP registry in which survival in PAH reached 75% at 3 years using new PAH-targeted therapies (3, 4). This clinical course resembles PVOD natural history and, in fact, in half of our patients there was a clinical suspicion for PVOD. The cause/s of this poorer outcome may be due to the mutation itself, the concurrence of modifier effects/genes or other unknown factors.

Our findings provide important data for diagnosis, carrier testing, preconception genetic diagnosis and genetic counseling of this devastating disease. In addition, it will facilitate calculation of recurrence risks in this particular ethnic group. Information on the identity of affected populations is important for public health intervention because it would allow the planning and facilitate the implementation of targeted prevention programs (9). Similarly to other ethnic groups in whom specific programs have already showed high efficacy in preventing diseases [such as Tay–Sachs disease among Ashkenazi Jews (23)], carrier testing should become available to the Gypsy population at high risk of developing this severe and disabling disorder (9). Further research needs to be performed in order to study a

more representative subgroup of Gypsies to better outline genotype–phenotype correlations.

Supporting Information

Additional supporting information may be found in the online version of this article at the publisher's web-site.

Acknowledgements

This project was supported in part by an unrestricted, educational grant from ACTELION and from "Spanish Pulmonary Hypertension National Association" (ANHP).

References

1. Simonneau G, Robbins IM, Beghetti M et al. Updated clinical classification of pulmonary hypertension. J Am Coll Cardiol 2009: 54: S43–S54.
2. Simonneau G, Gatzoulis MA, Adatia I et al. Updated clinical classification of pulmonary hypertension. J Am Coll Cardiol 2013: 62: D34–D41.
3. Crosswhite P, Sun Z. Molecular mechanisms of pulmonary arterial remodeling. Mol Med 2014: 20: 191–201.
4. Van de Veerdonk MC, Marcus JT, Bogaard HJ, Vonk Noordegraaf A. State of the art: advanced imaging of the right ventricle and pulmonary circulation in humans (2013 Grover Conference series). Pulmonary Circulation 2014: 4: 158–168.
5. Austin ED, Loyd JE. Heritable forms of pulmonary arterial hypertension. Semin Respir Crit Care Med 2013: 34: 568–580.
6. Bongers EM, Duijf PH, van Beersum SE et al. Mutations in the human TBX4 gene cause small patella syndrome. Am J Hum Genet 2004: 74: 1239–1248.
7. Best DH, Sumner KL, Austin ED et al. EIF2AK4 mutations in pulmonary capillary hemangiomatosis. Chest 2014: 145: 231–236.
8. Eyries M, Montani D, Girerd B et al. EIF2AK4 mutations cause pulmonary veno-occlusive disease, a recessive form of pulmonary hypertension. Nat Genet 2014: 46: 65–69.
9. Kalaydjieva L, Gresham D, Calafell F. Genetic studies of the Roma (Gypsies): a review. BMC Med Genet 2001: 2: 5.
10. Martinez-Frias ML, Bermejo E. Prevalence of congenital anomaly syndromes in a Spanish gypsy population. J Med Genet 1992: 29: 483–486.
11. Alvarez A, del Castillo I, Villamar M et al. High prevalence of the W24X mutation in the gene encoding connexin-26 (GJB2) in Spanish Romani (gypsies) with autosomal recessive non-syndromic hearing loss. Am J Med Genet A 2005: 137A: 255–258.
12. Barca-Tierno V, Aza-Carmona M, Barroso E et al. Identification of a Gypsy SHOX mutation (p.A170P) in Leri-Weill dyschondrosteosis and Langer mesomelic dysplasia. Eur J Hum Genet 2011: 19: 1218–1225.
13. Callen E, Casado JA, Tischkowitz MD et al. A common founder mutation in FANCA underlies the world's highest prevalence of Fanconi anemia in Gypsy families from Spain. Blood 2005: 105: 1946–1949.
14. Claramunt R, Sevilla T, Lupo V et al. The p.R1109X mutation in SH3TC2 gene is predominant in Spanish Gypsies with Charcot-Marie-Tooth disease type 4. Clin Genet 2007: 71: 343–349.
15. Cotarelo RP, Fano O, Raducu M et al. A double homozygous mutation in the POMT1 gene involving exon skipping gives rise to Walker-Warburg syndrome in two Spanish Gypsy families. Clin Genet 2009: 76: 108–112.
16. Diez O, Domenech M, Alonso MC et al. Identification of the 185delAG BRCA1 mutation in a Spanish Gypsy population. Hum Genet 1998: 103: 707–708.
17. Herrero-Morin JD, Rodriguez J, Coto E et al. Gitelman syndrome in Gypsy paediatric patients carrying the same intron 9 + 1 G>T mutation. Clinical features and impact on quality of life. Nephrol Dial Transplant 2011: 26: 151–155.
18. Mancebo E, Moreno-Pelayo MA, Mencia A et al. Gly111Ser mutation in CD8A gene causing CD8 immunodeficiency is found in Spanish Gypsies. Mol Immunol 2008: 45: 479–484.
19. Quental S, Macedo-Ribeiro S, Matos R et al. Molecular and structural analyses of maple syrup urine disease and identification of a founder mutation in a Portuguese Gypsy community. Mol Genet Metab 2008: 94: 148–156.
20. Sevilla T, Martinez-Rubio D, Marquez C et al. Genetics of the Charcot-Marie-Tooth disease in the Spanish Gypsy population: the hereditary motor and sensory neuropathy-Russe in depth. Clin Genet 2013: 83: 565–570.
21. Fessel JP, Flynn CR, Robinson LJ et al. Hyperoxia synergizes with mutant bone morphogenic protein receptor 2 to cause metabolic stress, oxidant injury, and pulmonary hypertension. Am J Respir Cell Mol Biol 2013: 49: 778–787.
22. Lu Z, Xu X, Fassett J et al. Loss of the eukaryotic initiation factor 2 alpha kinase general control nonderepressible 2 protects mice from pressure overload-induced congestive heart failure without affecting ventricular hypertrophy. Hypertension 2014: 63: 128–135.
23. Kaback M, Lim-Steele J, Dabholkar D, Brown D, Levy N, Zeiger K. Tay-Sachs disease – carrier screening, prenatal diagnosis, and the molecular era. An international perspective, 1970 to 1993. The International TSD Data Collection Network. J Am Med Assoc 1993: 270: 2307–2315.